Azotobacter vinelandii Nitrogenase: Multiple Substrate-Reduction Sites and Effects of pH on Substrate Reduction and CO Inhibition

By Hong Li

Dissertation submitted to the faculty of the Virginia Polytechnic Institute and State University in partial fulfillment of the requirement for the degree of

DOCTOR OF PHILOSOPHY

in

Biochemistry Department

APPROVED:

William E. Newton, Chair

Jiann-Shin Chen

Eugene M. Gregory

Timothy J. Larson

Robert H. White

May, 2002

Blacksburg, VA

Key word: Biological nitrogen fixation, amino acid substitution, altered nitorgenases, Mo-nitrogenase

Azotobacter vinelandii Nitrogenase: Multiple Substrate-Reduction Sites and Effects of pH on Substrate Reduction and CO Inhibition

by Hong Li

Committee Chairman: William E. Newton
Department of Biochemistry

Abstract

Mo-nitrogenase consists of two component proteins, the Fe protein and the MoFe protein. The site of substrate binding and reduction within the Mo-nitrogenase is provided by a metallocluster, the FeMo cofactor, located in the α-subunit of the MoFe protein. The FeMo cofactor's polypeptide environment appears to be intimately involved in the delicate control of the MoFe protein's interactions with its substrates and inhibitors (Fisher K *et al.*, 2000c). In this work, the α-subunit 278-serine residue of the MoFe protein was targeted because (i) a serine residue at this position is conserved both in the Mo-nitrogenase from all organisms examined and in the alternative nitrogenases (Dean, DR and Jacobson MR, 1992); (ii) its hydroxyl group hydrogen bonds to the Sγ of the α-subunit 275-cysteine residue that directly ligates the FeMo cofactor; and (iii) its proximity to the α-subunit 277-arginine residue, which may be involved in providing the entry/exit route for substrates and products (Shen J *et al.*, 1997).

Altered MoFe proteins of *A. vinelandii* nitrogenase, with the $\alpha 278^{Thr}$, $\alpha 278^{Cys}$, $\alpha 278^{Ala}$ and $\alpha 278^{Leu}$ substitutions, were used to study the interactions of H^+, C_2H_2, N_2 and CO with the enzyme. All strains, except the $\alpha 278^{Leu}$ mutant strain, were Nif^+. From measurement of the K_m for C_2H_2 (C_2H_4 formation) for the altered MoFe proteins, the $\alpha 278^{Ala}$ and $\alpha 278^{Cys}$ MoFe proteins apparently bind C_2H_2 similarly to the wild type, whereas the $\alpha 278^{Thr}$ and the $\alpha 278^{Leu}$ MoFe proteins both have a K_m ten-times higher than that of the wild type. Unlike wild type, these last two altered MoFe proteins both produce C_2H_6. These results suggest that C_2H_2 binding is affected by substitution at the α-278

position. Moreover, when reducing C_2H_2, the $\alpha278^{Ala}$ and $\alpha278^{Cys}$ MoFe proteins respond to the inhibitor CO similarly to the wild type, whereas C_2H_2 reduction catalyzed by the $\alpha278^{Thr}$ MoFe protein is much more sensitive to CO. Under nonsaturating concentrations of CO, the $\alpha278^{Leu}$ MoFe protein catalyzes the reduction of C_2H_2 with sigmoidal kinetics, which is consistent with inhibitor-induced cooperativity between at least two C_2H_4-evolving sites. This phenomenon was previously observed with the $\alpha277^{His}$ MoFe protein, in which the α-subunit 277-arginine residue had been substituted (Shen J *et al.*, 1997). Together, these data suggest that the MoFe protein has at least two C_2H_2-binding sites, one of which may be located near the α277-278 residues and, therefore, most likely on the Fe_4S_3 sub-cluster of the FeMo cofactor. Like the wild type, N_2 is a competitive inhibitor of the reduction of C_2H_2 by the $\alpha278^{Thr}$, $\alpha278^{Cys}$ and $\alpha278^{Ala}$ MoFe proteins. Apparently, the binding of N_2 in these altered MoFe proteins is similar to that with the wild type MoFe protein, suggesting that the αSer278 residue is not directly involved in N_2 binding and reduction. Previous work suggested that both a high-affinity and low-affinity C_2H_2-binding site were present on the MoFe protein (Davis LC *et al.*, 1979; Christiansen J *et al.*, 2000). Our results are generally consistent with this suggestion.

Currently, there is not much information about the proton donors and how the protons necessary to complete all substrate-to-product transformations are transferred. The dependence of activity on pH (activity-pH profiles) has provided useful information about the nature of the groups involved in proton transfer to the FeMo cofactor and the bound substrate. Approximately bell-shaped activity-pH profiles were seen for all products from catalysis by all the MoFe proteins tested whether under Ar, in the presence of C_2H_2 as a substrate, or with CO as an inhibitor. The profiles suggested that at least two acid-base groups were required for catalytic activity. The pK_a values of the deprotonated group and protonated group were determined from the pH that gave 50% maximum specific activity. These pK_a values for the altered α278-substituted MoFe proteins and the $\alpha195^{Gln}$ MoFe protein under various assay atmospheres were compared to those determined for the wild type. It was found that the pK_a value of the deprotonated group was not affected by either substitution or changing the assay atmosphere. The wild type MoFe protein has a pK_a (about 8.3) for the protonated group under 100% argon that was

not affected very much by the substitution by Cys, Ala and Leu, whereas the Thr substitution shifted the pK_a to about 8, which was the same as that of the wild type MoFe protein in the presence 10% CO. The pK_a values for the protonated group for all the altered MoFe proteins were not changed with the addition of 10% CO. These results suggest that the αSer278 residue, through hydrogen bonding to a direct ligand of the FeMo cofactor, is not one of the acid-base groups required for activity. However, this residue may "fine-tune" the pK_a of the responsible acid-base group(s) through interaction with the αHis195 residue, which has been suggested (Dilworth MJ *et al.*, 1998; Fisher K *et al.*, 2000b) to be involved in proton transfer to substrates, especially for N_2 reduction. The activity-pH profiles under different atmospheres also support the idea that more than one proton pathway appears to be involved in catalysis, and specific pathway(s) may be used by individual substrates.

Acknowledgment

I would like to thank my dear advisor Dr. William E. Newton first, for his patience, his support and caring all these years that I worked under his direction. Without his guidance in my study and research, I would not have come through this endeavor. I also would like to thank my committee members, Dr. J-S. Chen, Dr. Gregory, Dr. Larson and Dr. White, for their advice, encouragement and understanding. Many thanks to Dr. Bevan who also gave me a lot of valuable suggestions when I had my preliminary exam, and not to mention all the patience during my studying in his molecular modeling course. I will always treasure their care for me.

I would like to thank Christie Dapper in our lab. She was the first person who taught me how to work with nitrogenase. Her patience in helping me at the bench, discussion of the data, and her support and advice in dealing with difficulties during these years are of great importance to me.

I want to thank Dr. Karl Fisher, for all his help, generosity, and insightful advice in the experiments and discussion of the results. I also appreciate the help from Dr. Karin Kloos (now in Germany), Dr. Kanit Vichitphan (now in Thailand), Dr. Jaehong Han and Steve Paugh in our lab. All are great people to work with.

My appreciation to Dr. Kennelly, Dr. Sitz, Dr. Hess, Dr. Dean and all the other faculty members in the department for their effort to help me whenever I needed it. Thanks to Dr. Sunyoung Kim, who is willing to listen to me, and give me her shoulders. I am grateful to Ross Willis for his patience and help at anytime with the equipment and technical problems, and Steve Lowe, Mary Jo, Peggy, Karin, Sheila and Carolyn for their warm hearts and hard work. I have known many of the graduate students in this department, good friends like Brian, Farzana, Ken, Barbara, Hui, Hong Rui, Murat, to name a few. And my Chinese friends, Charlene, Xiling, Fang, Leong and Qun. It has been a pleasure to know them far away from my home.

Most important of all, I thank my beloved husband, Lei Ma, who is the inspiration of my life, whose love and support have always been with me.

(This work was supported by grant from NIH DK-37255.)

Table of Contents

List of Figures

List of Tables

Abbreviations

ADP	adenosine diphosphate
$ADP{\cdot}AlF_4^-$	adenosine diphosphate aluminium tetrafluoride
ATP	adenosine triphosphate
Av1	*Azotobacter vinelandii* MoFe protein
Av2	*Azotobacter vinelandii* Fe protein
B-medium	Burk medium without nitrogen source
BN-medium	Burk medium with nitrogen source (urea or ammonium acetate)
CD	circular dichroism
CHES	2-[N-cyclohexylamino] ethanesulfonic acid
Cp	*Clostridium pasteurianum*
CPK	creatine phosphokinase
DEAE	diethylaminoethyl cellulose
EDTA	ethylene diamine tetraacetic acid
EPR	electron paramagnetic resonance spectroscopy
ESEEM	electron spin echo envelope modulation
HEPES	N-[2-hydroxylethyl] piperazine- N-[2-ethanesulfonic acid]
HEPPS	N-[2-hydroxylehtyl] piperazine- N-[3-propanesulfonic acid]
^1H NMR	proton nuclear magnetic resonance spectroscopy
ICP-AES	inductively coupled plasma atomic emission spectroscopy
K_m	Michaelis constant
k_{obs}	observed rate constant
Kp	*Klebsiella pneumoniae*
MCD	magnetic circular dichroism
MWCO	molecular weight cut-off
M^N	FeMo cofactor in reduced state
M^{OX}	FeMo cofactor in oxidized state
NMF	*N*-methylformamide
P^N	P cluster in reduced state
P^{OX}	P cluster in oxidized state

SA	specific activity
SDS-PAGE	sodium dodecyl sulfate polyacrylamide gel electrophoresis
SF-FTIR	stopped-flow Fourier Transform Infrared Spectroscopy
$T_{1/2}$	doubling time or half life
Tris	tris (hydroxylmethyl) aminomethane
UV	ultraviolet

Chapter 1 Literature Review

A. Nitrogen fixation

Nitrogen is an essential nutrient for all life forms. It is the nutrient that is most commonly limiting for agricultural productivity and results in reduced agricultural yields throughout the world. Molecular nitrogen or dinitrogen (N_2) makes up four-fifths of the atmosphere but is metabolically unavailable directly to both higher plants and animals. During the past century, human activities clearly have accelerated the rate of nitrogen fixation on land, effectively doubling the annual transfer of nitrogen from the vast but unavailable atmospheric pool to the biologically available forms. The major sources of this enhanced supply include industrial processes that produce nitrogen fertilizers, the combustion of fossil fuels, and the cultivation of soybeans, peas, and other crops that host symbiotic nitrogen-fixing bacteria. Furthermore, human activity is also speeding up the release of nitrogen from long-term storage in soils and organic matter (Galloway JN *et al.*, 1995).

Industrial fixation of nitrogen for use as fertilizer currently produces approximately 80 Tg per year and represents by far the largest human contribution of new fixed nitrogen to the global cycle. That figure does not include manures and other organic nitrogen fertilizers, which represent a transfer of already-fixed nitrogen from one place to another rather than new fixation (Bockman OC, 1997). The process of manufacturing fertilizer by industrial nitrogen fixation was first developed in Germany during World War I, and fertilizer production has grown exponentially since the 1940s. In recent years, the increasing pace of production and use has been truly phenomenal. The amount of industrially fixed nitrogen applied to crops during the decade from 1980 to 1990 more than equaled all industrial fertilizer applied previously in human history (Newton WE, 1996). Until the late 1970s, most industrially produced fertilizer was applied in developed countries. Use in these regions has now stabilized whereas fertilizer applications in developing countries have risen dramatically. The momentum of human population growth and increasing urbanization ensures that industrial fertilizer production will continue at high and likely accelerating rates for decades in order to meet the escalating demand for food (Smil V, 1991).

In contrast to the largest industrial facilities required to produce ammonia economically, some microorganisms are capable of diazotrophy, the ability to use nitrogen gas as the sole source of nitrogen for growth (Young JPW *et al*., 1992). This process is called biological nitrogen fixation in which atmospheric nitrogen is converted to ammonia by the enzyme nitrogenase. Microorganisms that fix nitrogen are called diazotrophs. Biological nitrogen fixation requires energy. Those microbes, such as *Azotobacter* and *Clostridium* that fix nitrogen independent of other organisms, are called free living. The free-living diazotrophs require a chemical energy source if they are nonphotosynthetic, whereas the photosynthetic diazotrophs, such as the cyanobacteria, utilize light energy. The free-living diazotrophs contribute little fixed nitrogen to agricultural crops.

Associative nitrogen-fixing microorganisms are those diazotrophs that live in close proximity to plant roots (that is, either in the rhizosphere or within plants but not within their cells) and so can obtain energy materials from the plants (Newton WE, 1996). These associative organisms may make a modest contribution of fixed nitrogen to agriculture and forestry, but quantification of their potential has not been established. The more formalized symbiosis between legumes and the nitrogen-fixing rhizobia occurs within the plant's cells in specialized structures called nodules mainly on the roots and, in a few cases, on the stem (Burns RC and Hardy RWF, 1975). A similar symbiosis occurs between a number of woody plant species and the diazotrophic actinomycete *Frankia* (Newton WE, 1996). In these symbioses, the plant supplies energy materials to the diazotrophs, which reduce atmospheric nitrogen to ammonia. This ammonia is then transferred from the bacteria to the plant to meet some (or most) of the plant's nutritional nitrogen needs for the synthesis of proteins, enzymes, nucleic acids, chlorophyll, and so forth. These symbiotic associations are the greatest contributions of fixed nitrogen to agricultural systems.

Biochemical research into the workings of nitrogen fixation is generally centered on the enzyme complex called nitrogenase. The potential importance of biological nitrogen fixation research with the goal of increasing plant productivity is well documented (Newton WE, 2000 and references therein). However, nitrogenase research has achieved broader significance because the system has emerged as a model for more general

biochemical processes, such as signal transduction, protein-protein interaction, inter- and intramolecular electron transfer, complex metal cluster involvement in enzymatic catalysis, and prosthetic group assembly and insertion into polypeptides. Nitrogenase research also demonstrates the utility of various spectroscopic techniques as probes into enzymatic mechanism and chemistry (Rees DC and Howard JB, 2000).

B. Introduction to nitrogenase

Biological nitrogen fixation is the catalytic process performed by the nitrogenase complex, a two-component metalloenzyme. Three major types of nitrogenase have been identified: one containing molybdenum with iron, a second containing vanadium with iron, and a third apparently containing iron only. There have been reports of a fourth type of nitrogenase, also based on molybdenum but having many unique features, which will be discussed later in this review. This chapter will mainly describe the molybdenum-nitrogenase. This enzyme consists of the iron (Fe) and molybdenum-iron (MoFe) proteins. Substrate reduction by nitrogenase involves three basic types of electron transfer reactions: 1) the reduction of the Fe protein by electron carriers either ferredoxins and flavodoxins *in vivo* or dithionite ($Na_2S_2O_4$) *in vitro*; 2) transfer of single electrons from the Fe protein to the MoFe protein in a MgATP-dependent process; and 3) electron transfer to the substrate at the active site within the MoFe protein. Under optimal conditions, the overall stoichiometry of dinitrogen reduction can be written as follows:

$$N_2 + 24H_2O + 4S_2O_4^{2-} + 16MgATP^{2-} \rightarrow 2NH_4^+ + H_2 + 8SO_3^{2-} + 16MgADP^- + 16HPO_4^{2-} + 22H^+$$

The standard free energy change, ΔG^o, for the biological process using ferredoxin as reductant, is –15 kcal/mol (Alberty RA, 1994). Nitrogenase is a relatively slow enzyme, with a turnover rate per electron of about 5 s^{-1}.

Nitrogenase can reduce substrates other than N_2, such as acetylene, azide or hydrogen cyanide. In the absence of other reducible substrates, the enzyme will reduce protons to dihydrogen (Bulen WA *et al.*, 1965; Jackson EK *et al.*, 1968). The other small triple-bonded substrates will be discussed later. Larger substrates, such as 2-butyne, are

not reduced efficiently, indicating that physical limitations on access to the enzyme's active site (McKenna CE *et al.*, 1976). CO is a potent inhibitor of all nitrogenase substrate reductions except that of the proton to H_2. In the presence of CO, the overall rate of electron transfer is not inhibited, but all electrons go to the production of H_2 (Hardy *et al.*, 1965).

C. The Fe protein of molybdenum nitrogenase

1. Structure

The Fe protein component of the Mo-nitrogenase complex is a γ_2 homodimer with a molecular mass of 64,000 kDa. The subunits are encoded by the *nifH* gene. It contains one [4Fe-4S] cluster that bridges between the two identical subunits. Each subunit consists of a large, single domain of an eight-stranded β-sheet flanked by nine α-helices (Figure 1.1). This architecture is characteristic of the P-loop containing nucleotide triphosphate hydrolases (Howard JB and Rees DC, 1996). The two subunits of the Fe protein are related by a molecular 2-fold rotation axis that passes through the [4Fe-4S] cluster, which is located at the subunit-subunit interface. Each subunit is approximately 40 Å in length along the 2-fold axis and approximately 35 Å by 45 Å in girth (Georgiadis MM *et al.*, 1992). The [4Fe-4S] cluster is symmetrically coordinated by the thiol groups of Cys97 and Cys132 from each subunit (Hausinger RP *et al.*, 1983, Georgiadis MM *et al.*, 1992). (*A. vinelandii* primary sequence numbering will be used unless otherwise noted.) Both cluster ligands are located near the amino terminal end of α-helices that are directed toward the cluster. Amide nitrogens from residues within these helices form hydrogen bonds to the cluster and cluster ligands may provide stabilizing electrostatic interactions to this center. In addition to those involving the cluster, there are numerous van der Waals and polar interactions in the interface beneath the cluster that help stabilize the dimer structure. The [4Fe-4S] cluster appears to be highly solvent exposed. It is a loosely packed redox center that could serve as either a pivot or a hinge for conformational rearrangements between the subunits (Howard JB and Rees DC, 1996). As stated above, the Fe protein displays structural similarity to other nucleotide-binding

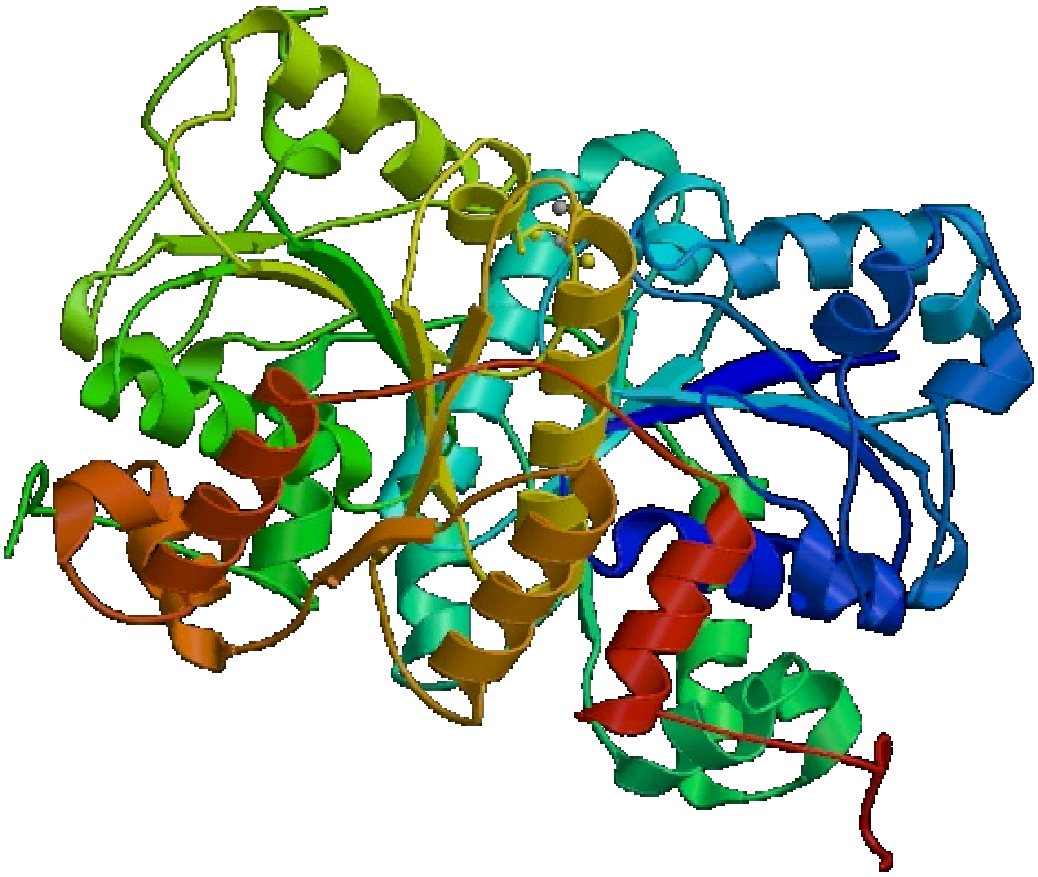

Figure 1.1 Ribbons diagram (with α-helices and β-sheets) of the Fe protein from *Azotobacter vinelandii* (Strop P *et al.*, 2001).

proteins, including signal transduction molecules, such as G-proteins and *Ras*, and energy transduction systems, such as myosin. They are all characterized by common core elements (Milner-White *et al.*, 1991; Sprang SR, 1997) consisting of: 1) predominantly parallel β-sheets flanked by α-helices; 2) a phosphate-binding loop, known as P-loop or a Walker A motif (Walker JE *et al.*, 1982), containing the G-X-X-X-G-K-S/T- consensus sequence (residues Gly9 to Ser16 in *A. vinelandii* Fe protein); and 3) two switch regions, Switch I and Switch II. These switch regions undergo conformational changes upon hydrolysis of the nucleotide triphosphate to the diphosphate, with consequent loss of the interaction with the terminal phosphate group. The Fe protein residues corresponding to Switch I and Switch II include residues 38 to 43 and 125 to 135, respectively. Switch I region includes the Asp39 residue, which interacts with the bound Mg^{2+} and may be involved in MgATP hydrolysis (Lanzilotta WN *et al.*, 1996). Amino acid residues in this region also connect to other residues in the region of residues 59-69, which interact with the MoFe protein (Jang SB *et al.*, 2000). Switch II region includes the conserved D-X-X-G sequence motif, known as the Walker B motif (corresponds to residues 125 to 128 in *A. vinelandii*), and the Cys132, which is the [4Fe-4S] cluster ligand.

2. Redox properties

Early work by electron paramagnetic resonance (EPR) and Mössbauer spectroscopies demonstrated that reduced Fe protein from *A. vinelandii* in the native state is heterogeneous. Approximately half of the molecules contain a $[4Fe\text{-}4S]^{1+}$ cluster with electronic spin S=1/2 and half contain a $[4Fe\text{-}4S]^{1+}$ cluster with spin S=3/2. The former yields the characteristic g = 1.94 EPR signal whereas the latter exhibits signals around g = 5. In the oxidized state, the protein exhibits Mössbauer spectra typical of diamagnetic $[4Fe\text{-}4S]^{2+}$ clusters (Lindahl PA *et al.*, 1985). Addition of MgATP results in a change both in the shape of the S=1/2 signal from rhombic to axial (Smith BE *et al.*, 1973) and in the proportion of the S=3/2 signal present (Lindahl PA *et al.*, 1987).

The reduced Fe protein can be reversibly oxidized from the 1^+ to the 2^+ state in four ways (Burgess BK and Lowe DJ, 1996). 1) By O_2, although the protein is ultimately inactivated by O_2, it is not because the $[4Fe\text{-}4S]^{2+}$ cluster is destroyed by O_2 but rather

because the protein is attacked by superoxide or some other reactive species (Thorneley RNF and Ashby GA, 1989). 2) By self-oxidation, as shown when the reduced Fe protein is incubated anaerobically and over time slowly self-oxidizes to the $[4Fe\text{-}4S]^{2+}$ state (Dao CJ-F, 1990; Watt GD and Reddy KRN, 1994). 3) By redox active dyes, such as thionine, methylene blue and indigodisulfonate (Anderson GL and Howard JB, 1984; Lindahl PA *et al.*, 1985). 4) Enzymatically by transfer of an electron to the MoFe protein when the Fe and MoFe proteins are combined with MgATP and a limiting amount of dithionite. As the dithionite is exhausted, the Fe protein EPR signal disappeared completely (Lindahl PA *et al.*, 1985). The conclusion of the experiment was that the Fe protein donates electrons to the MoFe protein and consequently loses its EPR signal as it is oxidized.

Until the mid-1990s, the Fe protein was regarded as a one-electron donor to the MoFe protein cycling between its 1^+ and 2^+ oxidation states during the turnover. However, it is now known that the protein can be reversibly reduced further to the $[4Fe\text{-}4S]^0$ state (Watt GD *et al.*, 1994; Angove HC *et al.*, 1997; Yoo SJ *et al.*, 1999). The redox potential for this reduction, at -460 mV, is within the physiological range and the reduction can be carried out by flavodoxin in the hydroquinone state as well as by the artificial electron donors, such as reduced methyl viologen and titanium(III) citrate. In combination with the MoFe protein, the $[4Fe\text{-}4S]^0$ cluster-containing Fe protein was able to support both H_2 and C_2H_4 production from C_2H_2 in nitrogenase turnover assays in the absence of added reductant. These data may imply that *in vivo*, the Fe protein may act as a two-electron donor to the MoFe protein (Watt GD *et al.*, 1994). The ATP utilization per electron pair transferred ($ATP/2e^-$) decreases from 4-5, typically observed with dithionite, to values near 2 (Angove HC *et al.*, 1997; Erickson JA *et al.*, 1999). This behavior was proposed to arise from operation of the $[4Fe\text{-}4S]^{2+}/[4Fe\text{-}4S]^0$ redox couple with transfer of two electrons to the MoFe protein accompanied by hydrolysis of only two ATP molecules. Because the $[4Fe\text{-}4S]^{1+}$ state of the Fe protein is clearly competent for substrate reduction as a one-electron donor and if the all-ferrous Fe protein functions mechanistically as a two-electron donor, this redundancy in reductant would be yet another unique property of nitrogenase (Rees DC and Howard JB, 2000).

3. Interactions with nucleotides

The binding of MgATP to the Fe protein induces global structural changes (Jang SB *et al.*, 2000; Chiu HJ *et al.*, 2001) that are manifested by alterations in the electronic properties of the [4Fe-4S] cluster (Chen L *et al.*, 1994). Such perturbations are readily detected by EPR, circular dichroism (CD), ^{1}H-nuclear magnetic resonance (NMR) and Mössbauer spectroscopies (Lindahl PA *et al.*, 1987; Meyer J *et al.*, 1988). The effect of metal chelating agents on the Fe protein provides additional information on cluster conformation (Walker GA and Mortenson LE, 1974). The MgATP-bound form of the Fe protein is considerably more susceptible to chelation of its cluster by compounds like α,α'-bipyridyl (Walker GA and Mortenson LE, 1974; Diets TL and Howard JB, 1989) than the nucleotide-free form. Such chelation assays (monitoring the formation of the Fe^{2+}-chelator complex at 520 nm) have been used to test the effect of substitutions on the Fe protein (see the later discussion in this section). The midpoint potential of the [4Fe-4S] cluster is lowered approximately 100mV when the Fe protein binds MgATP (Cordewener J *et al.*, 1983; Larsen C *et al.*, 1995).

Robson (Robson RL, 1984) was the first to recognize the Walker A nucleotide binding motif in the derived amino acid sequences of the Fe proteins. In the three dimensional structure of the Fe protein, these motifs are close to the inter-subunit interface, implying the existence of two nucleotide binding sites at the interface. Because the nucleotide-binding site is 15~20 Å from the [4Fe-4S] cluster and yet hydrolysis of MgATP is apparently associated with electron transfer from the cluster to the MoFe protein, nucleotide-induced changes in the electronic properties of the cluster cannot be the result of a direct interaction between MgATP and the cluster. A lack of direct interaction between the cluster and nucleotide is also indicated by spectroscopic comparison of the Fe protein in its nucleotide-free and nucleotide-bound states (Morgan TV *et al.*, 1990). Therefore, nucleotide-induced effects upon the [4Fe-4S] cluster must be communicated through the protein backbone by polypeptide conformational changes. Moreover, changes in the electronic properties of the cluster must result from the polypeptide environment rather than through structural rearrangement of the cluster (Lindahl PA *et al.*, 1987).

How is nucleotide binding communicated to the cluster? As noted before in discussion of the structure of Fe protein, two switch regions play important roles in the transduction pathway (Figure 1.2). The protein chain from Asp125 to Cys132, which are the residues in the switch II region, offers the shortest pathway from the nucleotide-binding site to the cluster. The Asp125 residue is known to be located in the nucleotide-binding site, probably functioning in the interaction with the Mg^{2+} associated with the nucleotide (Wolle D *et al.*, 1992). The Cys132 residue (one from each subunit) provides two of the four protein ligands to the [4Fe-4S] cluster. Studies of Fe proteins in which either Asp125 or Asp129 (Lanzilotta WN *et al.*, 1995) were changed to the amino acid Glu suggested a possible function of this protein domain in the nucleotide-induced conformational changes communicated to the [4Fe-4S] cluster. One of the most significant interactions between the P-loop and Switch II region is the salt bridge between Lys15 and Asp125. It is envisioned that MgATP binding triggers movement of switch II by breaking this salt bridge. Evidence supporting this model was provided by the characterization of altered Fe proteins substituted at either Lys15 (Ryle MJ *et al.*, 1995) or Asp125 (Wolle D. *et al.*, 1992a). Substitution by Gln at Lys15 position results in an altered Fe protein that remains able to bind MgATP, but this binding event is not communicated to the [4Fe-4S] cluster (Seefeldt LC *et al.*, 1992). Substitution by Glu at the Asp125 position results in an Fe protein that mimics certain properties of the MgATP bound form when it has MgADP, rather than MgATP, bound.

Deletion of amino acid Leu127 by site-directed mutagenesis in the protein chain between Asp125 and Cys132 results in a permanent protein conformational change resembling the MgATP-bound state in the absence of any bound nucleotides (Ryle MJ and Seefeldt LC, 1996a). Specifically, ^{1}H-NMR, EPR, and CD spectroscopic properties, along with Fe chelation assays, suggested that deletion of Leu127 (Δ127L) in the Fe protein results in changes in the electronic properties of the [4Fe-4S] cluster similar to those normally observed upon MgATP binding to the wild-type Fe protein. In addition, deletion of Leu127 of the Fe protein lowered the redox potential of the [4Fe-4S] cluster from -294mV for the wild type Fe protein to -412 mV, which is nearly identical to the lowering of the redox potential (by 120 mV) upon binding MgATP to the wild type Fe protein. The Δ127L Fe protein did not contain bound nucleotides that could have

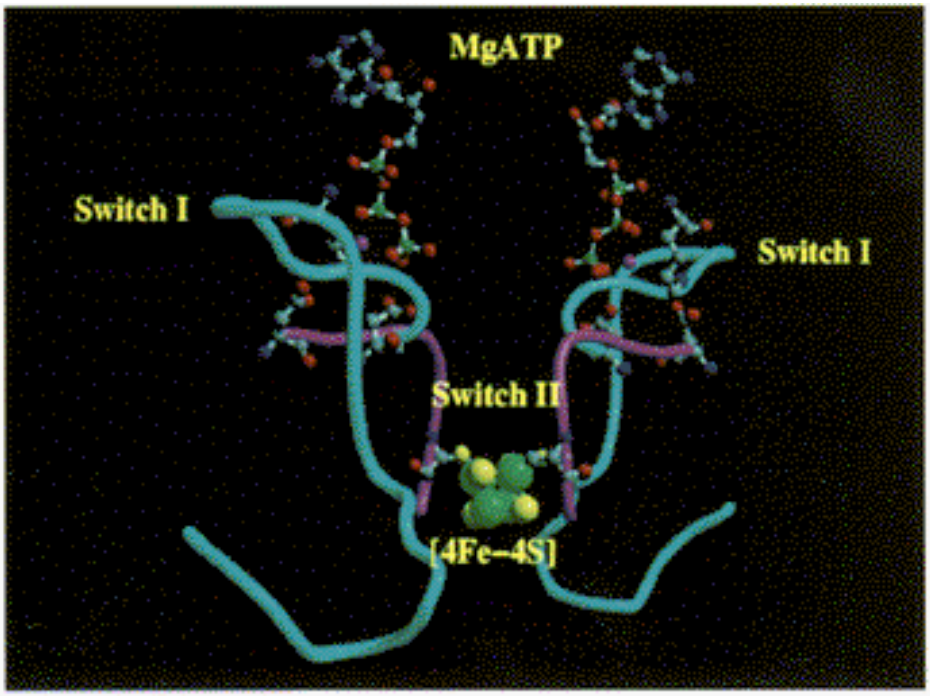

Figure 1.2 Ribbon diagram of the Fe protein, showing switch I, switch II, the [4Fe-4S] cluster, and the two bound MgATP molecules.

Switch I (cyan) and switch II (magenta) domains are highlighted to illustrate their spatial relationships to the [4Fe-4S] cluster and the MgATP binding sites (Seefeldt LC and Dean DR, 1997).

accounted for the observed conformational changes. These results thus support a model in which the protein chain from Asp125 to Cys132 acts as one pathway for MgATP signal transduction and suggest a mechanism for this transduction to the [4Fe-4S] cluster.

MgADP, which is the product of MgATP hydrolysis by nitrogenase, is also a potent physiological inhibitor of nitrogenase turnover. It appears to bind to the same sites as MgATP (Burgess BK, 1984). However, MgADP binds more tightly to the Fe protein than does MgATP and MgADP binds more tightly to oxidized $[4Fe\text{-}4S]^{2+}$ containing Fe protein than it does to the reduced $[4Fe\text{-}4S]^{1+}$ containing protein (Yates MG, 1992). By using the same spectroscopic techniques as were used for studies of the binding of MgATP, it was found that the conformational changes induced by the binding of MgADP are different from, and more mild than, those caused by MgATP (Chen L *et al.*, 1994). The cluster remains stable in the presence of metal chelation agents when MgADP is bound (Hausinger *et al.*, 1983, Anderson GL *et al.*, 1984) and the observed changes in the EPR spectrum with MgADP are less obvious than those observed for MgATP binding (Lindahl PA *et al.*, 1987).

D. The MoFe protein

1. Overall structure

The MoFe protein is an $\alpha_2\beta_2$ tetramer of Mr ~230 kDa, the α (~57 kDa) and β (~59 kDa) subunits being encoded by the *nifD* and *nifK* genes, respectively. The protein can be described as a dimer of $\alpha\beta$ dimers (Figure 1.3). It contains two unique metallosulfur clusters: the $MoFe_7S_9$·homocitrate cofactor (FeMo cofactor, also referred to the M center), and the Fe_8S_7 P cluster (or the P center). Neither of these two types of cluster has been observed elsewhere in biology nor have they been synthesized chemically. Each molecule of fully active MoFe protein contains two of each type of cluster. The total cluster content is equivalent to 2 Mo, 30 Fe and 32 S atoms per holoenzyme. The X-ray crystal structure of the MoFe protein component of the nitrogenase complex from *A. vinelandii* was initially determined at 2.7 Å resolution (Kim J and Rees DC, 1992 a,b), then at 2.2 Å resolution (Chan MK *et al.*, 1993), and most recently at 2.03 Å resolution (Peters JW *et al.*, 1997). Since then, the structure of the MoFe protein from *K. pneumoniae* has been determined at 1.6 Å resolution (Mayer SM *et al.*, 1999).

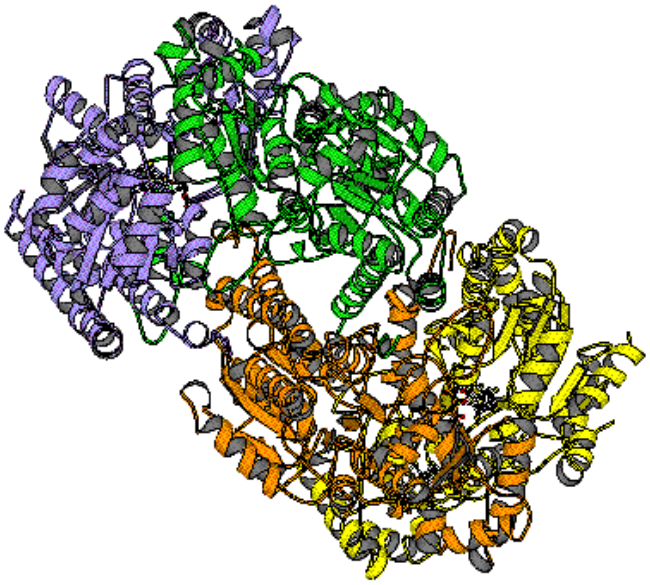

Figure 1.3a Ribbon representation of Mo-nitrogenase MoFe protein $\alpha_2ß_2$ tetramer structure.

Subunit color codes: α_1 = violet; $ß_1$ = green; α_2 = yellow; $ß_2$ = orange. From *Azotobacter vinelandii* (Peters JW *et al.*, 1997). All drawings were produced by using the program MOLSCRIPT (Kraulis PJ, 1991).

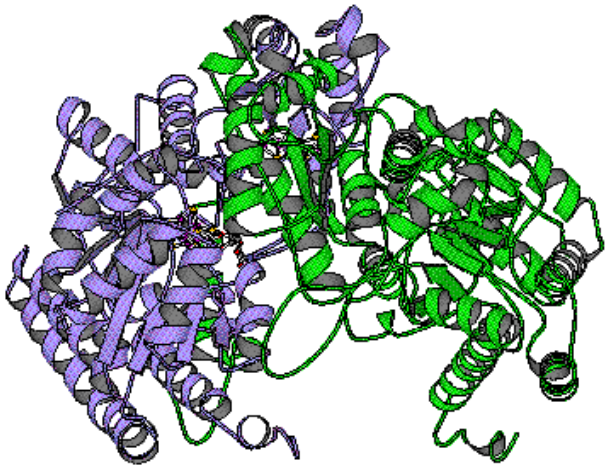

Figure 1.3b Ribbon representation of Mo-nitrogenase MoFe protein αß dimer structure (orientation as 1.3a).

Subunit color codes: α1= violet; ß1 = green.

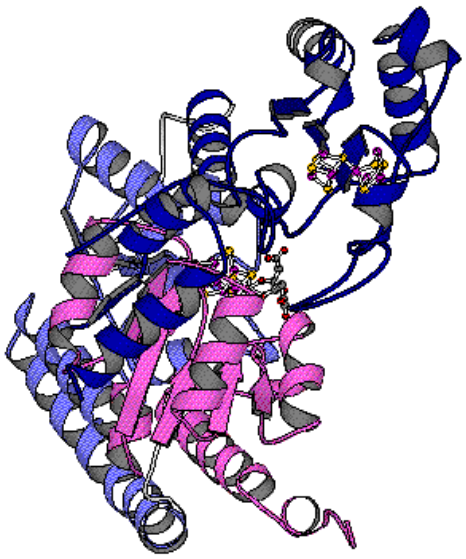

Figure 1.3c Ribbon representation of Mo-nitrogenase MoFe protein α-subunit structure (orientation as 1.3a).

Domain color codes: domain I = dark blue; domain II = light blue; domain III = magenta.

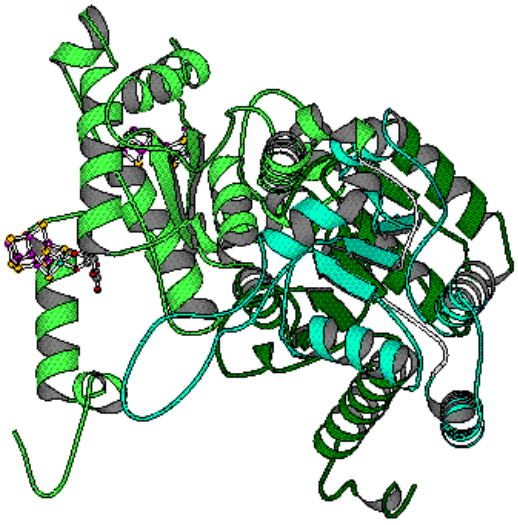

Figure 1.3d Ribbon representation of Mo-nitrogenase MoFe protein ß-subunit structure (orientation as 1.3a).

Domain color codes: domain I' = light green; domain II' = cyan; domain III' = dark green.

The α and β subunits of the MoFe protein exhibit similar polypeptide folds, which consist of three domains of the parallel β-sheet/α-helical type. At the interface between the three domains is a wide, shallow cleft. In the α subunit, the FeMo cofactor occupies the bottom of this cleft. The P-cluster is buried at the interface between a pair of α- and β-subunits with a pseudo-2-fold rotation axis passing between the two halves of the P-cluster and relating the two subunits. The extensive interaction between α and β subunits in an αβ dimer suggests they form the fundamental functional unit. An open channel of ~8 Å diameter exists between the two pairs of αβ dimers with the tetramer 2-fold axis extending through its center. The interface between the two αβ dimers is dominated by interactions between helices from the two β subunits, along with a cation-binding site, possibly for calcium, that aids in tetrameric stabilization (Howard JB *et al.*, 1996).

2. The FeMo cofactor

2.1 Structure

The iron-molybdenum (FeMo)-containing cluster (FeMo cofactor) can be extracted intact from acid-denatured protein into N-methylformamide (NMF) solution (Shah VK and Brill WJ, 1977) and has been extensively studied using a wide range of spectroscopic techniques both bound to the protein and in solution after extraction (Smith BE, 1999 and references therein). The extracted FeMo cofactor can be combined with the apo-MoFe protein, which is isolated from strains unable to synthesize the FeMo cofactor, to generate active MoFe protein.

The FeMo cofactor is essentially composed of two subclusters, $Mo_1Fe_3S_3$ and Fe_4S_3, which are bridged by 3 sulfides (S^{2-}) that link the opposing Fe atoms from each subcluster (Figure 1.4). The FeMo cofactor is buried ~10 Å beneath the protein surface, consistent with the results of spectroscopic studies (Oliver ME *et al.*, 1993), in an environment primarily provided by the α subunit. It is bound to the α subunit through residue Cys275, to a terminal tetrahedral iron atom, and through residue His442, to the molybdenum atom. The metal-metal distances within each 4Fe (or Fe_3Mo)-3S partial cubane are relatively typical, whereas pairs of trigonal iron atoms between the two

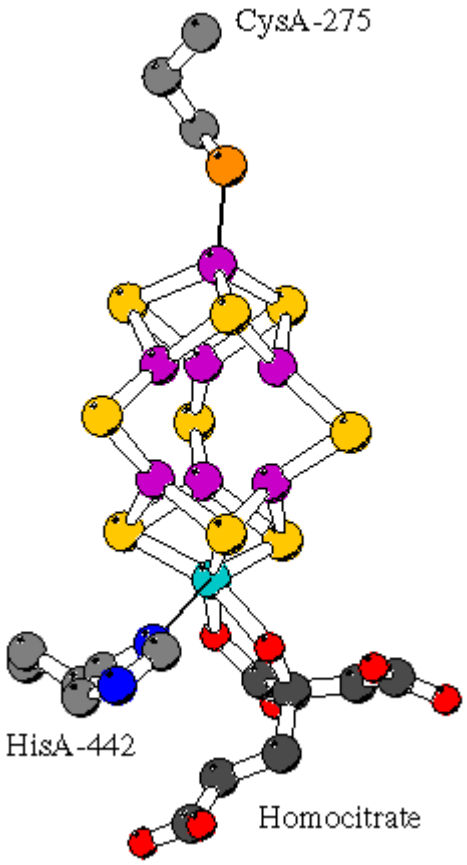

Figure 1.4 Ball and stick model of the *A. vinelandii* FeMo cofactor, homocitrate and direct ligands only (Peters JW *et al.*, 1997).

All drawings were produced by using the program MOLSCRIPT (Kraulis PJ, 1991).

(Note: A represents α.)

subclusters are separated by 2.5-2.6 Å and 3.6-3.7 Å, depending on the interactions. The distances from Mo to the Fe atoms of the other subcluster are ~5.0 Å, which is comparable to the distances from the tetrahedral Fe to the Fe atoms of the Mo-containing subcluster. The longest distance between the components in the cofactor is ~7.1 Å between the tetrahedral Fe and the Mo. Fe-Fe and Mo-Fe distances corresponding to these interactions are generally consistent with the results of EXAFS (Extended X-ray Absorbance Fine Structure) studies (Eidsnesss MK *et al.*, 1986; Conradson SD *et al.*, 1987). Overall, this structure has a central prismatic waist of six Fe atoms, each of which is ligated to three sulfides in a nearly trigonal planar geometry. These six Fe atoms are arranged such that three pairs of Fe atoms are shared at the intersection of three geometrically identical 4Fe-4S faces within the FeMo cofactor (Christiansen J *et al.*, 2000).

A unique feature of the FeMo cofactor is the coordinately unsaturated, and so potentially reactive, trigonal Fe atoms, which are unknown in model compounds. There may be some iron-iron bonding between the apparently trigonal Fe atoms in the center of FeMo cofactor (Smith BE, 1999). A further suggestion in an attempt to explain the existence of trigonal Fe atoms in FeMo cofactor was that they were ligated by hydride ions, which could be important during the nitrogenase turnover as a source of electrons/protons for reduction of N_2. However, ENDOR spectroscopic studies imply that this situation is unlikely (Howes BD *et al.*, 1994).

The octahedral coordination sphere of the Mo is completed by bidentate binding of the homocitrate. (R)-homocitrate is an integral component of the FeMo cofactor. It is coordinated to the Mo atom by its 2-hydroxyl and 2-carboxyl groups. It projects from the Mo atom of the FeMo cofactor toward the P-cluster. This Mo-homocitrate end of the FeMo cofactor is surrounded by many water molecules, which has led to the suggestion that homocitrate might be involved in proton donation to the active site during substrate reduction. In contrast, the Cys-ligated tetrahedral Fe end of the FeMo cofactor is virtually anhydrous (Howard JB and Rees DC, 1996).

2.2 Spectroscopy of the FeMo cofactor

The FeMo cofactor possesses a biologically unique EPR spectrum, which arises from a S=3/2 spin state and gives rise to EPR signals at g= 4.3, 3.7, 2.0 (Shah VK and Brill WJ, 1977). This spectrum is a useful spectroscopic fingerprint that is detectable in the dithionite-reduced state of whole cells, crude extracts, purified MoFe proteins, and the isolated FeMo cofactor (Newton WE and Dean DR, 1993). The S=3/2 signal has been used both in experiments to demonstrate the role of the FeMo cofactor as the active site of nitrogenase as well as for identifying amino acid residue in the proximal FeMo cofactor environment that are critical for nitrogenase action.

EPR spectroscopy and electrochemical titration experiments have been used to quantify the midpoint potentials of the redox centers of the MoFe protein. EPR and Mössbauer studies have shown that, when dithionite is used as the reducing source *in vitro*, the Fe protein transfers one electron at a time to the MoFe protein, and ultimately to the substrate, during catalysis (Orme-Johnson *et al.*, 1972). During this event, the EPR spectra of both the Fe and the MoFe proteins become bleached as the proteins become oxidized and reduced, respectively (Orme-Johnson *et al.*, 1972; Smith BE *et al.*, 1974).

Multiple variations of the S=3/2 signal have been observed for the MoFe protein from *K. pneumoniae* at either different pH values or during turnover (Lowe DJ *et al.*, 1978). In addition, EPR signals that are associated with the MoFe protein only in the presence of either CO (Cameron LM *et al.*, 1998) or C_2H_2 and C_2H_4 (Lowe DJ *et al.*, 1978) have been described. Electron-nuclear double resonance spectroscopy (ENDOR) under conditions of enzymatic turnover shows that one CO molecule is bound to the FeMo cofactor at a low CO pressure (pCO = 0.08 atm) but that two CO molecules are bound at high pressure (pCO = 0.5 atm) (Pollock RC *et al.*, 1995). Recently, ENDOR measurements from preparation using $^{13}C_2H_2$ reveal interactions with three distinct ^{13}C nuclei, indicating that at least two C_2H_2-derived species are bound to the FeMo cofactor of an altered MoFe protein with a Gln substitution at the αHis195 residue under turnover conditions (Lee H-I *et al.*, 2000).

Because numerous redox states that are likely involved in the reaction of nitrogenase are inaccessible by crystallography, rapid-mixing/rapid-freezing techniques, together with EPR spectroscopy, have been applied to explore any changes in the electronic

structure of the MoFe protein that occur during turnover. Such changes may indicate changes of either conformational state or protonation state of the FeMo cofactor itself (Fisher K *et al.*, 2001). Many other spectroscopic techniques, such as magnetic circular dichroism (MCD) (Johnson MK, 1988), ^{14}N electron spin echo envelope modulation (ESEEM) (Lee H-I *et al.*, 1998), have also yielded valuable data. Spectroscopy has played an important role in elucidating the structure and properties of the nitrogenase metal clusters.

2.3 The FeMo cofactor's polypeptide environment

The protein environment around the FeMo cofactor is primarily provided by hydrophilic residues, although there are some hydrophobic residues such as αVal70, αTyr229, αIle231, αLeu358 and αPhe381 (Howard JB and Rees DC, 1996). As shown in Figure 1.5, FeMo cofactor is tightly packed within the α subunit by residues that: (i) approach each of its three faces (αVal70, αArg359 and αPhe381); (ii) have the potential to hydrogen bond to the bridging sulfides (αArg96, αHis195, αGly356 and αGly367); and (iii) by αArg359, which has the potential to hydrogen bond to a S atom within the $MoFe_3S_3$ subcluster (Lee H-I *et al.*, 1998). Unusual for a buried center, the environment of the FeMo cofactor contains a number of neighboring charged groups. The environment surrounding the homocitrate is also relatively polar, with several potentially charged groups and water molecules within 8 Å. In addition, the terminal carboxyl groups of homocitrate forms hydrogen bonds to both the side chain of αGln191 and to the side chain of αGln440 (Howard JB and Rees DC, 1996).

It is believed that the FeMo cofactor is the site for substrate binding and reduction of nitrogenase. Evidence is provided by studies demonstrating that changes in either the FeMo cofactor itself or its environment directly affects substrate-reduction properties (Hawkes TR *et al.*, 1984). For example, certain mutant strains, which are incapable of synthesizing FeMo cofactor, produce a FeMo cofactor-deficient inactive and EPR silent MoFe protein (Shah VK *et al.*, 1977). Such inactive MoFe protein can be reconstituted by the addition of FeMo cofactor that has been extracted into NMF from native MoFe protein. The reconstituted MoFe protein regains not only its enzymatic activity but also the characteristic S = 3/2 EPR signal. If FeMo cofactor extracted from the *nifV*$^-$ mutant

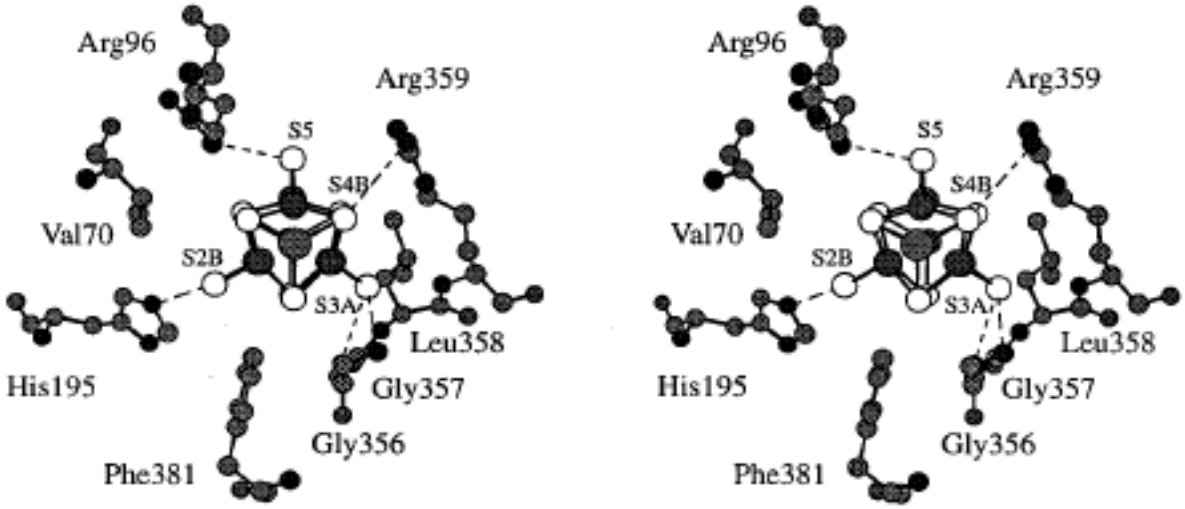

Figure 1.5 Stereoscopic views of the FeMo cofactor and the surrounding environment of the MoFe protein from *A. vinelandii* (Lee H-I *et al.*, 1998).

Dashed lines represent the possible hydrogen bonds revealed from the X-ray crystal structure. The figures are regenerated by using Chem 3D from the atomic coordinates obtained from Brookhaven Database.

is used for the reconstitution, the new MoFe protein exhibits the catalytic properties of the MoFe protein as isolated from the *nifV*$^-$ mutant strain (Hoover TR *et al.*, 1989). Altered MoFe proteins from mutant strains, each having a single substitution for a certain amino acid residue targeted as either providing or being located near FeMo cofactor-binding sites, simultaneously exhibit altered substrate reduction properties and changed EPR spectra (Scott DJ *et al.*, 1990).

2.4 Site-directed mutagenesis studies

Amino acid sequence conservation in a number of Mo-nitrogenases was used to target certain residues in the MoFe protein (Brigle KE *et al.*, 1985). These residues were suggested to be either bond directly to the FeMo cofactor or be close enough to the FeMo cofactor to influence its electronic environment and, thereby, modify substrate binding or reduction (Brigle KE *et al.*, 1987; Scott DJ *et al.*, 1992; Dilworth MJ *et al.*, 1998). For example, replacement of the αCys275 residue with alanine resulted in an altered MoFe protein (designated as $\alpha 275^{Ala}$) that exhibits native electrophoretic mobilities characteristic of the apo-MoFe protein (Kent HM *et al.*, 1990). The pool of available FeMo cofactor was also increased in extracts of this altered $\alpha 275^{Ala}$ MoFe protein (Kent HM *et al.*, 1989). Although such substitution studies are useful in the original assignment of potential FeMo cofactor ligands and are in agreement with the structural assignments, they are of little use in mechanistic studies because all substitutions placed at either the αCys275 or the αHis442 position tested so far lead to the complete loss of all MoFe protein activities. In contrast, the results for two other targeted α-subunit residues, αHis195 and αGln191, are different. Substitution of either of these residues was predicted to modify both the substrate/inhibitor binding and the spectroscopic properties of the resulting altered nitrogenases, but without loss of all activities. These suggestions proved to be true but the crystal structural data showed that neither of them is covalently linked to the FeMo cofactor. The αHis195 residue forms a putative hydrogen bond to one of the central bridging sulfides of the FeMo cofactor and αGln191 is hydrogen bonded to the carboxyl group terminating the shorter arm of the (R)-homocitrate entity (Figure 1.6).

Substitution of the αHis195 residue individually by a number of other amino acids (Asn, Tyr, Gln, Leu, Thr, or Gly) led to a variety of altered MoFe proteins (Kim C-H *et*

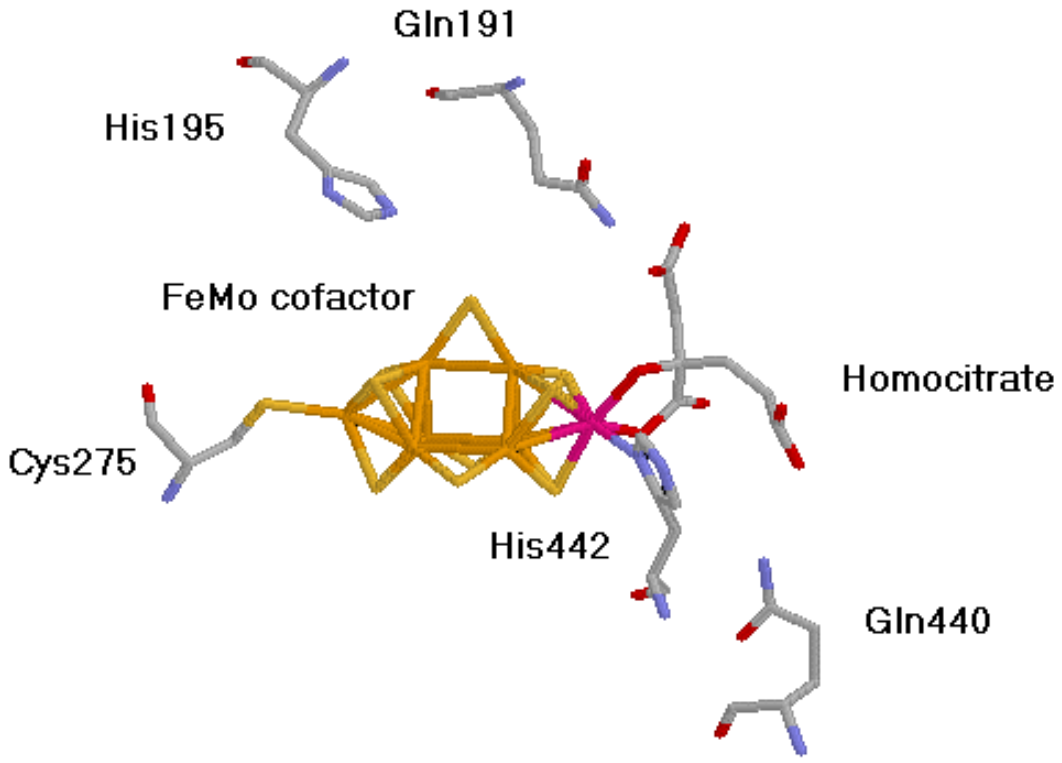

Figure 1.6 FeMo cofactor and selected residues in its immediate vicinity (Adapted from Peters JW *et al.*, 1997).

Fe and sulfide atoms are shown in yellow, Mo atom in purple, nitrogen in blue, oxygen in red, and carbon in gray.

al., 1995). None of these MoFe proteins, when complemented by the Fe protein, were able to reduce N_2 at appreciable rates, but they still catalyzed both proton reduction to H_2 and C_2H_2 reduction to C_2H_4 either alone or with some accompanying C_2H_6. The most active and interesting of these is the $\alpha 195^{Gln}$ MoFe protein. This altered MoFe protein reduces N_2 to NH_3 but at only 1~2% of the wild type rate (Dilworth MJ *et al.*, 1998). N_2 is, however, a potent inhibitor of both C_2H_2 and proton reduction and apparently inhibits substrate reduction by simple occupancy of a common active site. In doing so, it uncouples MgATP hydrolysis from substrate reduction without altering the overall rate of MgATP hydrolysis, suggesting that electron flow through nitrogenase may be controlled in part by the substrate serving as an effective electron sink (Kim C-H *et al.*, 1995). The inhibition constant (K_i) for CO inhibition of C_2H_2 reduction indicated that the $\alpha 195^{Gln}$ MoFe protein was 8-fold more sensitive to CO than wild type MoFe protein.

This $\alpha 195^{Gln}$ MoFe protein also functions very differently with respect to both azide and cyanide reduction compared to the wild type. Azide is a poor substrate for this altered MoFe protein and, with a NaCN solution, this altered MoFe protein recognizes and effectively reduces HCN but does not recognize CN^- and so suffers no flux inhibition. In contrast, CN^- acts as a potent inhibitor of electron flux to substrate with the wild type MoFe protein (Dilworth MJ *et al.*, 1998).

Another altered MoFe protein with asparagine at the $\alpha 195$ position was also characterized and compared to the wild type MoFe protein (Fisher K *et al.*, 2000 a,b). The data obtained have been interpreted as indicating that HCN, C_2H_2 and CO, but not N_2 and azide, either do not bind in the vicinity of the αHis195 residue or do not depend on this residue for effective binding, protonation, and/or reduction. Furthermore, it was suggested that the αHis195 residue is involved in proton transfer during substrate reduction. The last suggestion points to the different pK_a of an imidazole N-H compared to that of an amide N-H which could contribute to the different reactivity toward N_2 (Fisher K *et al.*, 2000a).

ESEEM spectroscopy on whole cells showed that the modulation arising from nitrogen coupled to the S=3/2 spin system of the FeMo cofactor was sensitive to changes in FeMo cofactor's polypeptide environment. The strain harboring the $\alpha 195^{Asn}$ MoFe protein did not exhibit this N-modulation and was also Nif^-, which led to the initial

suggestion that N coordination of the FeMo cofactor is essential for biological N_2 fixation (Thomann H *et al.*, 1991). In contrast, substitution to glutamine results in an altered MoFe protein that retains the wild type N1 ESEEM signature (Lee H-I *et al.*, 1998). On the basis of these data, it was concluded that the αHis195 residue does not contribute to the ESEEM signature, but rather, substitution at this position appears to perturb in the FeMo cofactor's polypeptide environment such that another N donor is displaced. The authors also suggested that the side chain of the αArg359 residue is the source of the deep ESEEM N1 modulation.

Although the αGln191 residue is situated only one turn of a helix away, the phenotypes of mutant strains substituted at this position are very different from those of the α-195 mutants. Five of the thirteen mutant strains constructed were able to grow diazotrophically, whereas the others were non-N_2-fixers. Unlike the altered α-195 MoFe proteins, when complemented with wild type Fe protein, most of these α191-substituted MoFe proteins exhibited H_2 evolution sensitive to varying extents to the presence of CO. For all the αGln191-substituted Mo-nitrogenases, C_2H_2 is a relatively poor substrate. Even so, both the $\alpha 191^{Lys}$ and $\alpha 191^{Glu}$ MoFe proteins produce small amounts of C_2H_6 as a product of C_2H_2 reduction (Scott DJ *et al.*, 1990, 1992). Using C_2D_2, a correlation was suggested to exist between the stereo-specificity of proton addition to give the products, *cis*- and *trans*- $C_2D_2H_2$, and the propensity of the nitrogenase to produce C_2H_6 (Fisher K *et al.*, 2000c). Also, it was indicated that the affinity for C_2H_2 is the major factor in producing C_2H_6 from C_2H_2. C_2H_6 production is achieved through a delicate balance between having an affinity for C_2H_2 that is high enough to have reasonable binding but not so high that it effectively displaces any bound intermediates. By comparing the altered α-191 and α-195 MoFe proteins with wild type MoFe protein and among themselves, it appears that the residue occupying the α-191 position will have a critical impact on the binding, protonation and/or reduction of all nitrogenase substrates, whereas the residue at the α-195 position will play a less important, but still mechanistically insightful role (Fisher K *et al.*, 2000b).

Another interesting substitution results from the histidine substitution for arginine at position α-277 (Shen J *et al.*, 1997). This residue was targeted for substitution due to its

proximity to the FeMo cofactor-binding ligand αCys275 residue and its potential role in a proposed pathway for the entry/exit of substrates/products. This same channel might also serve during the FeMo cofactor insertion (Kim J *et al.*, 1992b). This latter proposition was based on the crystal structure that noted a potential channel in the FeMo cofactor vicinity was formed by residues αArg277, αSer192 and αGly356. The EPR spectrum of the altered $\alpha 277^{His}$ MoFe protein in the resting state exhibits two sets of signals. One accounts for 80% of the overall intensity with g values close to the wild type signal; the other one accounts for 20% of the intensity with g = 4.52 and 3.48. The EPR signals may result from either two different orientations of the FeMo cofactor or two different turnover intermediate states of the FeMo cofactor. Furthermore, this altered MoFe protein cannot bind and reduce N_2 even though it has a comparable H^+ and C_2H_2 reduction rate to the wild type MoFe protein. When reducing C_2H_2 under an atmosphere containing a non-saturating concentration of CO, the $\alpha 277^{His}$ MoFe protein responded with sigmoidal kinetics, whereas with wild type MoFe protein, a typical hyperbolic response is observed. Thus, CO-binding induces cooperativity between at least two C_2H_4-evolving sites on the FeMo cofactor of the $\alpha 277^{His}$ MoFe protein.

A different strategy was developed for targeting residues in polypeptide environment of FeMo cofactor (Christiansen J *et al.*, 2000). Isolation of a mutant strain of *A. vinelandii* that exhibited *in vivo* N_2-fixing activity resistant to acetylene led to the construction of an altered MoFe protein with a serine substitution at the αGly69 position. The altered $\alpha 69^{Ser}$ MoFe protein had a K_m of about 0.14 ± 0.01 atm for C_2H_2, which is about 20-times higher than that of the wild type, but it could reduce N_2 with kinetic parameters almost identical to those observed for wild type MoFe protein. These data were interpreted to mean that, in the $\alpha 69^{Ser}$ MoFe protein, the elimination of a high affinity C_2H_2-binding site resulted in the observation of a second, but low affinity, C_2H_2-binding site to which C_2H_2 and N_2 were able to bind competitively. The 4Fe-4S face of the FeMo cofactor capped by the αVal70 residue was proposed to be the most likely region within FeMo cofactor to which C_2H_2 binds with high affinity (Christiansen J *et al.*, 2000). This hypothesis is supported by recent work (Mayer SM *et al.*, 2002) which shows that substitution of the αVal70 residue by Ala relaxes constraints within the substrate-

binding pocket so that effective reduction of the short chain alkynes, propargyl alcohol and propyne, which are not effectively reduced by the wild type enzyme, is now permitted.

In addition to these three residues, the positively charged αArg96 and αArg359 residues are also packed around the central bridging region of the FeMo cofactor (Howard JB and Rees DC, 1996). These residues could provide an electrostatic mechanism for stabilizing negatively-charged intermediates generated during substrate reduction (Lee H-I *et al.*, 1998). One recent study suggests that the side chain of the αArg96 residue could act as a gatekeeper, moving during turnover in order to permit accessibility of C_2H_2 or cyanide to the 4Fe-4S face of the FeMo cofactor capped by αVal70 (Benton PMC *et al.*, 2001).

All of the work described above supports the suggestion that the polypeptide environment of the FeMo cofactor plays an important role in the interactions between the FeMo cofactor and substrates and inhibitors (Newton WE and Dean DR, 1993). Because different substrates and inhibitors probably bind to different sites on the FeMo cofactor, substitutions, by impacting different part of the FeMo cofactor, alter the FeMo cofactor's interactions with different substrates and inhibitors. The altered MoFe proteins with substitutions in the FeMo cofactor's polypeptide environment offer a good opportunity to gain insights into the nitrogenase mechanisms.

3. The P cluster

3.1 Structure

As noted previously, the P cluster, which may function in electron transfer between the [4Fe-4S] cluster of the Fe protein and the FeMo cofactor, is bonded at the interface of the α and β subunits by cysteine ligands. It is located about 10 Å below the protein surface and on the 2-fold axis that approximately relates the α and β subunits. In striking contrast to the more polar FeMo cofactor pocket, the protein environment around the P cluster is mainly provided by hydrophobic residues.

There has been some controversy about the composition and structure of the P cluster, specifically concerning the number and bonding arrangements of the sulfur atoms

in this cluster. Generally, it was agreed that the P cluster contained eight Fe atoms. Models of the P cluster with either eight or seven S atoms have been proposed from X-ray diffraction data from *A. vinelandii* MoFe protein crystals. In the 8Fe-8S model, the P cluster has been described as a pair of 4Fe-4S cubanes bridged by a disulfide bond formed between sulfur atoms, one from each cubane cluster (Chan MK *et al.*, 1993). Two versions of 8Fe-7S P cluster have been described that can be formally derived from the 8Fe-8S model by removal of one of the sulfur atoms in the disulfide bond (Bolin JT *et al.*, 1993; Chan MK *et al.*, 1993). The differences among these models may reflect, at least in part, different redox states of the P cluster (Rees DC, 1993). Finally, in 1997, the structure of the MoFe protein from *A. vinelandii* was refined to 2.0 Å resolution in two redox states (Peters JW *et al.*, 1997, Figure 1.8 a,b). EPR studies on the crystals indicated that the structures correspond to the spectroscopically assigned oxidized (P^{ox}/M^{ox}) and the native or dithionite-reduced (P^{N}/M^{N}) forms of the enzyme (P refers to the P cluster and M refers to the FeMo cofactor). The 1.6 Å resolution X-ray crystal structure of *K. pneumoniae* MoFe-protein confirms these two redox states of the enzyme (Mayer SM *et al.*, 1999).

The P cluster is covalently coordinated to the MoFe protein through six cysteinyl ligands, three from the α subunit and three from the β subunit. The αCys62 and αCys154 residues terminally coordinate two Fe atoms in one cubane, whereas the αCys88 residue provides a bridging thiolate ligand. In an analogous manner, the βCys70 and βCys153 residues terminally coordinate two Fe atoms in the other cubane, whereas the βCys95 residue serves as a bridging ligand (Figure 1.7 a,b).

The P cluster in either oxidized or reduced state is an 8Fe-7S cluster. In the reduced state, the P cluster may be described as one containing bridged 4Fe-4S and 4Fe-3S subclusters that are bound to the α- and β-subunit, respectively. Upon reduction of the P^{OX} state to the P^{N} state, movement of two Fe atoms of the 4Fe-3S subcluster at the β-subunit end is accompanied by an exchange of covalent ligand, whereas the 4Fe-4S subcluster at the α-subunit end is not affected. In the oxidized state, two additional protein ligands are present (Peters JW *et al.*, 1997). The αCys88 residue coordinates the same Fe atom with its backbone amide nitrogen ligand in addition to its thiolate group, moreover, the Oγ of βSer188 coordinates a second Fe atom, which is also ligated by the

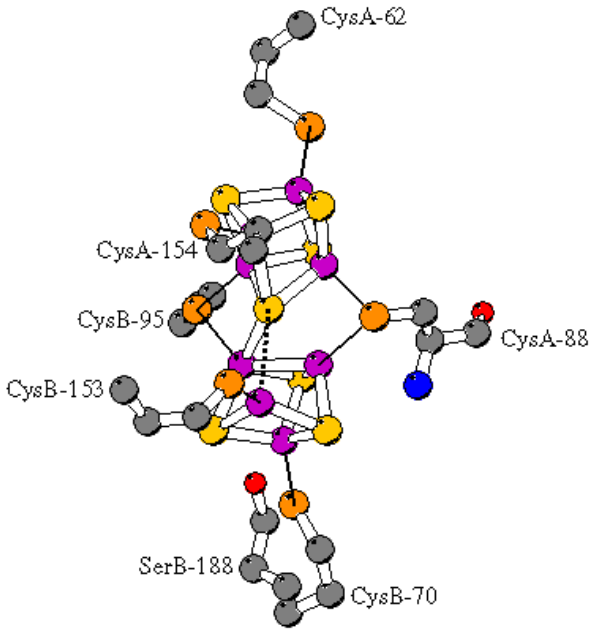

Figure 1.7a P cluster: the reduced (or P^N) state and its nearby amino acid residues (Peters JW *et al.*, 1997).

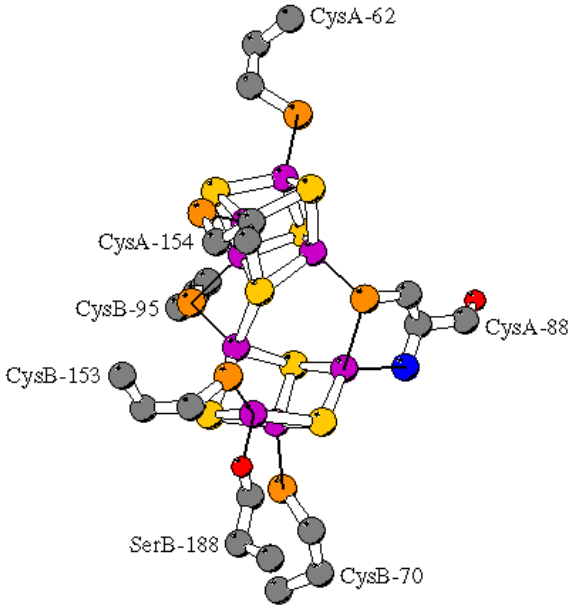

Figure 1.7b P cluster: the oxidized (or P^{OX}) state and its nearby amino acid residues. Sulfide atoms are shown in orange, Fe atoms in yellow, oxygen atoms in red and nitrogen atoms in blue.

thiolate group of the βCys153 residue. In the reduced state, these two non-cysteinyl ligands are replaced by interactions with the central sulfur atom. Hence, in both P^N and P^{ox}, all Fe atoms in the P cluster remain four-coordinated, although details of the coordination environments of some of the Fe atoms change with redox state (Peters JW *et al.*, 1997).

The structural differences between P^{OX} and P^N reflect movement of two Fe atoms by 1.4 Å and 0.9 Å, respectively, towards the central sulfide atom upon reduction. This net movement agrees with previous EXAFS data that indicate a contraction of Fe-Fe distances of the P clusters upon reduction (Christiansen J *et al.*, 1995). As mentioned above, oxidation of the P cluster is accompanied by the coordination of βSer188 and the amide nitrogen of αCys88 to the cluster Fe atoms. Because both of these ligands will be protonated in their free states and deprotonated in their bound states, it raises the intriguing possibility that the two-electron oxidation of the P cluster simultaneously releases two protons. Transfer of electrons and protons to the FeMo cofactor active site needs to be synchronized, and the crystal structures of the P cluster in the two redox states suggest that the coupling of proton and electron transfer may occur at the P cluster (Peters JW *et al.*, 1997; Lanzilotta WN *et al.*, 1998).

3.2 Redox and spectroscopic properties of the P cluster

In the presence of dithionite, the P clusters are EPR silent within the MoFe protein and there is a wealth of evidence (Smith BE *et al.*, 1992) using a variety of techniques that indicates the Fe atoms in these clusters are all reduced to the Fe^{2+} state. During the oxidation of the isolated MoFe protein, the P clusters are the first to be oxidized at about –340 mV. This redox potential was first measured using Mössbauer spectroscopy and exhibited a Nernst curve consistent with a two-electron oxidation process per P cluster to generate P^{2+} (Smith BE *et al.*, 1980). Initially, no EPR signal was observed from this oxidized form. Later, a weak signal near g=12 was detected (Lindahl PA *et al.*, 1988) and was finally confirmed, using parallel mode EPR spectroscopy (Surerus KK *et al.*, 1992), as arising from an integer spin system (S=3 or 4). Careful redox titration experiments allow the observation of two half-integer spin signals before the development of the g=12 signal (Surerus KR *et al.*, 1992; Pierik AJ *et al.*, 1993). The two signals arise from S=1/2

and S=5/2 spin systems with redox potentials very close to each other. It is proposed that they are from the one-electron oxidized P cluster and, as shown in the crystal structure, may be related to the breaking of two Fe-S bonds. Breaking one of these bonds would give rise to the S=1/2 state and breaking the other would give rise to the S=5/2 state (Pierik AJ *et al.*, 1993). Yet further oxidation after the P^{2+} state (g=12 signal) removes at least one more electron from each P cluster with an E_m (midpoint redox potential) of about +90 mV, and results in EPR signals from mixed spin states of S=1/2 and S=7/2 (Hagen WR *et al.* 1987; Peirik AJ *et al.*, 1993). Additional oxidation of the P cluster to the $P^{SUPEROX}$ state results in irreversible damage to the cluster.

3.3 Substitutions of the P cluster ligands and its nearby residues

Several altered MoFe proteins with substitutions for the cysteinyl ligands around the P cluster have been prepared by mutagenesis. Unlike the situation with the FeMo cofactor, some of the direct P cluster ligands may be substituted without complete loss of activity. For example, the βCys153 residue can be either substituted by serine or deleted and the resulting strains retain about 50% of the wild type diazotrophic growth rates and crude extract C_2H_2-reduction activity, and 100% of the S = 3/2 EPR signal intensity (May HD *et al.*, 1991). Substitution to alanine at this position leads to < 2% of the wild type activity (Kent HM *et al.*, 1989).

The $\beta153^{Ser}$ MoFe protein was purified and further tested for substrate-reduction patterns for comparison to wild type MoFe protein (May HD *et al.*, 1991). This altered protein was indistinguishable from the wild type with the notable exception of its response to an electron flux titration. The $\beta153^{Ser}$ and wild type MoFe proteins exhibit the same specific activity up to a 1:1 Fe protein to MoFe protein molar ratio but beyond that the $\beta153^{Ser}$ MoFe protein's activity slows dramatically relative to the wild type, e.g., its V_{max} is half of that of the wild type. The interpretation is that the intra-molecular delivery of electrons within the $\beta153^{Ser}$ MoFe protein has been slowed. Therefore, the P cluster probably functions in intra-molecular delivery of electrons to the FeMo cofactor. Note that βCys153 residue ligates the same Fe atom as the βSer188 residue, the residual activity of those βCys153 substituted MoFe proteins may be rationalized by assuming that the βSer188 residue alone can support some function of the P cluster.

Certain substitutions can also be tolerated for the αCys88 residues (Kent HM *et al.*, 1990; Dean DR *et al.*, 1990). Replacement of αCys88 residue in *A. vinelandii* by Ser, Thr, Asp or Gly resulted in the formation of partially active nitrogenase. It seems that the –OH group can act as a ligand in place of –SH. Removal of the side chain entirely (with a Gly substitution) appears to still allow normal polypeptide folding and assembly, but a methyl group (with Ala substitution) or larger side chain (with Val or Arg substitution) do not (Dean DR *et al.*, 1990). Interestingly, when both αCys88 and βCys95 residues are replaced by alanine, some activity is recovered. Although the proteins containing only one remaining bridging cysteine are inactive, the double mutant with both bridging cysteines substituted by alanine retains some activity (Kent HM *et al.*, 1990).

4. Relationship between the MoFe protein clusters

The protein environment between the FeMo cofactor and the P cluster may be important for electron transfer between the two clusters (Figure 1.8). The edge to edge distance from FeMo cofactor to the P cluster is about 14 Å (Kim J and Rees DC, 1992b). Hydrogen-bonded networks involving the NH of αGly61 (adjacent to the P cluster ligand αCys62), αGln191, and the homocitrate, as well as water molecules (not shown in this figure), can be identified that link these two metal centers. In addition, four helices have been recognized in the crystal structure that could participate in electron transfer between the two metal clusters (Kim J and Rees DC, 1992b). They are the helices from α63 to α74, from α88 to α92, from α191 to α209, and from β93 to β106, all of which are oriented in parallel between the two metal centers (only two of them are shown in Figure 1.8).

The βTyr98 residue is located on the helix including β93 to β106. It also approaches the terminal carboxyl of the homocitrate moiety of the FeMo cofactor and may indirectly interact with it by hydrogen bonding through water. A His for Tyr substitution, $\beta 98^{His}$, yielded an altered MoFe protein that had wild type MoFe protein metallocluster structure and electronic properties as determined by EPR and MCD (Peters JW *et al.*, 1995a). The altered $\beta 98^{His}$ MoFe protein had decreased substrate-reduction rates. In particular, it suffered inhibition of electron flux under a 10% C_2H_2 atmosphere compared to either a

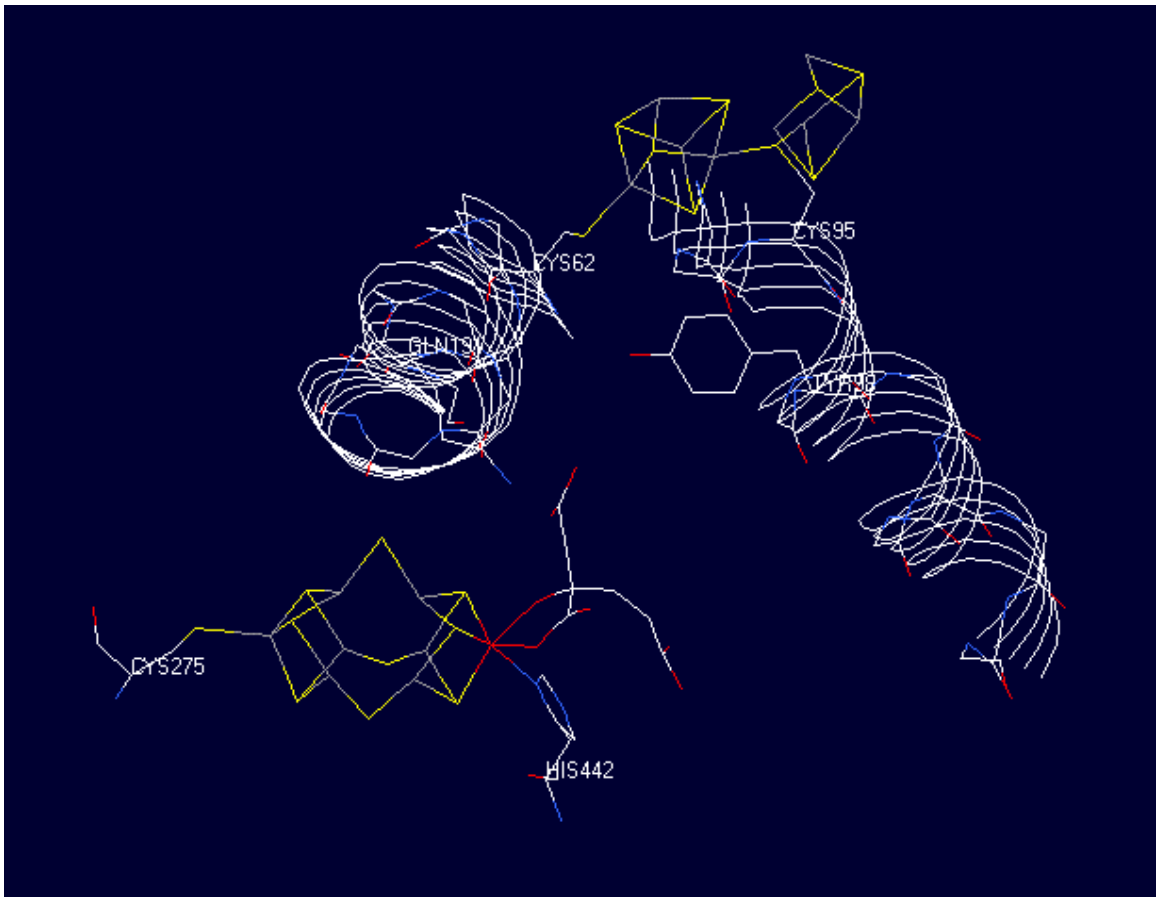

Figure 1.8 Protein environment between the FeMo cofactor and the P cluster of the MoFe protein from *A. vinelandii* (Adapt from Peters JW *et al.*, 1997).

Two helices, which include the αGln191 and βTyr98 residues, respectively, are shown in the figure.

100% N_2 or a 100% argon atmosphere. The inhibition of the electron flux under 10% C_2H_2 was partially relieved by CO, bringing it close to the same level observed under either 100% N_2 or 100% argon, and ATP hydrolysis was more coupled to substrate reduction in the presence of CO. It was suggested that the different substrates may be served by different or multiple electron-transfer pathways (Peters JW *et al.*, 1995a).

Whether or not this altered $\beta 98^{His}$ MoFe protein can transfer an electron from the P cluster to the FeMo cofactor was then investigated by stopped-flow spectrophotometry (Peters JW *et al.*, 1995a). Initially, the $\beta 98^{His}$ MoFe protein displayed a wild type dissociation rate of 6.0 sec^{-1} for the first 300 msec, then the rate dropped more than 2 fold to 2.5 sec^{-1}. The number of electrons delivered to the MoFe protein prior to the observed lowering in turnover rate was calculated as 2.4 electrons. This low dissociation rate was explained as a consequence of disturbing the intra-molecular electron transfer pathway. The capacity for the P cluster to accept electrons became saturated after about two rounds of component protein interaction and intermolecular electron transfer because the route of transferring the electrons to FeMo cofactor had been compromised. The uncoupling of ATP hydrolysis from electron transfer occurred because electron transfer from the Fe protein was inhibited but ATP hydrolysis continued as the two proteins dissociated.

E. Complex formation

The complex between the MoFe protein and Fe protein plays a central and critical role in the mechanism of nitrogenase, for it is in the complex that ATP hydrolysis is coupled to electron transfer between the two proteins (Imam J and Eady RR, 1980; Thorneley RNF *et al.*, 1991). Different approaches have been used to try to determine the factors that are important for complex formation and to locate the docking sites on both the Fe and MoFe proteins.

1. Chemical cross-linking

One approach to study complex formation was to use the chemical cross-linking reagent, 1-ethyl-3-[3-(dimethylamino)propyl]carbodiimide (Willing A *et al.*, 1989), which forms a link between residue Glu112 of the Fe protein and βLys400 of the MoFe protein (Willing A and Howard JB, 1990). Comparisons of the primary sequence of

nitrogenases from various bacterial species, however, identified these two residues as being variable. The Glu112 residue is part of a highly conserved patch, but itself is not conserved. The βLys400 is neither conserved nor located in a conserved region. The cross-linking reaction was found to be sensitive to high salt concentrations, which led to the prediction that ionic interactions between the two proteins may be the major force for both complex formation and cross-linking. This suggestion is supported by the observation that sodium chloride inhibits the rate of H^+, C_2H_2 and N_2 (Deits TL and Howard JB, 1990).

2. Site-directed mutagenesis affecting protein-protein interaction

A different approach used amino-acid substitution at the putative protein-protein docking surface. The surface of the Fe protein that interacts with the MoFe protein and some of the residues integral to protein-protein docking were identified before the X-ray crystal structure of the complex was determined. The Fe protein structural model reveals a crown of positively charged residues, Arg100, Arg140 and Lys143, located within the proposed docking surface that surrounds the Fe protein's [4Fe-4S] cluster. One of these residues, 100Arg, corresponds to the reversible ADP-ribosylation site involved in the regulation of Fe protein activity in *Rhodospirillum rubrum* (Pope MR *et al.*, 1985). ADP-ribosylation exerts its regulatory effect by preventing complex formation and subsequent intermolecular electron transfer. Altered Fe proteins in which His replaces Arg100 (Wolle D *et al.*, 1992b) or Gln replaces Arg140 or Gln replaces Lys143 (Seefeldt LC, 1994) all share similar biochemical phenotypes. They have decreased substrate reduction rates, which are also more sensitive to both high concentrations of MoFe protein and increasing salt concentrations. They also show various degrees of uncoupling of MgATP hydrolysis from substrate reduction. These changes indicate that the residues normally provide dominant ionic interactions with the MoFe protein during complex formation. However, the functional role of these residues cannot be assigned simply to ionic interactions because certain substitutions, such as when Arg100 is replaced by Tyr, only modestly affects catalytic activity and MgATP hydrolysis remains effectively coupled to electron transfer.

Another observation that gave clues to the docking site come from the knowledge that a heterologous mixture of the Fe protein from *Clostridium pasteurianum* (designated as Cp2) and the MoFe protein from *Azotobacter vinelandii* (designated as Av1) forms a very tight, catalytically inactive complex (Emerich DW *et al.*, 1978). Two studies have examined portions of the Fe protein that might be involved in the tight binding. In one case, the tight complex was found unlikely to be due to residues in the carboxyl terminus of the Fe protein (Jacobson MR *et al.*, 1990). The second case showed that the surface residues in a loop region (resides 59-67) of the Fe protein were critical for docking (Peters JW *et al.*, 1994).

In one docking model for the interactions between the Fe and MoFe proteins (Howard JB and Rees DC, 1994), the shortest distances from the [4Fe-4S] cluster of the Fe protein to the P cluster, from the P cluster to the FeMo cofactor, and from the [4Fe-4S] cluster to the FeMo cofactor are 18 Å, 14 Å and 32 Å, respectively (Howard JB and Rees DC, 1996). Hence, this model is suggestive of the following general sequence of electron transfer steps within the nitrogenase:

[4Fe-4S] → P cluster → FeMo cofactor → substrate

In this docking model, it is proposed that the MoFe protein undergoes conformational changes when it interacts with the Fe protein such that its cluster becomes more accessible to the Fe protein's cluster (Howard JB and Rees DC, 1994). Which MoFe protein residues might be involved in this change? A group of charged, possibly complementary residues on the surface of the MoFe protein from *A. vinelandii* was targeted. The αAsp161, αAsp162, βAsp160 and βAsp161 are all strictly conserved in the MoFe protein primary sequences of at least five nitrogen fixers (Dean DR and Jacobson MR, 1992). The side chains of αAsp162 and βAsp161 are solvent exposed and appear to be appropriately positioned to interact with one of the positively-charged residues that form the crown surrounding the Fe protein's [4Fe-4S] cluster. Thus, ionic interactions could be involved in complex formation and could coordinate the transmission of signals down short helices connecting αAsp161/αAsp162 and βAsp161/βAsp160 to the P cluster ligands, αCys154 and βCys153, respectively (Peters JW *et al.*, 1995b). Substitution of Asn at either αAsp162 or βAsp161 has minimal effect on nitrogenase activity (Kim C-H *et al.*, 1993). This lack of effect is also true for a double substitution of Asn at both

αAsp162 and βAsp161. Substitution of Asn for αAsp161 leads to a phenotype nearly identical to that of an Arg100-substituted Fe protein. This last result indicated that the αAsp161 residue is involved in protein-protein interaction, even though it is not at the protein surface.

3. Is MgATP-binding involved in complex formation?

Only the Fe protein-MoFe protein complex catalyzes MgATP hydrolysis at significant rates. This observation suggests that key residues in the Fe protein, which are necessary for the hydrolysis reaction, are not properly positioned until the MoFe protein binds. Given the distance between the nucleotide-binding site and the MoFe protein-binding surface, it is reasonable to say that protein conformational changes mediate the communication between the two regions, probably involving the two switch motifs mentioned earlier. In another words, the conformational changes are a prerequisite for the correct docking of Fe protein to the MoFe protein and, thus, for all the subsequent nitrogenase reactions, including MgATP hydrolysis, electron transfer and substrate reduction (Burgess BK and Lowe DJ, 1996; Seefeldt LC and Dean DR, 1997).

Examples of experiments used to test this theory include characterization of altered Fe proteins either with the Lys15 residue substituted by Gln (Seefeldt LC *et al.*, 1992) or with the Ala157 residue substituted by Ser (Gavini N and Burgess BK, 1992). Both of the resulting altered Fe proteins bind MgATP but do not undergo the MgATP-induced conformational changes. Although both of these altered Fe proteins appear to form normal chemical cross-linking complexes with the MoFe protein, neither of them is able to compete with the wild type Fe protein in an activity assay. Another mutant strain harboring the Gly157 altered Fe protein is able to grow under nitrogen-fixing conditions at 55% of the wild type rate (Bursey EH and Burgess BK, 1998). Purified Gly157 Fe protein only supports 20% of the substrate reduction rate of wild type Fe protein. EPR and CD spectroscopies and enzymatic activity data indicate that this altered Fe protein can adopt the conformational changes upon the binding of MgATP. However, kinetic data show that this Fe protein undergoes the change more slowly than the wild type. Thus the Ala157 residue appears to stabilize the proper initial Fe protein conformation upon MgATP binding. Conversely, there are other variants that are stuck in a MgATP-like

protein conformational changes, but cannot support MgATP hydrolysis. The altered Fe protein with substitution at Asp129 by Glu is an example. It can bind MgATP and undergo the conformational changes but unable to compete with wild type Fe protein in the assay (Lanzilotta WN *et al.*, 1995). Therefore, to be able to bind MgATP and undergo MgATP-induced conformational change is not the only requirement for an active Fe protein to support nitrogenase activity.

F. Structure of nitrogenase complex

1. Structure of the ADP·AlF_4^- stabilized nitrogenase complex

AlF_4^-·ADP or AlF_4^-·GDP have been previously used as analogous of nucleoside triphosphates with nucleotide-switch proteins. Structural evidence from myosin (Fisher AJ *et al.*, 1995) and the heterotrimeric G proteins (Coleman DE *et al.*, 1994; Sondek J *et al.*, 1994) indicate that the AlF_4^--nucleoside diphosphate might be mimicking the transition state during on-enzyme MgATP hydrolysis. The structure of a nitrogenase complex stabilized with ADP·AlF_4^- was determined in 1997 (Schindelin H *et al.*, 1997). The structure shows that the β-phosphate and AlF_4^- groups are stabilized through interactions with side chains of the nearby amino acids at the interface between the Fe protein subunits, and the metal centers in the two proteins are positioned to facilitate the electron transfer. The structure of the complex, when compared to the free component proteins, has provided mechanistic implications for nitrogenase function as well as additional insights into the general signal-transduction processes.

1.1 Overall structure

The structure of the complex is at 3.0 Å resolution (Schindelin H *et al.*, 1997) (Figure 1.9). It has a subunit composition of $(\alpha\beta\gamma_2)_2$, with one Fe protein (γ_2) dimer bound to each αβ-subunit pair of the MoFe protein, so two Fe protein dimers are bound per MoFe protein. The complex has a molecular mass of about 360,000 Da. The nitrogenase complex is elongated and has overall dimension of 190 Å and 65Å perpendicular to the pseudo-two-fold axis and 75 Å along this axis. As predicted in proposed models of the docked complex (Howard JB and Rees DC, 1994), the [4Fe-4S] cluster of the Fe protein and the P cluster of the MoFe protein are positioned along the

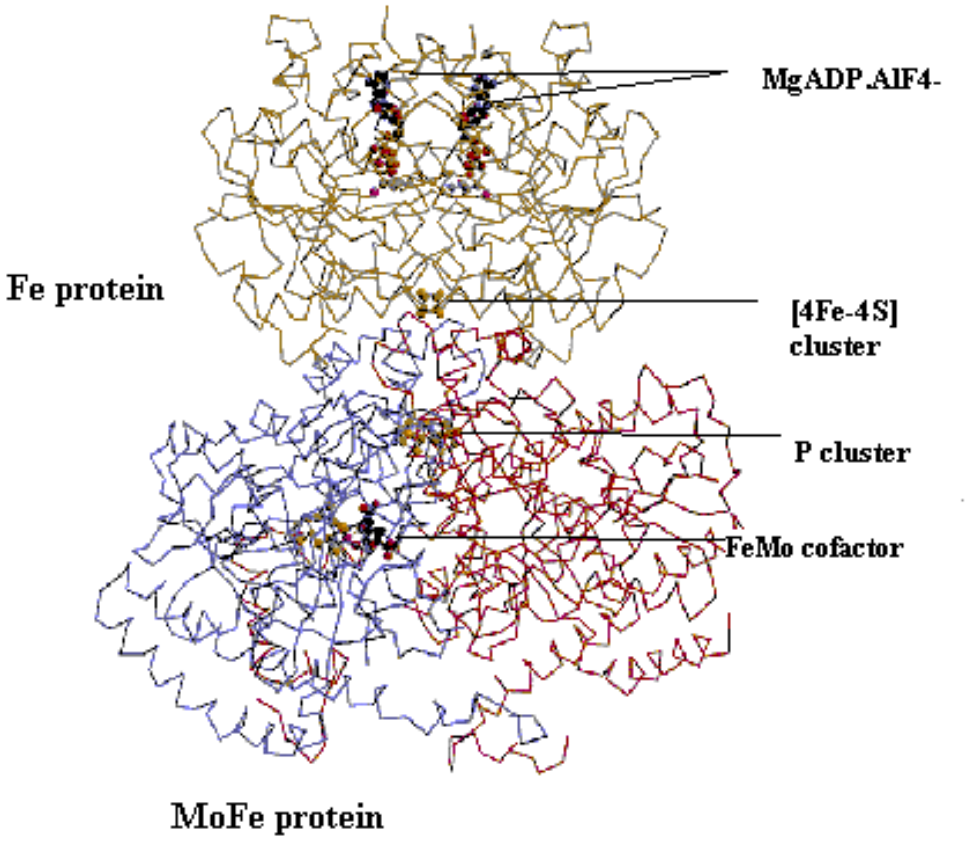

Figure 1.9 The overall structure of the ADP·AlF_4^--stabilized *A. vinelandii* nitrogenase complex (Schindelin H *et al.*, 1997).

Only one αβ pair of the MoFe protein is shown.

pseudo-two-fold axis relating the two proteins within the complex. Due to the conformational changes, particularly those in the Fe protein, the metal centers are closer than predicted. The distance from the [4Fe-4S] cluster to the P cluster is ~ 14 Å, measured as atom-to-atom distance, which is ~ 4 Å shorter than expected from the model building. Thus, in the complex, the P cluster is located essentially equidistant from the Fe protein [4Fe-4S] cluster and the FeMo cofactor. This arrangement strongly suggests that electrons are transferred from the Fe protein via the P cluster to the FeMo cofactor.

1.2 Interactions between component proteins

There are large numbers of contacts between the two proteins in the complex, which buries over 3500Å^2 of the surface area in each interface (Schindelin H *et al.*, 1997). The [4Fe-4S] cluster is completely buried in the Fe protein-MoFe protein interface region and is in van der Waals contact with the loop regions α157 to α159 and β156 to β158 of the MoFe protein. The Fe protein cluster ligand Cys97 from both subunits form main-chain hydrogen bonds to the carbonyl oxygens of the α123, α124 and β123, β124 from the MoFe protein. In addition to these main chain hydrogen bond interactions near the cluster, there are numerous side chain interactions between the two proteins in the complex. For example, the side chains of both Arg100 of the Fe protein form ionic bonds, multiple hydrogen bonds and van der Waals contacts with the MoFe protein residues. This structure information confirms the site-directed mutagenesis data that Arg100 is important for complex formation (see F.2 section).

1.3 Structural changes in the component proteins

Most of the structural changes that occur on complex formation occur in the Fe protein (Schindelin H *et al.*, 1997). The major change may be described as a ~ 13^o rotation of each monomer toward the subunit interface. In contrast, no large structural changes are detected for the MoFe protein. Five regions differ significantly when the Fe protein in the complex is compared to the free form of the Fe protein. These are: (1) The Walker A motif or phosphate-binding loop (P-loop). Binding of the nucleotide results in a tightening of the turn in the loop. (2) The protein-protein interface region of residues 51 through 75. Structural changes in this region appear to be coupled to those in the region from 88 to 118. (3) The residues 88 through 118, including the [4Fe-4S] cluster ligand,

Cys97, and the complex docking residue Arg100. The structural changes involve reorganization of residues 91 to 97, which permits proper positioning of Arg100 to contact with the MoFe protein. (4) Residues 127 to143, including the cluster ligand, Cys132. Notable changes involve the large movement of Gly128 and reorientation of Val130 and Val131. (5) Residues 151 through 176, which participate in an inter-subunit salt bridge that also stabilizes the adenosine ring of the bound nucleotide.

1.4 Fe protein and ADP·AlF_4^- interactions

Two ADP·AlF_4^- molecules are bound per Fe protein dimer, with each nucleotide primarily associated with one monomer in an orientation that is roughly parallel to the dimer interface. In this orientation, the phosphate groups interact with the P-loop and the nucleoside points away from the MoFe protein. The α,β phosphates and the AlF_4^- interact with the P-loop and the negative charges on the phosphate and AlF_4^- are compensated by Lys15 and Lys41. The Mg^{2+}-ion is coordinated by Ser16, the β-phosphate and two of the F-ligands of the AlF_4^-. The adenosine portion is fixed by hydrogen bond interactions to either the side chain or main chain amide of the Fe protein residues. There are other contacts to the second subunit that are very likely to be functionally significant (Schindelin H *et al.*, 1997). Most notable are Lys10 and Asp129. The Lys10 residue of the second subunit interacts across the interface with the terminal oxygen of the β-phosphate. The Asp129 residue is poised to interact with the AlF_4^- of the other subunit. Site-directed mutagenesis data have also indicated the possible roles for some of the above residues (see section C and D).

1.5 Mechanistic implications

The structure of the complex clearly shows the binding mode of MgATP to the Fe protein and establishes AlF_4^-·ADP as a mimic for the geometry of the ATP when bound and hydrolyzed to MgADP·P_i. The structure shows that the MoFe protein does not directly interact with the nucleotide and, hence, its role in nucleotide hydrolysis must be to stabilize an Fe protein-nucleotide intermediate that is not attainable by the Fe protein alone. Potential electron transfer pathways can be traced between the [4Fe-4S] cluster and the P cluster that would not exist without the structural changes in the Fe protein

induced by MgATP binding. The main connection between ATP hydrolysis and electron transfer may be the stabilization of the closed interface between the Fe protein subunits, providing the new conformation from which these processes can proceed. Once the nucleotide is hydrolyzed, the stabilization would be decreased and the subunits could move apart, driving protein dissociation.

2. MgATP-bound and nucleotide-free structures of a nitrogenase protein complex between the L127Δ Fe protein and the MoFe protein

A tight Fe protein-MoFe protein complex is formed when an Fe protein whose switch region has been shortened by one amino acid by deletion of 127Leu (L127Δ) is mixed with MoFe protein (Ryle M and Seefeldt LC, 1996a; Lanzilotta WN and Seefeldt LC, 1996). The crystal structure of this complex generated from *A. vinelandii* (designated as L127ΔFe-MoFe complex) has been determined at 2.2 Å resolution (in the absence of nucleotide) and 3.0 Å resolution (with bound MgATP) (Chiu H-J *et al.*, 2001). As observed in the AlF_4^-·ADP stabilized structure of *A. vinelandii* nitrogenase complex (see above), the most significant conformational changes in the L127Δ Fe-MoFe protein complex occur in the Fe-protein component. While the interactions at the interface between the MoFe-protein and Fe-protein are conserved in the two complexes, significant differences are evident at the subunit-subunit interface of the dimeric Fe-proteins, with the L127ΔFe protein structure having a more open conformation than the wild-type Fe protein in the complex stabilized by AlF_4^-·ADP (Chiu H-J *et al.*, 2001). Addition of MgATP to the L127ΔFe-MoFe protein complex results in a further increase in the separation between Fe-protein subunits so that the structure more closely resembles that of the wild type, nucleotide-free, uncomplexed Fe-protein, rather than the Fe-protein conformation in the AlF_4^-·ADP complex (Chiu H-J *et al.*, 2001). The ability of the L127ΔFe-MoFe protein complex to bind MgATP demonstrates that dissociation of the two component proteins is not required for nucleotide binding.

3. Long-range interactions between the Fe protein binding sites of the MoFe protein

During the past few years, investigation of the structures of stabilized complexes formed by nitrogenase components has utilized the altered forms of Fe protein. Such Fe proteins are either locked in the MgATP-bound conformation or form tight complexes with the MoFe protein (Lanzilotta WN and Seefeldt LC, 1996; Lanzilotta, WN *et al.*, 1997). Other studies have utilized the stable transition-state analogues formed with either BeF_3^- or AlF_4^- and MgADP (Schindelin H *et al.*, 1997; Clarke TA *et al.*, 1999). Tight complexes are also formed as heterologous nitrogenases that are comprised of component proteins purified from different nitrogen-fixing organisms. For example, the Fe protein from *C. pasteurianum* (Cp2) and the MoFe protein from *A. vinelandii* (Av1) or *K. pneumoniae* (Kp1) form a tight complex (Emerich DW *et al.*, 1976; Emerich DW *et al.*, 1978).

Recently, the potential catalytic properties of the heterologous nitrogenase formed by Av1 and Cp2 were reexamined (Clarke TA *et al.*, 2000). This complex has a low level of activity for H_2 evolution with a specific activity of 12 nmol (min×mg of Av1)$^{-1}$, which is about 0.5% that of the homologous Av-nitrogenase. This activity showed saturation kinetics when increasing amounts of Cp2 were added to the assay. When assayed with Av2, the isolated Av1·Cp2 complex showed full half site reactivity with a specific activity of 750 nmol C_2H_2 reduced (min×mg of Av1)$^{-1}$. The 1:1 reduced-Av1·oxidized-Cp2 ($Av1_{red}$·Cp2ox) complex is more stable than the 1:2 $Av1_{red}$·$(Cp2_{ox})_2$ complex, when comparing their rate of dissociation. The differences in the stability of the 1:2 and 1:1 complexes indicate cooperativity between the two Fe protein-binding sites of Av1 even though they are separated by 105 Å. These data indicate that the two Fe protein-binding sites of the MoFe protein alternately bind and release Fe protein in a shuttle mechanism associated with long-range conformational changes in the MoFe protein (Clarke TA *et al.*, 2000).

The Kp1 and Cp2 heterologous nitrogenase was also examined (Maritano S *et al.*, 2001). The isolated Kp1·Cp2 1:1 complex exhibits 25% of the activity of the Kp-nitrogenase, and reduces protons, acetylene and N_2. The formation of a tight complex between the Kp1 and Cp2 prevents Kp1 from binding to the homologous Kp2. Again, the conclusion is that long-range interactions across the $\alpha\beta$ subunit pairs of Kp1 must occur

to explain the non-equivalence of the two Fe protein binding sites leading to the formation of a stable 1:1 complex. Moreover, the reactivity of the Kp2 with the free site in the isolated Kp1·Cp2 complex is dependent on the redox state or nucleotide-bound conformation of the already bound Cp2. The differences in reactivity of Av1·Cp2 complex and Kp1·Cp2 complex could be due to the slower dissociation rate of the Cp2ox from the Av1·Cp2 complex than from the Kp1·Cp2 complex (Clarke TA *et al.*, 2000; Maritano S *et al.*, 2001).

G. Nitrogenase mechanism

The Thorneley and Lowe kinetic model for nitrogenase catalysis was developed in the early to mid 1980s, and has been of value in accounting for many aspects of nitrogenase catalysis. Since its original publication, many new results have been obtained and some of them have been successfully incorporated into the model. This scheme also has limitations because there are experimental observations that it cannot explain. Now, in this part of the review, this model will be described by breaking it down into two cycles, the Fe protein oxidation-reduction cycle and the MoFe protein cycle. Some of the assumptions used in the model will be also included in the discussion.

1. The Fe protein cycle

The Fe protein cycle is a redox cycle that describes the single electron donation from the Fe protein to the MoFe protein, the concomitant hydrolysis of MgATP, and the events necessary for re-reduction of the oxidized Fe protein in order to restart another round of cycle. The individual steps are shown in Figure 1.10, Cycle (a).

1.1 Reduced Fe protein and MoFe protein complex formation and dissociation

Only reduced Fe protein bound by two MgATP molecules is capable of transferring an electron to MoFe protein. So, the association of the reduced Fe protein·$(MgATP)_2$ and MoFe protein is the first step. Evidence for formation of such a protein complex is provided by an extensive series of kinetic studies (Thorneley RNF, 1975; Hageman RV and Burris RH, 1980; Thorneley RNF and Lowe DJ, 1984a). Using *K. pneumoniae* nitrogenase and monitoring the MgATP-induced electron transfer from the Fe protein to

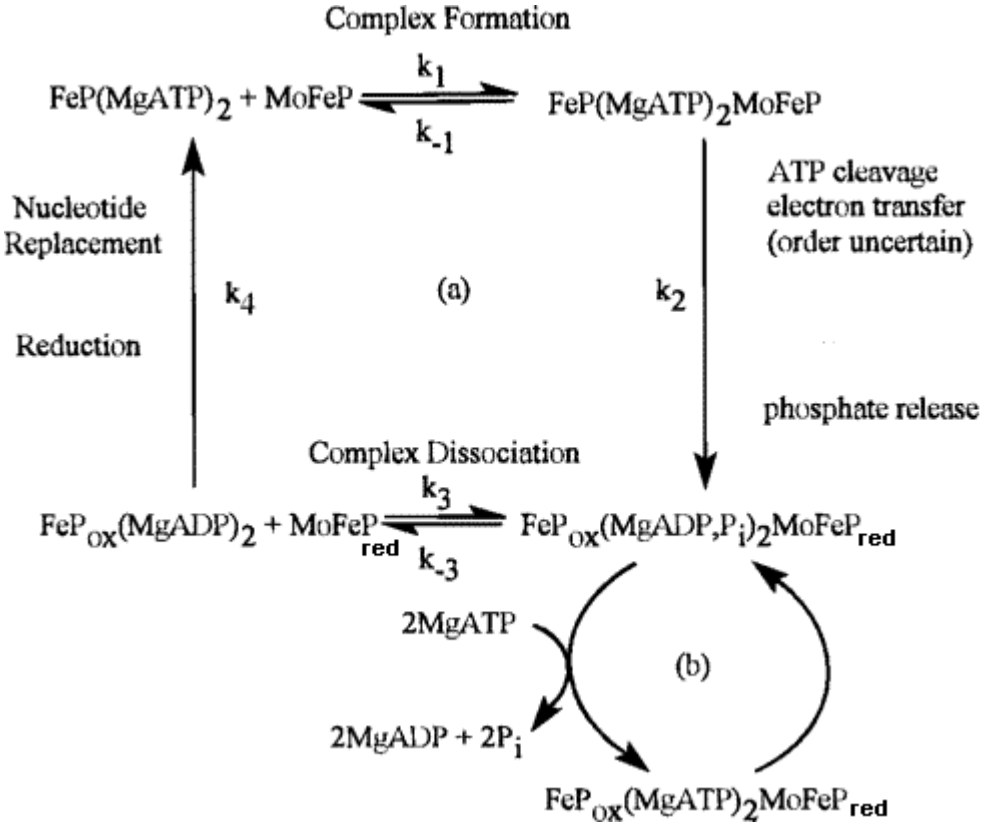

Figure 1.10 Oxidation-reduction cycle for the Fe protein of Mo-nitrogenase (Adapted from Thorneley RNF and Lowe DJ, 1985).

FeP^{red} and FeP^{ox} represent the one-electron reduced and oxidized Fe protein, respectively. Cycles a and b show reductant-dependent and -independent ATP hydrolysis. MoFeP represents the $\alpha\beta$ dimer of the MoFe protein. $MoFeP_{red}$ represents the MoFe protein one more electron reduced than MoFeP.

the MoFe protein as a function of the component protein concentrations at 23°C by stopped-flow spectrophotometry, k_1 was estimated to have a lower limit of 5×10^7 $M^{-1}s^{-1}$ (Lowe DJ and Thorneley RNF, 1984), which is close to the diffusion limit. The rate constant k_{-1} was estimated to be 15 s^{-1} assuming the association-dissociation rates of the nitrogenase complex are independent of the MoFe protein redox level. The reversible complex formation steps is responsible for the so-called "dilution effect" (Lowe DJ and Thorneley RNF, 1984). When low concentrations (<0.5 μM) of nitrogenase component proteins are used, a decrease in specific activity is observed due to the rate of association of the reduced Fe protein·$(MgATP)_2$ with MoFe protein becomeing rate-limiting (Thorneley RNF and Lowe DJ, 1984a).

1.2 Electron transfer from the Fe protein to MoFe protein and MgATP hydrolysis

In this step, intermolecular electron transfer occurs with concomitant hydrolysis of two ATP molecules. Stopped-flow experiments, monitoring the absorbance change of the Fe protein as it transfers one electron to the MoFe protein, have measured the rate constant for this electron transferring reaction. The value of k_2 was measured as 320 s^{-1} at 30°C (pH 7.4) (Hageman RV and Burris RH, 1978) for *A. vinelandii* Fe protein, and 200 s^{-1} at 23°C for *K. penumoniae* Fe protein (pH 7.4) (Thorneley RNF, 1975). The intermolecular electron transfer and MgATP hydrolysis steps are considered together because it is still not clear what the sequence of occurrence is. A number of studies have investigated the order in which these two reactions occur. Early work suggested that MgATP hydrolysis and electron transfer occurred simultaneously (Eady RR *et al.*, 1978). Later, stopped-flow microcalorimetry experiments at 6°C found that protons are released from the MgATP hydrolysis reaction at a rate faster than the electron transfer (Thorneley RNF *et al.*, 1989). Thus, MgATP hydrolysis would have to precede electron transfer. In contrast, stopped-flow spectrophotometry studies at 20°C indicated that protons were released slower than the electron transfer rate (Mensink RE *et al.*, 1992). It may be that the order can vary depending on the circumstances.

Although MgATP hydrolysis is not strictly required for electron transfer, the rate of MgATP-independent electron transfer is insignificant compared to the rate of electron transfer coupled to ATP hydrolysis (Lanzillota WN *et al.*, 1996). Likewise, electron

transfer is not required for ATP hydrolysis (Imam S *et al.*, 1980; Larson C *et al.*, 1995). More recently (Lowe DJ *et al.*, 1995), the kinetic scheme of the Fe protein cycle was modified to include the reductant-independent MgATP hydrolysis cycle (Figure1.10, Cycle b). Note that, in both cycles, ATPase activity is a property of the complex involving both proteins and not of either protein alone (Lowe DJ *et al.*, 1995). This reductant-independent ATPase activity can explain why the limiting stoichiometry of two molecules of MgATP hydrolyzed for each electron transferred to substrate is not maintained under some conditions, such as with the pH >8.5 or < 6.4 (Jeng DY *et al.*, 1970; Iman and Eady RR, 1980).

1.3 The dissociation of oxidized Fe protein from reduced MoFe protein: the rate-limiting step in the catalytic cycle for substrate reduction

A combination of stopped-flow spectrophotometry and EPR spectroscopy was used to study the kinetics of the reduction by dithionite of oxidized Fe protein in the presence of MgADP (Thorneley RNF and Lowe DJ, 1983). The inhibition of this reaction by added MoFe protein enabled the rate of dissociation of oxidized Fe protein·$(MgADP)_2$ from the MoFe protein to be measured as $k_{-3} = 6.4 \pm 0.8\ s^{-1}$ at 23°C and pH 7.4. Comparison with the steady-state rate of substrate reduction showed that the dissociation of the complex is the rate-limiting step, except at very low protein concentrations, where the k_1 becomes rate-limiting (Thorneley RNF and Lowe DJ, 1983). The rate constant k_3 for the reverse reaction was determined to be $4.4 \times 10^6\ M^{-1}s^{-1}$. Oxidized Fe protein has less affinity for the MoFe protein than does reduced Fe protein. Yet, under conditions of low electron flux through nitrogenase, when the Fe protein:MoFe protein molar ratio is decreased, the expected activity of the Fe protein is compromised by the re-association of oxidized Fe protein with the MoFe protein in the k_3 step. This phenomenon is referred to as “MoFe protein inhibition” because the excess MoFe protein prevents reduction by dithionite of the oxidized Fe protein that it binds. These experiments were performed in the absence of MgATP. It was also determined that reduced Fe protein·$(MgADP)_2$ binds the MoFe protein with the same affinity as oxidized Fe protein·$(MgADP)_2$. This observation underlies one of the assumptions of the Thorneley & Lowe model that ATP

concentration must be in excess compared to ADP and nucleotide exchange on the free reduced Fe protein is rapid.

Another conclusion from the complex dissociation data relates the slow dissociation rate with efficient N_2 reduction. It was suggested that because products are assumed to evolve only from the substrate-reduction site on the non-complexed MoFe protein, the slow dissociation rate may be necessary for the generation of a low-potential metal-hydride site capable of binding N_2 and displacing H_2. In other words, the value of k_{-3} may contribute to the preference for N_2 reduction over H_2 evolution (Lowe DJ and Thorneley RNF, 1984).

1.4 Reduction of oxidized Fe protein by $SO_2\cdot^-$

The reduction of oxidized Fe protein by dithionite actually involves $SO_2\cdot^-$ as the active reductant based on a linear dependence of k_{obs} on $[S_2O_4^{2-}]^{1/2}$ (Thorneley RNF and Lowe DJ, 1983). The rate constant k_4 for oxidized Fe protein·$(MgADP)_2$ reduction by $SO_2\cdot^-$ was measured at 23°C to be 3×10^6 $M^{-1}s^{-1}$.

Nitrogenase requires a low-potential source of electrons, such as dithionite or Ti^{3+}citrate or reduced methyl viologen *in vitro*, and either reduced flavodoxin or ferredoxin *in vivo*. The choice of electron source can have a significant impact on the overall kinetics of nitrogenase catalysis. We now know that both the $[4Fe\text{-}4S]^{2+}/[4Fe\text{-}4S]^{1+}$ and $[4Fe\text{-}4S]^{2+}/[4Fe\text{-}4S]^{0}$ redox couples of the Fe protein can function during catalysis (Erickson JA *et al.*, 1999; Nyborg AC *et al.*, 2000). Which of the couples is active is dependent on the reductant used and its concentration. The Thorneley-Lowe model was developed using dithionite as reductant and, consequently, this model applies only when the $[4Fe\text{-}4S]^{2+}/[4Fe\text{-}4S]^{1+}$ redox couple of the Fe protein is in use.

The Thorneley-Lowe model predicts that only free oxidized Fe protein is reduced. The requirement is based on the observation of "MoFe protein inhibition" (see above). In physiological terms, this means that when the oxidized Fe protein is bound to the MoFe protein, its [4Fe-4S] cluster will not be exposed to solvent and so cannot react with reductant. Its [4Fe-4S] cluster is, therefore, the site of Fe protein reduction as well as the site of electron transfer to the MoFe protein (Wilson PE *et al.*, 2001). After Fe protein reduction, the Fe protein cycle starts over again.

Recently, flavodoxin hydroquinone was used to reduce the oxidized Fe protein, instead of sodium dithionite as used in the Thorneley-Lowe model (Duyvis MG *et al.*, 1998). Evidence was presented that flavodoxin hydroquinone is able to reduce the Fe protein in nitrogenase protein complex after the MgATP-induced electron transfer and before dissociation of the complex. Thus, the dissociation of the nitrogenase complex is not necessary for reduction by flavodoxin (Duyvis MG *et al.*, 1998).

2. The MoFe protein cycle

One completion of the Fe protein cycle accounts for the transfer of one electron from Fe protein to MoFe protein. However, all nitrogenase substrates require 2n electrons ($n \geq 1$). For example, the reduction of N_2 to $2NH_3$ involves the transfer of at least of eight electrons (equivalent to eight turns of the Fe protein cycle) with obligatory reduction of at least $2H^+$ to H_2. The MoFe protein cycle accounts for the different redox states of the MoFe protein before a product is released (Figure 1.11) (Lowe DJ and Thorneley RNF, 1984). In Figure 1.11, E_0 corresponds to the level of reduction of MoFe protein isolated in the presence of dithionite. An assumption of this model is that the kinetics of the Fe protein cycle is independent of the redox state of the MoFe protein. This assumption has been shown to hold for the first two redox states of the MoFe protein (Fisher K *et al.*, 1991).

2.1 H_2 evolution and N_2 reduction

In the absence of alternative substrates, nitrogenase catalyzes the reduction of $2H^+$ to H_2. The first electron transferred from the Fe protein to the MoFe protein is assumed to be accompanied by a H^+ and, after complex dissociation, the species E_1H is formed (Lowe DJ *et al.*, 1990). After the second electron/proton is transferred, the MoFe protein is at the E_2H_2 level and is now capable of evolving H_2 and reforming E_0. This aspect of the model conforms to the previous suggestion that the lag phase before H_2 evolution occurs is caused by two slow dissociation steps (Hageman RV and Burris RH, 1978). Because only free MoFe protein is assumed to be capable of evolving product, if reduced Fe protein binds to the E_2H_2 state before H_2 is released, E_3H_3 can be generated. H_2 evolution from the E_2H_2 state happens under conditions where the more reduced redox

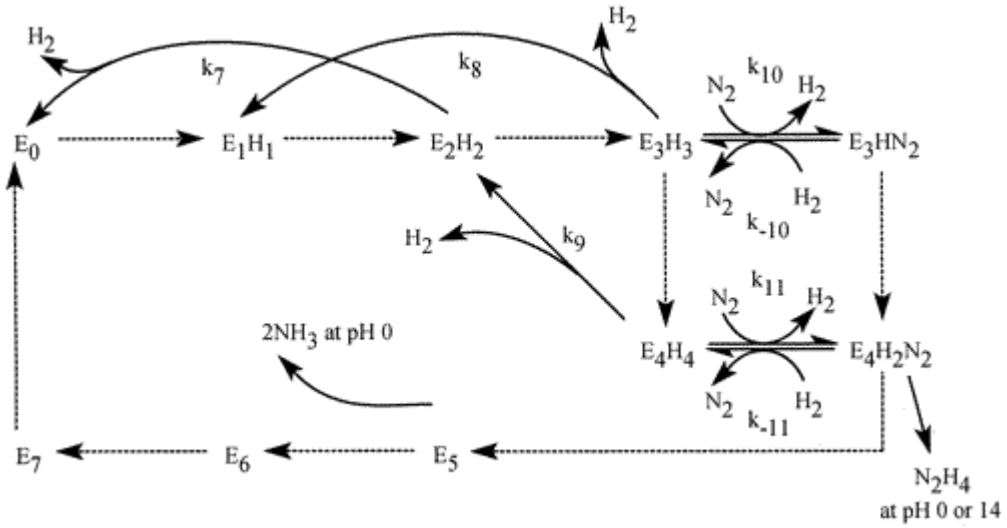

Figure 1.11 The MoFe protein cycle.

E_n represents the αβ dimer of the MoFe protein from *K. pneumoniae* nitrogenase, and n refers to the number of electron transferred from the Fe protein to the MoFe protein (Thorneley RNF and Lowe DJ, 1984b).

states of the MoFe protein cannot be reached, for example, at low electron flux generated by a low molar ratio of Fe protein-to-MoFe protien (Wherland S *et al.*, 1981; Guth JH and Burris RH, 1983). The model predicts that N_2 does not bind to the MoFe protein until the E_3H_3 or E_4H_4 redox state has been reached and this binding of N_2 results in the displacement of H_2. The presence of N_2 leads to an overall decrease in H_2 evolution as more of the electron flux goes to generating NH_3. However, H_2 evolution is never completely stopped even at high pressures of N_2 (Simpson FB and Burris RH, 1984). H_2 evolution from E_2H_2 is minimized by the slow complex dissociation step and the rapid conversion of E_2H_2 to E_3H_3 is due to the diffusion-limited association rate, k_1. In another words, any increase in the rate-limiting step would result in a decrease in N_2 reducing activity and an increase in H_2 evolving activity.

2.2 N_2 reduction

Thorneley and Lowe used a combination of rapid acid-quench and stopped-flow spectrophotometry in their attempts to detect intermediates in the N_2-reduction pathway (Lowe DJ and Thorneley RNF, 1984). Whereas product evolution normally comes from free MoFe protein, acid-quench releases substrate intermediates from both free MoFe protein and the Fe protein-MoFe protein complex. Therefore, by modeling the pre-steady-state kinetic data obtained with this method, they were able to gain insights into the enzyme-bound intermediates of N_2 reduction.

They found that some hydrazine, N_2H_4, is released from the MoFe protein when it is turning over in the presence of N_2 on quenching the reaction with either acid or base (see Figure 1.11) (Thorneley RNF *et al.*, 1978). The Thorneley & Lowe model proposes that the MoFe protein-bound intermediate, which is responsible for N_2H_4 production, is a bound dinitrogen-hydride intermediate formed at the E_4H_4 redox state (Thorneley RNF and Lowe DJ, 1984b). Based on work with synthetic model compounds, a hydrazido(2-) structure (=N-NH_2) was favored for the intermediate that yields N_2H_4 on quenching. A pre-steady-state time course for N_2H_4 formation from N_2 by rapid-quenching technique was performed under a 50% N_2/50% H_2 atmosphere. The decrease in N_2H_4 concentration at all the times measured indicates that H_2 inhibition of N_2 reduction must occur before the formation of the intermediate that yields N_2H_4 on quenching (E_4H_4). The results are

consistent with their prediction that N_2 binds to MoFe protein by the displacement of H_2 as discussed in 2.1.

Other experiments produced NH_3 formation data that support the suggestion made by Chatt (1980) that the triple bond of N_2 is weakened by progressive protonation of the β-nitrogen atom. These data are consistent with an intermediate bound to E_5H_5 that is likely to be a hydrazido(2-) derivative ($Mo{=}N\text{-}NH_3^+$) and that bound to E_6H_6 a nitrido derivative ($Mo{\equiv}N$). Both of these intermediates would be expected to hydrolyze rapidly under acid conditions to yield NH_3. The Thorneley-Lowe model is not definitive as to which intermediates normally release NH_3. Their data suggested the overall pattern of product release from the nitrogenase system under a N_2 atmosphere is H_2 and then NH_3.

2.3 C_2H_2 reduction

C_2H_2 binds MoFe protein at either of two redox states. These are E_1H_1 and E_2H_2. Pre-steady-state time course data show that C_2H_4 formation (from C_2H_2 reduction) is linear after an initial lag of 250 ms. C_2H_4 is, therefore, not released until either the E_3H_3 or E_4H_4 redox state is reached even though C_2H_2 binds at either the E_1H_1 or E_2H_2 redox state. This result is consistent with the observation that high electron flux, induced by a high Fe protein:MoFe protien molar ratio, favors C_2H_2 reduction over H_2 evolution (Lowe DJ *et al.*, 1990). Additionally, electron flux through nitrogenase is inhibited by C_2H_2 at high protein concentrations because the association rate between the MoFe protein and the oxidized Fe protein is enhanced by C_2H_2, leading to an increased steady-state concentration of the inactive complex of oxidized Fe protein·MoFe protein·C_2H_2. This inhibition effect is not relieved by CO even though CO eliminates C_2H_2 reduction (see later). Thus, CO and C_2H_2 must be bound at the same time to distinct sites on the enzyme.

H. Nitrogenase catalyzed substrate reduction

1. Substrate reduction

Nitrogenase is a relatively promiscuous enzyme with a wide range of neutral and anionic substrates containing NN, NO, NC or CC (Yates MG, 1992; Burgess BH, 1993) and more recently CO and CS triple or double bonds (Seefeldt LC *et al.*, 1995; Rasche

ME and Seefeldt LC, 1997). Hydrazine is the only single bonded substrate known. All products require the enzyme to supply multiples of two electrons with usually two protons. Some substrates give multiple products and, at high electron flux, products requiring larger numbers of electrons are favored.

1.1 Hydrogen evolution and dinitrogen reduction

Nitrogenase catalyzes an ATP-dependent H_2 evolution reaction (Bulen WA *et al.*, 1965) that has all the same requirements as N_2 fixation. At present, the mechanism and the site of H_2 evolution are still unknown. Like the other substrates of nitrogenase, protons are believed to be reduced at the FeMo cofactor although the possibility that H_2 could be produced from the P cluster has been discussed (Burgess BK and Lowe DJ, 1996).

H_2 evolution cannot be completely eliminated during N_2 reduction (Hadfield KL and Bulen WA, 1969). Even at 50 atm N_2 pressure, a minimum of 25% of the available electrons goes into H_2 evolution (Simpson FB and Burris RH, 1984). One explanation that has been offered for this seemingly obligatory H_2 evolution is that N_2 can only bind to nitrogenase by displacement of H_2, which would require a minimum 1:1 stoichiometry (Thorneley RNF and Lowe DJ, 1985).

Other features of H_2-N_2 interactions are 1) the specific inhibition of N_2 reduction by H_2 and 2) the nitrogenase-catalyzed formation of HD in the presence of N_2 and D_2. HD formation is dependent on MgATP, reductant, and N_2. It is not a simple D_2-H_2O exchange process because incubations under tritium-labeled H_2 produce insignificant radioactivity in the liquid phase (Burgess BK *et al.*, 1981). Electrons appearing as HD under a N_2 + D_2 atmosphere are diverted exclusively from NH_3 formation and, therefore, concomitant H_2 evolution is unaffected. The K_m of N_2 for HD formation is much lower than the K_m of N_2 for NH_3 production (Burris RH and Orme-Johnson WH, 1976; Li J-H and Burris RH, 1983). Because of the requirements for both HD formation and H_2 inhibition of N_2 reduction are the same, a number of models have been proposed to explain both phenomena (Dilworth MJ *et al.*, 1998 and reference therein).

The altered MoFe protein with His substituted by Gln at the α195 position ($\alpha 195^{Gln}$), which binds N_2 normally but reduces it at only 1~2% of wild type rate, offers

an opportunity to test some aspects of these models (Dilworth MJ *et al.*, 1998). With this altered MoFe protein, the rate of HD production and the fraction of total electron flow allocated to HD are similar to those for wild type MoFe protein under the same conditions. However, the electrons forming HD do not come from those normally producing NH_3 (as occurs in the wild type) but are equivalent to those whose evolution as H_2 had been inhibited by N_2 (Dilworth *et al.*, 1998). These observations are different from those with the altered $\alpha 195^{Asn}$ MoFe protein, which cannot reduce N_2 to NH_3 and form HD (Fisher K *et al.*, 2000a). It was suggested that the $\alpha 195^{Asn}$ MoFe protein is incapable of reaching the E_4H_4 redox state and, therefore cannot catalyze N_2-reduction and HD formation.

1.2 Hydrazine reduction

Nitrogenase catalyzes hydrazine reduction to NH_3. This reaction was first demonstrated using an *A. vinelandii* nitrogenase complex in 1976 and it was shown that the $N_2H_5^+$ is not a substrate for nitrogenase (Bulen WA, 1976).

$$N_2H_4 + 2e^- + 2H^+ \rightarrow 2NH_3$$

N_2H_4 is a poor substrate and its K_m is about 20 to 30 mM (Davis LC, 1980). N_2H_4 reduction is not inhibited by H_2 (Davis LC, 1980). Hydrazine is a likely intermediate of N_2 reduction but, if so, it remains enzyme-bound. Hydrazine can be detected if Mo-nitrogenase is quenched with either acid or alkali during turnover. In contrast, vanadium-containing nitrogenase (V-nitrogenase) releases hydrazine at a low rate during turnover under N_2 (Dilworth MJ and Eady RR, 1991).

1.3 Acetylene reduction

Acetylene reduction is routinely used for estimating the activity of preparations of nitrogenase because its product, ethylene, is relatively easy to quantify. The first demonstrated reduction of C_2H_2 to C_2H_4 used *C. pasteurianum* crude extracts (Dilworth MJ, 1966). Acetylene is a good substrate for nitrogenase with a K_m value ranging from about 0.003 to 0.02 atm depending on the source of the nitrogenase (Hardy RWF, 1979). In more recent research work, the K_m value is usually about 0.005 atm as measured with the *A. vinelandii* nitrogenase (Shen J *et al.*, 1995; Fisher K *et al.*, 2000b). It is reduced to

ethylene only by wild type Mo-nitrogense. Concentrations of C_2H_2 greater than 0.4 atm inhibit electron flux through the *A. vinelanedii* wild type Mo-nitrogenase (Hwang JC and Burris RH, 1972). C_2H_2 inhibits N_2 reduction non-competitively (Rivera-Ortiz JM and Burris RH, 1975). C_2H_6 is a minor product of C_2H_2 reduction by V-nitrogenase along with C_2H_4 (Dilworth MJ *et al.*, 1987). Some Mo-nitrogenases with altered MoFe proteins (Scott DJ *et al.*, 1990, 1992; Fisher K *et al.*, 2000c) also produce C_2H_6 from C_2H_2.

The stereochemistry of proton addition to the triple bond of C_2D_2 was reported to be completely *cis* with wild type *C. pasteurianum* nitrogenase (Dilworth MJ, 1966). Other studies, using various wild-type Mo-nitrogenases, suggested the formation of a trace amount of *trans*-$C_2D_2H_2$ (Kelly M, 1969; Hardy RWF *et al.*, 1968). Recently, a correlation was proposed between the stereospecificity of proton addition and the propensity of nitrogenase to produce ethane, where increased *trans*-$C_2D_2H_2$ production correlated with increased ethane production from acetylene (Fisher K *et al.*, 2000c).

C_2H_4 can be reduced to C_2H_6 by wild type in a reaction consuming < 1% of the total electron flux, even though no C_2H_6 could be detected when C_2H_2 is being reduced to C_2H_4 (Ashby GA *et al.*, 1987). C_2H_4 also inhibited total electron flux without uncoupling MgATP hydrolysis from electron transfer with the wild type Mo-nitrogenase (Ashby GA *et al.*, 1987; Fisher K *et al.*, 2000c). It was suggested that C_2H_4 interrupts both the electron transfer and MgATP hydrolysis. Possibly, bound C_2H_4 exerts its effect similarly to that of bound C_2H_2, which inhibits total electron flux by enhancing the MoFe protein-Fe protein association rate and so increasing the steady-state concentration of the inhibitory complex of the MoFe protein with oxidized Fe protein (Lowe DJ *et al.*, 1990). This interpretation requires that the inhibitory complex does not catalyze MgATP hydrolysis (Fisher K *et al.*, 2000c).

1.4 Cyanide reduction

Cyanide reduction was first demonstrated in 1967 (Hardy RWF and Knight E, Jr, 1967). Because HCN is a relatively weak acid, sodium cyanide solutions simultaneously contain both HCN and CN^-, the relative amounts varying with the pH of the solution. Under certain conditions, the Mo-nitrogenase produces "excess NH_3", which is an amount of NH_3 in excess of the amount of CH_4 produced (Li JG *et al.*, 1982; Fisher K *et*

al., 2000b). The reason for "excess NH_3" production has been explored. As shown in the scheme below (taken from Fisher K *et al.*, 2000b), HCN is proposed to be initially converted into CH_2=NH (methyleneimine) by two electrons and two protons and when this intermediate escapes from the active site, it is hydrolyzed to H_2C=O and NH_3 (Li JG *et al.*, 1982; Fisher K *et al.*, 2000b). Under these circumstances, NH_3 is produced without concomitant CH_4 production. In the next step, an additional two electrons and two protons produce CH_3NH_2, which can also escape and be detected. Finally, CH_4 and NH_3 are formed in equal quantities by the next pair of electrons and protons.

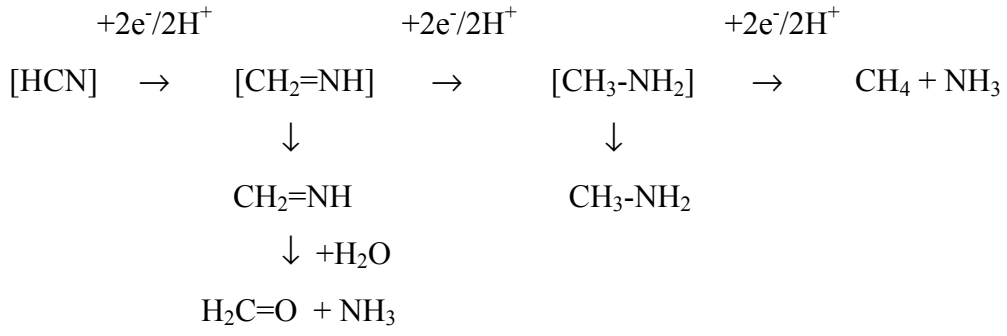

[] indicates substrate bound to the enzyme.

The anion, CN^-, acts as an electron flux inhibitor with wild-type Mo-nitrogenase, but it does not inhibit MgATP hydrolysis. Higher Fe protein to MoFe protein ratios favor H_2 release rather than HCN reduction (Li JG *et al.*, 1982). Thus, HCN may bind to a more oxidized state of the MoFe protein than the H_2-evolving state. On the basis of pre-steady-state data (Lowe DJ *et al.*, 1989), the early suggestion that CN^- and HCN bind at independent sites (Li JG *et al.*, 1982) has been questioned. The more recent interpretation suggests that both inhibitor and substrate bind at the same site and that CN^- only acts as an electron flux inhibitor until it is protonated to give the substrate HCN (Fisher K *et al.*, 2000b).

1.5 Azide reduction

Schöllhorn and Burris (1967) reported that both *C. pasteurianum* and *A. vinelandii* Mo-nitrogenase reduce azide ion (N_3^-) in a two-electron reaction to give stoichiometric amounts of N_2 and NH_3, a product balance also found by Hardy and Knight (1967). Later, Dilworth and Thorneley (1981) found that hydrazine is also a major product when hydrogen azide (HN_3) is reduced by *K. pneumoniae* and *A. vinelandii* nitrogenases and that it does not rebind to the enzyme for further reduction to NH_3. Like sodium cyanide solutions, sodium azide provides two species (HN_3 and N_3^-) in the solution (Rubinson JF *et al.*, 1985). But unlike those produced from sodium cyanide, both species can be reduced by Mo-nitrogense.

$$N_3^- + 2e^- + 3H^+ \rightarrow N_2 + NH_3 \quad (1)$$

$$HN_3 + 6e^- + 6H^+ \rightarrow N_2H_4 + NH_3 \quad (2)$$

$$N_3^- + 8e^- + 9H^+ \rightarrow 3NH_3 \quad (3)$$

Note that, in reaction (1) and (3), N_3^- can be reduced by unequal amount of electrons and protons, which is rarely seen in the nitrogenase catalyzed substrate reduction.

HN_3 binds to nitrogenase with a K_m of 12 μM in the six-electron reduction reaction (Rubinson JF *et al.*, 1985). HN_3 binds to and is reduced at a redox state of the MoFe protein more oxidized than the N_2-reducing state. "Excess NH_3" is always observed during azide reduction with more NH_3 produced than the sum of N_2 and N_2H_4 produced. This result has been interpreted as the N_2 produced from N_3^- reduction acting as a substrate and being further reduced to NH_3 (Dilworth MJ and Thorneley RNF, 1981; Rubinson JF *et al.*, 1985). However, an alternative explanation was given recently that reaction (3) may be utilized to produce "excess NH_3" (Fisher K *et al.*, 2000a).

N_3^- was found to induce electron-flux inhibition with both the $\alpha 195^{Asn}$ and $\alpha 195^{Gln}$ altered MoFe proteins but not with the wild type MoFe protein (Fisher K *et al.*, 2000a). Both of the altered MoFe proteins, however, retain the ability to reduce azide (HN_3 and N_3^-) to a similar extent. This observation led to the suggestion that N_3^- has two binding sites in these altered MoFe proteins. The first acts as a substrate-binding and reduction site, whereas the second site is an electron-flux inhibition site (Fisher K *et al.*, 2000a). A

possible alternative explanation is that only a single azide-binding site exists and this alternative can be compared with interaction of the HCN/CN^- pair with the enzyme. Details of the mechanism for the binding and reduction of azide (HN_3 and N_3^-) are still unknown.

2. Inhibitors of substrate reduction

CO is a potent non-competitive inhibitor of the reduction of all substrates except that of protons (Hardy RWF *et al.*, 1965). In the presence of CO, the rate of electron transfer through the system is generally not inhibited, but all electrons go toward the production of H_2 (Hardy RWF *et al.*, 1965; Hwang JL *et al.*, 1973). However, if either homocitrate is replaced by citrate (as in the $NifV^-$ phenotype) or the arginines surrounding the FeMo cofactor are substituted by lysine, proton reduction becomes sensitive to inhibition by CO in the normal assay (Newton WE *et al.*, 1995).

Under turnover conditions with CO present, two distinct EPR signals can be observed from the enzyme. At low partial pressures of CO (low-CO: 0.08 atm), a rhombic signal with g values of 2.09, 1.97 and 1.93 is seen and is replaced, under higher CO partial pressure (high-CO: 0.5 atm), by an axial signal with g values of 2.17 and 2.06 (Yates MG and Lowe DJ, 1976; Lowe DJ *et al.*, 1978; Davis LC *et al.*, 1979; Cameron LM and Hales BJ, 1998). Neither of these EPR signals showed broadening when ^{13}CO was used, however, ENDOR spectroscopy was successful in detecting signals in the presence of ^{13}CO (Pollock RC *et al.*, 1995). ^{57}Fe ENDOR spectroscopy in which either the P cluster or the FeMo cofactor of the MoFe protein were labeled with ^{57}Fe showed that these EPR signals arose from the FeMo cofactor (Christie PD *et al.*, 1996). The ^{13}C ENDOR data were interpreted to indicate that the signal, which appears at a low concentration of CO arises from a single CO molecule bound to the FeMo cofactor and the signal, which appears at a high concentration of CO, arises from two CO molecules bound to the FeMo cofactor (Lee H-I *et al.*, 1997). Under high concentration of CO, the two CO molecules were suggested to terminally ligate the FeMo cofactor, whereas the single CO under low concentration of CO may bridge the same two Fe atoms of the FeMo cofactor.

Other inhibitors of nitrogenase include NO, which is a well established, but difficult to work with, inhibitor (Burgess BK and Lowe DJ, 1996). It inactivates the Fe protein and possibly the MoFe protein irreversibly (Liang JH and Burris RH, 1988; Hyman MR *et al.*, 1992). Nitrite also inactivates the Fe protein irreversibly (Vaughn SA and Burgess BK, 1989).

3. Potential binding sites of substrates

The FeMo cofactor is believed to be the substrate binding and reduction site, but where and how do substrates bind and get reduced on the FeMo cofactor? As discussed in D2.3 and D2.4 sections, it is clear now that the polypeptide environment of the FeMo cofactor plays critical roles for its activity. Although substituting its immediate amino acid neighbors and studying the consequences of the modification on the catalytic, spectroscopic or redox function of the altered MoFe proteins have given us a wealth of information about the binding of the substrates and inhibitors, theoretical studies and spectroscopic investigations on wild type MoFe protein have also provided insights.

Since publication of the structure of the FeMo cofactor, theoretical calculations have been used in attempts to predict the mode of N_2 binding and the mechanism of its reduction. In one study, nine theoretically possible motifs were examined and three of them were proposed as the best candidates for activating N_2 for reduction (Deng H and Hoffman R, 1993). However, these studies focused on the apparently unsaturated Fe atoms at the center of the FeMo cofactor, and ignored the possibility that N_2 binding could occur at the Mo site, after dissociation of the homocitrate ligand (Grönberg KLC *et al.*, 1998; Durrant MC, 2001b). Kinetic studies on the reactivity of extracted wild type and NifV$^-$ cofactors show that the two clusters have different reactivities only when imidazole is bound to the isolated cofactor (Grönberg KLC *et al.*, 1998). The results suggest a new role for the homocitrate ligand in "tuning" the reactivity of the FeMoco in the enzyme during turnover. A model was proposed in which the carboxyl group of the homocitrate dissociates from the Mo atom, leaving it tethered by only its hydroxyl group. N_2 binding and reduction could then take place at the Mo site (Grönberg KLC *et al.*, 1998).

There are also reports on the reactions of isolated FeMo cofactor. EPR and EXAFS spectroscopies have been used to monitor the binding of reducible substrates and inhibitors, such as cyanide, of nitrogenase (Richards AJM *et al.*, 1994). The data revealed that more than one cyanide ion seems to bind per FeMo cofactor and one of the cyanide ions binds at the terminal tetrahedral Fe atom in competition with thiol (Richards AJM *et al.*, 1994) and the other site could be at the Mo atom of the FeMo cofactor (Liu HI *et al.*, 1994).

Freeze-quench EPR and both ^{13}C and ^{1}H ENDOR spectroscopies have been used to address substrate binding and reduction in both wild type MoFe protein and altered MoFe proteins (Lee H-I *et al.*, 2000; Ryle MJ *et al.*, 2000). Studies with the altered $\alpha 195^{Gln}$ MoFe protein by these methods indicated that at least two C_2H_2-derived species are bound to the FeMoco of the $\alpha 195^{Gln}$ MoFe protein under turnover conditions (Lee H-I *et al.*, 2000).

A relatively new technique of stopped-flow Fourier transform infrared spectroscopy (SF-FTIR) has also been applied to the study of nitrogenase (George SJ *et al.*, 1997). This technique has the potential to monitor directly vibrations associated with bound small molecules. During turnover under high CO conditions, three time-dependent infrared bands were observed, whereas, under low CO conditions, only a single band was observed. All bands identified correspond to different CO species bound to the FeMoco, because they all have different time courses. The interpretation of the data is that there is more than one metal site binding CO in the protein during turnover conditions. Because SF-FTIR can detect all species present, it has the potential to detect the binding and reduction of a wide range of nitrogenase substrates, provided that the appropriate spectroscopic range can be accessed (Smith BE, 1999). This technique may help to narrow down the possible modes of substrate binding and reduction, especially for N_2, the physiological substrate for this enzyme.

I. *nif* genes and their products

The biochemical complexity of nitrogenase is reflected in the genetic organization and in the regulation of expression of the components required for the synthesis of a catalytically competent nitrogenase. The organization and regulation of the genes were

revealed in the early 1980's. The organism that appears to have the simplest organization of nitrogen-fixation-specific (*nif*) genes, and which is the one best studied at the molecular genetic level, is the facultative anaerobe, *Klebsiella pneumoniae*. This organism has 20 *nif* genes organized into eight contiguous transcriptional units. The specific designations for individual *K. pneumoniae nif* genes are also used to denote genes whose products have homologous functions in other organisms (Figure 1.12).

1. Nitrogenase structural genes

The *nif* genes encoding the polypeptides of nitrogenase include *nifH* that codes for the Fe protein, *nifD* that codes for the α-subunit, and *nifK* that codes for the β-subunit of the MoFe protein, respectively.

2. Electron transport to nitrogenase genes

nifF and *nifJ* genes are involved in the reduction of the Fe protein of the nitrogenase. The *nifF* gene product is a flavodoxin that can donate one electron to the oxidized Fe protein. The re-reduction of the flavodoxin is accomplished through the catalytic activity of the *nifJ* gene product, a pyruvate-flavodoxin oxidoreductase.

3. Genes for the biosynthesis of the FeMo cofactor and their products

At least six gene products are involved in the biosynthesis of the FeMoco. These are the products of *nifQ*, *nifB*, *nifV*, *nifN*, *nifE*, and *nifH*.

The *nifQ* mutants exhibit a Nif^+ phenotype at normal Mo concentrations but, when the Mo concentration is lowered to the nanomolar range, then *nifQ* mutants of *K. pneumoniae* are Nif^- (Imperial J *et al.*, 1984). The gene product may be associated with a high affinity Mo transport system that provides Mo for the FeMo cofactor at an early step in its biosynthesis.

Mutations in *nifB* result in the formation of an immature MoFe protein that we now know lacks FeMo cofactor. It can be activated *in vitro* by adding FeMo cofactor that has been isolated from wild type MoFe protein (Roberts GP *et al.*, 1978). These and related data indicate that the immature MoFe protein and FeMo cofactor are synthesized

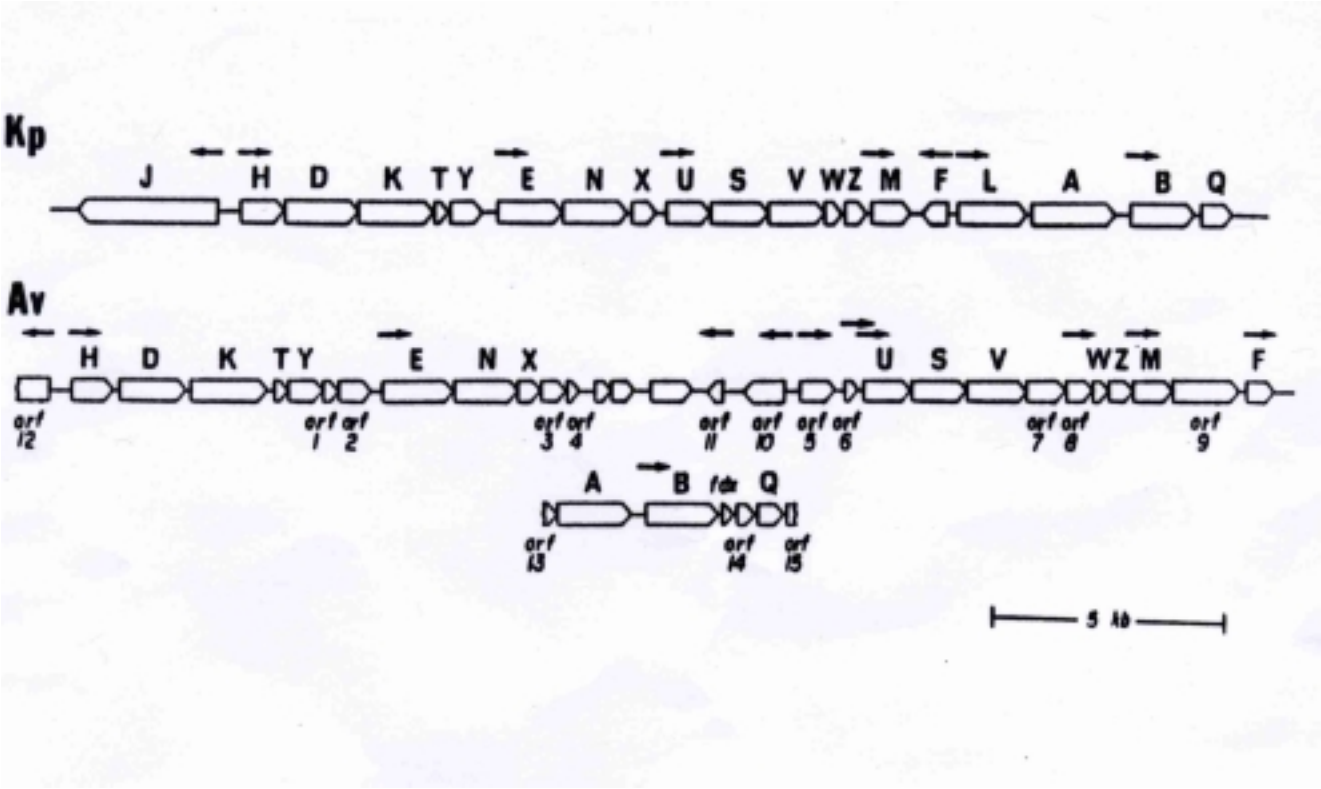

Figure 1.12 Comparison of the physical organization of the *nif* genes from *A. vinelandii* (Av) with that of *K. pneumoniae (*Kp*).*

Arrows indicate the position and direction for known or proposed transcription initiation sites (Arnold W *et al.*, 1988; Jacobson MR *et al.*, 1989a; Bennett LT *et al.*, 1988; Joerger RD and Bishop PE, 1988; Dean DR and Jacobson MR, 1992).

separately within the cell. The product of *nifB* can be solubilized in detergents and has been isolated as an iron-sulfur containing NifB cofactor (Shah VK *et al.*, 1994). This product is possibly an Fe-S cluster containing precursor of the FeMo cofactor itself.

DNA sequence analysis revealed that the products of the *nifE* and *nifN* genes exhibit considerable homology to those of the *nifD* and *nifK*, which may indicate some functional relationship. Because mutations in either *nifE* or *nifN* also prevent FeMo cofactor biosynthesis, it was suggested a $NifE_2N_2$ complex probably acts as a scaffold on which the FeMo cofactor is biosynthesized before being transferred to the MoFe protein (Brigle KE *et al.*, 1987).

Mutations in the *nifV* gene result in the formation of a nitrogenase with a bound citrate rather than homocitrate. The *nifV* product is homocitrate synthase (Zheng L *et al.*, 1997). Substitution of homocitrate using the *in vitro* synthesis of FeMo cofactor (see below) by a range of organic acids revealed that aberrant forms of the FeMo cofactor could be synthesized but they exhibited altered substrate specificities and inhibition susceptibilities (Hoover TR *et al.*, 1988). Specifically, the stereochemistry at the C1 position of homocitrate, chain length, and position of the hydroxyl group can have dramatic effects on the catalytic properties of the resulting nitrogenase.

The mature *nifH* gene product, the Fe protein, was thought of only as the electron donor for the MoFe protein. Then, its involvement in the biosynthesis of the FeMoco was demonstrated (Filler WA *et al.*, 1986). The *nifH* product has at least two functions. It is required for both formation of the FeMo cofactor and its insertion into the immature MoFe protein (Filler WA *et al.*, 1986; Robinson AC *et al.*, 1987). Active Fe protein is not essential. The *nifH* product is not involved in either stabilization of the preformed cofactor or control of the transcription of other *nif* genes (Shah VK *et al.*, 1988). In a later report, a mutant with Ala157 substituted by Ser, which cannot function in nitrogenase turnover and does not undergo the MgATP-induced conformational change, was shown to be active in FeMo cofactor biosynthesis (Gavini N and Burgess BK, 1992). Thus, it is clear that the roles for the Fe protein in the cofactor biosynthesis and in nitrogenase turnover are quite different.

A system for the *in vitro* synthesis of the FeMo cofactor has been developed (Allen RM *et al.*, 1994), which combines an extract from an *A. vinelandii* $nifB^-$ mutant strain

with one from a strain containing a mutation in either *nifN* or *nifE*, and includes added MoO_4^{2-}, homocitrate and MgATP. The system has been used to provide an enzymatic assay for the components required for the biosynthesis of the cofactor. More recently, using an *in vitro* FeMo cofactor synthesis assay, it has been shown that the *nifX* gene product is also necessary for the FeMo cofactor biosynthesis (Shah VK *et al.*, 1998). The products of the *nifW* and *nifZ* genes might also have some role in FeMo cofactor biosynthesis (Jacobson MR *et al.*, 1989a, Shah VK *et al.*, 1998). With *K. pneumoniae*, a small molecular weight protein, encoded by *nifY*, appears to be associated with the immature MoFe protein produced in strains lacking either *nifB* or *nifEN* activity. The *nifY* gene product may stabilize a particular conformation that is amenable to the FeMo cofactor insertion (White TC *et al.*, 1992; Homer MJ *et al.*, 1993). A different small molecular weight protein, which is called γ and is not encoded by *nifY*, appears to serve the same function in *A. vinelandii* (Homer MJ *et al.*, 1995).

4. Genes for Fe-S cluster biosynthesis

Two other *nif* gene products, those of *nifS* and *nifU*, catalyze reactions that are involved in the general mobilization of Fe and S for metallocluster assembly (Zheng L and Dean DR, 1994; Fu W *et al.*, 1994). The *nifS* gene codes for a pyridoxal phosphate-containing cysteine desulfurase (Zheng L and Dean DR, 1994) and catalyzes the *in vitro* reconstitution of an apo-Fe protein whose [4Fe-4S] cluster has been removed by chelation. Thus, the NifS protein is responsible for providing sulfur for the [4Fe-4S] cluster. The *nifU* product may function either as the iron source for [Fe-S] cluster formation or to provide a site for [Fe-S] cluster assembly (Dean DR *et al.*, 1993). The NifU protein is a homodimer that contains two identical [2Fe-2S] clusters (Fu w *et al.*, 1994). These clusters are unlikely to represent the source of iron necessary for nitrogenase [Fe-S] formation, because they are tenaciously bound within the NifU protein and cannot be removed by strong chelation reagents. Later work suggested that ferric ions are bound at individual mononuclear sites on the NifU protein and that these Fe^{3+} ions are rearranged on donation of sulfur by NifS to form a $[2Fe\text{-}2S]^{2+}$ cluster that is bridged between the two NifU subunits. These transient [2Fe-2S] cluster units are formed on

NifU and then released to supply the inorganic iron and sulfur necessary for maturation of the nitrogenase component proteins (Yuvaniyama P *et al.*, 2000).

5. Regulatory genes

Two of the *nif* genes, *nifL* and *nifA*, are regulatory genes (Arnold W *et al.*, 1988). Nif A is a *nif*-specific transcriptional activator protein (Dixon RA *et al.*, 1980; Buchanan-Wollaston V *et al.*, 1981), which interacts with the RNA polymerase σ-factor, σ^{54} (the product of *rpoN*) to initiate transcription at *nif* promoters (Morett E and Buck M, 1989). NifA belongs to a family of transcriptional activators all of which act in concert with an RNA polymerase holoenzyme containing the alternative σ^{54}. The formation of open complexes and transcription initiation is catalyzed by NifA and involves nucleoside triphosphate hydrolysis. Only the *A. vinelandii* NifA protein has been purified in its native form (Austin S *et al.*, 1994). The activity of NifA is usually regulated in response to two major environmental factors, dioxygen and fixed nitrogen.

The NifL protein is an inhibitor of *nif* gene transcription in *K. pneumoniae, A. vinelandii and Enterobacter agglomerans*. NifA activity is inhibited by NifL and requires stoichiometric amounts of the two proteins, implying that the mechanism of inhibition is by direct protein-protein interaction rather than by catalytic modification of the NifA protein (Shi L *et al.*, 1999). This interaction facilitates regulation of NifA activity in response to dioxygen, fixed nitrogen, and energy status, each of which is signaled by an independent pathway (Merrick MJ *et al.*, 2000).

Both *Av*NifL and *Kp*NifL are flavoproteins with FAD as the prosthetic group (Hill S *et al.*, 1996; Schmitz RA, 1997), which is bound to the N-terminal domain. The ability of NifL to inhibit NifA activity is affected by the redox state of the bound FAD, although physiological electron donors to NifL have not so far been identified (Macheroux P *et al.*, 1998). In many diazotrophs, it is clear that not only is *nifA* expression controlled by the global nitrogen regulation (*ntr*) system, but that, the activity of NifA is also responsive to the availability of fixed nitrogen. The mechanism whereby the NifL-NifA system responds to the nitrogen status to control nitrogen fixation is not well defined and it is variable in different organisms (Little R *et al.*, 2000).

6. Other *nif* genes

The primary translation products of the nitrogenase structural genes are not active. Many other *nif*-specific genes are required to activate these components. In the case of the Fe protein, the *nifM* gene product is required for its maturation (Howard KS *et al.*, 1986). The *nifM* gene product has not yet been isolated in an active form, but it appears to be a member of a family of peptidyl-prolyl isomerases (Rudd KE *et al.*, 1995), which assist protein folding by catalyzing the *cis* to *trans* isomerization of certain peptidyl-prolyl bonds.

In the nitrogenase system of *K. pneumoniae*, *nifT* is located between *nifDK*, and *nifY*. The products of all three genes are involved in nitrogenase maturation. It is, therefore, a reasonable hypothesis that the NifT protein might also have a role in the maturation of nitrogenase. However, the phenotypic characterization of *nifT* and *nifT*-overexpressing strains for effects on the regulation, maturation, and activity of nitrogenase identified no properties that were distinct from those of the wild type (Simon HM *et al.*, 1996).

J. The alternative nitrogenases

Two molybdenum-independent nitrogenases have been discovered: one containing vanadium (V), and the other containing only iron (Fe). It was found, that when the structural genes *nifHDK* for the Mo-nitrogenase were deleted in *Azotobacter*, the resulting deletion strains were capable of fixing N_2 in the absence of Mo (Bishop PE *et al.*, 1986). Subsequently, vanadium was shown to stimulate diazotrophic growth of such strains due to the presence of a V-nitrogenase. Later, the existence of a third nitrogenase system (Fe-nitrogenase) was demonstrated in *Azotobacter vinelandii* when it was grown under both Mo and V limitation (Chisnell JR *et al.*, 1988). Not all N_2-fixing organisms have three alternative nitrogenases and, moreover, there appears to be no logic to the way in which these nitrogenases are distributed among microorganisms. For example, *Klebsiella pneumoniae* has only Mo-nitrogenase, whereas *Azotobacter chroococcum* has both the Mo- and V-nitrogenases and *Rhodobacter capsulatus* has the Mo- and Fe-nitrogenases. All three nitrogenase types are found in *A. vinelandii*. Biochemical studies on the Mo-independent nitrogenases have been restricted to the V-nitrogenases from *A.*

chroococum and *A. vinelandii* and the Fe-nitrogenases from *A. vinelandii* and *R. capsulatus*.

1. Biosynthesis of the V- and Fe-only nitrogenases

A. vinelandii has genes encoding all three nitrogenases. The proteins involved in these three systems are encoded by the *nif*, *vnf* and *anf* genes, respectively (Jacobson MR *et al.*, 1989b). Some of the *nif* genes, namely, *nifB, nifM, nifS, nifV* and *nifU*, are required for the biosynthesis of all three nitrogenases (Newton WE, 1992; Eady RR, 1996). Each genetic system has a separate transcriptional activator gene, *nifA*, *vnfA* and *anfA*, respectively, and separate genes encoding the structural polypeptides. Expression of the *vnf* and *anf* systems is inhibited by molybdenum, that is, in its presence only the Mo-nitrogenase is synthesized. In the absence of molybdenum but the presence of vanadium, expression of the *vnf* system is activated, and in the absence of both molybdenum and vanadium, the *anf* system is activated.

In addition to the specific structural genes *vnfHDK* and the activator gene *vnfA*, the *vnf* system also contains specific homologous of the *nifEN* genes, *vnfEN*, which probably encode a scaffold protein on which the FeV cofactor is biosynthesized. NifM protein is required for maturation of VnfH, and NifS and NifU seem to be important for provision of sulfide and probably iron for the biosynthesis of the V-nitrogenase. The VFe protein could be activated *in vitro* by the addition of FeV cofactor to form a fully active protein.

The Fe protein of iron-only nitrogenase is very similar in sequence and properties to the Fe protein of the Mo- and V- nitrogenases. In addition to the *nif* genes mentioned above, the *vnfE* and *vnfN* genes are required for biosynthesis of the iron nitrogenase, implying that $VnfE_2N_2$ can act as a scaffold for the biosynthesis of FeFe cofactor as well as FeV cofactor.

2. Vanadium nitrogenase

The purified Fe proteins of V-nitrogenase from both *A. vinelandii* and *A. chroococum* have the physical and chemical properties characteristic of Mo-nitrogenase Fe proteins. The proteins are dimeric with Mr of about 63 kDa and one [4Fe-4S] cluster per dimer. The EPR spectrum of the dithionite-reduced V-nitrogenase Fe protein and the

redox potential of its [4Fe-4S] cluster are very similar to those of the Fe proteins from Mo-nitrogenase (Smith BE, 1999). The VFe protein has subunits that are highly homologous in amino-acid sequence to the Mo-nitrogenase including the residues that ligate the metalloclusters. The VFe protein, however, also possesses a small (~15 kDa), extra δ-subunit that is encoded by *vnfG* that is essential for activity (Waugh SI *et al.*, 1995). In the VFe protein isolated from *A. chroococcum*, the δ subunit is present in a 1:1:1 stoichiometry with the other subunits (Eady RR *et al.*, 1987). The VFe protein isolated from *A. vinelandii*, exhibits a variable stoichiometry of the α and β subunits and no stoichiometry has been established for the δ subunit (Blanchard CZ and Hales B, 1996).

The amino acid residues involved in binding the P clusters and the FeMo cofactor within the MoFe proteins are strictly conserved in the primary sequence of the VFe protein (Eady RR, 1996). This observation provides a very strong presumptive case for the presence of homologous redox centers in the VFe proteins. More recently, EPR, MCD, Mössbauer, and X-ray absorption spectroscopies and cofactor extrusion studies have confirmed the presence of redox centers that are homologous to the P clusters and the FeMoco (with V replacing Mo) in these VFe proteins (Eady RR, 1996 and references therein).

The requirements for V-nitrogenase activity are very similar to those of the Mo-nitrogenase. Both the Fe protein and the VFe protein are essential, and MgATP is required as is a low-potential reductant, normally dithionite, and the absence of oxygen. Pre-steady-state kinetic studies of V-nitrogenase are few, but the rate of electron transfer between the two component proteins was significantly lower than the equivalent rate for the Mo-nitrogenase (Thorneley RNF *et al.*, 1989b). Substrate reduction by V-nitrogenase has not been investigated nearly as extensively as has that of Mo-nitrogenase, but there are clear differences. For example, C_2H_2 is a poor substrate for V-nitrogenase and N_2 does not compete as effectively with protons for the electrons available during turnover. Therefore, high levels of H_2 evolution occur in the presence of these substrates. Furthermore, C_2H_2 is reduced by V-nitrogenase to both C_2H_4 and C_2H_6 (Eady RR *et al.*, 1987).

3. Fe-only nitrogenase

The FeFe protein of the third nitrogenase was first purified from a *nifHDK*-deletion strain of *A. vinelandii* and, subsequently this protein was characterized from both *R. capsulatus* (Schneider K *et al.*, 1991) and *R. rubrum* (Lehman LJ and Roberts GP, 1991; Davis R *et al.*, 1996). Both of the FeFe proteins were characterized as $\alpha_2\beta_2\delta_2$ hexamers containing only Fe. Spectroscopic studies on these proteins are limited to EPR spectroscopy, which has been used extensively to probe the types of redox center that these proteins contain. Substrate reduction by the Fe-nitrogenase is more like V-nitrogenase than Mo-nitrogenase. C_2H_2 is a poor substrate compared with protons and N_2 reduction is accompanied by high levels of H_2 evolution (Schneider K *et al.*, 1997). The Fe-nitrogenase also produces C_2H_6 in addition to C_2H_4 when it reduces C_2H_2. Although substrate reduction by this alternative nitrogenase has not been investigated really as extensively as with Mo-nitrogenase, it is clear that differences in the cofactor centers and their interaction with neighboring amino acid residues modulate the reactivity of these systems (Smith BE, 1999).

K. Nitrogenase from *Streptomyces thermoautotrophicus*

Streptomyces thermoautotrophicus is a thermophilic, aerobic and obligately chemolithoautotrophic bacterium. It is able to fix dinitrogen with either CO alone or H_2 plus CO_2 as growth substrates. Although CO and H_2 are known as inhibitors of the classical Mo-nitrogenase activity, *S. thermoautotrophicus* is able to fix N_2 in the presence of these gases. It contains an unusual N_2-fixing system. The N_2 fixation reaction was reported (Ribbe M *et al.*, 1997) to require less MgATP to be hydrolyzed per electron pair transferred to substrate ($ATP/2e^- = 2$) than the classical Mo-nitrogenase ($ATP/2e^- = 4$). H_2 also appears to be obligatorily evolved when N_2 is reduced.

This N_2-fixing system is composed of three enzymes, a heterotrimeric molybdenum-containing carbon monoxide-dehydrogenase (called Mo-CODH or St3), a heterotrimeric molybdenum-containing dinitrogenase (St1) and a homodimeric manganese-containing superoxide oxidoreductase (St2). The Mo-CODH couples the oxidation of CO to the reduction of O_2 to generate $O_2^{\cdot -}$ and therefore supplies electrons to St2 by reoxidation of

the superoxide radicals. St2 then delivers the electrons to St1, where N_2 is reduced. St1 contains one molybdenum atom, 14-22 iron atoms and 9-15 acid-labile sulfides per molecule (Ribbe M *et al.*, 1997; Hofmann-Findeklee C *et al.*, 2000). The N-terminal amino-acid sequences of the three subunits of St1 show insignificant sequence similarities with the MoFe protein of classical dinitrogenases and genomic DNA from *S. thermoautotrophicus* did not hybridize with *nifHDK*-probes derived from either *Frankia alnus* or *Klebsiella pneumoniae*. The N-terminal amino-acid sequence of St2 showed high similarity to Mn-superoxide dismutases of bacilli but were unrelated to the Fe protein sequences of classical nitrogenases.

The classical Mo-nitrogenase components are very oxygen-sensitive; however, both nitrogenase proteins of *S. thermoautotrophicus* are stable to the presence of O_2. Moreover, for the formation of ammonia, O_2 is absolutely necessary. In contrast to the direction of electron flow in other nitrogenase systems, which is from ferredoxin/flavodoxin via the Fe protein to the MoFe protein, this superoxide-dependent nitrogenase uses superoxide as a very efficient reductant. The flow of electrons may be described as:

$$4CO + 4H_2O \rightarrow 4CO_2 + 8H^+ + 8e^-$$
$$8O_2 + 8e^- \rightarrow 8O_2\cdot^-$$
$$N_2 + 8O_2\cdot^- + 8H^+ \rightarrow 2NH_3 + 8O_2 + H_2$$

For effective catalysis, the two components of classical Mo-nitrogenase associate in a transient complex (Schindelin H *et al.*, 1997) after the Fe protein has bound MgATP and undergone substantial conformational changes. MgATP hydrolysis and electron transfer then occur. The residues involved in MgATP-binding and hydrolysis are highly conserved among classical nitrogenases and are arranged in Walker A motif and Walker B motifs (Schindelin H *et al.*, 1997). In contrast, this combination of motifs is absent from the superoxide-dependent nitrogenase system (Hofmann-Findeklee C *et al.*, 2000). Finally, this nitrogenase does not catalyze the reduction of C_2H_2 to C_2H_4. The stability of the nitrogenase components towards O_2 makes them ideal candidates for the transformation into plants.

L. Summary and outlook

Considerable progress has been made in understanding the mechanism of action of nitrogenase, particularly since 1970. In the recent past, the major part of nitrogenase research has been focused on the structure of nitrogenase, elucidation of the compositions and functions of all of the *nif*-gene products. The challenge now is to put all the known information together and, with the combined application of biochemical, biophysical and genetic techniques, to determine where and how N_2 binds and is reduced to NH_3. If we understand how nitrogenase functions at the molecular level, we might be able to improve the enzyme's efficiency and increase its fixed-N output. For example, if the obligatory evolution of H_2 during N_2 reduction could be eliminated, up to 25% of the expended ATP could be recovered. Moreover, perhaps the requirement for ATP could be completely circumvented by providing alternatives to the obligatory Fe protein (Newton WE, 2000).

Genetic manipulation of N_2 fixation is the ultimate solution for providing fixed nitrogen input to crop plants and for increasing global food supplies. This solution will also decrease reliance on fossil fuel energy inputs to fertilizer production, costs for transportation and industrial installations, and the potential hazard to the natural ecosystem. Recent genetic manipulation of the recognition and infection processes could result in both new and enhanced symbiotic associations because many plants appear to already have most genes necessary to produce a nodule-like structure. In addition, the success of transferring the *nif* genes from one bacterial genus to another has opened up the possibility of their transfer to crop plants (Merrick M and Dixon R, 1984). However, genetic transfer is not enough. Not only are adequate energy supplies required, but also the nitrogenase proteins must be protected from destruction by O_2. Some success has already been achieved in that some *nif* genes have been transferred into plant cells and been expressed (Dixon R *et al.*, 2000).

The first active cell-free preparation of nitrogenase was isolated in 1960 (Carnahan JE *et al.*, 1960). We have learned a great deal over the years since then; however, many years of research work will be required before we can fully understand this enzyme system and manipulate it for agricultural benefit.

Chapter 2 Materials and Methods

A. General Materials

All general materials were purchased from Fisher Scientific Company (Pittsburgh, PA) unless otherwise specified. The following buffers, purchased from Sigma Chemical Co. (St. Louis, MO), were used in the studies: Trizma Base, Bis-Tris, CHES, HEPPS, HEPES. The desired pH values were obtained through the addition of either HCl or NaOH and KOH.

Sodium dithionite was purchased from Mallinckrodt Chemical Company (Berkeley, CA). Cylinder gases used, such as nitrogen, argon, hydrogen, helium and air, were purchased from AirCo (Randor, PA). Carbon monoxide was purchased from Matheson Products, Inc. (East Rutherford, NJ).

Calibration gases used on the gas chromatograph, including 1000 ppm C_2H_4 in helium, 1000 ppm C_2H_6 in helium, 1000 ppm CH_4 in helium and 1% H_2 in N_2, were purchased from either Alltech Associates, Inc. (Deerfield, IL) or Scott Specialty Gases (Plumsteadville, PA). Aluminum caps, and rubber septa were purchased from Aldrich Organics and Inorganics (Milwaukee, WI). Grey slotted stoppers for the assay vials were purchased from Fisher Scientific Company (Pittsburgh, PA). Disposable test tubes for the protein estimation, creatine assay and ammonia assay were also purchased from Fisher Scientific Company.

B. Anaerobic Techniques

Because nitrogenase is extremely oxygen labile, all of the procedures were performed in anaerobic buffer under an argon atmosphere using the anaerobic Schlenk Line that was designed to replace air with an inert gas, argon, in a closed system. The Schlenk Line is a two-way manifold system with one line connected to an inert gas (argon) tank and the other connected to a vacuum source. The manifold consists of four lines, each of which can be connected to either a gas line or a vacuum line independently via individual stopcocks. Positive argon atmosphere is produced by carefully opening the regulator on the argon gas tank. Constant positive pressure (ca. 1.1 atm) is maintained in

the gas line to prevent the leakage of air into the sample vessels and flasks. The negative pressure generated by the vacuum line is monitored by a mercury manometer, whereas a bubbler is used to monitor the argon flow into the system. A dry ice trap is also used in order to prevent moisture generated by the vacuum from mixing with the pump oil. In order to replace the air with argon, the buffer-containing flask (or other container) is first degassed by applying vacuum over the closed system for about 10 minutes depending on the volume of the buffer, the flask was then filled with argon, followed by the addition of sodium dithionite to produce 2 mM final concentration in the buffer. Finally, the flask was evacuated again and then filled with argon before being kept under a positive pressure of argon. If the atmosphere in an empty container was to be replaced, a cycle of repeated evacuation and flushing with argon was applied. The anaerobicity was checked by methylviologen-soaked filter paper**,** where development of a deep blue color indicated the presence of dithionite and, therefore, essentially no O_2.

C. Construction of Site-Directed Mutant Strains

1. Site-directed mutagenesis using the pALTER vector

Site-directed mutagensis was performed using the pALTER vector (Promega, Madison, WI). As template for the site-directed mutagenesis reaction, the 2.9 kb *Sal*I fragment from pDB14 (Brigle KE *et al.*, 1985, obtained from Dr. Dean of Virginia Tech) containing the complete *nifD* (encodes the α-subunit of the MoFe protein of *A. vinelandii* nitrogenase) as well as parts of *nifH* (encodes the Fe protein subunit of *A. vinelandii* nitrogenase) and *nifK* gene (encodes the β-subunit of the MoFe protein of *A. vinelandii* nitrogenase) was used. The complete purified *Sal*I fragment was cloned into the corresponding sites of the pALTER vector. The reaction was performed according to the manufacturer's guidelines on single stranded DNA. The initial use of a degenerate oligonucleotide to mutate the triplet encoding αSer278 of the *nifD* gene resulted in the mutation to cysteine and leucine only. Specific oligonucleotides were then used to obtain the changes for alanine and threonine.

The resulting plasmid was first transformed into the repair-deficient strain E. *coli* ES 1301 *mutS* for amplification before being transformed into *E. coli* JM109. The

concomitant repair of the knocked out ampicillin-resistant gene of pALTER in the mutagenesis reaction allows an initial screening for ampicillin-resistant clones. All mutations were identified by sequencing on double stranded or single stranded DNA using the Sequenase Kit (USB, Cleveland, OH). The plasmid carrying the single codon mutation is referred to as the mutation vector DNA. In addtion, the Nif$^-$ strain DJ769 carrying a mutation to arginine was constructed by J. Shen.

2. Transformation of the mutated gene into *A. vinelandii*

Retransformation of the altered DNA fragment into *A. vinelandii* was done as described previously (Brigle KE *et al.*, 1987). The selection of the transformable strains is dependent on the proposed phenotype of the transformed mutant strain. If the mutation causes loss of diazotrophy, then a wild type *A. vinelandii* strain is used; if the mutation retains the diazotrophic trait, then rescue of a Nif$^-$ *A. vinelandii* strain would verify its integration into the bacterial chromosome.

The first step in transformation is the growth of an *A. vinelandii* culture that is capable of taking up exogenous plasmid DNA. Using the metal starvation method (Page WJ and von Tigerstrom M, 1979), competent cells were grown on Burk medium (See this chapter section D.1.) without either molybdate or iron. The overnight culture was typically a bright, fluorescent green color due to the overproduction of the Fe-importing siderophores in the medium. Transformable cells were then used in a transformation reaction mixture with 200 μL of competent cells, 25 μL of the mutation vector DNA and 200 μL of 1 × MOPS buffer. Potential Nif$^-$ transformants required an additional selectable marker, in this case rifampicin resistance (rif^R, kindly supplied by Dr. Dean.), which is introduced into the *A. vinelandii* cells simultaneously with the mutation vector DNA by the method of congression. The technique involved the addition of *A. vinelandii* chromosomal DNA, which carries an uncharacterized rif^R marker, to the transformation reaction. The concentration of mutation vector DNA is about 25-fold higher than the rif^R DNA to insure that incorporation of mutation vector accompanies the acquisition of antibiotic resistance.

Nif$^-$, rif^R transformants were selected by outgrowth of the transformation reaction mixture on Burk medium + rifampicin (5 mg/mL) agar plates with or without a fixed

nitrogen source (either urea or ammonium acetate). Double cross-over recombinants grew on the fixed-N^+ plus Rif^+ plates, but not on fixed-N^- plus Rif^+ plates. The phenotypes were verified prior to growing confluent agar plates, which were then used for freezer stocks for subsequent culturing.

D. Cell Growth: Media and Nitrogenase Derepression

1. Nif phenotype screening on solid media

Initial screening of mutant *A. vinelandii* strains was accomplished by growth on agar plates incubated at 30°C. Agar plates consist of a 2% agar in Burk modified medium plus or minus a fixed nitrogen source (either 24 mM urea or 30 mM ammonium acetate). Burk modified medium (Strandberg GW and Wilson PW, 1968) is a minimal bacterial growth medium comprised of 2% sucrose, phosphate buffer (1.5 mM KH_2PO_4, 4.6 mM K_2HPO_4), 0.8 mM $MgSO_4 \cdot 7H_2O$, 0.5 mM $CaCl_2 \cdot 2H_2O$, 40 μM $FeCl_3 \cdot 6H_2O$, 10 μM $NaMoO_4 \cdot 2H_2O$. The agar, sucrose, Mg^{2+} and Ca^{2+} salts were added to distilled/deionized water, autoclaved and then allowed to cool. The phosphate buffer was autoclaved separately. Both the Mo and Fe solution and the urea (or ammonia acetate) solution were filter-sterilized separately as concentrated solutions. They were then added separately to the cooled autoclaved mixture. All mutant strains that were Nif^+ grew on nitrogen-free plates, whereas Nif^- and Nif^{slow} strains do not grow (or grow slowly) on nitrogen-free plates. They were, therefore, grown on urea-supplemented plates.

2. Growth on liquid media and measurement of doubling time ($t_{½}$)

The next step for characterization of a mutant strain is to determine its doubling time during the logarithmic stage of growth on liquid Burk medium. The liquid Burk medium has the same ingredients as in section D.1 above except the agar and a fixed-nitrogen source are omitted. Mutant and wild type strains were first cultured on agar plates containing a fixed nitrogen source (denoted as BN-medium) and then transferred to 250-mL Klett flasks filled with 50 mL of BN-medium. The design of a Klett flask allows the turbidity to be measured on the cell culture as a closed system and so minimizes the risk of contamination. Cell cultures were grown in a G-25 Incubator Shaker (New Brunswick Scientific Co. Inc., Edison, NJ) at 30°C and aerated by shaking at 250-300 rpm. Turbidity

of the cell culture was monitored using a Klett-Summerson meter (Klett Mfg. Co. Inc., NY) fitted with a green No. 54 filter. After the BN-medium liquid cultures had grown to a Klett reading of 150~200 units, which is considered to be a mid-log phase, the entire contents of the flasks were centrifuged using a Sorvall RC-5B Refrigerated Superspeed Centrifuge (DuPont Instruments, Wilmington, DE) and a GSA-type rotor at 8,000×g for ~10 minutes at 4°C. The cell pellet was resuspended in 10 mL of Burk nitrogen-free medium (B-medium), centrifuged again, and the pellet was resuspended in 10 mL of B-medium and used as an inoculum for new Klett flasks. Enough inoculum was added to bring the culture to an initial Klett reading of ~50 units. The flasks were returned to the shaker and the turbidity was measured periodically. The doubling time, $t_{½}$, was then calculated. The doubling time determination was derived from at least two independent cultures for each strain.

For larger batches, 20-50 mL of the mid-log phase cell culture was transferred to Fernbach flasks (2.8-L capacity). Each flask contained 500 mL of BN-medium. The culture was grown to a Klett of ~200 units at which time it was harvested by centrifugation as above, rinsed with 10 mL B-medium, centrifuged, and resuspended in another 10 mL fresh B-medium. The cell suspension was then transferred into new sterilized Fernbach flasks, containing 500 mL B-medium for the synthesis of nitrogenase proteins. The cultures were shaken for 3-4 hours. The cells were harvested by centrifugation and the cell pellet was stored in the –80°C freezer until use.

3. Fermentor batch growth and derepression

Large scale *A. vinelandii* cultures were grown in a 24-L working capacity fermentor (New Brunswick Scientific Co. Inc., Edison, NJ) on modified BN-medium. 200 mL to 400 mL of cells from mid-log growth cultures in Fernbach were used to inoculate the fermentor. Fermentation consists of overnight (12-18 hours) growth at 30°C, a 250 rpm agitation rate, and a 35-40 L/min aeration rate. All mutant strains, both Nif^- and Nif^+ phenotypes, were derepressed for nitrogenase expression.

Derepression of the culture was accomplished as follows. A membrane cassette filter apparatus was used first to filter the cells from the BN-medium and to concentrate the cell-culture volume. A 24-L batch of cells is usually concentrated to less than 2 L. It is

then washed 2-3 times with 2 L of phosphate buffer while still in the fermentor and concentrated again to less than 2 L after each wash. The cell culture is then diluted with 24 L of B-medium and the culture is allowed to derepress for 3-4 hours. After derepression, the cells are harvested by concentration to ~1.5 L, using the membrane cassette filter, and then washed with 5 L of phosphate buffer. The concentrated cell culture is then transferred to several 500-mL centrifuge bottles and centrifuged in the Sorvall RC-5B in a GS-3 rotor at 7,000 × rpm for 20 minutes. The cell pellets are scraped into large plastic bags and stored in the –80°C freezer until used.

E. Crude Extract Preparation

For crude-extract preparation, the frozen cells were thawed and diluted anaerobically at 4°C in degassed 50 mM Tris-HCl buffer, pH 8.0, containing 2 mM sodium dithionite, at the approximate ratio of 1.0 g of cells to 2.0 mL of buffer. A model XL 2015 sonicator (Heat Systems Inc., Farmingdale, NY), which was mounted in a sound dampening polyacrylic box, was used for cell disruption. A low-O_2 atmosphere was maintained by flushing the rosette cell containing the cell suspension with argon both prior to and during the sonication. Small-scale sonication was performed in the 10-mL rosette cell using the micro-probe and a 50% power output. Sonication consisted of 6 cycles of 30 seconds on/off intervals in order to cool the probe in ice. Large-scale sonication was performed in the 250-mL rosette cell, using the large probe, with 100% power output. Sonication consisted of 6 cycles of 1 minute on/off intervals. After sonication, the crude extract was transferred to a degassed, argon-flushed Schlenk flask if the heat-treatment step was to be used. Alternatively, the extract was removed from the rosette cell and transferred into either 10-mL or 60-mL capacity argon-flushed ultracentrifuge tubes using a syringe rinsed with dithionite-containing buffer.

A heat treatment at 55-56°C for 5 minutes was performed for the heat-stable altered nitrogenases. Use of the heat step requires a prior small-scale activity test of the temperature stability of the crude extract. After heating, the extract was rapidly cooled to ~15°C in an ice water bath. This step removed approximately 50% of the soluble proteins from the extract after centrifugation. The soluble cytosolic fraction of the crude extract was separated from the insoluble cellular debris by ultracentrifugation for 90 minutes at

98,000×g at 4°C in a Beckman L5-50B ultracentrifuge (Beckman Instruments, Inc., Palo Alto, CA). The nitrogenase component proteins were located in the dark brown supernatant. This supernatant was transferred anaerobically from the centrifuge tubes to a previously degassed separatory funnel, frozen as droplets into liquid nitrogen, and the frozen pellets stored until used.

F. Protein Purification

1. Chromatographic separation of the nitrogenase components

Crude extract was typically in the volume range of 250-300 mL and had a protein concentration of 30-40 mg/mL. The crude extract was loaded onto a 5 × 15 cm Q-sepharose column (Pharmacia LKB, Uppsala, Sweden). The ion-exchange column had been pre-equilibrated and made anaerobic by passing ~4 L of 25 mM Tris, 2 mM dithionite, pH 7.4 buffer, slowly through the column overnight. This buffer also contained 25 mM NaCl to help dithionite reduce the column. Prior to the crude-extract loading, the anaerobicity of the column was confirmed by 1 mM methylviologen-soaked filter paper, to confirm the presence of dithionite in the column effluent. The extract was loaded by a Rabbit Plus peristaltic pump (Rainin, Instruments Co. Inc., Woburn, MA) at a rate of ~300 mL/hr. The loading was followed by a short wash with 25 mM Tris buffer, pH 7.4, 2 mM dithionite. A linear salt gradient was initiated using an additional peristaltic pump that added a 25 mM Tris, 1 M NaCl (pH 7.4) solution into the low (25 mM NaCl) salt buffer at half of the rate of the pump loading onto the column. By this technique, a linear NaCl gradient passed through the column and resulted in separation of the MoFe protein from the Fe proteins.

Protein elution from the column was monitored at 405 nm by a UA-5 Absorbance/Fluorescence Detector (ISCO Lincoln, NE). The Q-sepharose column was developed with a 0.025 M-to-1 M NaCl gradient. The MoFe protein eluted at ~0.3 M NaCl and the Fe protein eluted at 0.5 M-0.6 M NaCl. The two nitrogenase component proteins were collected in separate anaerobic Schlenk flasks, each protein fraction was concentrated, and then frozen in liquid nitrogen. Concentration was achieved by use of a 300-mL Amicon stirred-cell concentrator, using a molecular weight cut-off (MWCO) membrane (Amicon Inc., Beverly, MA). Prior to use, the concentrator cells were made

anaerobic by rinsing the cell with dithionite-containing buffer. Anaerobicity was verified by methylviologen paper. The MoFe protein was concentrated with a 100K MWCO membrane, whereas the Fe protein was concentrated with a 30K MWCO membrane.

2. Further MoFe protein purification

The MoFe protein fraction as it elutes from the ion-exchange column contains some Fe protein as well as other low molecular weight proteins. For further purification, a large S-200 Sephacryl (Pharmacia LKB, Uppsala, Sweden) column (8 × ~45 cm) was used. This gel filtration chromatography separates proteins based on molecular size. The column was equilibrated overnight with 25 mM Tris, 200 mM NaCl, 2 mM dithionite, pH 7.4 buffer. After 70-100 mL of the MoFe protein fraction was loaded onto the column, the MoFe protein was eluted as one large absorbance peak and was collected as three or four fractions. Each fraction was concentrated using an Amicon cell fitted with a 100K MWCO membrane.

The next step for purifying the MoFe protein was achieved by hydrophobic-interaction chromatography, which relies on the interactions between the hydrophobic sites on the column and the hydrophobic patches on the proteins. Usually, the fraction with the highest activity from the gel-filtration column was purified on a Phenyl Sepharose column (2.5 × 15-20 cm, Pharmacia LKB, Uppsala, Sweden), which was pre-equilibrated with 500-1000 mL of 25 mM Tris, pH 7.4, 400 mM $(NH_4)_2SO_4$, 2 mM dithionite buffer. The addition of ammonium sulfate was to assist in binding the MoFe protein to the hydrophobic phenyl group on the resin matrix. Therefore, the MoFe protein sample was also made 400 mM in $(NH_4)_2SO_4$ before it was loaded onto the column. Proteins were eluted from the column by a decreasing ammonium sulfate gradient. The MoFe protein eluted at ~ 100 mM $(NH_4)_2SO_4$. This peak was typically broad and of low absorbance. Fractions were collected, concentrated, and then frozen in liquid nitrogen. Purity was assessed by a combination of SDS-PAGE, specific activity enhancement, and metal analysis. The highest-activity fraction was exchanged into 25 mM HEPES, 200 mM NaCl, 2 mM sodium dithionite, pH 7.4 buffer by using a small S-200 Sephacryl (Pharmacia LKB, Uppsala, Sweden) gel-filtration column (2.5 × ~40 cm). The MoFe

protein in this buffer was used for all structural, kinetic and spectroscopic characterization.

3. Further Fe protein purification

The Fe protein fraction, which was collected from the ion-exchange column, usually was purified further to obtain a sample with high specific activity for use in an assay. The Fe protein was purified via a second anion-exchange column (2.5 × 15~20 cm). Because the Fe protein fraction eluted from the first column was in high salt concentration, the fraction was diluted with sufficient 25 mM Tris, 2 mM sodium dithionite pH 7.4 buffer to reduce the salt concentration to ~ 100 mM prior to loading. An increasing NaCl gradient from 0.05 M to 1 M was applied to elute the Fe protein from the column. A peak of absorbance was collected in 3-4 fractions and then concentrated using an Amicon cell fitted with a 30 K MWCO membrane. The highest activity fractions were buffer exchanged into 25 mM HEPES, 200 mM NaCl, 2 mM sodium dithionite pH 7.4 buffer.

4. Metal affinity chromatography

A recently developed protein purification technique was explored as an alternative method to purify the MoFe protein from *A. vinelandii*. The method employs attaching a poly-histidine tail to the carboxy-teminus of the α-subunit of the MoFe protein. Poly-histidine polypeptides are known to bind selectively divalent metal cations. Metal affinity chromatography resin is saturated with a divalent metal salt and the bound metal ion acts as an exchange site for the retention and elution of proteins possessing the poly-His tag. Zn^{2+} was chosen for MoFe protein purification in this work.

The procedure used in purifying poly-His-modified MoFe proteins was taken from the His-Bind Resin manufacture's recommendations (Novagen Inc., Madison, WI). All metal affinity chromatography solutions consisted of various concentrations of imidazole combined with a 25 mM Tris, 500 mM NaCl, 1 mM dithionite, pH 7.9 buffer solution.

Preparation of the crude extract proceeded by the prescribed method except that 0.2% sucrose was added into the resuspension buffer to protect the nitrogenase component proteins (Ramos JL and Robson RL, 1985). After centrifugation, the supernatants were pooled and then loaded onto the 100 mM $ZnSO_4$-saturated metal-

affinity column. The column had a resin volume of ~100 mL. It had been pre-equilibrated overnight with 25 mM Tris buffer containing 5 mM imidazole. Imidazole was used in a step gradient to separate the poly-His MoFe protein from other column-bound proteins. After loading, the column was washed with 5 mM imidazole, 25 mM Tris buffer until the effluent was clear. Next, the column was washed with a 40 mM imidazole, 25 mM Tris buffer, which resulted in the elution of a light brown band. This fraction had little MoFe-protein activity in it. The column was then washed with a 250 mM imidazole, 25 mM Tris buffer, which eluted the poly-His MoFe protein. The collected MoFe protein was either diluted into the 25 mM HEPES buffer or purified further by anion-exchange chromatography using a small (2.5 × 15 cm) DEAE-Sepharose (Pharmacia LKB, Uppsala, Sweden) column. Using a linear 0.025 M-to-1 M NaCl gradient, the MoFe protein was eluted from this column as one large peak, which was collected, concentrated, and then frozen for later use.

At each stage of the purification process, the purity and specific activity of the various collected fractions were assayed.

G. Gel Electrophoresis

SDS-PAGE (sodium dodecyl sulfate-polyacrylamide gel electrophoresis) was used to estimate and compare the purity of the fractions as well as to evaluate the effectiveness of nitrogenase derepression during cell growth. Gel electrophoresis was performed with a model SE250 mini-gel apparatus (Hoefer Scientific Instruments, San Francisco, CA). Samples and gels were prepared according to Laemmli (1970). Optimal resolution conditions were obtained from a 4% total acrylamide plus 0.1 % cross-linker stacking gel and a 12% total acrylamide plus 0.32% cross-linker separating gel. Samples were denatured by boiling in SDS- and β-mercaptoethanol-containing sample-fixing solution for 5 minutes. Proteins (5-10 μg) were loaded into each well. Gel electrophoresis was performed at 25 mA constant current for 1-1.5 hours. Gels were stained at room temperature overnight in a 0.1% R-250 Coomassie blue stain (Bio-Rad laboratories, Richmond, CA), destained in a mixture of 40% methanol and 10% acetic acid, and then stored in 5% methanol with 7% acetic acid. A 667 instant film Polaroid photograph (Polaroid Corp., Cambridge, MA) was taken as a permanent record of each gel.

H. Protein Determination

Proteins were estimated using the Lowry method with the Folin-Ciocalteau modification for increased protein sensitivity (Lowry OH *et al.*, 1951). A bovine serum albumin (BSA) stock solution (2 mg/mL in 0.9% NaCl and 0.05% NaN_3 water solution) was used to generate a standard curve. Absorbance was measured at 750 nm on the model 8452 Diode Array Spectrophotometer (Hewlett-Packard, Palo Alto, CA).

I. Metal Analysis

An alternative indicator of nitrogenase purity is the metal content of the proteins. By measuring the molybdenum and iron concentrations from a known concentration of protein, it was possible to estimate the number of metal atoms per molecule of either MoFe protein or Fe protein. Ideally, a pure sample of MoFe protein will have 2 g-atoms of Mo and 30 g-atoms of Fe per mole of protein. The closer any particular MoFe-protein sample came to these values for metal content, the purer the sample was considered to be. The relative concentration of Mo and Fe in a MoFe protein was also used to estimate the concentration of the two types of metal centers, the FeMo cofactor and the P cluster. Again, the ideal MoFe protein would have a Fe:Mo ratio of 15:1 if both clusters were found in equal proportion.

Purified MoFe protein samples were analyzed for metal content using inductively coupled plasma atomic emission spectrometry (ICP-AES). Metal analysis was performed by C.H. Dapper (Department of Biochemistry, Virginia Tech), using a Plasma 400 Emission Spectrometer (Perkin-Elmer, Rockville, MD). Samples generally consisted of 3-5 mg of purified protein in a 5 mL of 25 mM HEPES, 200 mM NaCl, pH 7.4 buffer. The volume of all the samples allowed for at least three replicate readings for Mo and Fe contents, and the concentration was high enough so that the readings of each sample were within the reading ranges of the standard solution. Results were recorded as parts per million (ppm) of either Mo or Fe. After subtraction of the buffer blank, data were then converted to concentrations to yield g-atoms of Mo and Fe per mole of sample.

J. Steady-state Assays of Purified Proteins

Once the component proteins of nitrogenase were purified, steady-state assays were performed to characterize the wild type and altered MoFe protein. Specific activity measurements were obtained from the steady-state H_2-evolution or C_2H_2-reduction assays. The substrate-reduction rate was measured in nanomoles of product evolved per minute per mg of the component protein under study in the presence of an optimal amount of the complementary component protein.

1. H_2 evolution

This assay was routinely used to measure the activity of both component proteins. Assays were performed at 30^{o}C in 9.00 – 9.25 mL capacity reaction vials. Each 1.0-mL reaction solution consisted of nitrogenase component proteins, sodium dithionite, a MgATP-regenerating system, and anaerobic, argon atmosphere of just more than 1 atm pressure. The MgATP-regenerating system (stock reaction mixture) contained a final concentration of 0.1 M ATP, 0.25 M $MgCl_2$, 0.3 M creatine phosphate, and 500 units/mL of creatine phosphokinase in 25 mM HEPES buffer, pH 7.4. Each assay vial contained 0.3 mL of stock reaction mixture. All vials were kept on ice both to minimize turnover of the regenerating system and to prevent denaturation of the kinase during preparation. The vials were then capped by crimping an aluminum seal over a rubber septum. The vials were subjected to four alternating cycles of 100 seconds of vacuum-degassing and 15 seconds of argon-flushing via a custom-made vacuum/gas manifold (Corbin JL, 1978). During the process, a 200 mM sodium dithionite solution was prepared by adding solid sodium dithionite (0.348 g) to anaerobically prepared 25 mM HEPES, pH 7.4 buffer (10 mL).

After the vials had been degassed and filled with argon, they were placed in a model G76 Gyrotory Water bath Shaker (New Brunswick Scientific Co. Inc., Reno, NV) for 2-3 minutes. An aliquot (100 μL) of the 200 mM dithionite solution was added to each vial using a gas-tight syringe (Hamilton Co., Reno, NV). Then, each vial was vented to atmospheric pressure. After these steps, the component proteins of nitrogenase were added. Usually, purified Fe protein was added first, and then the MoFe protein was added

to initiate the reaction. After a preset time interval, reactions were stopped by addition of 0.3 mL of 0.5 M EDTA, pH 8.0 solution by injecting it through the rubber septum.

The gas contents of each assay vial were analyzed by removal of a 200 μL gas sample using a pressure-Lok, lockable gas-tight syringe (Precision Sampling Corp., Baton Rouge, LA), and injection of the sample into a Model 8A gas chromatograph (Shimadzu, Kyoto, Japan) fitted with a thermal conductivity detector (katharometer). H_2 produced during the nitrogenase reaction was determined by separation of the gas sample components over a 1 m × 2 mm I.D. molecular sieve 5-Å, 60/80 mesh column (Supelco Inc., Bellefonte, PA) operating at an oven temperature of 40°C. Argon was the carrier gas at a flow rate of 70 mL/minute. Retention times were recorded and peak areas were integrated by a CR501 Chromatopac integrator (Shimadzu, Kyoto, Japan). Peak areas were calibrated by reference to a 1% H_2 in N_2 standard (Scott Specialty Gases, Plumsteadville, PA). H_2 was identified by its retention time, which distinguished it from any remaining O_2 and N_2 peaks from air, as the sample passed through the detector.

2. C_2H_2 reduction

The procedure for the C_2H_2-reduction assay was essentially the same as for the H_2 evolution assay, except that the atmosphere of the anaerobic assay vials was 10% C_2H_2/90% argon. The C_2H_2 gas was prepared by the reaction of CaC_2 with water. After the venting of excess pressure from the argon filled vials, 1 mL of C_2H_2 gas was added to each assay vial, and the vials are replaced in the shaker water bath for 2-3 minutes at 30°C. These vials were then vented to atmospheric pressure again prior to initiating the enzymatic reaction. After the assay, the products were analyzed on a model GC-14A gas chromatograph (Shimadzu, Kyoto, Japan) equipped with a flame ionization detector. A 200 μL gas sample was removed from each assay vial and injected into a 3 m × 2 mm Porapak N (Supelco Inc., Bellefonte, PA) column operating at a column oven temperature of 80°C with a helium carrier gas flow rate of 90 mL/min. The injector temperature was set at 180°C and the detector temperature was 200°C. The C_2H_4 peak eluted after about 1.1 minutes and peak area was integrated using a C_2H_4 gas standard of 1000 ppm C_2H_2 in helium. A separate 200 μL gas sample was also assayed for H_2 content using the Shimadzu GC-8A gas chromatograph as described above. In some cases, C_2H_6

was also produced. In such cases, peak areas were integrated using a C_2H_6 gas standard, which was 1000 ppm C_2H_6 in helium.

3. NH_3 production

Ammonia production was assayed by the indophenol method (Chaney AL and Marbach EP, 1962). Although this colorimetric assay is reasonably specific and sensitive, it is also prone to interference by reagents used in the nitrogenase reaction, for example, dithionite, Tris buffer, and creatine. Therefore, the Tris buffer used for all purification protocols was always replaced by HEPES buffer before NH_3 measurements were undertaken. Using a modified indophenol method (Dilworth MK and Eldridge ME, 1992), reactions were terminated by addition of 0.3 mL of 0.5 M EDTA (pH 7.5). After all gas products were quantified using gas chromatography, the liquid mixture (1.0 mL) was removed from the assay vial and passed through a Bio-Gel AG 1×2 (Bio-Rad, Hercules, CA) anionic exchange resin (Cl^- form, 200-400 mesh). The resin bound most of the inhibitory reagents of the color development reaction. An individual disposable column (2.5 cm × 0.6 cm) was used for each assay sample and was made from a glass Pasteur pipette plugged with Pyrex fiberglass wool (Corning Inc., Corning, NY).

After the 1.0 mL sample was applied to the column, two 0.5-mL water rinses were used to wash the ammonia from the column. A fraction of the effluent (0.5-0.9 mL, depending on the activity of the MoFe protein) was used for the assay and the total volume was brought up to 1.5 mL with distilled water. A 0.3 mL aliquot of sodium phenate solution (5% phenol, 2.5% NaOH) was added, followed by the simultaneous addition of 0.45 mL of 10% sodium hypochloride and 0.45 mL of 0.02% sodium nitroprusside. After 40 minutes incubation at room temperature, samples were transferred individually to a 1-cm path length disposable cuvette and the sample's absorbance was measured at 630 nm in the model 8452 diode array spectrophotometer. Ammonia concentration was determined by comparison with an $(NH_4)_2SO_4$ standard curve, which was linear in the range of 0-200 nmols of NH_4^+. A spiked blank (carried 100 nmols of $(NH_4)_2SO_4$), which consisted of a nitrogenase activity assay that had been inactivated with EDTA prior to initiation of the enzymatic reaction, was used to determine ammonia

recovery. Based on this recovery, a correction factor for the ammonia concentration values was determined.

4. ATP hydrolysis determination by the creatine assay

ATP hydrolysis was measured indirectly through determining the released creatine by the creatine colorimetric detection method (Ennor AH, 1975). The protocol used also included using small anion-exchange columns to remove interfering compounds from the nitrogenase activity assay mixture. The reaction was stopped by 0.3 mL of 0.5 M EDTA (pH 7.5), and all fractions were kept on ice throughout the assay to minimize the generation of creatine after cessation of the enzyme activity assay. The procedure used was the same as described for the ammonia assay. A smaller fraction of the aqueous effluent was used for the assay compared to that for the ammonia assay. Usually, 0.03 mL to 0.1 mL of solution was used for the creatine assay. The sample was brought to 0.5 mL with distilled water, 1.0 mL of a 1% naphthol, 6% NaOH, 16% Na_2CO_3 solution was added to each sample, followed by 0.5 mL of 0.05% diacetyl solution to initiate the reaction. After 20 minutes incubation, the reaction was stopped by the addition of 2.5 mL of distilled water. The creatine content was then calculated by measurement of the absorbance of each sample at 530 nm in the spectrophotometer. A creatine standard curve ranging from 0 to 250 nmols was used to calibrate the absorbance reading after correction with a killed blank, which consisted of a nitrogenase activity assay that had been inactivated with EDTA prior to initiation of the enzymatic reaction.

5. K_m for C_2H_2 (C_2H_4 formation) and C_2H_2 concentration titration

The Michaelis constant, K_m, is the substrate concentration at which the specific activity of the enzyme is half the value of the maximum specific activity. The value of K_m is an indicator of the apparent binding affinity of the active site for the substrate. The lower the value of K_m, the tighter the substrate apparently binds to the enzyme. The K_m for C_2H_2 was obtained from the nitrogenase activity assays in the presence of non-saturating C_2H_2 concentrations. Different concentrations of C_2H_2 were added to each assay vial. The volumes of the C_2H_2 gas added were chosen to produce concentrations that range 5-10-times both lower and higher than the K_m. The assay was duplicated for

each concentration of C_2H_2. The rate of C_2H_4 production was determined for each assay and a double reciprocal (Lineweaver-Burk) plot of substrate concentration versus specific activity of C_2H_4 production was used to derive the K_m and V_{max} values.

High concentrations of acetylene in the nitrogenase assay are known to cause a decrease of total specific activity for the wild type Mo-nitrogenase (Hwang JC and Burris RH, 1972; Fisher K *et al.*, 2000c). The procedure used to generate the higher C_2H_2 concentrations involved flushing with 100% C_2H_2, followed by dilution with argon. In this way, a complete titration over the range 0 to 100% C_2H_2 was available for use in the assays.

6. Response to the inhibitior, CO

The responses of wild type and altered MoFe proteins to a saturating (10%) concentration of CO were compared. Nitrogenase activity assays were performed under different gas atmospheres, 100% Ar, 100% N_2 and 10% C_2H_2/90% argon, in the absence and presence of 10% CO. CO (1 mL) was added to the assay vials containing the designated gas phase at atmosphere pressure. The assay vials were then equilibrated in a shaker water bath for 2-3 minutes at 30^{o}C and vented to atmosphere pressure before the addition of the nitrogenase component proteins to start the reaction.

7. Electron flux titration assays

The response of the nitrogenase system to a varying electron flux has proven to be an important diagnostic of the overall mechanism. Alterations in total substrate-reduction rates, ATP-hydrolysis rates, and patterns of electron allocation to alternative products are some of the consequences of changing the electron flux through nitrogenase. Electron flux was controlled by varying the molar ratio of the Fe protein to the MoFe protein in fixed-total-protein activity assays. The total protein was fixed at either 0.5 or 1.0 mg per 1 mL assay. The amounts of both Fe and MoFe protein were varied in compensatory fashion to give the desired molar ratio while maintaining a constant total protein concentration. Electron flux ranged from a low flux-producing Fe protein:MoFe protein ratio of 1:10 to a high flux ratio of 60:1.

K. Electron Paramagnetic Resonance

In addition to charge and mass, an electron also has angular momentum and spin. A spinning electron generates a magnetic field and the strength of this magnetic field is referred to as the magnetic moment of the electron. An externally applied magnetic field forces the magnetic moment of an electron to assume one of the two possible orientations. Either the electron spin is aligned with the external magnetic field and is assigned a –1/2 spin, or the electron is aligned against the external magnetic field and has a +1/2 spin. If two electrons are paired, their spins oppose and cancel each other resulting in a diamagnetic state. If a molecule contains one or more unpaired electrons, the molecule is paramagnetic and can be studied by electron paramagnetic resonance (EPR), sometimes known as electron spin resonance (ESR) spectroscopy. The EPR spectrum gives information about the immediate environment of an unpaired electron, the spin concentration, and the interaction of the unpaired electron spins with nuclear spins. EPR has been proven useful in the study of Fe-S cluster proteins because these clusters often have unpaired electrons in various surroundings.

The EPR spectrum of the MoFe protein of nitrogenase can only be observed at temperatures below 30K. The analyses were run in our laboratory by Dr. Fisher on a Varian E-line spectrometer (Varian Associates, Palo Alto, CA). The EPR spectra of the samples were recorded at a microwave frequency of about 9.2 GHz and a microwave power of 20 mW with a 100 kHz field modulation of 1.6 mT (millitesla) at 12 K maintained by liquid helium.

Purified MoFe protein was prepared for EPR analysis and placed in an anaerobic ~20 cm × 3 mm I.D. quartz EPR tube (Wilmad Glass Co. Inc., Buena, NJ) that had been degassed several times and flushed with argon. Sample concentrations varied around 15 mg/mL or higher. Sample volume was 300 μL and was injected into the EPR tube by a gas tight syringe. The sample tube was then slowly frozen in liquid nitrogen and kept in the liquid nitrogen until analyzed.

Chapter 3

Azotobacter vinelandii α278 Mutant Strains: Growth and Characterizations of the Crude Extracts

A. Introduction

Mo-nitrogenase is a metalloenzyme consisting of two component proteins, called the Fe protein and the MoFe protein. During nitrogenase turnover, the specifically required Fe protein delivers single electrons sequentially to the MoFe protein, which contains the substrate-reduction site. Each electron transfer involves the association and subsequent dissociation of the two component proteins. Because all the substrate reduction requires at least two electrons, at least two association-dissociation cycles must occur between the reduced Fe protein and the MoFe protein to accumulate sufficient electrons. The MoFe protein is known to contain two types of metalloclusters, the FeMo cofactor and the P cluster. It is generally believed that the P clusters are redox centers involved in the initial acceptance of electrons from the Fe protein (Peters JW *et al.*, 1995a; Lanzilotta WN and Seefeldt LC, 1996; Schindelin H *et al.*, 1997). The FeMo cofactor is responsible for the biologically unique S=3/2 EPR signal that is observed in whole cells, crude extracts and purified MoFe protein. It provides the site of substrate binding and reduction (Scott DJ *et al.*, 1990, 1992).

The FeMo cofactor consists of a metal-sulfur framework ($MoFe_7S_9$) and one molecule of (R)-homocitrate (Chan MK *et al.*, 1993). This framework is constructed from S-bridged $MoFe_3S_3$ and Fe_4S_3 cluster sub-fragments. The cofactor is buried within the MoFe protein α-subunit and is covalently attached to the protein by the thiolate side chain of αCys275 and by the δ-nitrogen of the side chain of αHis442, which bind to the terminal Fe and Mo atoms, respectively. Although these two residues provide its only covalent ligands, the FeMo cofactor is tightly packed within the MoFe protein by (i) residues that approach each of its three faces (αVal70, αArg359 and αPhe381), (ii) residues that have the potential to hydrogen bond to the bridging sulfide atoms (αArg96,

αHis195, αGly356 and αGly357), and (iii) a residue that has the potential to hydrogen bond to a S atom contained within the $MoFe_3S_3$ sub-cluster fragment (αArg359) (Lee H-I *et al.*, 1998). The special arrangement of these residues in relation to the FeMo cofactor is shown in Figures 1.6 and 3.1. It is possible to locally perturb the active center of the MoFe protein by placing appropriate amino-acid substitutions in its environment and then to use the resulting disruption of catalytic, spectroscopic or redox function as a means to gain insight into the nitrogenase mechanism.

The 278-serine residue of the α-subunit of the nitrogenase MoFe protein was targeted for substitution in this work because of (i) its proximity to αArg277, which seems to be involved in the control of the protein's ability to bind and to reduce substrates (Shen J *et al.*, 1997), (ii) its hydroxyl group hydrogen bonds to the Sγ of αCys275 that ligates the FeMo cofactor, and (iii) the conservation of the Ser residue at this position for the Mo-nitrogenases from other organisms and in the alternative nitrogenases (Dean DR and Jacobson MR, 1992). To determine the functional role of this residue in catalysis by nitrogenase, five mutant strains were constructed by site-directed mutagenesis at this position. In this chapter, initial characterization of the five *A.vinelandii* mutant strains is described at the crude extract-level.

B. Methods

1. Mutant strain construction and diazotrophic growth

The techniques used to construct the mutant strains harboring the altered MoFe proteins with substitution at the α-278 position were described in the Materials and Methods chapter (see Chapter 2.C.1). The pALTER vector was used for the site-directed mutagenesis. Specific oligonucleotides were used to construct the $\alpha278^{Thr}$ and $\alpha278^{Ala}$ strains, whereas a degenerate oligonucleotide was used for the $\alpha278^{Cys}$, $\alpha278^{Leu}$ and $\alpha278^{Arg}$ strains. Purified plasmids were separately transformed into competent wild type *A. vinelandii* cells as in Chapter 2.C.2 section. The recombinants with the desired phenotype were cultured and made into freezer stocks. The major part of the mutant strain construction was done by Dr. Kloos. The $\alpha278^{Arg}$ strain was made by Dr. Shen.

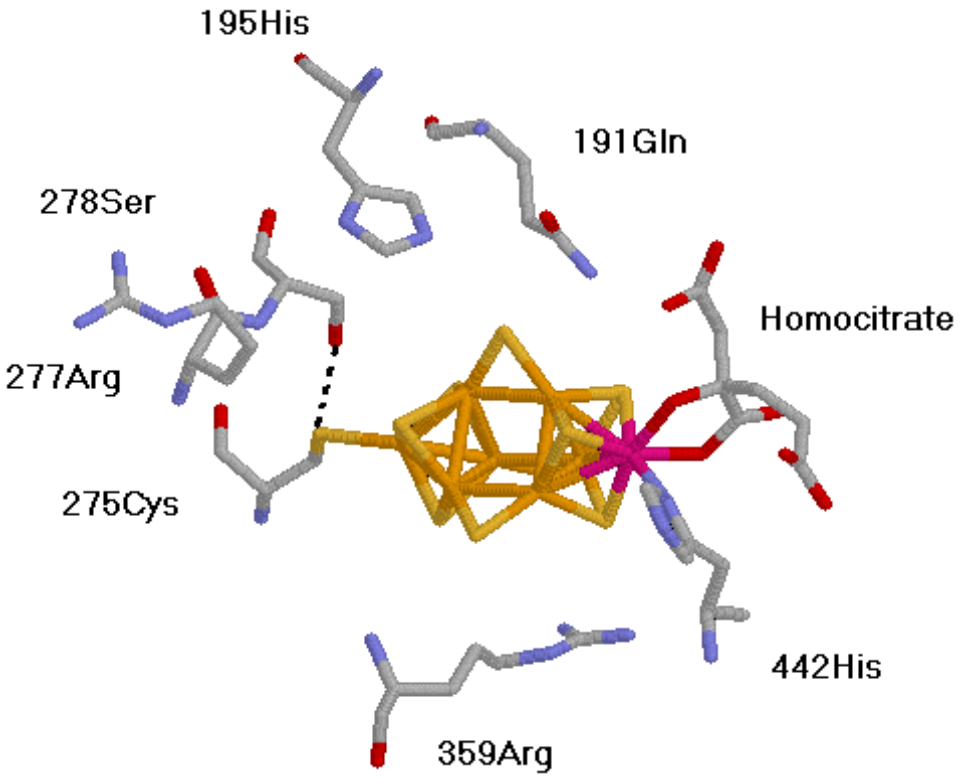

Figure 3.1 FeMo cofactor and selected residues in its surrounding environment. αSer278 is hydrogen bonded to αCys275 as indicated by the dashed line. This figure is adapted from Peters JW *et al.*, 1997 and is prepared using the SpdbViewer program (Guex N *et al.*, 1997).

Each mutant strain constructed was subjected to a diazotrophic growth experiment for the purpose of determining its Nif phenotype and, if applicable, the doubling time ($t_{1/2}$) of the strain. The doubling time determination experiment was performed as in Chapter 2.D.2.

Small batches of *A. vinelandii* wild type and mutant strains were grown at 30°C in Fernbach flasks on a modified Burk medium containing 10 μM Na_2MoO_4, which is sufficient to repress the alternative nitrogenase systems. When required, a fixed-nitrogen source of filter-sterilized urea was added to a final concentration of 20 mM. Large-scale *Azotobacter* cultures were grown in 24-L fermentor on the same medium as above. All mutant strains that did not grow in nitrogen-free medium were grown on urea-supplemented medium and then derepressed for nitrogenase synthesis. As described in Chapter 2.D.3 section, the culture was concentrated in the fermentor to ~ 2 L to remove as much of the fixed-nitrogen source as possible, and then reinoculated into Burk nitrogen-free medium to a final volume of about 24 L. After derepression for 3 hours, cells were harvested and then stored at –80°C until used.

2. Crude extract preparation and characterization

To prepare the crude extract for the nitrogenase activity assay, ~ 3 g of cells were used. After the cells were thawed, they were diluted in ~ 6 mL of degassed 50 mM Tris-HCl, pH 8.0, containing 2 mM sodium dithionite. The cell suspension was broken using a Heat System Sonicator as described in Chapter 2.E section. The extract was transferred anaerobically into centrifuge tubes and centrifuged for 90 minutes at 98,000 × g at 4°C. The supernatant was frozen into liquid nitrogen and stored until used.

Protein content of the crude extract was estimated using the Lowry method (Lowry OH *et al.*, 1951) with bovine serum albumin (0-0.1 mg/mL) as a standard. MoFe-protein and Fe-protein specific activities were measured in the crude extracts in the presence of an optimal amount of the purified complementary protein. When needed, either CO or C_2H_2 were added by gas-tight Hamilton syringe to the appropriate assay vial, which contained either a 100% argon or a 100% N_2 atmosphere.

C. Results

The five α-278 mutant strains exhibit a variety of Nif phenotypes. Two of them, which carry the altered MoFe protein with substitution to leucine or arginine, cannot fix N_2. The other three strains are capable of diazotrophic growth. However, they have impaired growth rates under diazotrophic conditions in nitrogen-free medium compared to the wild type strain, which is indicated by their longer doubling times (see Table 3.1).

The MoFe-protein and the Fe-protein specific activities in the crude extracts prepared from the derepressed cell cultures of the wild type and α-278 mutant strains are summarized in Table 3.2. The comparable specific activities of the Fe protein in the mutant strain crude extracts to that of the wild type indicate effective nitrogenase derepression during cell growth. This is also confirmed by the SDS-PAGE results (Figure 3.2), which shows that both the MoFe protein and the Fe protein have been synthesized in comparable amounts by the wild type strain and the mutant strains.

The different nitrogen-fixation phenotypes shown by these mutant strains correlated well with their C_2H_2- and H^+-reduction activities in the crude extracts, which range from 0.5% to 95% of the wild-type activity (Table 3.2). Crude extracts of the $\alpha 278^{Cys}$ and $\alpha 278^{Ala}$ strains, exhibit about a 50% reduction in activity under both 100% argon and 10% C_2H_2 in argon when compared to the wild type. The substitution to threonine exhibits only a slightly reduced overall specific activity. The two Nif^- strains, $\alpha 278^{Leu}$ and $\alpha 278^{Arg}$, are highly impaired in H_2 evolution as well as in acetylene reduction. The activities of $\alpha 278^{Leu}$ and $\alpha 278^{Arg}$ crude extracts are 6% and 0.5% of the wild type activity, respectively.

Substitutions at the α-278 position not only changed the specific activity of the altered MoFe protein, but also influenced its distribution of electron flux among the products formed (Table 3.2). The strains with substitution by either cysteine or alanine gave very similar results. Under 100% N_2, about 5% less of the electron flux goes to ammonia production and under 100% N_2, about 20% less of the electron flux goes to C_2H_4 production, compared to those of wild type. The homologous threonine substitution gave rise to more dramatic changes in the electron distribution, with only about 50% of the total electron flux going to ammonia under 100% N_2 and about 50% to C_2H_4 under

Table 3.1 Nif phenotype and diazotrophic growth rates of the wild type and α-278 mutant strains.

Strain	**Nif phenotype**	**Doubling time (hrs)**
Wild type	+	2.4±0.1
$\alpha278^{Thr}$	+	3.3±0.1
$\alpha278^{Cys}$	+	3.1±0.1
$\alpha278^{Ala}$	+	2.7±0.1
$\alpha278^{Leu}$	–	NG
$\alpha278^{Arg}$	–	NG

NG= no growth

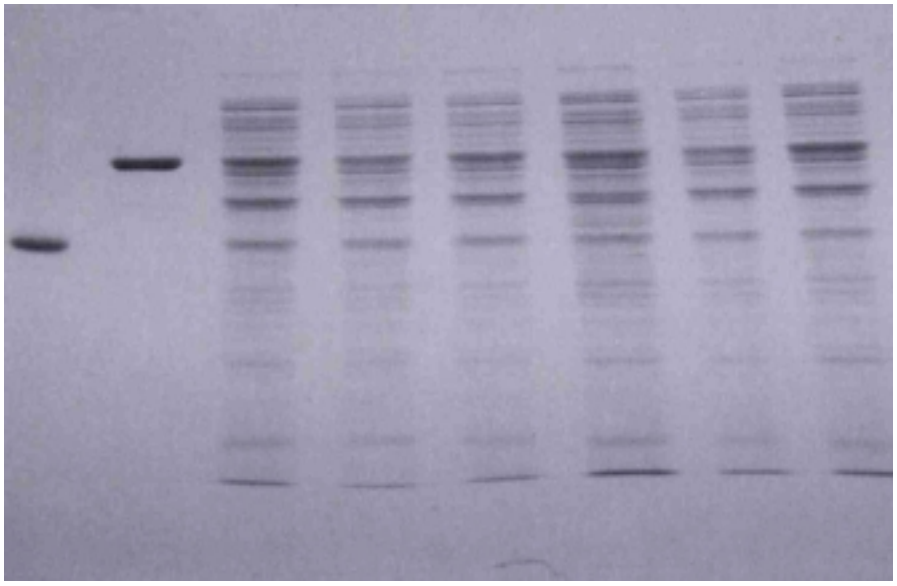

A B C D E F G H

Figure 3.2 SDS-PAGE of crude extracts from the α-278 mutant strains and wild type. Lane A: purified wild type Fe protein; Lane B: purified wild type MoFe protein; Lane C: wild type crude extract; Lane D: $\alpha 278^{Thr}$ crude extract; Lane E: $\alpha 278^{Cys}$ crude extract; Lane F: $\alpha 278^{Ala}$ crude extract; Lane G: $\alpha 278^{Leu}$ crude extract; Lane H: $\alpha 278^{Arg}$ crude extract.

Table 3.2 The MoFe protein and Fe protein specific activities in the crude extract of α-278 mutant strains under different assay atmospheres.

Strain[a]	**Under Ar**[b]		**Under 10% C_2H_2**[c]		**Under 100% N_2**[e]
	MoFe, H_2	Fe, H_2	C_2H_4 (%e^-)[d]	H_2 (%e^-)	H_2 (% e^-)[f]
Wild type (αSer278)	130	80	105 (89%)	13 (11%)	45 (35%)
α278^{Thr}	125	110	54 (48%)	58 (52%)	60 (48%)
α278^{Cys}	75	115	43 (68%)	20 (32%)	29 (39%)
α278^{Ala}	75	108	50 (71%)	20 (29%)	31 (41%)
α278^{Leu}	8.0	102	2 (29%)	5 (71%)	8.0 (100%)
α278^{Arg}	<1.0	100	0.6 (86%)	0.1 (14%)	<1.0 (100%)

All values are the results of at least four replicate measurements. The error range is less than 10%.

[a] All strains are deleted for the uptake hydrogenase structural genes resulting in Hup$^-$ phenotype.

[b] MoFe protein and Fe protein specific activities in the crude extract are listed as nmol of H_2 produced per minute per mg of total protein in the crude extracts under a 100% argon atmosphere. All assays were performed with optimal amount of purified complementary protein present.

[c] MoFe protein specific activity in the crude extract are listed as nmol of C_2H_4 and H_2 produced per minute per mg total protein in the crude extracts under a 10% C_2H_2 / 90% argon atmosphere in the presence of optimal amount of purified wild type Fe protein.

[d] Numbers in parentheses represent the percentage of total electron flux to each product.

[e] MoFe protein specific activity in the crude extract is listed as nmol of H_2 produced per minute per mg total protein in the crude extracts under a 100% N_2 atmosphere in the presence of optimal amount of purified wild type Fe protein.

[f] Numbers in parentheses represent the percentage of total electron flux to H_2 evolution under 100% N_2 compared to that of under 100% argon. For those strains which can fix N_2, this number indicates the approximate percentage of total electron flux to H_2 evolution under 100% N_2.

10% C_2H_2 compared to 65% and 85% with the wild type. The leucine substitution produced a much lower activity as well as much lower percentage of total electron flux used for C_2H_4 production when reducing C_2H_2. It did not reduce N_2 to NH_3.

The addition of 10% CO has no effect on the hydrogen evolution under 100% argon and the total activities under either 100% N_2 or 10% C_2H_2 for all of these mutants (data not shown).

D. Discussion

Amino acid sequence comparison reveals that the αSer278 is a strictly conserved residue among the MoFe proteins of Mo-nitrogenases from other organisms and the alternative nitrogenases (Dean DR and Jacobson MR, 1992). This residue is also hydrogen bonded to the direct ligand of the FeMo cofactor, αCys275 residue (Kim J and Rees DC, 1992 a,b). All of these indicate that this residue may play a role in nitrogenase function.

Three of the five mutant strains with substitutions at residue αSer278 gave a Nif^+ phenotype. Crude extracts prepared from these three mutant strains, $\alpha278^{Thr}$, $\alpha278^{Cys}$ and $\alpha278^{Ala}$, also have comparable activities to that of the wild type strain. Thus, a serine residue at this position is not absolutely required for nitrogenase activity. However, both of the leucine and arginine substitutions, which have bigger side chains than the other substitutions, cause a dramatic loss of activity. The size of these side chains probably significantly perturbs the environment of the cofactor so that the FeMo cofactor in these altered MoFe proteins may not be able to either accept electrons/protons or reach the redox state required for substrate reduction. The αSer278 residue is next to the αArg277, which was suggested to be involved in providing a possible entry/exit route for substrates and products (Kim J and Rees DC, 1992 a,b; Shen J *et al.*, 1997). Therefore, maybe substitution to either leucine or arginine also interrupts the entry of the substrates into the interior of the α subunit, resulting a low activity for the leucine-substituted mutant strain and essentially no activity for the arginine-substituted strain.

For the $\alpha 278^{Thr}$, $\alpha 278^{Cys}$ and $\alpha 278^{Ala}$ mutant strains, the substitutions also influenced the electron distribution among the products. Placing a threonine at α-278, which is a conservative substitution for serine, gave rise to more dramatic changes in the electron distribution among the products than the other two high-activity substitutions, cysteine and alanine, neither of which has the hydroxyl group. This result indicates that the extra methyl group in threonine disrupts the ability of the FeMo cofactor to engage in the reduction of both N_2 and C_2H_2. Another possibility could be that threonine residue interacts with the nearby residues, such as the αArg277 or the αHis195, close to the FeMo cofactor. Without changing the overall activity of the altered MoFe protein much, the resulting disturbed polypeptide environment of the FeMo cofactor may subtly alter its interaction with different substrates and differentiate among the various substrates.

The crude extract of the $\alpha 278^{Leu}$ mutant strain also exhibited an altered allocation of electron flux with only about 30% of its total electron flux going to C_2H_4 production when assayed under 10% C_2H_2. It seems that the threonine and leucine substitutions affect C_2H_2 reduction more than the cysteine and alanine substitutions do. Recall that previous work (Shen J *et al.*, 1997) on the $\alpha 277^{His}$ MoFe protein suggested one of the C_2H_2-binding sites is close to the [Fe_4-S_3] subcluster of the FeMo cofactor. It is then reasonable to expect some changes for C_2H_2 reduction in these altered α-278 mutant strains. Purification and characterization of the altered MoFe proteins from these mutant strains will allow us to compare the electron distribution pattern among the products in more detail and, by doing so, we will also know if the purification process affects the properties of the protein.

Chapter 4
Purification and Characterization of the Altered α-278 MoFe Proteins

A. Introduction

The αSer278 residue hydrogen bonds to the Sγ of the αCys275 that ligates the FeMo cofactor to the MoFe protein. This observation as well as the conservation of a serine residue at this position for both the Mo-nitrogenases from other sources and the alternative nitrogenases indicates a functional role for this residue (Dean DR and Jacobson MR, 1992). Initial characterization using the crude extracts of the α-278 mutant strains confirmed this suggestion. Therefore, the altered α-278 MoFe proteins were purified in order to characterize their catalytic properties further.

B. Methods

The altered α-278 MoFe proteins from the mutant strains and the wild type MoFe proteins were purified using the same method and in parallel. As described in Chapter 2.F.1 & 2, crude extract was prepared by sonication on a large scale. A heat step of 55^{o}C for 5 minutes was applied to all extracts except that with limited heat stability of the MoFe protein in the mutant strain (the $\alpha278^{Leu}$ crude extracts), before centrifugation at 98,000×g at 4^{o}C for 90 minutes. Purification of the MoFe protein started with anion exchange chromatography on a Q-sepharose column, followed by gel-filtration chromatography on a Sephacryl S-200 column. Further purification was achieved by hydrophobic interaction chromatography on a phenyl-sepharose column. The purified MoFe protein from this last step was exchanged into 25 mM HEPES, 200 mM NaCl, 2 mM sodium dithionite, pH 7.4 buffer by passage through a small S-200 Sephacryl (Pharmacia LKB, Uppsala, Sweden) gel-filtration column (2.5 × ~40 cm). The MoFe proteins in this buffer were used for kinetic and spectroscopic characterization.

The Lowry method was used for protein estimation with bovine serum albumin as standard (Lowry OH *et al.*, 1951). The activity of the MoFe protein and the Fe protein were then measured by the nitrogenase activity assay in the presence of an optimal amount of the purified complementary component protein as described in Chapter 2.J.1. The purity of the MoFe protein was checked by SDS-PAGE.

Inductively coupled plasma atomic emission spectroscopy was utilized to determine the Mo and Fe contents of the purified MoFe proteins from wild type and α-278 mutant strains. The concentration and volume used in the determinations allowed for at least three replicate readings for Mo and Fe. The EPR spectra of the purified MoFe proteins were recorded on a Varian Associates E-line instrument at a microwave frequency of about 9.2 GHz and a microwave power of 20 mW with a 100-kHz field modulation of 1.6 mT at 12 K maintained by liquid helium boil-off.

C. Results

1. Purification of the altered α-278 MoFe proteins

Because the Thr substitution did not decrease the C_2H_2-reduction activity very much, but only altered the distribution of the electron flux among the products (C_2H_4 and H_2), the $\alpha 278^{Thr}$ MoFe protein was the first chosen for purification in parallel with the wild type MoFe protein. Similar levels of purification were achieved for both proteins as shown by their activities and migration on SDS-PAGE at all stages of purification (Table 4.1). After exchanging into HEPES buffer, the wild type and $\alpha 278^{Thr}$ MoFe proteins have specific activities of 2380 and 2730 nmols of H_2 (min×mg of protein)$^{-1}$, respectively. The $\alpha 278^{Cys}$, $\alpha 278^{Ala}$ and $\alpha 278^{Leu}$ MoFe proteins were also purified using the same methodology. Both of the $\alpha 278^{Cys}$ and $\alpha 278^{Ala}$ MoFe proteins were purified with lower yield than the wild type. The $\alpha 278^{Leu}$ MoFe protein was more difficult to purify than the others. The purification yield for this last MoFe protein was about 1/10 that of the wild type (Table 4.2). The specific activities of these purified MoFe proteins were 2280, 1560 and 130 nmols of H_2 (min×mg of protein)$^{-1}$, respectively. All the MoFe proteins were purified into homogeneity, with the $\alpha 278^{Leu}$ MoFe protein was less pure than the other MoFe proteins shown on the SDS-PAGE gel (Figure 4.1).

Table 4.1. Purification table for the wild type and $\alpha 278^{Thr}$ MoFe proteins.

	Total protein[b]		**Total activity[c]**		**Specific activity[d]**		**Fold purified**		**Yield (%)**	
Step[a]	WT	$\alpha 278^{Thr}$	WT	$\alpha 278^{Thr}$	WT	$\alpha 278^{Thr}$	WT	$\alpha 278^{Thr}$	WT	$\alpha 278^{Thr}$
CE	5.6	5.4	0.69	0.81	120	150	1.0	1.0	100	100
Q-seph	1.6	1.7	0.62	0.76	390	452	3.3	3.0	90	94
Sephacryl-200	0.55	0.53	0.51	0.59	930	1120	7.8	7.5	74	72
Phenyl-sepharose	0.10	0.13	0.24	0.35	2400	2700	20	18	35	43
Buffer change	0.076	0.10	0.18	0.21	2380	2730	20	18	26	26

[a] Crude extract was prepared with the heat step before centrifugation. Purification was performed as in Chapter 2.F.1 & 2.

[b] Total protein is expressed in units of grams.

[c] Total activity is expressed as H_2 evolved in units of millimoles per minute.

[d] Specific activity is expressed as H_2 evolved in units of nmols $(min \times mg\ protein)^{-1}$.

Table 4.2 Purification table for the wild type and altered α-278 MoFe proteins.

MoFe protein	**Crude extract[a] Specific activity**	**Purified protein Specific activity[b]**	**Fold purified**	**Yield (%)**
Wild type	120	2380	20	26%
$\alpha 278^{Thr}$	150	2730	18	26%
$\alpha 278^{Cys}$	80	2280	28	13%
$\alpha 278^{Ala}$	80	1560	20	12%
$\alpha 278^{Leu}$	6	130	20	3%

a Crude extract was prepared with the heat step before centrifugation. Purification was performed as in Chapter 2.F.1 & 2. Heat step was not applied for the $\alpha 278^{Leu}$ MoFe protein.

b Specific activity is expressed as H_2 evolved in units of nmols (min×mg protein)$^{-1}$.

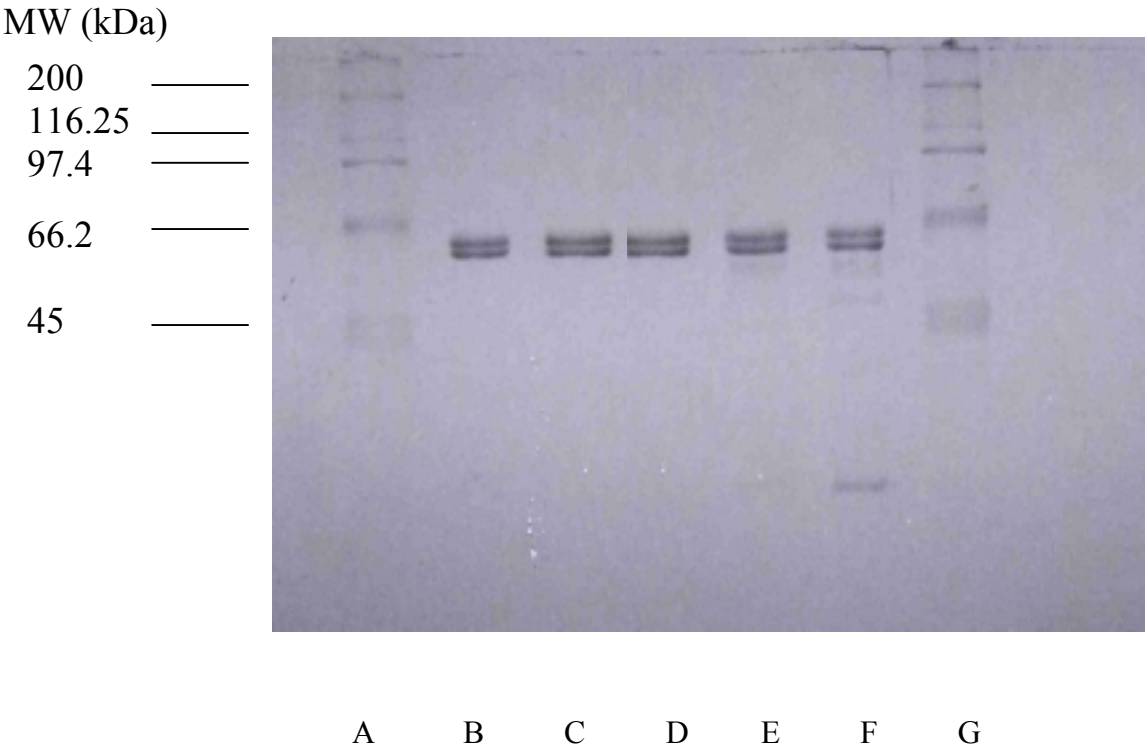

Figure 4.1 SDS-PAGE of MoFe proteins purified from the α-278 mutant strains and wild type.

Lane A: Molecular weight marker (Myosin 200,000, β-galactosidase 116,250, Phosphorylase b 97,400, Serum albumin 66,200, Ovalbumin 45,000.); Lane B: wild type MoFe protein; Lane C: $\alpha 278^{Thr}$ MoFe protein; Lane D: $\alpha 278^{Cys}$ MoFe protein; Lane E: $\alpha 278^{Ala}$ MoFe protein; Lane F: $\alpha 278^{Leu}$ MoFe protein; Lane G: Molecular weight marker (same as Lane A).

Because the MoFe-protein specific activity in the crude extract of the $\alpha 278^{Arg}$ mutant strain was less than 1 nmol of H_2 (min×mg of protein)$^{-1}$, purification and further characterization of this altered MoFe protein were not attempted.

2. General properties of the altered α-278 MoFe proteins

After the purification of these altered MoFe proteins, the next step was the characterization of their general properties under 100% argon, 10% C_2H_2/90% argon and 100% N_2. The results are shown in Table 4.3.

Two altered MoFe proteins, the $\alpha 278^{Thr}$ and the $\alpha 278^{Cys}$, have comparable specific activities to the wild type. The $\alpha 278^{Ala}$ MoFe protein has about 60% and the $\alpha 278^{Leu}$ MoFe protein has about 5% of the wild type specific activity. All of the altered MoFe proteins except the $\alpha 278^{Leu}$ can reduce N_2 to ammonia.

The $\alpha 278^{Cys}$ and the $\alpha 278^{Ala}$ MoFe proteins are similar to the wild type in terms of the electron distribution among the products either under 10% C_2H_2/90% argon or under 100% N_2. The electron distribution pattern changes in the $\alpha 278^{Thr}$ MoFe protein compared to the wild type. Under 10% C_2H_2/90% argon, about 50% of the total electron flux goes to the C_2H_4 formation in this altered MoFe protein, compared to nearly 90% in the wild type MoFe protein. Under 100% N_2, about 50% of the total electron flux goes to ammonia formation, compared to nearly 70% in the wild type MoFe protein. The $\alpha 278^{Leu}$ MoFe protein is a poor C_2H_2 reducer compared to other altered α-278 MoFe proteins. It uses only 26% of its total electron flux for the C_2H_4 formation. Unlike the wild type MoFe protein, both of the $\alpha 278^{Thr}$ and $\alpha 278^{Leu}$ MoFe proteins can produce marginal amount of C_2H_6 when they reduce C_2H_2, although both of them are relatively poor at reducing C_2H_2.

Because the optimal stoichiometry during inter-molecular electron transfer is 2 MgATP hydrolyzed per electron transferred, an often-used measure of the efficiency of substrate reduction is the ATP/2e^- ratio. This index of the number of molecules of MgATP hydrolyzed for each pair of electrons appearing as product is usually measured as 4-5/1 with wild type Mo-nitrogenase. Because this ratio approaches 4/1, wild type Mo-nitrogenase is described as having MgATP hydrolysis tightly coupled to electron transfer.

Table 4.3 Substrates, products, and electron distribution for the purified wild type (αSer278), α278^{Thr}, α278^{Cys}, α278^{Ala} and α278^{Leu} MoFe proteins.

MoFe protein	**Substrates and Products** [a,b]					
	100% Ar	**10% C_2H_2 / 90% Ar**			**100% N_2**	
	H_2	**H_2**	**C_2H_4**	**C_2H_6**	**H_2**	**NH_3**
Wild type	2380	260(12%)[c]	1970(88)	0	670(31%)	1500(69%)
α-278^{Thr}	2730	1280(52%)	1180(48%)	2(<1%)	1190(53%)	1060(47%)
α-278^{Cys}	2280	480(23%)	1620(77%)	0	850(40%)	1280(60%)
α-278^{Ala}	1560	230(16%)	1220(84%)	0	450(32%)	950(68%)
α-278^{Leu}	130	81(74%)	28(26%)	0.4(<1%)	120	0

[a]All values are the results of at least four replicate measurements. Error range is less than 10%.

[b] Specific activity is expressed as nmols of electron pairs (min×mg MoFe protein)$^{-1}$ appearing in each product in the presence of a 20-fold molar excess of wild type Fe protein.

[c] Numbers in parentheses represent the percentage of total electron flux to each product. Total electron flux is calculated as nmols of electron pairs (min×mg MoFe protein)$^{-1}$ appearing in all measured products per assay.

In Table 4.4, the total electron fluxes and ATP/$2e^-$ ratios of the altered α-278 MoFe proteins were compared to those of wild type under 100% argon, 10% C_2H_2 and 100% N_2. For the $\alpha278^{Thr}$, $\alpha278^{Cys}$ and $\alpha278^{Ala}$ MoFe proteins, electron transfer was also tightly coupled to ATP hydrolysis under the different assay conditions, whereas for the $\alpha278^{Leu}$ MoFe protein, the ATP/$2e^-$ ratios were increased by about 2-fold to about 10-13/1.

Consistent with the results from the crude extracts of these mutant strains, H_2 evolution by any of the purified MoFe proteins was unaffected by the addition of 10% CO to the assays, and the ATP/$2e^-$ ratios were the same as those measured under 100% argon (data not shown). 10% CO was also added to the assays under 10% C_2H_2 and 100% N_2 and there were no effects on the total electron flux with all the altered MoFe proteins (data not shown). Like with the wild type MoFe protein, CO diverts all the electron flux to H_2 evolution and ATP hydrolysis is still tightly coupled to electron transfer.

3. Metal analysis of the purified MoFe proteins

The altered α-278 MoFe proteins have different Mo and Fe contents (Table 4.5). When their specific activity is adjusted for the Mo content, all become comparable to that of the wild type except for the $\alpha\text{-}278^{Leu}$ MoFe protein, which contains much less Mo and has a very low specific activity. The ratio of the Fe and the Mo concentrations of the wild type and altered MoFe proteins, except for the $\alpha278^{Leu}$ MoFe protein, is around 15/1, which is the expected ratio. In the $\alpha278^{Leu}$ MoFe protein, the ratio is increased 2.3-fold, indicating the existence of some co-purified apo-MoFe protein that likely contains a full complement of P cluster but lacks FeMo cofactor.

4. EPR spectra of the altered MoFe proteins

The FeMo cofactor is the source of the unique EPR spectrum of nitrogenase, which is characteristic of an S=3/2 spin system. As shown in Figure 4.2 D, the S=3/2 EPR signal of the FeMo cofactor in the wild type MoFe protein shows apparent g values of 4.3 and 3.7. The third g value at 2.0 is not shown. For the $\alpha\text{-}278^{Ala}$ (Figure 4.2(A)) and $\alpha\text{-}278^{Cys}$ (Figure 4.2(B)) MoFe proteins, the EPR spectra are only slightly changed in g

Table 4.4 Total electron flux and ATP/$2e^-$ ratio for the wild type and the altered α-278 MoFe proteins during substrate reduction.

Substrate		**100% Ar**	**10% C_2H_2 / 90% Ar**	**100% N_2**
Wild type	Total specific activity [a]	2380	2230	2170
	ATP/$2e^-$ [b]	4.6	4.8	5.2
α-278^{Thr}	Total specific activity	2730	2460	2250
	ATP/$2e^-$	4.3	4.4	6.1
α-278^{Cys}	Total specific activity	2280	2100	2130
	ATP/$2e^-$	4.4	4.8	5.1
α-278^{Ala}	Total specific activity	1560	1450	1400
	ATP/$2e^-$	5.4	5.2	5.5
α-278^{Leu}	Total specific activity	130	110	120
	ATP/$2e^-$	10	13	11

[a] Total specific activity is expressed as nmols of electron pairs (min×mg MoFe protein)$^{-1}$ appearing in all measured products per assay in the presence of a 20-fold molar excess of wild type Fe protein.

[b] The error range is less than 10% for both the total specific activity and the ATP/$2e^-$ ratio.

Table 4.5 Mo content of wild type and α-278 altered MoFe proteins.

Mo and Fe concentrations are the average of two independent analysis with each analysis having triplicate measurements. The error range is less than 10%.

MoFe proteins	**Specific activity[a]**	**Mo / MoFe**	**Specific activity / Mo**	**[Fe] / [Mo]**
Wild type	2380	1.8	1320	15
α-278^{Thr}	2730	2.0	1360	14
α-278^{Cys}	2280	1.7	1340	14
α-278^{Ala}	1560	1.2	1300	16
α-278^{Leu}	120	0.33	360	34

[a] Specific activity is expressed as nmols H_2 evolved (min×mg MoFe protein)$^{-1}$ under a 100% argon atmosphere in the presence of a 20-fold molar excess of wild type Fe protein.

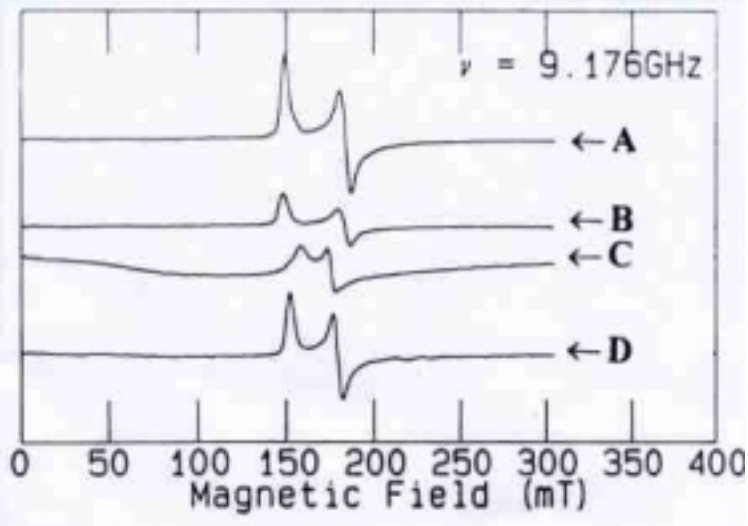

Figure 4.2 EPR spectra of purified $\alpha 278^{Ala}$ (A), $\alpha 278^{Cys}$ (B), $\alpha 278^{Thr}$ (C) and wild type (D) MoFe proteins.

Spectra are shown the g=4 region only. The Mo active site concentration calculated for $\alpha 278^{Cys}$, $\alpha 278^{Thr}$ and wild type were about 120 μM, and 160 μM for the $\alpha 278^{Ala}$ MoFe protein.

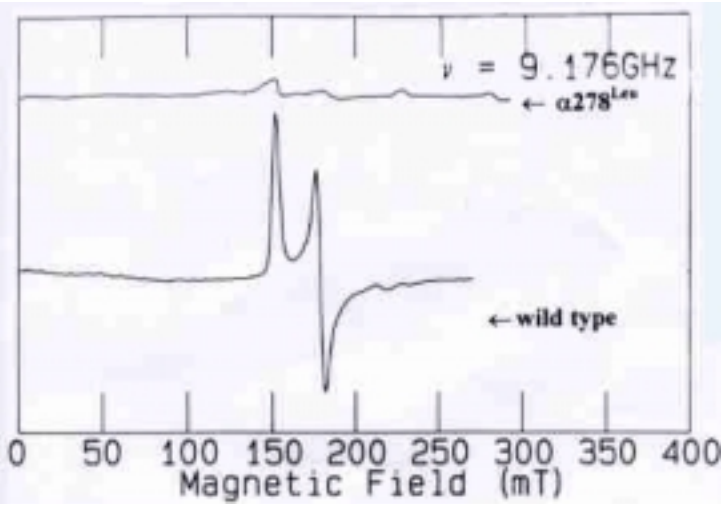

Figure 4.3 EPR spectra of purified $\alpha 278^{Leu}$ and wild type MoFe proteins.

The Mo active site concentration calculated for the $\alpha 278^{Leu}$ MoFe protein was about 90 μM and 120 μM for the wild type MoFe protein.

value to 4.4 and 3.6. For the α-278^{Thr} MoFe protein (Figure 4.2(C)), the EPR spectrum is changed not only in the g values to 4.1 and 3.7, but also in the shape of the line. The g =4.1 line in the spectrum is broader but the g =3.7 line is sharper than those in the wild type spectrum. The spectrum of α-278^{Leu} MoFe proteins has very low intensity, compared to that of the wild type, as expected from its low Mo concentration and low specific activity. The g values for this spectrum are close to wild type's at 4.3 and 3.5 (Figure 4.3).

D. Discussion

Four altered α-278 MoFe proteins have been purified in parallel with the wild type MoFe protein. The electron distribution pattern among the products from these purified MoFe proteins is consistent with that found in the crude extracts. These observations indicate that no changes were introduced by the purification methods.

Of the four altered MoFe proteins, those with the α278^{Cys} and the α278^{Ala} substitutions show either little or no change in substrate specificity and EPR spectra when compared to the wild type MoFe protein. Because the alanine substitution eliminates the hydroxyl group, the hydrogen bond interaction observed in the crystal structure between the αSer278 and the αCys275 residues cannot be absolutely required for nitrogenase activity. However, the leucine substitution has an enormous impact on catalytic activity, even if one allows for its lower Mo content, which suggests the presence of FeMo cofactor-deficient apo-MoFe protein. This deleterious effect on activity is confirmed by the amount of ATP hydrolyzed in the assays, which was only about 10~15% of that for the wild type MoFe protein. If the rate of ATP hydrolysis is adjusted for the Mo content of the α278^{Leu} MoFe protein and compared with that for the wild type MoFe protein, the rates are comparable even though the rates of substrate reductions are not. This result suggests that the substitution does not affect Fe protein-MoFe protein association and dissociation but does impact electron transfer. Interestingly, this altered MoFe protein reduces C_2H_2 to both C_2H_4 and C_2H_6, even though only 25% of the total electrons are used for C_2H_2 reduction.

In contrast, substitution by threonine, which retains the hydroxyl functional group, affects both the electron distribution among the products of C_2H_2 and N_2 reduction

and the EPR spectrum of the MoFe protein, while retaining a wild-type level of catalytic activity. Compared to the wild type MoFe protein, C_2H_2 is not as good a substrate for this altered MoFe protein, which allocates only about half of its total electron flux to the C_2H_4 production and it produces C_2H_6. These data suggest that, in this altered MoFe protein, the substitution causes a local disturbance of the FeMo cofactor's polypeptide environment and by doing so, changes its ability to catalyze the reduction of the different substrates.

As shown in Figure 4.2 (C), the line shape and the g values of the EPR spectrum from the $\alpha 278^{Thr}$ MoFe protein is similar to that of the $\alpha 191^{Lys}$ altered MoFe protein (Scott DJ *et al.*, 1990; Scott DJ *et al.*, 1992), although these two altered MoFe protein have different catalytic properties. For example, the $\alpha 191^{Lys}$ mutant strain cannot fix N_2 and the purified $\alpha 191^{Lys}$ MoFe protein has about half of the wild type MoFe protein activity. Different from the $\alpha 278^{Thr}$ MoFe protein, the $\alpha 191^{Lys}$ MoFe protein exhibits H_2 evolution sensitive to CO and has a K_m of 0.35 atmosphere for C_2H_4 formation (Fisher K *et al.*, 2000c), which is about 6-times higher than that of the $\alpha 278^{Thr}$ MoFe protein. Maybe both substitutions affect the electronic structure of the FeMo cofactor similarly and so result in a similar EPR spectrum in the dithionite-reduced MoFe proteins. However, this similarity may not carry over to the more reduced redox states required for catalytic activity.

Chapter 5

C_2H_2 Reduction Catalyzed by the α-278 Altered MoFe Proteins

A. Introduction

The next step, after the purification of these altered α278 MoFe proteins, was the characterization of the kinetic parameters of each of the altered MoFe proteins in specific nitrogenase assays. From their general properties (Table 4.3), catalyzed C_2H_2 reduction in these altered MoFe proteins is different from that of the wild type MoFe protein. For example, changes occur in the electron distribution of some of the altered MoFe proteins between H_2 evolution and C_2H_4 formation and the ability to produce C_2H_6 during the C_2H_2 reduction. Previous work on the αArg277 residue, which is next to the αSer278, shows interesting and unusual kinetics of CO inhibition of C_2H_2 reduction by the altered $\alpha 277^{His}$ MoFe protein (Shen J *et al.*, 1997). Therefore, further studies on C_2H_2 reduction with or without inhibitors, such as CO, catalyzed by the altered α278 MoFe proteins could provide additional insights into the binding of C_2H_2 and CO to the FeMo cofactor. Of particular interest is to determine how the substitution affects both C_2H_2 binding and reduction and the interactions between C_2H_2 and either CO or N_2 with these altered MoFe proteins.

B. Methods

1. K_m for C_2H_2 (C_2H_4 formation)

The procedure for the C_2H_2 reduction assay is detailed in Chapter 2.J.2. To determine the K_m for C_2H_2, a known amount of C_2H_2 was added to pre-degassed, argon-flushed assay vials to produce a final concentration ranging between 0.001 and 0.30 atm pressure. The specific concentrations used ranged from 0.02 K_m to 10 K_m. Gas tight syringes with hypodermic needles were used to transfer the different amounts of 100% C_2H_2. Sometimes, dilution of the 100% C_2H_2 with argon was required before adding the gas to the assay vials. The production of C_2H_4 was used to determine the K_m for C_2H_2. For abbreviation, we use the term of "K_m for C_2H_4 formation" to represent "K_m for C_2H_2 (C_2H_4 formation)" in this chapter.

2. Inhibition of C_2H_2 reduction by either CO or N_2

Non-saturating concentrations of CO were added to the C_2H_2-reduction assay vials, which were set up as described above and then vented to atmospheric pressure. The amount of CO added was calculated to provide the required final concentrations of both C_2H_2 and CO in the vial. Serial dilutions of CO with argon were sometimes used to ensure the accuracy of the final concentration.

For wild type MoFe protein, the K_i of N_2 inhibition of C_2H_2 reduction is reported to be in the range of 0.10-0.20 atm (Hardy RWF, 1979; Davis LC and Wang YL 1980; Kim C-H *et al.*, 1995). Therefore, high concentrations of N_2 ranging from 0.1 to 0.8 atm were used in the experiments. For the lower concentrations in this range, a known amount of N_2 gas was added to argon-flushed vials, whereas, for higher concentrations, a calculated amount of argon gas was added to N_2-flushed vials.

3. C_2H_2 reduction at high C_2H_2 concentration

Catalyzed C_2H_2 reduction was measured at concentrations ranging from 10% C_2H_2 in argon to 100% C_2H_2 with the wild type and all the altered α-278 MoFe proteins. After the gaseous products were measured by gas chromatography, the amount of creatine released during the assay as a measure of MgATP hydrolysis was determined as described in Chapter 2.J.4 section.

4. Is the inhibition of total electron flux through the $\alpha278^{Leu}$ MoFe protein by C_2H_2 reversible?

Assays to determine if the inhibition of total electron flux by C_2H_2 was reversible were performed under 10% C_2H_2/90% argon for 12 minutes with the $\alpha278^{Leu}$ MoFe protein and the H_2, C_2H_4 and C_2H_6 production was quantified every 4 minutes. The assay vial was then rapidly evacuated and refilled with 100% argon through the Schlenk line. The experiment was continued for a further 18 minutes and the products again quantified every 4 minutes. Effective removal of C_2H_2 was monitored by gas chromatography. Control assays under 100% argon and under 10% C_2H_2/90% argon were run at the same time.

5. Treatment of the kinetic data

A double-reciprocal plot of the experimental data points was used to obtain K_m and K_i values. Each series of assays was independently run two or three times with individual data points always having duplicate measurements. The error range for the assay duplicates was less than 5% and, for the different series, it was less than 10%. K_m values were obtained using the equation $1/V_0 = 1/V_m + K_m/V_m \times 1/S$. Inhibition patterns were derived from the double-reciprocal plots. For competitive inhibition, the equation $1/V_0 = 1/V_m + K_m/V_m (1 + [I]/K_i) \times 1/S$ was used. For non-competitive inhibition, the equation $1/V_0 = (1 + [I]/K_i) \times 1/V_m + K_m/V_m (1 + [I]/K_i') \times 1/S$ was used. A secondary plot of the slope of each equation was used to obtain K_i. The R^2 values for the data points in these plots were higher than 0.99.

6. Stereospecficity of proton addition to C_2D_2

C_2D_2 was generated by the addition of anaerobic D_2O to a predetermined amount of CaC_2 in a 25 mL sealed and evacuated flask. Typically, 70 mg of CaC_2 was weighed into a flask, which was then capped and filled with argon at atmospheric pressure after four cycles of evacuation and filling. A 0.5 mL aliquot of D_2O (99.9% purity, Sigma) was then added and the reaction allowed to proceed to completion for at least 1 hour. Prior experiments had shown this combination would produce approximately 24 mL of C_2D_2 (Fisher K *et al.*, 2000c). A 5 mL aliquot of gas was then removed and transferred by gastight syringe to an assay flask under argon. The assay flask was vented to atmospheric pressure after 5 min at 30°C. The assay procedure for the C_2D_2 assay is the same as the C_2H_2 assay described before (Chapter 2. J.2), only the amount of reaction mixture, sodium dithionite and component proteins used is 10-times of those used in the normal assay. After the assay was terminated by addition of 3.0 mL of 0.5 M EDTA-Na_2, pH 8.0, gas samples (0.1-0.2 ml) were then removed for gas-chromatographic analysis for C_2H_4, C_2H_6 and H_2. The liquid contents of the flask were frozen by partial immersion in a dry ice bath and the gaseous contents then allowed to equilibrate through the gastight connecter to a previously evacuated infrared gas cell of 100 mL capacity. The amounts of *cis*- and *trans*-$C_2D_2H_2$ were estimated by Fourier transform infrared spectroscopy, using the height of the bands at 843 and 988 cm^{-1}, respectively. A MIDAC (Irvine, CA) model

M2004 spectrometer with Grams 32 software was used. Because the trans isomer has a molar absorptivity at 988 cm^{-1} of about half that of the cis isomer at 843 cm^{-1} (Lin-Vein D *et al.*, 1989), its measured height was doubled.

A similar protocol was used for the $\alpha 278^{Thr}$ MoFe protein, except that 50 mL C_2D_2 was added to the assay flask (5 mL C_2D_2 was used for both wild type and the $\alpha 278^{Ala}$ MoFe proteins).

C. Results

1. Kinetic parameters of acetylene reduction for the wild type, $\alpha 278^{Thr}$, $\alpha 278^{Cys}$, $\alpha 278^{Ala}$ and $\alpha 278^{Leu}$ MoFe proteins.

K_m values for C_2H_4 production were measured to compare the apparent binding affinity of these altered MoFe proteins for C_2H_2. As shown in Table 5.1, wild type MoFe protein has a K_m of about 0.006 atm, which is within the range reported previously (Kim C-H *et al.*, 1995; Fisher K *et al.*, 2000c). Both the $\alpha 278^{Cys}$ and the $\alpha 278^{Ala}$ MoFe proteins have similar K_m values and apparently bind C_2H_2 similarly to the wild type. Both the $\alpha 278^{Thr}$ and the $\alpha 278^{Leu}$ MoFe proteins, however, have K_m values that are 10-times higher than that of wild type. This difference is consistent with their lower allocation of total electron flux to C_2H_4 production under 10% C_2H_2. The K_m values for C_2H_6 production from C_2H_2 for the $\alpha 278^{Thr}$ and $\alpha 278^{Leu}$ MoFe proteins were the same as their individual K_m values for C_2H_4 production from C_2H_2 reduction (data not shown). These last two altered MoFe proteins showed an increase in both C_2H_4 and C_2H_6 production as the C_2H_2 partial pressure is increased.

Under 10% C_2H_2, wild type MoFe protein reduces C_2H_2 to C_2H_4 accompanied by H_2 evolution, which uses about 10% of the total electron flux. With the addition of 10% CO, the total electron flux through the wild type MoFe protein remains unchanged but H_2 is the only observed product (Hardy RWF *et al.*, 1965; Bulen WA *et al.*, 1965). When non-saturating concentrations of CO were added to the C_2H_2-reduction assay vials, partial inhibition of C_2H_2 reduction was observed. The wild type MoFe protein gave linear double-reciprocal plots that indicated a non-competitive pattern of inhibition. This

Table 5.1 K_m for C_2H_4 production, K_i of CO and N_2 inhibition of C_2H_2 reduction in the wild type and the altered α-278 MoFe proteins.

MoFe protein	**K_m C_2H_2 [a] ($atm\times10^2$)**	**K_i CO [b] ($atm\times10^4$)**	**K_i N_2 [c]**
Wild type	0.6	3	0.15
$\alpha278^{Thr}$	6.0	0.1	0.32
$\alpha278^{Cys}$	0.8	8	0.20
$\alpha278^{Ala}$	0.6	13	0.18
$\alpha278^{Leu}$	8.0	? [d]	Not determined

[a] K_m is expressed in the unit of atmosphere (atm) for the catalyzed production of C_2H_4.

[b] CO is a non-competitive inhibitor for all the MoFe proteins catalyzed C_2H_2 reduction and K_i is expressed in atm.

[c] N_2 is a competitive inhibitor for catalyzed C_2H_2 reduction by all the MoFe proteins.

[d] Under a non-saturating concentration of CO, $\alpha278^{Leu}$ MoFe protein catalyzed the reduction of C_2H_2 with sigmoidal kinetics (see Figure 5.1).

inhibition pattern was also observed for all the α-278 altered MoFe proteins except for the $\alpha 278^{Leu}$ MoFe protein (see below). For the $\alpha 278^{Cys}$ and the $\alpha 278^{Ala}$ MoFe proteins, C_2H_2 reduction is somewhat less sensitive to CO inhibition compared to wild type, whereas the $\alpha 278^{Thr}$ MoFe protein is much more sensitive to CO (Table 5.1).

For the $\alpha 278^{Leu}$ MoFe protein, C_2H_2 reduction responded to the non-saturating concentrations of CO differently to wild type. This altered MoFe protein catalyzed C_2H_2 reduction with sigmoidal kinetics in the presence of CO (Figure 5.1 panel A). The double-reciprocal plot of C_2H_4 production activity vs. C_2H_2 concentration was not linear (Figure 5.1 panel B). From a Hill plot, a value of n = 1.3 was found for the number of C_2H_2-binding sites on the altered MoFe protein. This result suggests that CO induces cooperativity between at least two C_2H_2-binding sites on the $\alpha 278^{Leu}$ MoFe protein.

N_2 is a competitive inhibitor of C_2H_2 reduction with the wild type MoFe protein (Rivera-Ortiz JM and Burris RH, 1975). The K_i for N_2 inhibition of C_2H_2 reduction determined in this work was about 0.15 atm for the wild type, which is within the range reported previously (Hardy RWF, 1979). For the $\alpha 278^{Thr}$, $\alpha 278^{Cys}$ and $\alpha 278^{Ala}$ MoFe proteins, which can reduce N_2 to NH_3, N_2 was also a competitive inhibitor of C_2H_2 reduction and the K_i values found for N_2 inhibition were 0.32, 0.20 and 0.18 atm, respectively (Table 5.1).

2. C_2H_2 reduction under high C_2H_2 concentrations

As shown above, under 10% C_2H_2, the $\alpha 278^{Thr}$ MoFe protein uses about 50% of its total electron flux and the $\alpha 278^{Leu}$ MoFe protein uses about 25% of its total electron flux for C_2H_4 production. To determine if higher concentrations of C_2H_2 would increase C_2H_4 production in these two altered MoFe proteins, C_2H_2 reduction under high electron flux (obtained by using a 20:1 molar ratio of the Fe protein to the MoFe protein in the assays) was performed with the concentration of C_2H_2 ranging from 10% to 100% for the wild type and all four altered α-278 MoFe proteins. Table 5.2 compares the resulting distribution of electron flux to C_2H_4 production under 10% and 100% C_2H_2. The $\alpha 278^{Cys}$ and $\alpha 278^{Ala}$ MoFe proteins again were similar to the wild type MoFe protein all showing

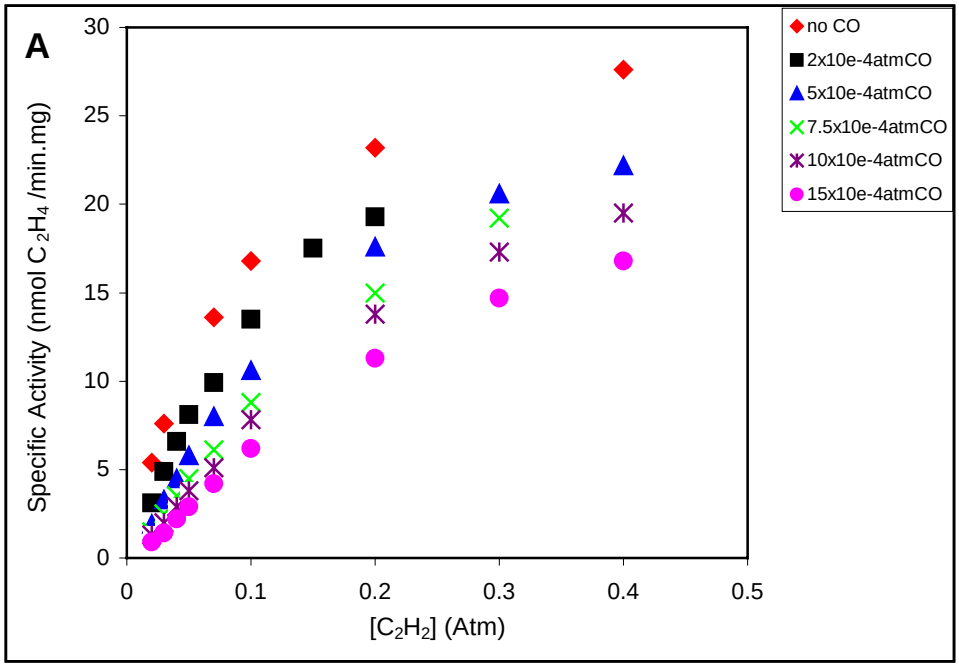

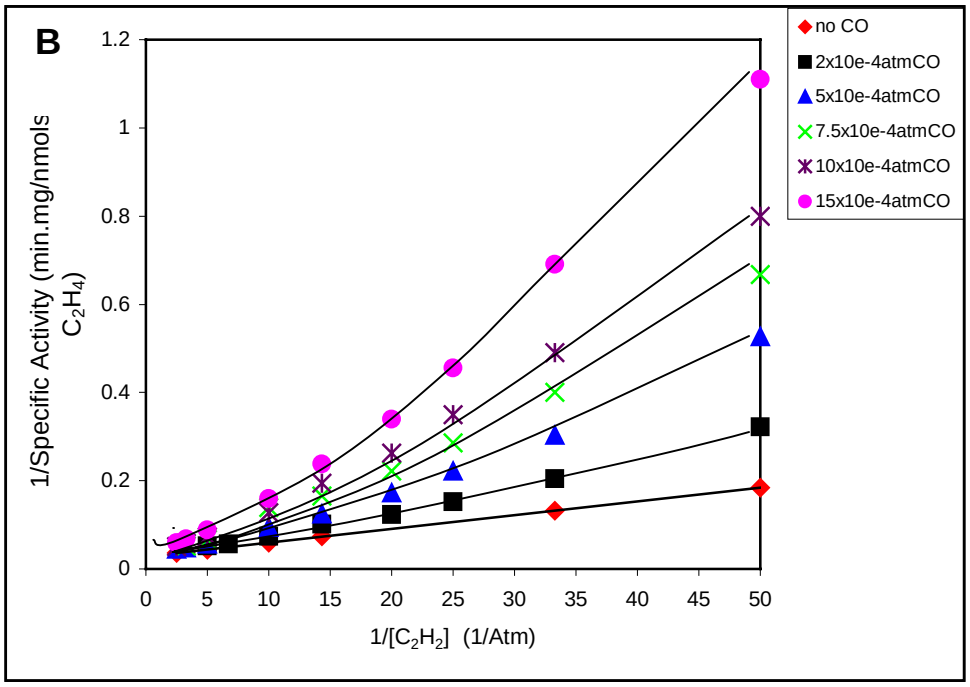

Figure 5.1 Michaelis-Menton (panel A) and Lineweaver-Burk (panel B) plots of $\alpha 278^{Leu}$ MoFe protein C_2H_2-reduction reactions in the absence and presence of CO.

Table 5.2 Effect of varying C_2H_2 (10% vs. 100%) concentration on the distribution of electron flux to C_2H_4 formation and the resulting ATP/$2e^-$ ratio with wild type and the altered MoFe proteins.

MoFe protein	**10% C_2H_2**		**100% C_2H_2**	
	% e^- [a]	ATP / $2e^-$ [b]	% e^-	ATP / $2e^-$
Wild type	88%	4.7	90%	4.4
$\alpha 278^{Thr}$	46%	4.4	86%	4.3
$\alpha 278^{Cys}$	78%	4.6	85%	4.5
$\alpha 278^{Ala}$	85%	5.4	89%	5.4
$\alpha 278^{Leu}$	25%	14	53%	40

[a] % of total electron flux to C_2H_4 formation under 10% and 100% C_2H_2.

[b] Error range is less than 10%.

only a small increase in distribution to C_2H_4. The $\alpha278^{Thr}$ MoFe protein showed a significant increase in C_2H_4 production to match that of the wild type when the C_2H_2 concentration was increased to 100%. No similar response occurred with the $\alpha278^{Leu}$ MoFe protein, where C_2H_4 production was increased only to about 50% at 100% C_2H_2.

Three observations were made when the concentration of C_2H_2 was gradually increasing from 10% to 100%. 1) C_2H_4 formation activities were maximal at about 20% C_2H_2 for the wild type, $\alpha278^{Cys}$ and $\alpha278^{Ala}$ MoFe proteins, at about 40% C_2H_2 for the $\alpha278^{Thr}$ MoFe protein, and at about 50% C_2H_2 for the $\alpha278^{Leu}$ MoFe protein. Under these maximal electron flux concentrations of C_2H_2, C_2H_4 production accounted for 95%, 89%, 93%, 72% and 50% of the total electron flux for each of the above MoFe proteins, respectively. 2) For the $\alpha278^{Thr}$ and the $\alpha278^{Leu}$ MoFe proteins, the C_2H_6 produced was maximized at about 30-40% C_2H_2 concentration. 3) When the C_2H_2 concentration reached 100% (1 atm), the total electron flux had decreased by 40% for the wild type and $\alpha278^{Thr}$ MoFe proteins and by about 50% for the $\alpha278^{Cys}$, $\alpha278^{Ala}$ and the $\alpha278^{Leu}$ MoFe proteins, compared to their total electron flux under 100% argon.

ATP hydrolysis was also measured for these assays. In Table 5.2, ATP/$2e^-$ ratios with these altered MoFe proteins are listed for both 10% and 100% C_2H_2 concentrations. For the wild type, $\alpha278^{Thr}$, $\alpha278^{Cys}$ and $\alpha278^{Ala}$ MoFe proteins, the decrease in total electron flux with the increase in C_2H_2 concentration was accompanied by a decrease in the rate of ATP hydrolysis. Thus, the overall ATP/$2e^-$ ratios were unchanged. However, for the $\alpha278^{Leu}$ MoFe protein, the rate of ATP hydrolysis under 100% C_2H_2 was increased by about 33% compared to that under 10% C_2H_2/90% argon. This increase in the rate of ATP hydrolysis plus the concomitant decrease in total electron flux resulted in an elevated ATP/$2e^-$ ratio. As shown in Table 5.2, the ATP/$2e^-$ increased to about 40 under 100% C_2H_2 from about 14 under 10% C_2H_2.

3. Inhibition of total electron flux by C_2H_2 through the $\alpha278^{Leu}$ MoFe protein

By comparing the effect of high C_2H_2 concentration on the total electron flux and the ATP/$2e^-$ ratios in the assays, we found that the rate of ATP hydrolysis by the $\alpha278^{Leu}$ MoFe protein responded differently to increasing C_2H_2 concentration compared to the

wild type and the other α-278 altered MoFe proteins. To obtain further information about C_2H_2 inhibition of the electron flux through this altered MoFe protein and the increased rate of ATP hydrolysis in the presence of high concentrations of C_2H_2, 10% CO was added to the C_2H_2 reduction assays. CO should eliminate C_2H_2 acting as a substrate, but should allow C_2H_2 to continue to act as an inhibitor. Under these conditions, total electron flux is used for H_2 evolution only.

The H_2 evolution activity was measured under various concentrations of C_2H_2 in argon plus 10% CO and compared to the activity under argon plus 10% CO. In Figure 5.2, the reciprocal of the C_2H_2 concentration is plotted against the reciprocal of the loss of H_2 evolution activity, which was determined as the difference in H_2 evolution between assays without added C_2H_2 and those with C_2H_2. The pseudo-K_i for C_2H_2 inhibition of H_2 evolution as calculated from the double-reciprocal plot was 0.17 atm. Therefore, when the C_2H_2 concentration was increased to this level, the total activity dropped to 50% of that under argon with 10% CO. We performed the same experiment with wild type (data not shown). When C_2H_2 concentration was 0.40 atm (in the presence of 10% CO), the total electron flux was inhibited by only 18%.

ATP hydrolysis was measured for all the above assays. Compared to that under argon plus 10% CO, ATP hydrolyzed by the $\alpha 278^{Leu}$ MoFe protein was increased by 40% when the added C_2H_2 concentration was 0.4 atm. Because of this elevated rate of ATP hydrolysis and the decrease (by about 75%) of the H_2 evolution activity, the ATP/$2e^-$ ratio was increased from ~12 (under argon plus 10% CO) to ~ 70 (under 40% C_2H_2 plus 10% CO) (data not shown). For the wild type MoFe protein, as expected, the decrease in total electron flux with the increase in C_2H_2 concentration was accompanied by a decrease in the rate of ATP hydrolysis, resulting in an unchanged ATP/$2e^-$ ratio.

The reversibility of this inhibition of total electron flux through the $\alpha 278^{Leu}$ MoFe protein by added C_2H_2 was tested in assays in which the initial 10% C_2H_2/90% argon assay atmosphere was switched after 12 minutes to 100% argon. The rates of product formation were quantified during both stages of the experiments. These rates were compared with those obtained from uninterrupted assays under either 100% argon or 10% C_2H_2/90% argon. The result was that, after the removal of C_2H_2, all the original activity

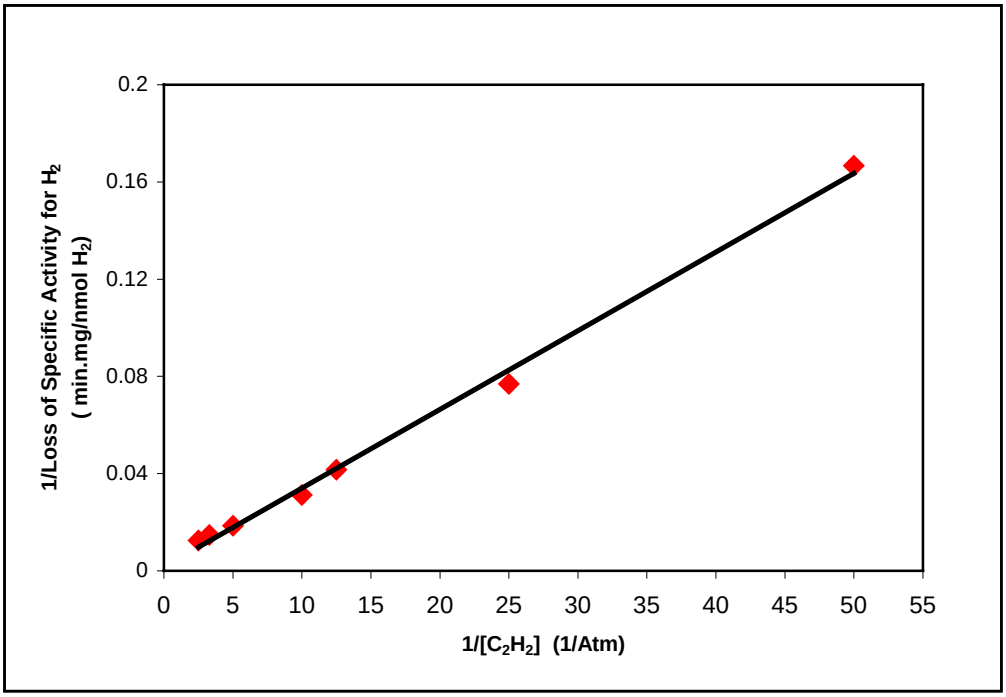

Figure 5.2 Measurement of the pseudo K_i (K_i=0.17atm) of C_2H_2 as an inhibitor of H_2 evolution under 10% CO with the $\alpha 278^{Leu}$ MoFe protein.

The difference in the specific activity for H_2 evolution under a mixed atmosphere of C_2H_2 and argon plus 10% CO versus under 90% argon/10% CO was used in this plot. ATP hydrolyzed was measured for each assay (data not shown). 10% CO was used to eliminate C_2H_4 production from C_2H_2 and drive all electron flux to H_2 evolution.

could not be recovered and, the level of the inhibition did not change over time after the C_2H_2 was removed. When measuring the hydrocarbon products in these assays by gas chromatography, we found that C_2H_2 originally added to the assay vials was not removed completely and about 1-2% C_2H_2 remained, probably reflecting the high solubility of C_2H_2 in water. Even so, as our data (section C.2 and Figure 5.2) indicate this low amount of C_2H_2 would be insufficient to cause such high inhibition (40%) of total electron flux. Therefore, the inhibition must be mostly irreversible.

4. Formation of *trans*- and *cis*-$C_2D_2H_2$ from C_2D_2

The wild type, $\alpha 278^{Ala}$ and $\alpha 278^{Thr}$ MoFe proteins were used to detect the stereospecificity of proton addition across the acetylenic triple bond. The distribution of trans and cis isomers in the dideuterated product, $C_2D_2H_2$, was estimated by Fourier transform infrared spectroscopy. The wild type and the $\alpha 278^{Ala}$ MoFe proteins produced small amount (about 8%) of trans isomer, which is similar to the published data for the wild type (Fisher K *et al.*, 2000c). The $\alpha 278^{Thr}$ MoFe protein, however, produced about 30% of the *trans*-$C_2D_2H_2$.

D. Discussion

C_2H_2 is one of the earliest established alternative nitrogenase substrates (Dilworth MJ, 1966). Wild type Mo-nitrogenase reduces C_2H_2 to C_2H_4 only, although some altered MoFe proteins (Scott DJ *et al.*, 1990, 1992; Fisher K *et al.*, 2000c) and the alternative nitrogenases (Dilworth MJ *et al.*, 1987, 1988) can produce C_2H_6 as well. Steady-state and pre-steady-state kinetic work on the *Klebsiella pneumoniae* nitrogenase has indicated that C_2H_4 formed from C_2H_2 reduction is not released on quenching the enzyme with acid until the E_3 redox state (after three electrons have been accepted) of the MoFe protein has been reached (Lowe DJ *et al.*, 1990). C_2H_2, therefore, must bind at more oxidized redox states of the enzyme (Lowe DJ *et al.*, 1990).

However, where the C_2H_2 molecule binds on the FeMo cofactor and how C_2H_6 is produced from C_2H_2 in those altered MoFe proteins is still not clear. Previous work has suggested that amino acid substitution, by impacting different parts of the FeMo cofactor's structure, are differentially altering its interaction with substrates and inhibitors

(Fisher K *et al.*, 2000c). In this Chapter, C_2H_2 reduction experiments were performed to see if substitution at the αSer278 position would affect C_2H_2 binding and reduction and would affect the interaction between this substrate and the inhibitor CO. CO is a non-competitive inhibitor of C_2H_2 reduction and, therefore, it could bind either at a different site or to a different redox state of the same site (Burgess BK, 1985).

1. Interaction of C_2H_2 with MoFe protein

Both the $\alpha 278^{Cys}$ and $\alpha 278^{Ala}$ MoFe proteins have low K_m values for C_2H_4 formation from C_2H_2. These K_m values are very close to that of the wild type MoFe protein. None of these MoFe proteins produces C_2H_6 from C_2H_2. Wild type MoFe protein has been shown to have a much higher apparent affinity for C_2H_2 than for C_2H_4 (Ashby GA *et al.*, 1987; Fisher K *et al.*, 2000c). Therefore, it is likely that, as soon as C_2H_4 is formed from C_2H_2 at the active site, it is outcompeted by another molecule of C_2H_2 and so C_2H_4 does not remain long enough at the active site to be further reduced to C_2H_6 (Dilworth MJ *et al.*, 1988; Scott DJ *et al.*, 1992). If an enzyme has a lower apparent affinity for C_2H_2, it is likely that the bound intermediate would stay longer and might be further reduced to C_2H_6 by accepting two more electrons and protons. Our results with the $\alpha 278^{Thr}$ and the $\alpha 278^{Leu}$ MoFe proteins are consistent with this suggestion. Both have a K_m value that is 10-times higher than the wild type, and both produce C_2H_6 from C_2H_2, although less than 1% of total electron flux goes to C_2H_6 formation. This observation is consistent with the suggestion that the appropriate apparent affinity for C_2H_2 is critical for the production of C_2H_6 from C_2H_2 (Fisher K *et al.*, 2000c). The apparent affinity of C_2H_2 should be low enough to let the bound C_2H_4 stay long enough to get two more electrons and protons to give C_2H_6, but also high enough to bind initially.

Another correlation with these altered MoFe proteins is between the percentage of total electron flux going to C_2H_4 formation under 10% C_2H_2 and the ability to produce C_2H_6 during the C_2H_2 reduction. Comparing the percentage of total electron flux going to C_2H_4 formation in these MoFe proteins under 10% C_2H_2 (Table 5.2), the $\alpha 278^{Thr}$ and $\alpha 278^{Leu}$ MoFe proteins have less percentage of electron flux for C_2H_4 formation than those in the wild type, $\alpha 278^{Cys}$ and $\alpha 278^{Ala}$ MoFe proteins and both produce C_2H_6. Therefore, the electron distribution between the H_2 evolution and C_2H_4 formation under

10% C_2H_2 also appears to reflect the apparent affinity of the enzyme for C_2H_2 and, thus, indicate whether or not the enzyme can produce C_2H_6 when reducing C_2H_2. However, this is not a tight correlation because the altered $\alpha 195^{Gln}$ MoFe protein, although it has the same K_m for C_2H_4 production from C_2H_2 as the wild type, uses only 55% of the total electrons for the C_2H_4 formation (Fisher K *et al.*, 2000c).

2. Multiple binding sites of C_2H_2 on the MoFe protein

C_2H_4 production from C_2H_2 by the $\alpha 278^{Leu}$ MoFe protein under non-saturating concentrations of CO exhibits sigmoidal kinetics, which indicates the presence of at least two C_2H_4-evolving sites. Previous studies have also indicated the presence of at least two binding sites for C_2H_2. First, Davis *et al.* suggested that two enzyme forms exist for wild type nitrogenase preparations from *Clostridium pasteurianum*, a low K_m (for C_2H_2) form and a high K_m (for C_2H_2) form (Davis LC *et al.*, 1979). Second, EPR studies were interpreted to indicate the presence of two binding sites for acetylene on the MoFe protein from *Klebsiella pneumoniae* (Lowe DJ *et al.*, 1978). Third, ENDOR measurements with $^{13}C_2H_2$ indicated that at least two C_2H_2-derived species are bound to the FeMo cofactor of the $\alpha 195^{Gln}$ MoFe protein under turnover conditions (Lee H-I *et al.*, 2000). Fourth, the kinetic properties of the altered $\alpha 69^{Ser}$ MoFe protein are also consistent with the MoFe protein containing at least two C_2H_2-binding/reduction sites; one of which is the high-affinity site that is primarily accessed during typical C_2H_2 reduction assays (Christiansen J *et al.*, 2000). Finally, with the altered $\alpha 277^{His}$ MoFe protein, non-saturating levels of CO induce cooperativity between at least two C_2H_4-evolving sites (Shen J *et al.*, 1997). It seems then that, in the wild type MoFe protein, normally the two C_2H_2-binding sites coexist either on or close to the FeMo cofactor. The second, low-affinity site might be masked by the high-affinity site under the normal assay conditions and only under certain circumstances can these two sites either communicate with each other or exhibit two separate K_m values for C_2H_2 reduction.

In this work, when CO binds to the $\alpha 278^{Leu}$ MoFe protein, it affects the FeMo cofactor and/or the polypeptide environment of the cofactor such that cooperativity is induced with the two-C_2H_2 binding sites to give C_2H_4 production. Taken together, these data indicate that at least one of the C_2H_2-binding sites is close to the α277-278 residues.

CO is normally a non-competitive inhibitor for C_2H_2 reduction and our data clearly indicate that CO binds simultaneously with C_2H_2 and, therefore, at a distinct site on the MoFe protein.

2.1.1 Insights from K_m values for C_2H_2 (C_2H_4 formation)

Both the $\alpha 278^{Thr}$ and $\alpha 278^{Leu}$ MoFe proteins are poor C_2H_2-reducers. Their K_m values are about 10-times than that of the wild type. These results may indicate that the high-affinity C_2H_2-binding site has been affected in these two altered MoFe proteins. When we increase the C_2H_2 concentration to 100%, which is about 10-15 times their K_m values, they respond differently to one another. The $\alpha 278^{Thr}$ MoFe protein is able to achieve the same percentage distribution to C_2H_4 production as the wild type, whereas the $\alpha 278^{Leu}$ MoFe protein cannot.

Why cannot the $\alpha 278^{Leu}$ MoFe protein recover to the wild type level under 100% C_2H_2, which is about 12-times of its K_m value. There are several factors that might cause a low allocation of total electron flux to C_2H_4 formation. First is the electron flux through the system. As shown above in section B.2, when C_2H_2 concentration was increased to 100%, the total electron flux decreased by about 40% in the $\alpha 278^{Thr}$ and about 50% in the $\alpha 278^{Leu}$ MoFe protein. Thus, the effect of 100% C_2H_2 on electron flux through these two systems is similar and so is unlikely to be the reason for different responses. A second factor is the rate of proton delivery for C_2H_4 formation. Because C_2H_2 reduction to C_2H_4 needs two protons and two electrons, if there is a slower rate of proton delivery to the C_2H_2 binding site(s) in the $\alpha 278^{Leu}$ MoFe protein, C_2H_4 will not be produced as efficiently as in the $\alpha 278^{Thr}$ MoFe protein. When the C_2H_4 formation activity vs. pH profiles for both altered MoFe proteins are compared, they are also similar to each other (see results in Chapter 6). Therefore, the rate of proton delivery should not be a deciding factor. The third factor is the binding of C_2H_2. The K_m for C_2H_4 formation reflects the apparent binding of C_2H_2 to the MoFe protein. Both altered MoFe proteins apparently bind C_2H_2 similarly, because their K_m values are close. Thus, it seems likely that substitution with the bulky leucine at the α-278 position somehow disrupts the high-affinity C_2H_2-binding/reduction site such that it just cannot bind and reduce to C_2H_2 even at high C_2H_2 concentrations. In contrast, with the $\alpha 278^{Thr}$ MoFe protein, this high-affinity

binding site may still be functioning, but now its apparent binding affinity for C_2H_2 is substantially lowered by the substitution. Or maybe the high-affinity site is eliminated, but the low-affinity site has increased affinity for C_2H_2.

2.1.2 Insights from flux inhibition by high C_2H_2 concentrations

So-called substrate self-inhibition at high C_2H_2 concentrations has been observed previously (Hwang JC and Burris RH, 1972; Fisher K *et al.*, 2000c). The inhibition of total electron flux by a high concentration of C_2H_2 occurred with the wild type and all the altered α-278 MoFe proteins and supported the concept of a separate flux-inhibition site for C_2H_2. Again, under normal assay conditions, this site, which likely has a relatively low affinity for C_2H_2, is probably inactive. Only under higher concentrations of C_2H_2 does it inhibit the total electron flux. CO cannot relieve this electron-flux inhibition by C_2H_2 and so must not bind to the same site (this work; Fisher K *et al.*, 2000c). In the presence of 10% CO, the electron-flux inhibition is clearer because CO eliminates C_2H_2 reduction. Under 40% C_2H_2 (+10% CO), the rate of H_2 evolution by $\alpha 278^{Leu}$ MoFe protein is only about 25% of that under argon (+ 10% CO), whereas for the wild type MoFe protein, it is about 82% of the H_2 evolution under argon (+ 10% CO). These results indicate that the C_2H_2 binding flux-inhibition site on the wild type MoFe protein has been affected by the substitution in the $\alpha 278^{Leu}$ MoFe protein. This flux-inhibition site could be the same one as that in the wild type MoFe protein, but its affinity for C_2H_2 has been increased. This flux-inhibition site likely constitutes a third C_2H_2-binding site on the MoFe protein, although it is also possible that it is the low-affinity C_2H_2-binding site that can bind C_2H_2, but not reduce it to C_2H_4, when CO is present (Lowe DJ *et al.*, 1990; Fisher K *et al.*, 2000c).

Another difference of the inhibition of total electron flux by high C_2H_2 concentrations with the $\alpha 278^{Leu}$ MoFe protein when compared with the wild type MoFe protein is their different rates of ATP hydrolysis. The decrease in electron flux on C_2H_2 binding is accompanied by a similar decrease in the rate of ATP hydrolysis with the wild type MoFe protein. The result is an unchanged ATP/$2e^-$ ratio (Table 5.2). It indicates that both electron flux to products and ATP hydrolysis are interrupted by the binding of C_2H_2 to the flux inhibition site. It has been suggested previously that either (a) the bound C_2H_2

inhibits total electron flux by enhancing the MoFe protein-Fe protein association rate and so increasing the steady-state concentration of a ternary complex of the MoFe protein plus bound C_2H_2 with oxidized Fe protein (Lowe DJ *et al.*, 1990), which must also not catalyze the reductant-independent hydrolysis of ATP (Fisher K *et al.*, 2000c) or (b) the bound C_2H_2 prevents association of the two component proteins and, thus, inhibit both electron transfer and ATP hydrolysis equally (Fisher K *et al.*, 2000c).

The $\alpha 278^{Leu}$ MoFe protein, though, reacts differently to increasing concentrations of C_2H_2. The total electron flux still decreases as before, but the rate of ATP hydrolysis increases with increasing C_2H_2 concentration. Thus, the ATP/$2e^-$ ratio increases dramatically with this altered MoFe protein. It may be in this case that the complex of oxidized Fe protein and altered MoFe protein formed on C_2H_2 binding inhibits electron transfer but not the reductant-independent hydrolysis of ATP. But, although this situation would increase the ATP/$2e^-$ rates, it would not reasonably explain the enhanced rate of MgATP hydrolysis. Such a rate enhancement is only likely for two reasons. One, if the dissociation rate of the complex (i.e. the step involving ATP hydrolysis) increased in the presence of C_2H_2 but does not always result in electron transfer. Two, if reductant-independent ATP hydrolysis by the ternary complex occurs simultaneously, but separately, from ATP hydrolysis that is accompanied by electron transfer. However, this explanation requires that C_2H_2 specifically stimulates reductant-independent ATP hydrolysis only when electron transfer is inhibited by its binding.

2.1.3 Insights from C_2H_6 production

C_2H_6 is only formed directly from C_2H_2 by those altered MoFe proteins ($\alpha 278^{Thr}$ and $\alpha 278^{Leu}$) with the high K_m values for C_2H_4 production from C_2H_2. As discussed above, these altered MoFe proteins likely have their high-affinity binding sites disrupted by these substitutions. If so, then a reasonable conclusion is that the low-affinity C_2H_2-binding site is also responsible for C_2H_6 production. Moreover, an extension of this conclusion, based on the previous correlation of C_2H_6 production with loss of stereospecificity of proton addition to C_2D_2 (Fisher K *et al.*, 2000c), is that the $\alpha 278^{Thr}$ and $\alpha 278^{Leu}$ MoFe proteins should produce more *trans*-$C_2D_2H_2$ from C_2D_2 than does wild

type. We, therefore, measured the proportions of both $C_2D_2H_2$ isomers produced by the $\alpha 278^{Ala}$ and $\alpha 278^{Thr}$ MoFe proteins. It turned out that our results are consistent with this conclusion. The $\alpha 278^{Ala}$ MoFe protein, which has a wild type K_m value for C_2H_4 formation and cannot produce C_2H_6, produces an identical percentage of *trans*-$C_2D_2H_2$ as does the wild type, i.e., less than 10% of the *trans*-isomer under 5% C_2D_2 in argon. The $\alpha 278^{Thr}$ MoFe protein with its much higher K_m value and ability to produce C_2H_6, gives about 30% of the products as *trans*-$C_2D_2H_2$. These results are consistent with the longer-lived, ethylenic intermediate on the enzyme suggested to be responsible for both ethane production and the loss of proton-addition stereospecificity (Fisher K *et al.*, 2000c), but further, that this intermediate occurs only at the low-affinity site.

3. Interactions of N_2 with the altered α-278 MoFe proteins

Three of the four altered α-278 MoFe proteins can reduce N_2 to NH_3 at rates comparable to that of the wild type MoFe protein (see Table 4.2). As shown in Table 5.1, the apparent binding affinity of these altered MoFe proteins for N_2 is not changed much compared to the wild type. The biggest change occurs with the $\alpha 278^{Thr}$ MoFe protein, which has a 2-fold higher K_i for N_2 inhibition of C_2H_2 reduction compared to wild type, consistent with its use of only about 50% of its total electron flux for NH_3 formation (see Table 4.2). In contrast, the $\alpha 278^{Leu}$ MoFe protein does not bind and reduce N_2 (see Table 4.2). This substitution may cause a change in the MoFe protein so that it cannot reach the redox state required for N_2 binding. Its H_2-evolution activity on the basis of Mo content is only about 25% of that of the wild type MoFe protein. Assuming the Mo content represents the amount of active FeMo cofactor present, it appears that the FeMo cofactor in this altered MoFe protein is not as active as in the wild type.

From the results of N_2 reduction by these altered MoFe proteins, it is clear that the αSer278 residue is not directly involved in N_2-binding and reduction and that substitution at this position has little effect on the interaction with N_2. These results support the concept that N_2 binding does not occur at the high-affinity C_2H_2-binding site because this site is ineffective in the $\alpha 278^{Thr}$ MoFe protein, which is still able to bind and reduce N_2. Thus, it is likely that N_2 binds at, and so shares, the low-affinity C_2H_2-binding site.

4. Structure-function insights

Substitution at the α278 position can result in several changes in the kinetic properties of nitrogenase. First, the K_m for C_2H_4 formation may increase up 10-times that of the wild type. Second, electron flux inhibition by high C_2H_2 concentrations is enhanced. Third, C_2H_6 may be produced as a minor product. Fourth, non-saturating concentrations of CO induce cooperativity in C_2H_4 production from C_2H_2. These data are consistent with the presence of two C_2H_2-binding sites, one (at least) of which is close to αSer278 residue.

A previous investigation of the kinetic properties of the altered $\alpha 69^{Ser}$ MoFe protein suggested that both a high-affinity and low-affinity C_2H_2-binding site were present on the MoFe protein (Christinansen J *et al.*, 2000). The high-affinity C_2H_2-binding site was eliminated by substitution of the αGly69 residue to serine leaving only the low-affinity C_2H_2-binding site. It was further suggested that N_2 shared this site with C_2H_2. Our results generally support this model, but a concern is the fact that substitution at α278 can result in loss of the high-affinity site just as occurs with substitution at α69. How might these two sets of results be rationalized? One possibility is that the αSer278 may hydrogen bond to αHis195 (see Chapter 6, Figure 6.5-6.7), which is itself hydrogen bonding to one of the central sulfide atoms of the FeMo cofactor. This sulfide is a member of the 4Fe-4S face of the FeMo cofactor capped by αVal70. So, interruption of this hydrogen-bonding network could impact reactivity at this putative high-affinity site. However, this suggestion cannot be the whole story because this $\alpha 69^{Ser}$ MoFe protein does not produce C_2H_6 directly from C_2H_2 and produces only a wild-type level of trans-$C_2D_2H_2$ (Benton PM *et al.*, 2001).

In addition, the αCys275, αSer278 and αHis195 residues may be involved in proton delivery to the FeMo cofactor (Pham DN and Burgess BK, 1993; Dilworth MJ *et al.*, 1998; Fisher K *et al.*, 2000a,b). Substitution at αSer278 could also affect proton delivery to bound substrate and thus affect the kinetics of the C_2H_2 reduction. This suggestion is addressed in Chapter 6.

Chapter 6

Activity Versus pH profiles of the Altered α-278 MoFe proteins

A. Introduction

There is compelling evidence that the FeMo cofactor provides the substrate binding and reduction sites (Shah VK and Brill WJ, 1977; Hawkes TR *et al.*, 1984; Scott DJ *et al.*, 1990, 1992; Kim C-H *et al.*, 1995; Shen J *et al.*, 1997). Besides dinitrogen, nitrogenase also catalyzes the reduction of a variety of other substrates, such as the H^+ and C_2H_2. Most of the substrate reductions require equal amount of electrons and protons. However, both the proton donors and the proton-transfer process are unknown.

A three-component buffer system (Pham DN and Burgess BK, 1993) used for the nitrogenase activity assays in the pH range of 5.0-9.8 eliminates the problems encountered when different buffers are used individually to cover a pH range. For catalyzed H_2 evolution and N_2 reduction to occur with the wild type MoFe protein, an acid-base group(s) with a pK_a of about 6.3 must be deprotonated and another acid-base group(s) with a pK_a of about 9.0 must be protonated (Pham DN and Burgess BK, 1993). Both groups are located close to the FeMo cofactor because their pK_a values are disturbed by the presence of either substrates or inhibitors. For example, CO affects only the group(s) with the higher pK_a value. The responsible acid-base groups were not identified, but the strictly conserved αCys275 and αSer278 were suggested as possibly responsible for the higher pK_a value. Now that four α-278-substituted MoFe proteins have been purified, we can perform activity vs. pH experiments to determine if the αSer278 residue is responsible for that higher pK_a value and involved in the proton transfer to substrate.

B. Method

1. Activity vs. pH experiments

Nitrogenase activity assays, under 100% argon, 100% nitrogen, 90% argon + 10% CO, 90% argon + 10% C_2H_2 and 80% argon + 10% CO + 10% C_2H_2, were performed as described in Chapter 2.H section. The difference in the activity vs. pH experiments from

the usual assay is that a three-buffer system was used instead of the 25 mM HEPES (pH 7.4) buffer in all the assays. This buffer system contains 75 mM Bis-Tris, 38 mM HEPPS and 38 mM CHES. The pH of the buffer was measured by a Fisher Scientific Accumet AR15 pH meter (Fisher Scientific, Pittsburgh, PA). The resolution was 0.01-pH unit. Stock reaction mixture was prepared in the three-buffer system and its pH was adjusted to 7.4. The reaction mixture was then distributed to different assay vials and was adjusted to the desired pH by addition of either 6 M HCl or 6 M NaOH. The assay vials were then degassed and flushed with argon as usual and were ready for the nitrogenase activity assays. All of the activity-pH assays were performed in the presence of a 20-fold molar excess of wild type Fe protein. In these experiments, four assays for each pH value were performed. One assay under argon was an activity control, one assay was used for checking the turnover pH, and the other two served as duplicate experimental samples. After the activity assays were stopped by 0.5 M EDTA (pH 8.0), the assay vial used for measuring the turnover pH was taken out of the water bath-shaker, opened, and the pH immediately measured. No significant pH changes occurred in any of the vials during the assay. This three-buffer system was both stable and consistent in the experiments.

2. S-PLUS program and pH profiles

To interpret the activity vs. pH data more accurately, a computer program called S-PLUS was used. S-PLUS is a language specially created for exploratory data analysis and statistics (S-PLUS 2000, Programmer's Guide). S-PLUS uses a specific model in attempting to describe the relationship and structure in the provided data. There are different models used in S-PLUS to analyze the data. The model used for the activity vs. pH data is called a non-linear local regression model. This model gives predictions based on the experimental data points, which are activity/pH pairs, to generate a reliable and smooth curve. Each point on the curve depends more on the nearest neighbor (local) experimental data points.

Shown in Figure 6.1 is an example of the profiles generated by the S-PLUS program. This activity vs. pH profile is of the wild type MoFe protein under 100% argon. Activity values used are the percentage of activity compared to the maximum specific activity in that set of assays and they are plotted as a function of pH. The Y-axis can also

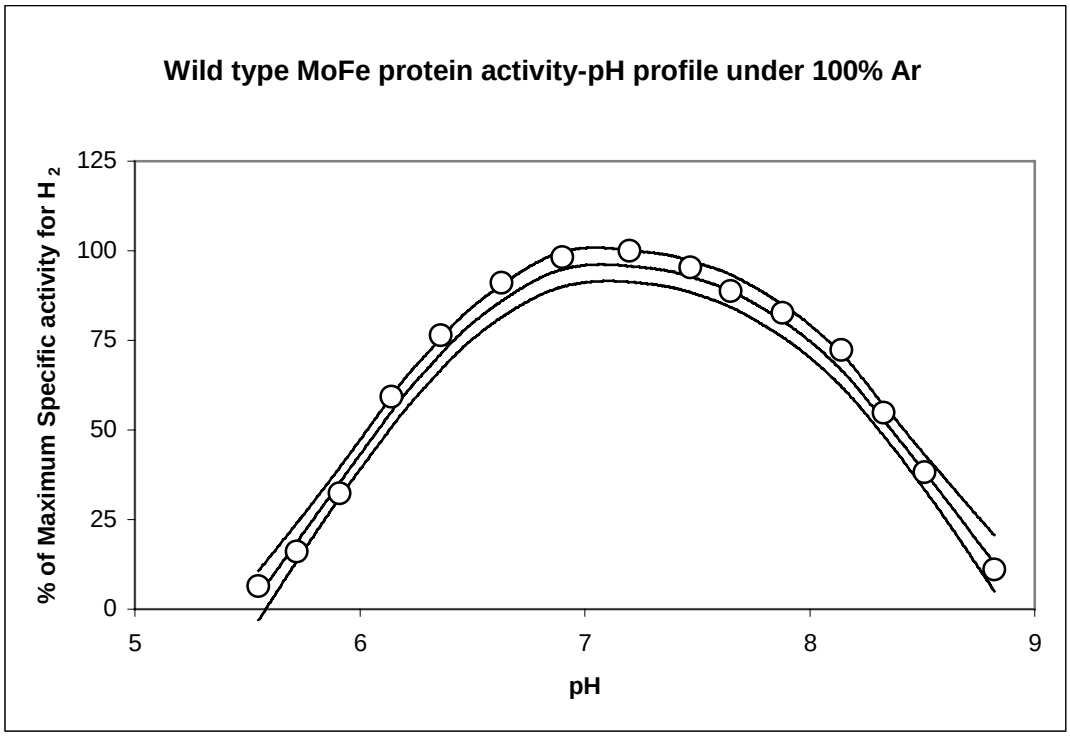

Figure 6.1 Activity-pH profile of the wild type MoFe protein under 100% argon generated by the S-PLUS program.

The specific activity for each pH value was normalized as a percentage of the highest activity in that series of assays.

be plotted in actual specific activities. There are three lines generated by the program. The middle line is called the fit line, which is the direct prediction by S-PLUS; the other two lines are called the upper line and the lower line, respectively, which are the 95% confidence boundaries for the fit line. With the higher and lower boundary to the fit line, an error range can be derived for the data, which indicates the reliability of the experiments. The error ranges for the two pK_a values of each profile were not more than ± 0.08 pH units in these experiments. The activity-pH profile for each assay atmosphere was repeated at least twice and a control profile from assays under 100% argon were always performed to ensure consistency among the results.

The bell-shape curve suggests two apparent pK_a values, which are the pH values where 50% of the maximum activity occurs. As shown in Figure 6.1, for the wild type MoFe protein under 100% argon, an acid-base group with a pK_a of about 6 (6.08 ± 0.04) must be deprotonated and another acid-base group with a pK_a of about 8.3 (8.31 ± 0.04) must be protonated for H_2 evolution to occur. Although there are only two apparent pK_a values indicated by this profile, it could be that more than one acid-base group actually contributes to each of the pK_a values. For abbreviation, the pK_a value for the deprotonated group is designated as the lower pK_a and the pK_a value for the protonated group is designated as the higher pK_a in the pH profile. The pH profile also indicates an approximate pH value for the maximum activity. In this case, the pH for the maximum activity is about 7 (7.09 ± 0.01).

C. Results

The activity vs. pH experiments for the wild type and the four altered α-278 MoFe proteins were performed under 100% argon, 90% argon + 10% CO, 90% argon + 10% C_2H_2, 80% argon + 10% C_2H_2 + 10% CO, and 100% N_2. These experiments were also done using the $\alpha 195^{Gln}$ MoFe protein, which was kindly provided by Dr. K. Fisher.

1. Activity-pH profiles under argon with and without 10% CO

Data in Table 6.1 show that, for all five MoFe proteins whether or not CO was present, the pK_a values for the deprotonated group were generally the same, which was

Table 6.1 The pK_a values for the deprotonated and protonated groups and the pH for the maximum activity of the wild type and the altered α-278 MoFe proteins.

MoFe protein	**pK_a of the deprotonated group**		**pH for maximum activity**		**pK_a of the protonated group**	
	Ar	Ar +10%CO	Ar	Ar +10%CO	Ar	Ar +10%CO
Wild type	6.08±0.04	6.02±0.05	7.09±0.01	6.99±0.01	8.31±0.04	8.06±0.06
$\alpha 278^{Thr}$	6.07±0.04	6.04±0.06	7.06±0.01	7.09±0.01	8.07±0.03	8.09±0.08
$\alpha 278^{Cys}$	6.06±0.03	6.04±0.04	7.03±0.04	7.08±0.04	8.22±0.03	8.21±0.04
$\alpha 278^{Ala}$	6.06±0.03	6.08±0.07	7.12±0.01	7.17±0.01	8.28±0.03	8.31±0.06
$\alpha 278^{Leu}$	5.90±0.04	5.88±0.08	6.94±0.01	6.98±0.01	8.38±0.04	8.23±0.08

about 6. This situation also happened for the pH for the maximum activity, all of which were around 7 and again were unaffected by added CO.

In contrast, the higher pK_a value did respond to both substitution and addition of CO. With wild type MoFe protein under 100% argon, the higher pK_a value was 8.31. With the $\alpha278^{Cys}$, $\alpha278^{Ala}$ and $\alpha278^{Leu}$ MoFe proteins, the higher pK_a values were very close to that of the wild type (Table 6.1), whereas with the $\alpha278^{Thr}$ MoFe protein, this value shifted in the acid direction, to about 8.07.

For wild type MoFe protein, the addition of 10% CO shifted the pK_a to ~8, that is by about -0.3 pH units, whereas for the $\alpha278^{Thr}$ MoFe protein, the addition of 10% CO did not change the pK_a value. For this $\alpha278^{Thr}$ MoFe protein, the pK_a values both with and without CO were the same as the wild type plus 10% CO (Figure 6.2 and Table 6.1). For the $\alpha278^{Cys}$, $\alpha278^{Ala}$ and $\alpha278^{Leu}$ MoFe proteins, the addition of 10% CO did not change the pK_a much, remaining the same as (or close to) that of the wild type under argon only, as shown in Figure 6.3, where the profile of the $\alpha278^{Ala}$ MoFe protein is used as a representative. The actual specific activities were also plotted in the Y-axis for the profiles under 100% argon and 90% argon plus 10% CO (data not shown) and yielded the same results. In a pH range from about 6.5 to 7.5, which covers the normal nitrogenase activity assay pH condition, added CO did not inhibit H_2 evolution in any of the MoFe proteins tested in this work.

2. Activity-pH profiles of the $\alpha195^{Gln}$ MoFe protein

From the activity-pH profiles under 100% argon +/- 10% CO with the wild type and the altered α-278 MoFe proteins, a possible interaction between the αSer278 and the αHis195 was indicated (see discussion D.1). To obtain more information on whether or not the αHis195 residue is the responsible group or at least one of the responsible acid-base groups contributing to the protonated pK_a value observed for the wild type MoFe protein, the activity-pH profiles under different assay atmospheres with the $\alpha195^{Gln}$ MoFe protein were constructed.

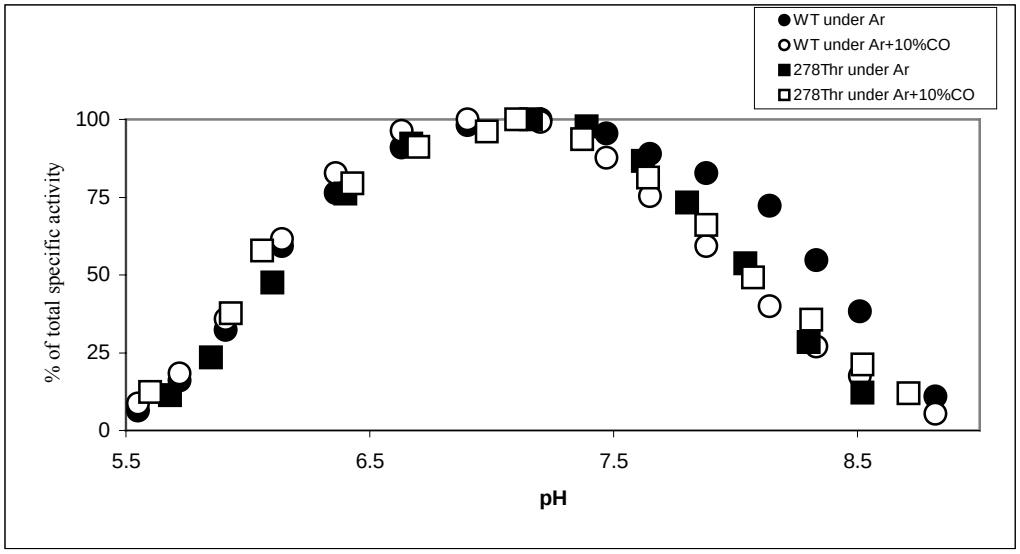

Figure 6.2 Activity vs. pH profiles of the wild type and the α-278^{Thr} MoFe protein under Ar +/- 10% CO.

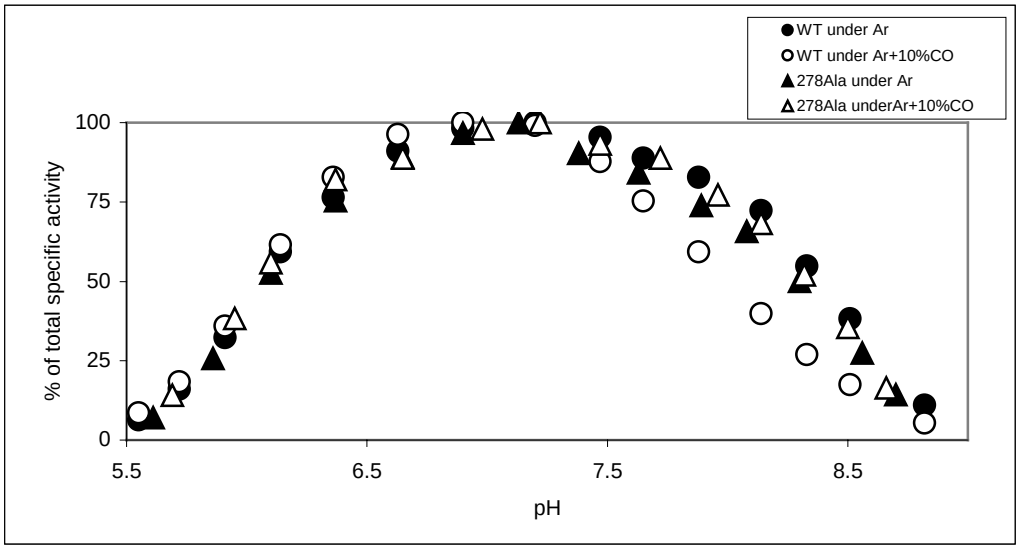

Figure 6.3 Activity vs. pH profiles of the wild type and the α278^{Ala} MoFe protein under Ar +/- 10% CO.

The data for the α278^{Ala} MoFe protein is also representative of the activity-pH profiles for the α278^{Cys} and the α278^{Leu} MoFe proteins under Ar +/- 10% CO.

Table 6.2 shows the results. Generally, both the pK_a values and the pH for maximum activity were unaffected under all assay atmospheres except N_2 and by the substitution. However, the shift of the pK_a value for the protonated group with this altered MoFe protein was more dramatic than that of the wild type when the atmosphere was changed from 100% argon to 100% N_2 atmosphere. The higher pK_a value for H_2 evolution with the wild type MoFe protein shifted to 8.00 (by -0.31 pH units) from 8.31 under 100% argon. With the $\alpha 195^{Gln}$ MoFe protein, it shifted to 7.34 (by -0.84 pH units) from 8.18 under 100% argon. Figure 6.4 compares the actual specific activity (panel A) and normalized activity (panel B) of H_2 evolution either under 100% argon or under 100% N_2 for the $\alpha 195^{Gln}$ and the wild type MoFe proteins. H_2 evolution under argon with both the wild type and the $\alpha 195^{Gln}$ MoFe proteins maximized at pH values within the range of normal assay pH. The profiles were similar to each other. Again, under 100% N_2, the H_2 evolution activity-pH profile of the $\alpha 195^{Gln}$ MoFe protein (panel B) was significantly shifted, compared both to that under 100% argon and to those of the wild type MoFe protein (under both argon and N_2). The maximum activity for H_2 evolution under 100% N_2 of the $\alpha 195^{Gln}$ MoFe protein was at a pH of about 6.50, a shift of about -0.4 pH units (compared to that of the wild type).

3. Activity-pH profiles for the altered α-278 MoFe proteins under 100% N_2

How then would the altered α-278 MoFe proteins respond to N_2? As shown in Table 6.3, the pK_a value of the deprotonated group and the pH for maximum activity were not changed much (by no more than ~0.1 pH unit) by either substitution or changing the assay atmosphere. For those which can reduce N_2, namely the $\alpha 278^{Thr}$, $\alpha 278^{Ala}$ and $\alpha 278^{Cys}$ MoFe proteins, the pK_a values for the protonated group(s) for the H_2 evolution under 100% N_2 shifted by -0.1 to -0.2 pH units compared to those under 100% argon. The actual pK_a values of the protonated group(s) for the $\alpha 278^{Ala}$ and $\alpha 278^{Cys}$ MoFe protein are similar to those of the wild type both before and after the change in atmosphere. For the $\alpha 278^{Thr}$ MoFe protein, the pK_a value starts out lower and finishes lower than wild type. These results are consistent with their Nif^+ phenotype and the electron distribution to both H_2 and NH_3 production under 100% N_2. For the $\alpha 278^{Leu}$

Table 6.2 The pK_a values for the deprotonated and protonated group(s) and the pH for maximum activity in the $\alpha 195^{Gln}$ and the wild type MoFe proteins under different assay atmospheres.

Under 100% N_2, only the H_2 evolution data were used to generate the activity-pH profiles.

MoFe protein /Assay atmosphere	**pK_a of the deprotonated group**	**pH for maximum activity**	**pK_a of the protonated group**
Wild type			
Under Ar	6.08±0.04	7.09±0.01	8.31±0.04
Under Ar + 10%CO	6.02±0.05	6.99±0.01	8.06±0.06
Under Ar + 10% C_2H_2	6.01±0.05	7.04±0.01	7.92±0.05
Under 100% N_2	5.96±0.05	6.90±0.01	8.00±0.07
$\alpha 195^{Gln}$			
Under Ar	6.04±0.02	6.99±0.01	8.18±0.03
Under Ar + 10%CO	5.98±0.06	7.03±0.01	8.08±0.06
Under Ar + 10% C_2H_2	6.01±0.05	6.89±0.01	7.99±0.07
Under 100% N_2	5.88±0.03	6.50±0.01	7.34±0.04

A

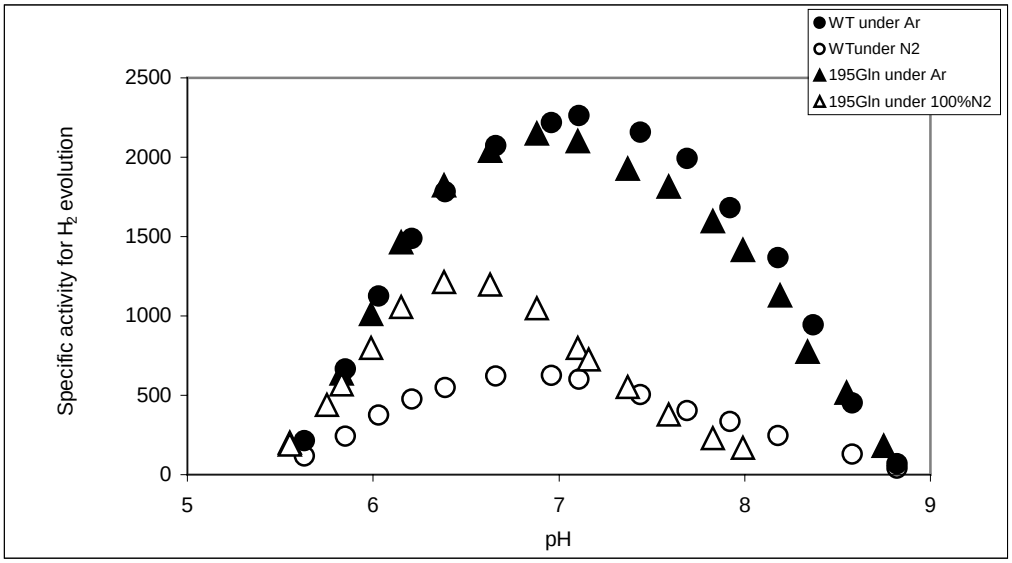

B

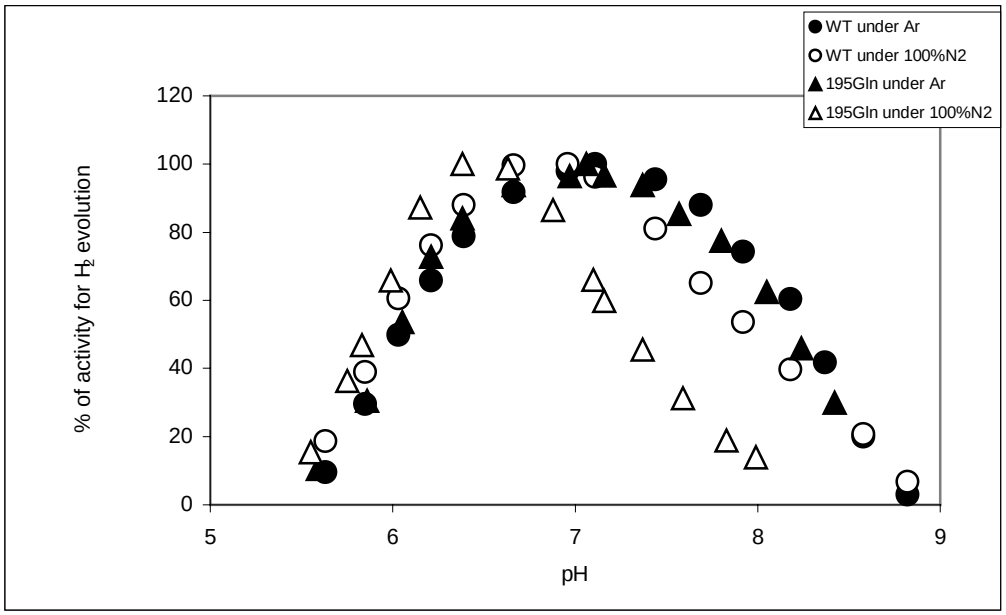

Figure 6.4 Activity vs. pH profiles of the $\alpha 195^{Gln}$ and wild type MoFe proteins under 100% argon and 100% N_2.

Panel A shows plots of the specific activity of H_2 evolution versus pH; panel B is plot of the percentage of maximum H_2 evolution activity vs. pH.

Table 6.3 The pK_a values of the deprotonated and protonated groups and the pH for the maximum activity for the H_2 evolution with the wild type and the altered α-278 MoFe proteins under 100% argon and 100% N_2.

MoFe protein	**pK_a of the deprotonated group**		**pH for maximum activity**		**pK_a of the protonated group**	
	Ar	100%N_2	Ar	100%N_2	Ar	100%N_2
Wild type	6.08±0.04	5.96±0.05	7.09±0.01	6.90±0.01	8.31±0.04	8.00±0.07
$\alpha278^{Thr}$	6.07±0.04	5.99±0.05	7.06±0.01	6.89±0.01	8.07±0.03	7.84±0.06
$\alpha278^{Cys}$	6.06±0.03	5.90±0.05	7.03±0.04	6.80±0.04	8.22±0.03	8.09±0.07
$\alpha278^{Ala}$	6.06±0.03	5.91±0.05	7.12±0.01	6.86±0.01	8.28±0.03	8.07±0.07
$\alpha278^{Leu}$	5.90±0.04	5.85±0.05	6.94±0.01	6.84±0.01	8.38±0.04	8.23±0.06

MoFe protein, which cannot bind and reduce N_2, the pK_a value was not affected much and remained close to the pK_a under argon.

4. Activity-pH profiles for the altered α-278 MoFe proteins under 90% argon/10% C_2H_2

As discussed in Chapter 5, our data suggest that one of the C_2H_2-binding sites is at the Fe_3S_4 subcluster of the FeMo cofactor. Therefore, the activity-pH profiles under 90% argon/10% C_2H_2 for these altered MoFe proteins were determined. Again, the pK_a values of the deprotonated group(s) required for either H_2 evolution or C_2H_4 formation were the same as those under 100% argon and so were unaffected by the substitution. This situation was also held for the pH for maximum activity. Therefore, Table 6.4 shows only the results of the pK_a values of the protonated group. Compared to the pK_a values of the protonated group under 100% argon, the wild type, α-278^{Cys}, α-278^{Ala} and α278^{Leu} MoFe proteins exhibited a shift for both H_2 evolution (ΔpH = -0.27, -0.21, -0.34 and -0.56, respectively) and C_2H_4 formation (ΔpH = -0.35, -0.10, -0.11 and -0.54, respectively) under 90% argon/10% C_2H_2. With the α278^{Thr} MoFe protein, the corresponding pK_a values were not changed at all.

Under 90% argon/10% C_2H_2, the pK_a value of the protonated group for the total specific activity for the wild type, the α278^{Cys}, α278^{Ala} and α-278^{Leu} MoFe proteins shifted from 8.31 to 7.92 (by -0.39 pH units), from 8.22 to 8.14 (by -0.08 pH units), from 8.28 to 8.15 (by -0.13 pH units) and from 8.38 to 7.84 (by -0.54 pH units), respectively. For the α278^{Thr} MoFe protein, it was not changed at all. They were still around 8.0.

Among the altered α-278 MoFe proteins, both the α278^{Thr} and the α278^{Leu} MoFe proteins can reduce C_2H_2 to C_2H_4 plus C_2H_6. When performing the activity vs. pH experiments under 90% argon/10% C_2H_2, the profiles of the C_2H_6 production for these two altered MoFe proteins were investigated (Table 6.5). Table 6.5 compares the profiles of the two products of C_2H_2 reduction. The pK_a values of the deprotonated, maximum activity and protonated groups required for C_2H_6 formation by the α278^{Thr} MoFe protein were shifted in the basic direction compared to those required for C_2H_4 formation. The pK_a value of the deprotonated group shifted from 6.05 to 6.87 (by +0.82 pH units), and the pKa value of the protonated shifted from 8.04 to 8.55 (by +0.51 pH units), respectively. The pH for maximum activity shifted from 7.07 to 7.95 (by +0.88 pH units).

Table 6.4 The pK_a values of the protonated group the wild type and the altered α-278 MoFe proteins under 100% argon and 90% argon/10% C_2H_2.

MoFe protein	**pK_a of the protonated group**			
	Ar	Ar+10%C_2H_2		
	H_2	H_2	C_2H_4	Total [a]
Wild type	8.31±0.04	8.04±0.08	7.96±0.05	7.92±0.05
$\alpha278^{Thr}$	8.07±0.03	8.06±0.08	8.04±0.05	8.07±0.05
$\alpha278^{Cys}$	8.22±0.03	8.01±0.09	8.12±0.07	8.14±0.04
$\alpha278^{Ala}$	8.28±0.03	7.94±0.06	8.17±0.07	8.15±0.03
$\alpha278^{Leu}$	8.38±0.04	7.82±0.10	7.84±0.08	7.84±0.05

[a] Total specific activity (expressed as nmols of electron pairs per min×mg MoFe protein appearing in all measured products) under 90% argon/10% C_2H_2 was used to generate activity-pH profiles for these MoFe proteins.

Table 6.5 Under 90% argon/10% C_2H_2, the pK_a values of the deprotonated group, protonated group and the pH for the maximum activity for the C_2H_4 and C_2H_6 production in the altered $\alpha 278^{Thr}$ and the $\alpha 278^{Leu}$ MoFe protein.

Assay atmosphere (10%C_2H_2)	**pK_a of the deprotonated group**		**pH for maximum activity**		**pK_a of the protonated group**	
Product / MoFe protein	C_2H_4	C_2H_6	C_2H_4	C_2H_6	C_2H_4	C_2H_6
$\alpha 278^{Thr}$	6.05±0.06	6.87±0.10	7.07±0.01	7.95±0.01	8.04±0.05	8.55±0.07
$\alpha 278^{Leu}$	5.80±0.10	5.78±0.07	6.79±0.01	7.02±0.01	7.84±0.10	8.25±0.06

For the $\alpha 278^{Leu}$ MoFe protein, the shifts were different from those with the $\alpha 278^{Thr}$ MoFe protein. There was no shift for the pK_a value of the deprotonated group for the C_2H_6 formation compared to the C_2H_4 formation. The pK_a value of the protonated group shifted from 7.84 to 8.25 (by +0.41 pH units) and the pH for maximum activity shifted from 6.79 to 7.02 (by +0.23 pH units).

Activity vs. pH profiles of the altered MoFe proteins under argon with both 10% CO and 10% C_2H_2 were also performed. Table 6.6 shows the results. When 10% CO is present, it is sufficient to completely inhibit all catalyzed substrate reductions. As expected, the pK_a values for the protonated group are the same as those under argon with just 10% CO present (see Table 6.1) for the wild type, the $\alpha 278^{Thr}$, the $\alpha 278^{Cys}$ and the $\alpha 278^{Ala}$ MoFe protein. Apparently, the effect of CO on the deprotonation/protonation of the acid-base groups dominates that of C_2H_2. However, for the $\alpha 278^{Leu}$ MoFe protein, the pK_a of the protonated group shifted to around 8 (8.04 ± 0.09), which is in between the pK_a under 10% CO (8.23 ± 0.08) and the pK_a under 10% C_2H_2 (7.84 ± 0.05).

D. Discussion

The FeMo cofactor of the Mo-nitrogenase is buried about 10 Å from the protein surface (Kim J and Rees DC, 1992a,b). Currently, there is little information about how protons are transferred from the solvent to the FeMo cofactor. The αSer278 residue is hydrogen bonded to the αCys275, one of the direct ligands to the FeMo cofactor. This interaction was used to argue that it could be one of the acid-base groups required for nitrogenase activity (Pham DN and Burgess BK, 1993). In addition, we find both the $\alpha 278^{Thr}$ and $\alpha 278^{Leu}$ MoFe proteins allocate lower percentage electron flux for C_2H_4 formation compared to that with the wild type and both produce C_2H_6 when reducing C_2H_2. C_2H_2 reduction catalyzed by the $\alpha 278^{Thr}$ MoFe protein also becomes much more sensitive to CO compared to the wild type (see Chapter 5). One possible reason for these changes is that the substitution might be interrupting proton delivery to C_2H_2-binding/reduction site. Activity vs. pH profiles of the nitrogenase-catalyzed reactions may provide useful information about the nature of the groups involved in proton transfer to the FeMo cofactor and bound substrate and any intermediates formed.

Table 6.6 The pK_a values of the deprotonated and protonated group, the pH for the maximum activity for the altered α-278 MoFe proteins under argon + 10% CO + 10% C_2H_2.

MoFe protien	**pK_a for the deprotonated group**		**pH for the maximum activity**		**pK_a for the protonated group**	
	Ar	Ar+10%C_2H_2 +10%CO	Ar	Ar+10%C_2H_2 +10%CO	Ar	Ar+10%C_2H_2 +10%CO
Wild type	6.08±0.04	5.93±0.09	7.09±0.01	6.93±0.02	8.31±0.04	8.02±0.1
$\alpha278^{Thr}$	6.07±0.04	6.09±0.07	7.06±0.01	7.08±0.01	8.07±0.03	8.11±0.08
$\alpha278^{Cys}$	6.06±0.03	5.99±0.06	7.03±0.04	7.08±0.01	8.22±0.03	8.20±0.06
$\alpha278^{Ala}$	6.06±0.03	6.02±0.07	7.12±0.01	7.09±0.01	8.28±0.03	8.33±0.07
$\alpha278^{Leu}$	5.90±0.04	5.82±0.07	6.94±0.01	6.65±0.01	8.38±0.04	8.04±0.09

1. Effect of amino acid substitution and CO binding on the activity-pH profiles

Under 100% argon only the higher pK_a values of the altered α-278 MoFe proteins shift compared to the wild type MoFe protein (Table 6.1). The change to Thr, which is the conservative substitution for Ser (wild type), shifted the pK_a of the protonated group from 8.3 to 8.1. All the other substitutions, which do not have the hydroxyl group, do not change the pK_a much, all of which remained close to that of the wild type MoFe protein under argon (~8.3) (Figure 6.3). If, as proposed, the αSer278 residue is responsible for this higher pK_a (Pham DN and Burgess BK, 1993), the three substitutions without this functional group would be more likely to affect the pK_a rather than the Thr substitution. Therefore, neither the $\alpha 278^{Ser}$ nor this hydrogen-bond interaction between the αSer278 and αCys275 residues is directly responsible for the higher pK_a required for the catalysis.

Added CO had the same effect on the pK_a of the protonated group(s) as the substitution of Thr for Ser at the α-278 position. As shown in Figure 6.2, the profiles of the $\alpha 278^{Thr}$ MoFe protein under argon with or without 10% CO resembled the profile of wild type MoFe protein under argon in the presence of 10% CO. As a first simple explanation, the Thr residue may have assumed a position in the structure similar to that taken up by the Ser in the CO-bound state of the wild type MoFe protein. In this case, the subsequent binding of CO to the α-278^{Thr} MoFe protein would not affect this state.

By using the published structure of MoFe protein (Peters JW *et al.*, 1997) and a computer program (SpdbViewer, Guex N *et al.*, 1997), a possible scheme has been devised for what may be occurring. The interaction of αSer278 with αCys275 in the wild type MoFe protein may be affected by the binding of CO to the FeMo cofactor. The αSer278 may switch from its "argon state" (Figure 6.5) to its "CO bound state" (Figure 6.6), in which the hydroxyl group of the Ser is hydrogen bonded to the δ-nitrogen of the $\alpha 195^{His}$ residue. It has been previously suggested that the αHis195 residue, which is hydrogen bonded to one of the central sulfide atoms of the FeMo cofactor, is involved in proton delivery to the FeMo cofactor (Dilworth MK *et al.*, 1998; Fisher K *et al.*, 2000b). When CO binds and the hydroxyl group of αSer278 flips towards αHis195, this electron-withdrawing hydrogen bond would facilitate the leaving of the proton from the ε-nitrogen of the His residue and result in a lower (observed) pK_a value for this last group.

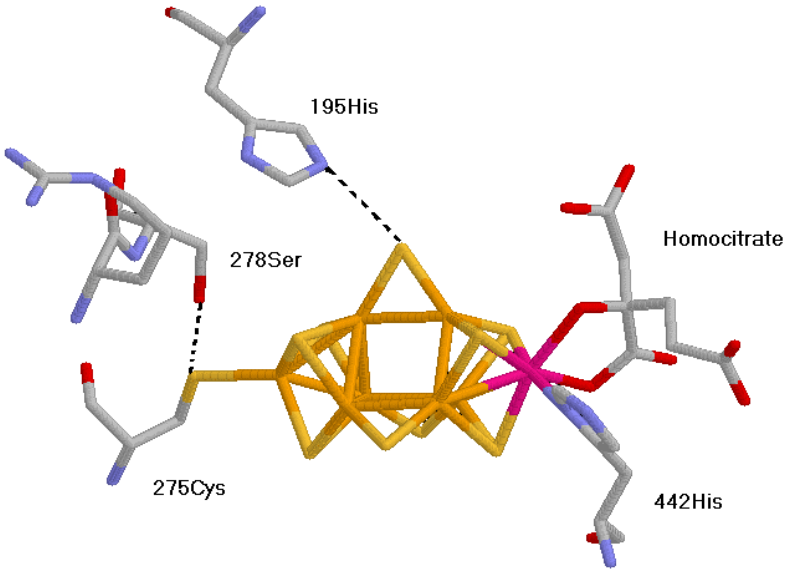

Figure 6.5 Wild type MoFe protein under 100% argon.

Structure is adapted from Peters JW *et al.*, 1997. Computer modeling is done by the SPdbViewer program (Guex N *et al.*, 1997).

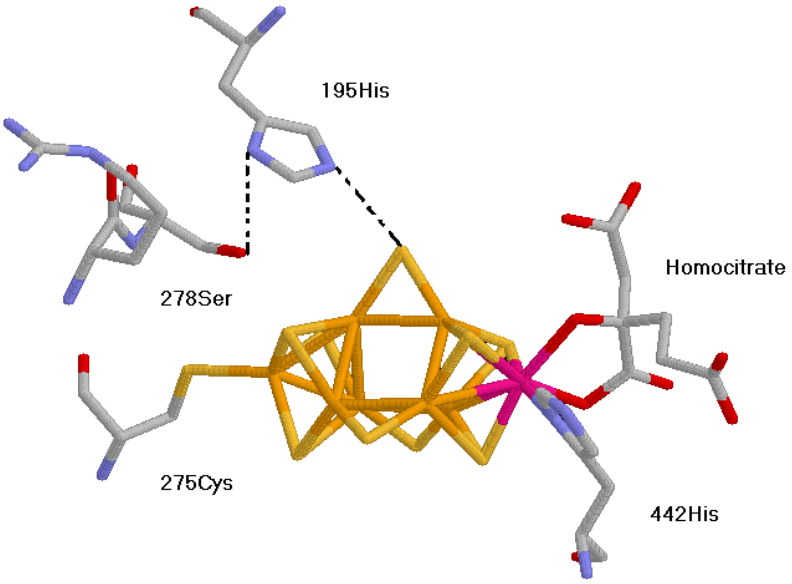

Figure 6.6 Wild type MoFe protein under 10% CO showing the hypothetical “flip”.

Applying this scheme to the other altered α-278 MoFe proteins by exploring the computer-generated model structures, we found that the hydroxyl group of Thr in $\alpha 278^{Thr}$ MoFe protein may already be hydrogen bonded to the δ-nitrogen of the αHis195 (Figure 6.7). The SpdbViewer computer program not only can measure the distance of two atoms but also can do molecular modeling to generate amino-acid substitution(s) on the known three-dimensional structure. In support of this suggestion, the measured distances from the oxygen atom of the hydroxyl group to both the nearest Fe atom in the FeMo cofactor and to the δ-nitrogen of the αHis195 residue are the same as in the computer-generated structure of the wild type MoFe protein in the presence of 10% CO. As shown in Figure 6.7, the methyl group of the Thr residue may provide steric hindrance, so that hydroxyl group of the Thr residue may not "flip" back when CO is removed from the FeMo cofactor of the $\alpha 278^{Thr}$ MoFe protein. In the $\alpha\text{-}278^{Ala}$, $\alpha\text{-}278^{Cys}$ and $\alpha\text{-}278^{Leu}$ MoFe proteins, no such interaction is expected and none occurs. These different interactions are consistent with the lack of a pK_a change for these last three altered MoFe proteins when CO is added.

2. The involvement of αHis195 residue in proton transfer

An interaction between the αHis195 and the αSer278 residue as a possible proton delivery system is proposed above. The αHis195 approaches to within 3.2 Å (Howard JB and Rees DC, 1996) and forms a putative hydrogen bond to one of bridging sulfide atoms of the FeMo cofactor. It has also been proposed to be involved in one of the likely proton-transfer routes to the FeMo cofactor (Durrant MC, 2001). The altered $\alpha 195^{Gln}$ MoFe protein can catalyze the reduction of H^+ and C_2H_2 at comparable rates to the wild type MoFe protein, but reduces N_2 to NH_3 only at 1-2% of the wild type rate (Kim C-H, *et al.*, 1995; Dilworth MJ *et al.*, 1998). This altered MoFe protein binds N_2 similarly to the wild type MoFe protein, yet it only uses about 1% of its total electron flux for NH_3 formation compared to about 70% in the wild type MoFe protein. Therefore, the question arises as to whether the αHis195 residue is the responsible group (or at least one of the responsible acid-base groups) contributing to the protonated pK_a value observed for the wild type MoFe protein. Could it be a specific proton donor for N_2 reduction to NH_3? In

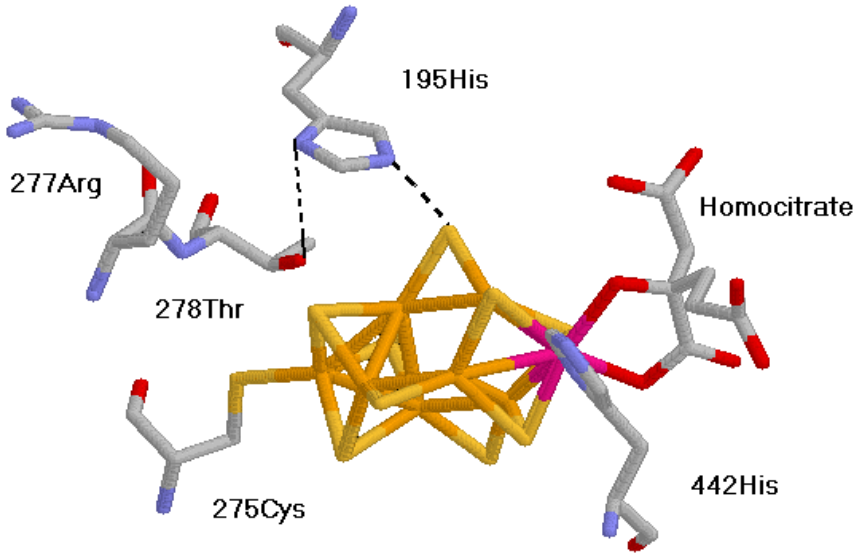

Figure 6.7 The $\alpha 278^{Thr}$ MoFe protein under argon with or without 10% CO, generated the SPdbViewer program.

order to answer these questions, the activity-pH profiles of $\alpha 195^{Gln}$ MoFe protein were determined.

It is known that the hydrogen bond to the central sulfide still exits in the $\alpha 195^{Gln}$ MoFe protein, and the amide group can still form hydrogen bond to the sulfide atom (Sorlie M *et al.*, 2001). As proposed before (Dilworth MJ *et al.*, 1998; Fisher K *et al.*, 2000a,b), although the $\alpha 195^{Gln}$ MoFe protein can bind N_2, it is the difference in the hydrogen bonds formed (the amide NH→ S hydrogen bond vs. the imidazole ε-NH→ S hydrogen bond) that produces different N_2 reduction activity. The results of activity-pH experiments show that the $\alpha 195^{Gln}$ substitution significantly affects the protonation state of the acid-base group(s) required for H_2 evolution under 100% N_2. Considering the much lower N_2 reduction activity of the $\alpha 195^{Gln}$ MoFe protein compared to that of the wild type, this big difference in the pK_a value of the protonated group for H_2 evolution in this altered MoFe protein (about 7.3 as compared to 8.0 for the wild type) supports the suggestion that the hydrogen bond formed between the αHis195 and the sulfide atom of the FeMo cofactor is important for the reduction of N_2.

Under 100% N_2, the pK_a of the protonated group(s) shifted in the acid direction with both the wild type and $\alpha 195^{Gln}$ MoFe proteins. It is likely that under N_2, different acid-base group(s) are used for the H_2 evolution activity compared to those used under 100% argon. This switch makes sense because, even though the $\alpha 195^{Gln}$ MoFe protein has a very different profile for H_2 evolution under 100% N_2 to wild type, its profile under 100% argon is similar to that of the wild type, which is consistent with its comparable H_2 evolution activity under argon. It is both the substitution to Gln and being under 100% N_2 that change the activity. So, what does the pK_a value of the protonated group for H_2 evolution under 100% N_2 in the $\alpha 195^{Gln}$ MoFe protein tell us about the reduction of N_2 in this altered MoFe protein? Two possible scenarios are as follows.

If under 100% N_2, both H_2 evolution and NH_3 formation used the same acid-base group(s), then (as shown in Figure 6.4) only about half of the required acid-base group(s) are actually protonated under normal assay conditions at pH 7.4 compared to that of the wild type. Therefore, this situation would also affect the protonation of bound N_2 and its

further reduction to NH_3 and support the suggestion that the αHis195 residue is involved in direct protonation of the bound N_2.

If under 100% N_2, both H_2 evolution and NH_3 formation use different acid-base group(s) for activity, an alternative explanation might involve a more intimate relationship between the ability to protonate bound N_2 and effective H_2 evolution, which cannot be completely suppressed during N_2 reduction, even when very high partial pressures of N_2 are employed (Simpson FB and Burris RH, 1984). A general accepted feature of catalysis by nitrogenase is that the arrival of each electron at the FeMo cofactor is intimately coupled with the movement of a proton (Durrant MC, 2001). In the Lowe-Thorneley scheme, this electron-proton coupling is indicated by the association of H_n with each E_n redox state (Thorneley RNF and Lowe DJ, 1984 a,b, 1985). The production of each successive redox state in this scheme is contingent upon the previous step. Therefore, the inability to protonate acid-base group(s) for H_2 evolution under 100% N_2 within the $\alpha 195^{Gln}$ MoFe protein would also affect formation of the next redox state because electron transfer could not occur. Thus, the result would be decreased (or no) reduction of N_2 by this altered MoFe protein.

The results (see Table 6.3) of the H_2 evolution activity-pH profiles for the altered α-278 MoFe proteins under 100% N_2 are correlated well with the above rationale. The $\alpha 278^{Cys}$ and $\alpha 278^{Ala}$ MoFe proteins, with a very similar electron distribution pattern between H_2 evolution and NH_3 formation to the wild type, have pK_a values for the protonated group similar to that of the wild type. In contrast, for the $\alpha 278^{Thr}$ MoFe protein, this value is slightly changed from that of the wild type, which is consistent with its allocation of lower percentage of electron flux to NH_3 formation. The Thr residue in this altered MoFe protein, as we proposed above, may have some interaction with the αHis195. Therefore, if the αHis195 residue is involved in proton delivery for N_2 reduction, the interaction could affect NH_3 production in the $\alpha 278^{Thr}$ MoFe protein and cause changes in the electron distribution between H_2 evolution and NH_3 formation.

The pK_a value of the protonated group for H_2 evolution in the $\alpha 278^{Leu}$ MoFe protein under 100% N_2 does not shift very much compared to that under argon. As we discussed before, it may be that the $\alpha 278^{Leu}$ MoFe protein cannot reach the redox state required for the binding and reduction of N_2, therefore, the proton-transfer mechanisms for H_2

evolution under both 100% argon and under 100%N_2 are likely to be the same. Interestingly, this situation happened with the altered $\alpha 277^{His}$ MoFe protein, which also cannot bind and reduce N_2. The pK_a of the protonated group for H_2 evolution does not change when the assay atmosphere was switched from 100% argon to 100% N_2, with the observed pK_a of 8.18 ± 0.06 and 8.15± 0.07, respectively. When reducing C_2H_2, this $\alpha 277^{His}$ altered MoFe protein also induces cooperativity between at least two C_2H_4-evolving sites under non-saturating concentrations of CO (Shen J *et al.*, 1997).

3. pH-dependence of C_2H_2 reduction

In the presence of 10% C_2H_2, there is no shift for the pK_a values of the deprotonated group(s) with the wild type and the altered α-278 MoFe proteins from those under 100% argon. This result indicates that the deprotonated acid-base group(s) required for activity is not affected by C_2H_2 binding and reduction and so could be used for nitrogenase activity under both 100% argon and 90% argon/10% C_2H_2.

The pK_a of the protonated group for both H_2 evolution and C_2H_4 formation, however, shifts in the acid direction with the wild type MoFe protein when 10% C_2H_2 is added. The same situation occurs for the $\alpha 278^{Cys}$, $\alpha 278^{Ala}$ and $\alpha 278^{Leu}$ MoFe proteins, with the $\alpha 278^{Leu}$ MoFe protein exhibiting the greatest shift. The corresponding pK_a values for the $\alpha 278^{Thr}$ MoFe protein are not changed at all with added C_2H_2. When comparing the pK_a values for H_2 evolution with all these altered MoFe proteins to that of the wild type when reducing C_2H_2, they are all similar. It suggests that the substitution at the α-278 residue may not affect the acid-base group(s) required for H_2 evolution when reducing C_2H_2. Probably, when C_2H_2 binds to the wild type, the $\alpha 278^{Cys}$, $\alpha 278^{Ala}$, $\alpha 278^{Leu}$ and $\alpha 278^{Thr}$ MoFe proteins, a different acid-base group(s) is used for H_2 evolution from that under 100% argon. For the $\alpha 278^{Thr}$ MoFe protein, it could be that the steric bulk of the Thr substitution has mimicked the effect of binding C_2H_2 to the FeMo cofactor such that no further change in pK_a is required (or possible).

Both the $\alpha 278^{Thr}$ and $\alpha 278^{Leu}$ MoFe proteins can produce C_2H_6 when reducing C_2H_2. This observation correlates with their lower K_m values for C_2H_4 production from C_2H_2 compared to that of the wild type (see Chapter 5). For C_2H_6 formation from C_2H_2,

bound C_2H_4 (from C_2H_2 reduction) needs to remain long enough to receive two more protons and electrons (Fisher K *et al.*, 2000c). Therefore, the C_2H_6 formation activity-pH profiles were investigated and compared to those of C_2H_4 production in these two altered MoFe proteins. From the results (see Table 6.5), it seems that the reduction from C_2H_2 to C_2H_4 and the reduction from C_2H_2 to C_2H_6 use different acid-base groups. Furthermore, we observed that the $\alpha 278^{Thr}$ was able to produce more C_2H_6 at pH 8.0 than at pH 7, even though K_m values for C_2H_4 formation at pH 7.0 and pH 8.0 are the same for the $\alpha 278^{Thr}$ MoFe protein. This result implies that both apparent affinity for C_2H_2 binding and the rate of proton delivery could affect C_2H_6 formation.

When an additional 10% CO was present with 80% argon/10% C_2H_2, all the altered α-278 MoFe proteins diverted their electron flux to H_2 evolution. This result is consistent with that of the activity-pH profiles (see Table 6.6). In the presence of both 10% CO and 10% C_2H_2, no change of the pK_a values of the deprotonated and protonated groups compared to those under 100% argon, except for the pK_a value of the protonated group of the $\alpha 278^{Leu}$ MoFe protein. What could have happened in this altered MoFe protein? Although there is no CO inhibition of H_2 evolution, C_2H_2 irreversibly inhibits part (at least) of total electron flux with the $\alpha 278^{Leu}$ MoFe protein (see Chapter 5). Possibly, both CO and C_2H_2 contribute to the pK_a shift with this altered MoFe protein.

Finally, these altered MoFe proteins responded to C_2H_2 differently to their response to CO, except for the $\alpha 278^{Thr}$ MoFe protein (see Table 6.1 and Table 6.4). When comparing their pK_a values for the protonated group(s), all of the altered MoFe proteins have the same response to CO, whereas the addition of 10% C_2H_2 has different effects on either C_2H_4 formation or total activity. These effects range from no change (Thr substitution) through a small change (Cys and Ala substitutions) to a big change (Leu substitution). Thus, the protonation of the acid-base group(s) must have been affected differently by C_2H_2 and CO. Comparing the changes of the pK_a for the protonated group under 100% N_2 and under 10% C_2H_2 (see Table 6.3 and Table 6.4), they are different, too. Therefore, different substrates and inhibitors may affect the deprotonation and protonation of the responsible acid-base groups in different ways. In other words, different substrates may use specific acid-base group(s) and so different proton pathway(s) exist through which the acid-base group(s) get the protons.

4. Proton pathways in the nitrogenase catalysis

The data presented in this chapter shows that the deprotonation of the acid-base group required for catalysis does not change either with different MoFe proteins tested or with changing assay atmospheres. This phenomenon is also seen with other altered MoFe proteins with substitutions at different positions (Newton WE *et al.*, 2002). It could be either that the responsible residue(s) has not been targeted yet or that this residue(s) is located elsewhere other than the polypeptide environment of the FeMo cofactor. It may be on the P cluster or from the residues close to the P cluster. Therefore, studying the consequences of the substitutions at the residues around the P cluster may help to discover the responsible deprotonated group(s).

Studies on the FeS cluster of ferredoxin have indicated that protonation of the cluster itself in the physiological condition could facilitate the increase of the negative charge on the cluster (George SJ *et al.*, 1984; Stephens PJ *et al.*, 1991; Pham DN and Burgess BK, 1993). In the wild type MoFe protein, when different substrates or inhibitors (CO in this work) are present, the activity-pH profiles seem to be only disturbed at the higher pH range. Substrates and inhibitors are believed to bind at the FeMo cofactor (Scott DJ *et al.*, 1992; Kim C-H *et al.*, 1995; Shen J *et al.*, 1997; Fisher K *et al.*, 2000c). Therefore, for Mo-nitrogenase, one possibility could be that the FeMo cofactor itself is the source of acid-base group(s). In this case, protons may reside on sulfide atoms of the cluster before they go to the substrates. The central three sulfide atoms, which are found to be considerably more basic than the sulfide atoms within both the $MoFe_3S_3$ sub-cluster and the Fe_4S_3 sub-cluster (Rod TH *et al.*, 2000; Durrant MC, 2001), are the most likely sites. In the Lowe-Thorneley scheme, the arrival of each electron at the FeMo cofactor is coupled with the movement of a proton (Lowe DJ and Thorneley RNF, 1984). The protonation of the cofactor is, thus, likely to be affected by its electronic structure and oxidation state. Moreover, the FeMo cofactor may bind different substrates or inhibitors at different sites, or even at different redox states. These substrates exhibit both competitive and noncompetitive kinetic interactions between each other and with inhibitors, such as CO. They could bind to one or more of the Fe, Mo and S sites of the FeMo cofactor. Therefore, binding of these molecules would certainly influence the protonation of the cofactor and, thus, change the higher pK_a in those titration curves, too.

How do those protons get to the FeMo cofactor? They could come through different proton pathways or channels. One mechanism would be by shuttling from one amino acid to another, using the side chains of Asp, His and Glu, as well as through water molecules. There are several possible pathways within the MoFe protein as indicated by the crystal structure. For example, a channel runs from the "water pool" located around the homocitrate to the protein surface (Howard JB and Rees DC, 1996). It could provide an efficient path for diffusion, not only of protons, but also for dinitrogen "in" and ammonia "out", between the buried FeMo cofactor and the exterior of the protein (Durrant MC, 2001). In addition, the αHis195 could accept a proton from the protein surface through αTyr281 and a water molecule and then transfer it to one of the central sulfide atoms through the hydrogen bond that connects to the ε-nitrogen of the imidazole ring of αHis195 residue. Mutations at residues either on these pathways or interacting with these pathways would interrupt proton transfer to the FeMo cofactor and so change the protonation state of the FeMo cofactor. Therefore, instead of using individual acid-base group(s) close to the FeMo cofactor for the catalysis, the FeMo cofactor may obtain protons through several different pathways and then stay in the protonated state required for substrate reduction.

In this work, the αSer278 residue, though hydrogen bonding to a direct ligand of the FeMo cofactor, seems not to be on one of the proton pathways discussed above. However, this residue may play a supporting role and "fine-tune" a pK_a value through its interaction with the αHis195 residue, which may be in one of the proton pathways to substrates. The αHis195 residue may be especially important for N_2 protonation, because a bigger shift of the pK_a of the protonated group(s) for H_2 evolution under 100% N_2 compared to that of the wild type (-0.66 pH units) was observed with the $\alpha 195^{Gln}$ altered MoFe protein. Activity-pH profiles under different atmospheres with the altered α-278 MoFe proteins also support the idea that more than one proton pathway appears to be involved in catalysis (Peters JW *et al.*, 1995; Howard JB and Rees DC, 1996), and specific pathway(s) may be used by individual substrates (Dilworth MJ *et al.*, 1998; Fisher K *et al.*, 2000 b,c).

Chapter 7
Hydrogen Cyanide Reduction with the Altered α-278 MoFe Proteins

A. Introduction

Mo-nitrogenase not only catalyzes the reduction of dinitrogen to ammonia, but also of many other alternative substrates, including cyanide reduction to CH_4, NH_3 and CH_3NH_2 (Hardy RWF and Knight Jr. E, 1967; Rivera-Ortiz JM and Burris RH, 1968; Li JG *et al.*, 1982). HCN is a weak acid (pK_a = 9.11), therefore, sodium cyanide solutions contain both HCN and CN^-, the relative amounts varying with the pH of the solution. The actual substrate of nitrogenase is HCN. It is believed to be reduced by series of two-electron/two-proton steps to give the different products as shown in the following scheme (taken from Fisher K *et al.*, 2000b).

$$
\begin{array}{ccccccc}
 & +2e^-/2H^+ & & +2e^-/2H^+ & & +2e^-/2H^+ & \\
[HCN] & \rightarrow & [CH_2{=}NH] & \rightarrow & [CH_3\text{-}NH_2] & \rightarrow & CH_4 + NH_3 \\
 & & \downarrow & & \downarrow & & \\
 & & CH_2{=}NH & & CH_3\text{-}NH_2 & & \\
 & & \downarrow +H_2O & & & & \\
 & & H_2C{=}O + NH_3 & & & &
\end{array}
$$

[] indicates either substrate or putative intermediate bound to the enzyme.

Kelly *et al.*. (1967) also observed very small amounts of C_2H_4 and C_2H_6 (0.08% of CH_4 for each) during cyanide reduction catalyzed by nitrogenase. They suggested that these C_2 products were formed by interaction of adjacent C_1 radicals on adjacent cyanide-binding sites. Under some conditions, an excess amount of NH_3 compared to the CH_4

formed in the reduction of HCN can be produced (Li GJ *et al.*, 1982; Fisher K *et al.*, 2000b).

The anion, CN^-, acts not as a substrate of the wild type enzyme but as a potent inhibitor of electron flux. However, CN^- does not inhibit the rate of MgATP hydrolysis during the reaction. The result is an increase of the ATP/$2e^-$ ratio. The inhibition effect of CN^- is very different from that of CO, which is a non-competitive inhibitor for all the catalyzed substrate reductions except H^+ reduction. When 10% CO is added to an assay with wild type enzyme, all electron flux goes to H_2 evolution and neither the total electron flux nor the rate of ATP hydrolysis are affected. The result is an unchanged ATP/$2e^-$ ratio.

In this part of the work, we have used the wild type and the altered α-278 MoFe proteins to explore the effect of substitution at the αSer278 residue on the interactions of HCN/CN^- with the MoFe protein. In addition, previous studies have shown that addition of C_2H_2 to the wild type Mo-nitrogenase, when reducing HCN, enhances CH_4 production (Rivera-Ortiz JM and Burris RH 1975; Biggins DR and Kelly M 1970; Fisher K *et al.*, 2000b), implying that both HCN and C_2H_2 are bound simultaneously to separate sites on nitrogenase. Our data indicate that one of the C_2H_2-binding sites is close to the αSer278 residue (see Chapter 6) and, therefore, we determined what effect (if any) substitutions at this position have on the interactions between C_2H_2 and HCN/CN^-.

B. Methods

Unless otherwise stated, all activity assays were performed at 30°C in 9.00–9.25 mL assay vials containing either 0.5 mg or 1.0 mg total nitrogenase proteins with a 20:1 Fe protein:MoFe protein molar ratio. For the HCN reduction assay, an anaerobic 100 mM NaCN stock solution was prepared in advance. After flushing the desired amount of solid NaCN in a sealed serum vial with argon, degassed 25 mM HEPES (pH 7.4) was added, followed by a predetermined amount of degassed 6 N HCl to obtain the desired pH (in this work, pH 7.4). Appropriate aliquots of the stock solution were then added to each anaerobic assay vial that had been flushed with argon before the incubation procedure. 100 μL of 200 mM sodium dithionite solution was added, followed by first the Fe protein

and then the MoFe protein to start the reaction. The reaction was terminated by the addition of 0.3 mL of 0.5 EDTA (pH 7.5). In the experiments with C_2H_2, 5% C_2H_2 was added after the addition of the stock NaCN solution but before both proteins.

The K_m for CH_4 formation from HCN was determined for the wild type and each altered MoFe protein except the $\alpha 278^{Leu}$ MoFe protein. CH_4 production was measured by taking an aliquot of the atmosphere for GC analysis after the termination of the reaction. The NaCN concentrations used were in the range of 0.2 mM to 10 mM at pH 7.4. The relative amount of HCN and CN^- in each buffered solution was calculated using following equation (Li JG *et al.*, 1982).

$$[CN^-] = [NaCN]/[\text{antilog}\ (9.11 - pH) + 1] \text{ and } [NaCN] = [HCN] + [CN^-]$$

H_2 evolution and C_2H_4 production were measured as described before in Chapter 2 J.1. & 2. CH_4 was measured using a Porapak N column and FID detector. The standard gas used was 1000 ppm of CH_4 in helium (Scott Specialty Gases, Inc., Plumsteadville, PA). The creatine assay that was used for the measurement of ATP hydrolysis was performed as described in Chapter 2. J. 4.

The total amounts of methylamine and ammonia produced in the HCN reduction were measured by a modified indophenol method (Dilworth MJ and Fisher K, 1998) as follows. After 1.0 mL of the liquid contents of the assay had been passed through a 2.5 cm × 6 mm column of Dowex 1X2 (Cl^- form), the column was washed two times with 0.5 mL deionized water and collected. The effluent (1.8 mL) was then passed through a 1.5 × 6 mm column of Dowex 50W-X8 (Na^+ form). The Dowex 50W-X8 resin of 100-200 mesh was prepared for these experiments as follows. The resin was boiled for 15 min in 4 M HCl and then used to pack the column. It was washed extensively with deionized water, and then converted to the Na^+ form by flushing with 0.5 M NaCl until the effluent was no longer acid. After application of the sample, this column was washed twice with 0.5 mL deionized water, followed by two 0.5 mL washes with 0.25 M of NaCl to remove the creatine. Lastly, two 1 mL washes with 2 M NaCl were applied to elute the ammonia plus methylamine from the column. Duplicate aliquots (0.95 mL) of the effluent were then used for the modified indophenol assay (Dilworth MJ and Eldridge ME, 1992).

C. Results

Table 7.1 lists the production of CH_4 and NH_3 from the catalyzed reduction of HCN in a 5 mM NaCN solution, plus the H_2 evolved in the assays. Methylamine, which is produced by the wild type MoFe protein during HCN reduction, was not measured separately in these experiments. Therefore, total electron flux in the table was calculated using only the production of CH_4, NH_3 and H_2. Under these conditions, total electron flux through the wild type, $\alpha 278^{Thr}$, $\alpha 278^{Cys}$, $\alpha 278^{Ala}$ and $\alpha 278^{Leu}$ MoFe proteins was inhibited by CN^- by 71%, 81%, 49%, 59% and 80%, respectively. This decrease of total electron flux was accompanied by an increase in the ATP/$2e^-$ ratio, because the added 5 mM NaCN did not significantly affect the rate of ATP hydrolysis in these assays. When the rate of CH_4 formation by the $\alpha 278^{Thr}$, $\alpha 278^{Cys}$ and $\alpha 278^{Ala}$ MoFe protein was compared with that of wild type, the rates were 100%, 210% and 210% of the wild type rate, respectively. The $\alpha 278^{Leu}$ MoFe protein could not reduce HCN, although its total electron flux was inhibited by CN^-.

When 10% CO was added to the 5 mM NaCN-containing reaction vials, the total electron flux was fully recovered or slightly enhanced for all the MoFe proteins. All electron flux was diverted to H_2 evolution, and ATP hydrolysis became tightly coupled to electron transfer again to give ATP/$2e^-$ ratios as observed under 100% argon.

In separate experiments, the K_m for CH_4 formation from HCN reduction of all the MoFe proteins, except the $\alpha 278^{Leu}$ MoFe protein, was measured using a range of concentrations of NaCN solution at pH 7.4. For all the MoFe proteins, the rate of CH_4 formation was maximized at about 5 mM NaCN concentration (data not shown). With each increase in the concentration of NaCN in the solution, the rate of H_2 evolution decreased and so did the total electron flux as calculated from the combined production of CH_4, H_2 and NH_3. The K_m values for CH_4 formation were: wild type, 1.5 mM HCN; $\alpha 278^{Thr}$, 0.7 mM HCN; $\alpha 278^{Cys}$, 2.0 mM HCN; $\alpha 278^{Ala}$, 1.1 mM HCN.

Table 7.1 Product formation, total electron flux and ATP/$2e^-$ ratio for HCN reduction without and with 10% CO. [NaCN] = 5 mM, pH = 7.4.

MoFe protein	Conditions	**Electron pairs (nmols)**			**Total Electron Pairs**	**ATP/$2e^-$**
		H_2	CH_4	NH_3		
Wild type	Ar alone	1576	0	0	1576	4.4
	+ NaCN	243	107	113	463	20
	+ NaCN/CO	1580	4	0	1584	4.4
α-278^{Thr}	Ar alone	1712	0	0	1712	4.0
	+ NaCN	106	108	104	318	31
	+ NaCN/CO	1761	2	0	1763	4.0
α-278^{Cys}	Ar alone	1253	0	0	1253	4.8
	+ NaCN	238	225	180	643	10
	+ NaCN/CO	1276	8	0	1284	4.7
α-278^{Ala}	Ar alone	1412	0	0	1412	4.6
	+ NaCN	162	225	192	579	14
	+ NaCN/CO	1430	12	0	1442	4.7
α-278^{Leu}	Ar alone	116	0	0	116	13
	+ NaCN	18	5	0	23	84
	+ NaCN/CO	125	1	0	126	14

Table 7.2 shows the results of the addition of 5% C_2H_2 on the rate of production of both CH_4 and NH_3 from HCN in 5 mM NaCN solution at pH 7.4. For the wild type MoFe protein, added 5% C_2H_2 had no effect on HCN reduction, whereas the rate of H_2 evolution was decreased. This lowered rate was not fully compensated by the C_2H_4 evolution rate from C_2H_2 reduction and resulted in an additional 12% decrease in the total electron flux and a slightly increased ATP/$2e^-$ ratio. For all the altered MoFe proteins, the addition of 5% C_2H_2, as in the wild type MoFe protein, did not change the rate of HCN reduction. For the $\alpha 278^{Thr}$ MoFe protein, H_2 evolution was not changed much either, whereas for the $\alpha 278^{Cys}$ and $\alpha 278^{Ala}$ MoFe proteins, it was decreased about 50% and the C_2H_4 production from C_2H_2 compensated quite well for this loss so the total electron flux was not changed much overall. Overall, for these three altered MoFe proteins, total electron flux and the ATP/$2e^-$ ratio remained unchanged. The $\alpha 278^{Leu}$ MoFe protein was ineffective in HCN reduction and the addition of C_2H_2 had no effect on its HCN reduction and total electron flux, which is consistent with its much higher K_m for C_2H_4 formation (see Chapter 6) than that of the wild type.

D. Discussion

Cyanide reduction was first demonstrated in 1967 (Hardy RWF and Knight Jr. E, 1967). Further studies have shown that HCN, the actual substrate in the solution, can be reduced to CH_4, NH_3 and CH_3NH_2 (Li JG *et al.*, 1982). More recent work focused on the impact of selected amino acid substitutions on (i) the relative rates of product formation during HCN reduction, (ii) the inhibition of electron flux by CN^-, and (iii) the effect of added C_2H_2, C_2H_4 or CO (Fisher K *et al.*, 2000b). In this work, we used the altered α-278 MoFe proteins to investigate if the reduction of HCN is affected by the substitutions and if the effect of adding either CO or C_2H_2 is changed with these altered MoFe proteins.

1. Effect of substitution on HCN and CN^- interactions with Mo-nitrogenase

To gain insights into the effect of substitution at the αSer278 position on HCN and CN^- interactions, we first investigated the response of the wild type MoFe protein to increasing concentrations of NaCN. The wild type MoFe protein has a K_m of 1.5 mM HCN for CH_4 formation when reducing HCN, which is close to the published data

Table 7.2 Product formation, total electron flux and ATP/$2e^-$ ratio for HCN reduction with and without 5% C_2H_2. [NaCN] = 5mM, pH =7.4.

MoFe protein	Conditions	Electron pairs (nmols)				Total Electron Pairs	ATP/$2e^-$
		H_2	CH_4	NH_3	C_2H_4		
Wild type	+ NaCN	330	140	130	0	600	20
	+ NaCN/ 5% C_2H_2	85	142	148	150	525	24
α-278^{Thr}	+ NaCN	133	130	126	0	389	33
	+ NaCN/ 5% C_2H_2	120	132	131	50	433	31
α-278^{Cys}	+ NaCN	297	247	211	0	755	11
	+ NaCN/ 5% C_2H_2	148	250	210	86	694	11
α-278^{Ala}	+ NaCN	180	227	205	0	612	15
	+ NaCN/ 5% C_2H_2	90	250	214	65	619	15
α-278^{Leu}	+ NaCN	20	6	0	0	26	86
	+ NaCN/ 5%C_2H_2	17	4	0	3	24	91

(Fisher K *et al.*, 2000b). We compared the rates of CH_4 and NH_3 production at 1 mM NaCN and 5 mM NaCN. There was "excess NH_3", an amount of NH_3 in excess of the CH_4, produced at 1 mM NaCN, and the difference was greatly diminished at 5 mM NaCN (data not shown). It has been proposed that the "excess NH_3" arises from the escape and subsequent hydrolysis of the CH_2=NH intermediate (Li JG *et al.*, 1982). Therefore, at low electron flux, any intermediate in the HCN reduction reaction might stay longer at the active site and so be more likely to escape and result in "excess NH_3" (see scheme in the introduction; Fisher K *et al.*, 2000b). Also, when the affinity for HCN is higher, the intermediate is more likely to be displaced by HCN and hydrolyzed to again produce "excess NH_3". Therefore, one might expect that either a lower electron flux or a higher affinity for HCN would result in the MoFe protein producing more "excess NH_3". Consistent with these suggestions, when the concentration of NaCN is increased to 5 mM NaCN, the "excess NH_3" becomes zero with the wild type MoFe protein, indicating that higher concentrations of NaCN lower the electron flux through the system and/or lower the apparent affinity for HCN resulting in less displacement of the intermediate and no "excess NH_3" (Fisher K *et al.*, 2000b).

Table 7.1 shows that substitution to Thr, Cys and Ala at the α-278 position resulted in HCN reduction activity either comparable to or greater than that of the wild type and all of the altered MoFe proteins suffer electron flux inhibition by CN^-. The $\alpha278^{Leu}$ MoFe protein does not reduce HCN, although CN^- in the 5 mM NaCN solution still inhibits the total electron flux in this altered MoFe protein. This MoFe protein reduces H^+ and C_2H_2 at only about 5% of the wild type rate, and cannot reduce dinitrogen at all. Therefore, it appears to be that the Leu substitution impairs the similar overall activity of the enzyme, not just any one substrate-reduction activity. These results, plus the Km value for CH_4 production for these altered MoFe proteins, indicate that the αSer278 residue is not an important factor in HCN/CN^- binding.

An interesting difference to wild type was noted with the $\alpha278^{Thr}$ MoFe protein. At either 1 mM NaCN or 5 mM NaCN, there was no "excess NH_3" produced, whereas wild type produces at 1 mM NaCN (data not shown). This altered MoFe protein has the lowest K_m (although only 2-fold lower than wild type) for CH_4 formation from HCN reduction among all the altered α-278 MoFe proteins that reduces HCN. Why can it not produce

"excess NH_3" at 1 mM NaCN when it has a higher apparent affinity for HCN than the wild type MoFe protein? The answer may be in the fact that this altered MoFe protein suffers much greater inhibition of total electron flux at 1 mM NaCN than the wild type MoFe protein (data not shown). Again, the low electron flux through this altered MoFe protein may well decrease the apparent affinity for HCN and so not provide an opportunity for the intermediate to escape from the active site.

2. Effect of added CO on HCN and CN^- interactions with wild type and the altered α-278 MoFe proteins

As shown in Table 7.1, CO exerted its inhibition effect on the wild type and all the altered α-278 MoFe proteins by eliminating product formation from HCN reduction and diverting all the electron flux to H_2 evolution. CO also relieves the electron flux inhibition by CN^-, resulting in the decrease of ATP/$2e^-$ ratio to the same level as that under argon. Thus, CO still acted as the expected non-competitive inhibitor of HCN reduction by both wild type and the altered MoFe proteins. There appears to be no change in the effect of CO on HCN/CN^- in these altered MoFe proteins.

3. Effect of added C_2H_2 on HCN and CN^- interactions

When 5% C_2H_2 was added to assays containing wild type MoFe protein at 5 mM NaCN solution, HCN reduction was not affected much but H_2 evolution was significantly decreased. Moreover, the production of C_2H_4 from C_2H_2 reduction did not balance out the loss in H_2 evolution and resulted in an additional ~10% decrease in the total electron flux. For all the altered MoFe proteins, the addition of 5% C_2H_2 also had no effect on the rate of HCN reduction. There were different degrees of make up by the C_2H_4 production from C_2H_2 for the decrease of H_2 evolution with the altered MoFe proteins. In the $\alpha 278^{Cys}$ and the $\alpha 278^{Ala}$ MoFe proteins, both of which have a wild type K_m value for C_2H_2 (C_2H_4 formation), the total electron flux was not changed much, and their ATP/$2e^-$ ratio was not changed either. For the $\alpha 278^{Leu}$ MoFe protein, which has very low activity towards C_2H_2 (K_m for C_2H_2 is 10-times higher than that of the wild type) and is unable to reduce HCN, added C_2H_2 did not affect the overall electron flux through this enzyme.

Again, the $\alpha 278^{Thr}$ MoFe protein was a little different from the others. H_2 evolution in this altered MoFe protein was not decreased much by added 5% C_2H_2 and therefore, with the additional C_2H_4 produced, the total electron flux may be somewhat increased. This MoFe protein has an apparent affinity for C_2H_2 that is 10-times lower than the wild type. It could be that the poorer binding of C_2H_2 has little or no effect on the interaction with HCN/CN^- and both substrates are reduced by the $\alpha 278^{Thr}$ MoFe protein without interfering with each other.

Because HCN reduction catalyzed by the wild type and all the altered MoFe proteins was not affected by the addition of 5% C_2H_2, and because C_2H_4 production occurred at the expense of H_2 evolution, HCN is reduced at a site that is in a more oxidized redox state than the sites for C_2H_2 and proton reduction. In addition, this result confirms that HCN and C_2H_2 bind to different sites on the enzyme. As discussed in Chapter 5, one of the C_2H_2-binding sites is close to the $\alpha 277$-$\alpha 278$ residues and now it appears that the binding site for HCN/CN^- is not near these two residues, which are in the vicinity of the Fe_4S_3-subcluster of the FeMo cofactor. This last conclusion supports previous reported insights of where the HCN/CN^- binding site is (Fisher K *et al.*, 2000b). Characterization of altered α-191 MoFe proteins showed that substitution of the amino acid residue (Gln) at the α-191 position (and the likely subsequent disruption of its interaction with homocitrate) clearly affect HCN/CN^- binding and reduction. These results place the HCN/CN^- binding site either at or near the $MoFe_3S_3$-homocitrate subcluster.

Chapter 8

Summary and Outlook from Work on αSer278

Evidence has accumulated that small-molecule substrates and inhibitors interact with sites on the MoFe protein component of *Azotobacter vinelandii* Mo-nitrogenase, specifically at the FeMo cofactor (Hawkes TR *et al.*, 1984; Scott DJ *et al.*, 1990, 1992). The three-dimensional crystal structures of both component proteins of Mo-nitrogenase, both individually and as a complex, have been solved by X-ray techniques (Kim J and Rees DC, 1992 a,b; Peters JW *et al.*, 1997; Schindelin H *et al.*, 1997; Chiu H-J *et al.*, 2001). These structures have defined the bonding of the FeMo cofactor within the MoFe protein. Substitution of the amino acids in the polypeptide environment of the FeMo cofactor and subsequent monitoring of the effects on the catalytic, spectroscopic and redox function of the enzyme have proved to be an effective approach to gain insights into the nitrogenase mechanism. This thesis is focused on the αSer278 residue, which is hydrogen bonded to one of the direct ligands of the FeMo cofactor. Two major goals drove this study. The first was to determine if substitution at this residue affects substrate binding and reduction and the pattern of inhibition of certain inhibitors, such as CO. What role does this residue play in nitrogenase catalysis? The second goal was to determine if this residue is an acid-base group required for nitrogenase activity. By analyzing activity vs. pH profile data, insights into the proton donors and proton-transfer mechanisms for substrate reduction by nitrogenase should occur.

Four altered MoFe proteins, with substitution of αSer278 by Thr, Cys, Ala and Leu, were purified and their catalytic and spectroscopic properties were characterized to initiate the investigation. The following conclusions were drawn from the results of these studies.

1). Three of the four altered MoFe proteins have comparable activity (H_2 evolution, C_2H_2 and N_2 reduction) to the wild type, indicating that a serine at this position is not absolutely required for nitrogenase activity. Substitution by Leu, though, dramatically decreases the enzyme activity. Probably, a bulky residue at this position, such as Leu,

significantly disrupts the environment of the FeMo cofactor and impairs the overall enzyme activity.

2). The EPR spectra of the $\alpha 278^{Cys}$ and $\alpha 278^{Ala}$ MoFe proteins are very similar to that of the wild type, whereas the spectrum of the $\alpha 278^{Thr}$ MoFe protein shows changes in both the line shape and g values. These results are correlated with their substrate-reduction activity. The $\alpha 278^{Leu}$ MoFe protein exhibits much lower EPR signal intensity than wild type, which is consistent with its low H_2-evolution activity under argon and its low Mo content compared to the wild type.

3). There is clear evidence that at least two C_2H_2-binding sites are located within the MoFe protein (Lowe DJ *et al.*, 1978; Davis LC *et al.*, 1979; Shen J *et al.*, 1997; Christiansen J *et al.*, 2000). One of these is a high-affinity C_2H_2-binding site and is the one primarily accessed during the normal nitrogenase activity assays. The other is a low-affinity C_2H_2-binding site and is where N_2 also binds. The K_m values for C_2H_2 (C_2H_4 formation) by the $\alpha 278^{Cys}$ and $\alpha 278^{Ala}$ MoFe proteins are close to that of the wild type (about 0.006 atm). The K_m values for C_2H_2 for the $\alpha 278^{Thr}$ and $\alpha 278^{Leu}$ MoFe proteins are both about 10-times higher (0.06 atm and 0.08 atm, respectively) than the K_m of the wild type and are similar to the reported value for the low-affinity C_2H_2-binding site (0.14 atm, Christiansen J *et al.*, 2000). Therefore, it is likely that the high-affinity C_2H_2-binding site has been severely affected (or may be inaccessible for use) by the substitution of Thr and Leu, and only the low-affinity C_2H_2-binding site is left.

However, several pieces of information suggest that the situations within these two altered MoFe proteins are different. First, with the $\alpha 278^{Thr}$ MoFe protein, CO is a non-competitive inhibitor of C_2H_2 reduction, whereas with the $\alpha 278^{Leu}$ MoFe protein, non-saturating concentrations of CO induces cooperativity between two C_2H_2-binding sites. This observation may indicate that the Leu substitution does not completely disrupt the high-affinity site, but causes it to be normally inaccessible for use. Only the low-affinity site remains generally available to substrate and it shows the higher K_m. Non-saturating concentrations of CO somehow make that high-affinity binding site accessible again and, further, induce the communication between the high- and low-affinity sites for C_2H_2 binding. Second, under a 100% C_2H_2 atmosphere, the $\alpha 278^{Thr}$ MoFe protein can recover to the wild type level (about 90%) of electron flux used for C_2H_4 formation from only

about 50% under 10% C_2H_2, whereas the $\alpha 278^{Leu}$ MoFe protein cannot (only about 50% achieved under 100% C_2H_2). These data suggest that the $\alpha 278^{Thr}$ MoFe protein still can access the high-affinity C_2H_2-binding site, which possibly has a lowered affinity for C_2H_2 as indicated by its increased K_m value for C_2H_2. Alternatively, substitution to Thr could eliminate the high-affinity C_2H_2-binding site, but simultaneously increase the affinity for C_2H_2 at the low-affinity C_2H_2-binding site. In contrast, the Leu substitution affects access to the high-affinity C_2H_2-binding site such that it remains unavailable even under 100% C_2H_2. If, as suggested earlier, both the high- and low-affinity C_2H_2-binding sites are close to the 4Fe-4S face of the FeMo cofactor that is capped by the αVal70 residue (Christiansen J *et al.*, 2000), substitution at the α-278 position could impact both sites through that 4Fe-4S face, possibly by interrupting the hydrogen bond formed between the αSer278 and αHis195 residues (see Chapter 6, Figure 6.5-6.7).

4). N_2 binding and reduction is not affected by substitution with Thr, Cys and Ala at the α278 position, indicating that the low-affinity-C_2H_2/N_2-binding site is unaffected. The $\alpha 278^{Leu}$ MoFe protein, however, cannot bind and reduce N_2 and its H_2-evolution and C_2H_2-reduction activities are also very low compared to those of the wild type. It appears that this Leu substitution affects all substrate reductions not specifically N_2 reduction. Therefore, the α Ser278 residue is unlikely to be involved in N_2 binding and reduction.

5). The H_2-evolution activity vs. pH profiles for all the nitrogenases were somewhat distorted bell shapes, indicating that at least two acid-base groups are required for catalysis. The profile of the altered α-278 MoFe proteins under argon +/- 10% CO suggest that neither the α Ser278 nor the hydrogen-bonding interaction between this residue and the αCys275 is responsible for the higher pK_a value observed with the wild type MoFe protein under 100% argon. However, the αSer278 residue could interact with the nearby αHis195 residue, which is hydrogen bonded to one of the central sulfides of the FeMo cofactor. The αHis195 residue has been suggested to be involved in proton transfer to the FeMo cofactor (Kim J and Rees DJ, 1992 a,b; Durrant MC, 2001a) and may be involved in proton delivery to bound N_2 (this work; Dilworth MJ *et al.*, 1998; Fisher K *et al.*, 2000 a,b). Either substitution by Thr at the αSer278 residue or binding of

CO to the wild type MoFe protein may interrupt the proton-transfer pathway through an interaction with the αHis195 and, thus, affect substrate reduction.

6). The substrate-reduction activity-pH profiles of the altered α-278 and $\alpha 195^{Gln}$ MoFe proteins indicate that different substrates may use specific acid-base group(s) and so different proton pathway(s) through which the acid-base group(s) gets the protons. Therefore, substitutions in the polypeptide environment of the FeMo cofactor may not only impact different substrate-binding sites, but also may interrupt the delivery of electrons/protons to the substrates. By doing so, the environment of the FeMo cofactor delicately controls the MoFe protein's ability to bind substrates, deliver protons and allocate electrons among substrates, as well as to interact with the CO inhibitor.

7). Both the $\alpha 278^{Thr}$ and $\alpha 278^{Leu}$ MoFe proteins have a K_m for C_2H_2 (C_2H_4 formation) that is 10-times higher than that of the wild type and can produce C_2H_6 in addition to C_2H_4 when reducing C_2H_2. This result is consistent with the correlation proposed earlier between the K_m for C_2H_2 (C_2H_4 formation) and the ability to produce C_2H_6 (Fisher K *et al.*, 2000c). If as suggested (see conclusion 3.), these two altered MoFe proteins likely have their high-affinity C_2H_2-binding sites disrupted by the substitution, one possibility is that the low-affinity C_2H_2-binding site is responsible for the production of C_2H_6. In addition, their C_2H_6 formation-pH profiles are different from the C_2H_4 formation-pH profiles, indicating that different acid-base groups are used. This suggestion makes sense, because two more protons are needed to further reduce C_2H_2 to C_2H_6. Either extra protonation/deprotonation cycles or different acid-base group(s) are used. Although the $\alpha 278^{Thr}$ MoFe protein has the same K_m value for C_2H_2 (C_2H_6 formation) at both pH 7 and pH 8, it produces more C_2H_6 at pH 8. Therefore, both the apparent affinity for C_2H_2 and the rate of proton delivery appears to affect C_2H_6 formation from C_2H_2-reduction.

8). The amino acid substitutions to Thr, Cys and Ala at the αSer278 residue does not much affect HCN-reduction activity and electron flux-inhibition by CN^-. Again, the Leu substitution impairs all substrate reduction activities, including HCN reduction, significantly and similarly. Thus, it is reasonable to conclude that the HCN and CN^- binding site(s) is not close to the αSer278 residue.

Overall, our kinetic data suggest that the αSer278 residue is not absolutely required for nitrogenase activity. However, this residue still appears to be important for normal nitrogenase function. Substitution by residues with small side chains at this position may slightly modify the enzyme function, such as the apparent affinity for substrate, interactions with inhibitors, and electron distribution among the products. Dramatic changes, such as occur with substitution of this residue by an amino acid with a bulky and/or charged side chain, can significantly impair and may cause the loss of activity.

Although considerable progress has been made in understanding the mechanism of nitrogenase, the familiar question of where and how substrates interact with the FeMo cofactor remains. Multiple approaches are being used to answer this question, including the use of altered nitrogenases constructed by site-directed mutagenesis, alternative substrates and inhibitors, a variety of spectroscopic techniques, model chemistry and theoretical methods. A better understanding of this biological system may prove beneficial for agriculture and human health especially in poorer countries. If it aids in the development of N_2-fixing plants, such knowledge should contribute to the long-term solution of the world food supply problem. However, a full appreciation of this fascinating enzyme will require a lot more work in the future.

Chapter 9
Preliminary Studies of the Effect of Substitution at αHis442 and αGln440

A. Introduction

As described in the introduction to Chapter 3, the substrate binding and reduction site(s) on the MoFe protein are provided by the FeMo cofactor (Scott DJ *et al.*, 1990; Kim C-H *et al.*, 1995; Fisher K *et al.*, 2000a,b). Crystallographic analysis has shown that the FeMo cofactor is covalently attached to the protein by the residues αCys275 and αHis442 only (Kim J and Rees DC, 1992a,b). The polypeptide environment of the FeMo cofactor plays critical functions in substrate binding and reduction. For example, it may electronically fine-tune the substrate reduction site to ensure productive delivery of protons and electrons to the bound substrate reduction site (Kim C-H *et al.*, 1995; Shen J *et al.*, 1997; Fisher K *et al.*, 1998). The impact of the local environment has been clearly demonstrated using altered nitrogenases with site-specific amino acid substitutions. They show substrate reduction properties that distinguish them from the native enzyme (Scott DJ *et al.*, 1992; Kim C-H *et al.*, 1995; Shen J *et al.*, 1997; Fisher K *et al.*, 2000c).

Upon substitution of αCys275 by Ala in *K. pneumoniae* MoFe protein, free FeMo cofactor could be detected by EPR spectroscopy in the crude extract of the mutant strain. The crude extract from this mutant strain could also be used to reconstitute an extract from a mutant strain (NifB$^-$) deficient in FeMo cofactor biosynthesis. Furthermore, non-denaturing gels showed that the major form of the MoFe protein in the $\alpha 275^{Ala}$ extracts ran as a band that migrates more slowly than did the native MoFe protein in wild type extracts (Kent HM *et al.*, 1990), but similarly to the "apo-MoFe protein" in NifB$^-$ strains. The interpretation of these results is that the FeMo cofactor is loosely attached to the MoFe protein matrix in this mutant. These data are consistent with the crystal structure, which shows that αCys275 provides one of only two covalent ligands from the protein environment to the cofactor.

The structural information also revealed that αHis442 provides the second direct coordination to the Mo atom and that αGln440 is hydrogen bonded to a terminal carboxylate of homocitrate (Figure 9.1). Substitution of αGln440 by glutamate has no apparent effect on either diazotrophic growth or catalytic activity (Newton WE and Dean DR, 1993). In contrast, substitution of αHis442 by Asn results in the complete inactivation of MoFe protein activity and also eliminates the S = 3/2 EPR signal characteristic of the protein-bound FeMo cofactor. Thus, αHis442 appears to play a major role in anchoring the FeMo cofactor to the polypeptide matrix (Newton WE and Dean DR, 1993).

Electron spin echo envelope modulation (ESEEM) spectroscopy had provided evidence for a N-atom coupled to the S = 3/2 spin system of the FeMo cofactor (Thomann H *et al.*, 1987). It was later proposed that αHis442 could be the source of this ESEEM modulation (Lee H-I *et al.*, 1998). Related studies on the $NifV^-$-extracted FeMo cofactor, in which homocitrate has been replaced by citrate, also suggest a possible role for the αHis442 in nitrogen fixation. The observed reactivities of the extracted $NifV^-$ FeMo cofactor with PhS^- were the same as with the isolated wild type FeMo cofactor when they were complexed with CN^-, N_3^-, or H^+. However, when imidazole was bound, the kinetics of the reactions of PhS^- with the two cofactors were different. The results indicate that by forming hydrogen bond to the (R)-homocitrate, αHis442 could be one of the components of the proton delivery system and this hydrogen bond may be crucial for the binding and protonation of bound N_2 (Grönberg KLC *et al.*, 1998).

Six mutant strains with substitutions at position α-442 in the MoFe protein were constructed by either Dr. Peters or Dr. Kloos at Virginia Tech. Four mutant strains with substitutions at position α-440 were constructed by Dr. Peters. Together with Dr. Kloos, I constructed another *A. vinelandii* mutant strain with a MoFe protein that has αHis442 changed to Cys plus seven His residues added to the carboxyl terminus of the α-subunit. Preliminary studies were performed on the α-440 and the α-442 mutant strains by characterizing their substrate-reduction activities at the crude-extract level. The crude extract of the $\alpha 442^{Cys}$ strain had the highest activity among the α-442 mutant strains and was chosen for purification of its altered MoFe protein by the traditional method first.

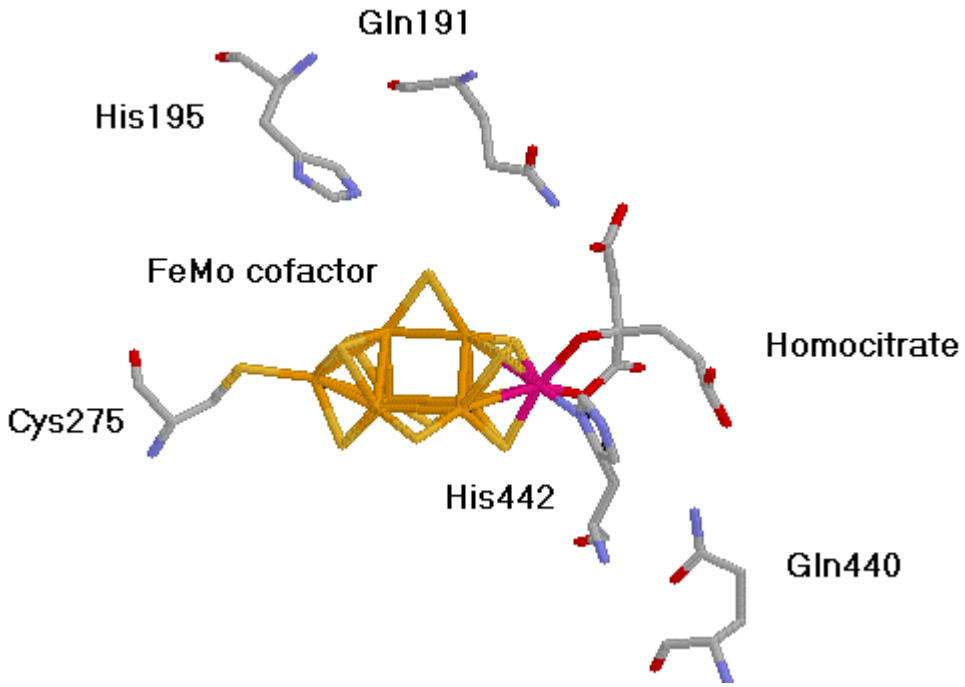

Figure 9.1 The FeMo cofactor and selected residues in its immediate vicinity.

The close approach of αGln191 and αGln440 to the homocitrate and its direct ligands, the αCys275 and αHis442 residues, are shown. Adapted from Peters JW *et al.*, 1997.

Metal affinity chromatography was later used to purify the $\alpha 442^{Cys}$ MoFe protein that has the His-tag at the carboxyl terminus of its α subunit. Both partially purified MoFe proteins were characterized and compared. The results are discussed in this chapter.

B. Methods

1. Construction of the *A. vinelandii* mutant strains

Six α-442 mutant strains and four α-440 mutant strains were previously constructed by either Dr. Peters or Dr. Kloos. The method is described in Chapter 2, section C.

The poly-His $\alpha 442^{Cys}$ mutant strain was constructed by transformation of a mutation vector, which carries the $\alpha 442^{Cys}$ mutation, into an *A. vinelandii* strain that has seven histidine codons placed between codons 481 and 482 of the wild type *nifD* gene (DJ995) (kindly provided by Dr. Dean of this department). The site-directed mutagenesis and the transformation procedures were performed as in Chapter 2, section C. (Page WJ and von Tigerstrom M, 1979; Brigle EK *et al.*, 1987).

2. Cell growth and nitrogenase derepression

Wild type and the mutant strains of *A. vinelandii* were cultured on a modified Burk medium (Strandberg GW and Wilson PW, 1968) that was supplemented with filter-sterilized urea to a final concentration of 24 mM when a fixed nitrogen source was required. Cell growth conditions and derepression for all these mutant strains were as described in Chapter 2.D.1&3 sections.

Derepression of the $\alpha 442^{Cys}$ (without the His-tag) mutant strain was monitored as described below. The mutant strain was grown overnight in the 24-L fermentor on modified Burk medium, plus Na_2MoO_4 and urea. The air flow rate into the fermentor was about 35–40 L/min with stirring at a speed of 250 rpm. At a cell density of about 200 Klett units, the cultures were derepressed for nitrogenase synthesis as described in Chapter 2. Nitrogenase expression was then monitored by whole cell C_2H_2 reduction assays. Aliquots (0.2 mL) of the atmosphere were removed and assays performed every 40 minutes. The production of C_2H_4 and C_2H_6 were determined by gas chromatography on a Model GC-14A.

3. Crude extract preparation and characterization

Characterization of the crude extracts from the α-440 mutant strains was undertaken jointly with C.H. Dapper. The α-442 mutant strains were characterized without assistance.

To prepare the crude extract for the nitrogenase activity assay, about 3 g of cells were thawed and diluted with about 6 mL of degassed 50 mM Tris-HCl, pH 8.0, containing 2 mM sodium dithionite. The cell suspension was broken using a Heat System Sonicator as described in Chapter 2, section E. The extract was anaerobically transferred into centrifuge tubes and centrifuged for 90 minutes at 98,000×g at 4^{o}C. The supernatant was frozen in liquid nitrogen and stored at –80^{o}C until used.

Protein content of the crude extract was estimated using the Lowry method (Lowry OH *et al.*, 1951) with bovine serum albumin (0-0.1 mg/mL) as a standard. The MoFe protein and Fe protein specific activities were individually measured in the crude extract in the presence of an optimal amount of the purified complementary protein. When needed, either CO or C_2H_2 were added by a gas-tight Hamilton syringe to the assay vial. Nitrogenase activity assays were performed as described in Chapter 2.H.

4. Purification of the altered α442^{Cys} (without/with His-tag) MoFe protein

A traditional purification method, which was described in Chapter 2.F.1&2 was used to purify the altered α442^{Cys} MoFe protein without the His-tag, whereas the α442^{Cys} MoFe protein with the His-tag was purified using the metal affinity chromatography (IMAC) method described in Chapter 2.F.4. The procedure used for purifying the poly-His-modified MoFe proteins was taken from the His-Bind Resin manufactures recommendations (Novagen Inc., Madison WI). All solutions used in the metal affinity chromatography method consisted of various concentrations of imidazole combined with a 25 mM Tris, 500 mM NaCl, 1 mM dithionite, pH 7.9 buffer solution.

Crude extracts were directly loaded onto the 100 mM $ZnSO_4$-saturated metal affinity column, which was pre-equilibrated overnight with 25 mM Tris buffer containing 5 mM imidazole. Imidazole was used in a step gradient to separate the poly-His MoFe protein from other column-bound proteins. After loading, the column was washed with 5 mM imidazole-containing 25 mM Tris-buffer until the column effluent was clear. Next, the

column was treated with a 40 mM imidazole, 25 mM Tris-buffer, which resulted in the elution of a light brown band during the first 100 ml of this wash buffer. This fraction had very little MoFe protein activity in it. The column was washed with more of this buffer until the effluent was relatively clear. The poly-His MoFe protein was then eluted from the column using 250 mM imdazole, 25 mM Tris-buffer. The eluted dark brown band contained MoFe protein with higher H_2-evolution activity. The MoFe protein collected from this column was then further purified on a small (2.5 × 15~20 cm) DEAE-Sepharose column (Pharmacia LKB, Uppsala, Swenden). Purified His-tagged MoFe protein was frozen and stored in liquid nitrogen for further characterization.

5. Reconstitution of the DJ42 mutant strain by the crude extract of $\alpha 442^{Cys}$ mutant strain

A crude extract of derepressed *A. vinelandii* DJ42 mutant strain, which is Δ*nifYENX* and unable to synthesize the FeMo cofactor, was incubated with the crude extract of the $\alpha 442^{Cys}$ mutant strain at room temperature for 30 minutes and an aliquot of the combined extracts were then assayed for MoFe protein activity under 10% C_2H_2. Different ratios (volume/volume) of the DJ42 crude extract to the $\alpha 442^{Cys}$ crude extract were used in these potential reconstitution assays. The ratios used were 4:1, 2:1, 1:1, 1:2 and 1:4. After the incubation, selected volumes of the mixed crude extracts were used for MoFe protein C_2H_2-reduction assays to ensure that there was always 25 μL of the DJ42 crude extract in the assay. The assay procedure is described in Chapter 2.H.

C. Results

1. Crude extract activities of the α-442 mutant strains

None of the α-442 mutant strains can fix N_2, which indicates the importance of this residue to the function of nitrogenase. The altered nitrogenases were synthesized in the mutant strains to a similar amount to those in the wild type strain, as indicated by their comparable Fe protein activities (Table 9.1). However, all substitutions resulted in very low (or no) MoFe protein activity. The crude extract from the $\alpha 442^{Cys}$ strain had the highest activity among all the α-442 mutant strains, but the activity was still only about

Table 9.1 Nif phenotype of the α-442 mutant strains and their crude extract MoFe-protein and Fe-protein activities[a].

Strain	**Nif phenotype**	**100% Ar**		**10% C_2H_2, 90% Ar**		
		MoFe H_2	**Fe H_2**	**C_2H_4**	**C_2H_6**	**H_2**
Wild Type	Nif^+	110	88	86	0	14
$\alpha 442^{Cys}$	Nif^-	2.2	64	0.2	<0.01	2.0
$\alpha 442^{Asn}$	Nif^-	0.8	78	0.1	0	0.9
$\alpha 442^{Gln}$	Nif^-	0.7	80	0.1	0	0.8
$\alpha 442^{Ala}$	Nif^-	0.5	72	0.1	0	0.8
$\alpha 442^{Arg}$	Nif^-	0.5	70	0	0	0
$\alpha 442^{Tyr}$	Nif^-	0.2	80	0	0	0

[a] MoFe-protein and Fe-protein specific activities in the crude extract are listed as nmol of the product produced per min×mg of total protein in the crude extract either under a 100% argon atmosphere or under 10% C_2H_2/90% argon atmosphere. All assays were performed as described in Chapter 2 with an optimal amount of purified complementary protein present.

2% of the wild type. Even with such a low activity, a small amount of C_2H_6 was observed when assaying the crude extract from this mutant strain under 10% C_2H_2. Further studies were performed with this mutant strain to confirm its ability to produce C_2H_6. As shown in Figure 9.2, derepression of the $\alpha 442^{Cys}$ mutant strain was monitored during the five-hour derepression time by using the whole cell C_2H_2 assay. The results indicated that nitrogenase synthesis kept increasing in this mutant strain up to three and half hours after starting derepression. It also confirmed that the altered nitrogenase in this mutant was able to reduce C_2H_2 to both C_2H_4 and C_2H_6.

2. Crude extract activities of the α-440 mutant strains

Three of the four α-440 mutant strains were able to grow diazotrophically (αGln440 to Glu, Asn or Lys). Both the αGln440 and $\alpha 440^{Asn}$ strains have comparable H_2-evolution and C_2H_2-reduction activities to the wild-type crude-extract activity (Table 9.2). The $\alpha 440^{Lys}$ strain can fix N_2 even though the doubling time for cell growth was about 3-times longer than the wild type (Dr. Peters and Dean, personal communication). The only substitution that caused the loss of the diazotrophic growth was with Arg. Under 10% C_2H_2, the Glu and Asn substitutions did not affect the electron distribution to H_2 and C_2H_2, which remained very close to that of the wild type. The two lower-activity substitutions, Lys and Arg, diverted less of the electron flux to C_2H_4 production. None of these altered mutant strains produce C_2H_6 when reducing C_2H_2 (Table 9.2), and none of them had H_2-evolution activity that was sensitive to the presence of CO (data not shown).

3. Purification of the altered $\alpha 442^{Cys}$ (without and with His-tag) MoFe protein

The $\alpha 442^{Cys}$ was chosen for purification in parallel with the wild type MoFe protein by the traditional three-step chromatography method as listed in Table 8.3. The partially purified $\alpha 442^{Cys}$ MoFe protein had a final specific activity of only 44 nmols H_2 (min×mg protein)$^{-1}$, which is about 2% of that of the wild type (Table 9.3) and consistent with the crude-extract results.

Table 9.4 shows the comparison of activities between the purified wild type and the $\alpha 442^{Cys}$ MoFe proteins. The altered MoFe protein has a much less activity than the wild

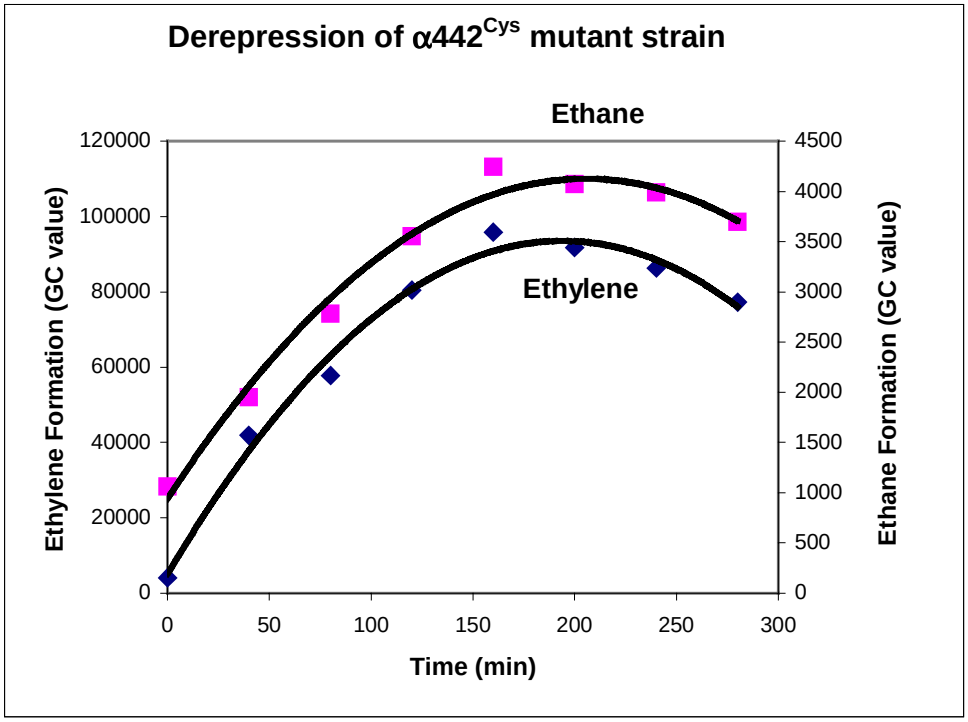

Figure 9.2 Time course of the production of C_2H_4 and C_2H_6 from C_2H_2 in the whole-cell assay during the derepression of the $\alpha 442^{Cys}$ mutant strain.

The production of C_2H_4 and C_2H_6, which were measured by gas chromatography on a Model GC-14A, were plotted as the GC value integrated by a CR501 Chromatopac integrator (Shimadzu, Kyoto, Japan) as a function of the derepression time.

Table 9.2 Nif phenotype of the α-440 mutant strains and their crude extract MoFe protein activities under 100% argon and 10% C_2H_2/90% argon.

Strain	**Nif phenotype**	**100% Ar**	**10% C_2H_2, 90% Ar**		
			C_2H_4	**C_2H_6**	**H_2**
DJ910 ($\alpha 440^{Glu}$)	Nif^+	78	54(84%) [b]	0	10(16%)
DJ948 ($\alpha 440^{Asn}$)	Nif^+	70	69(89%)	0	8(11%)
DJ946 ($\alpha 440^{Lys}$)	Nif^+	18	13(65%)	0	7(35%)
DJ950 ($\alpha 440^{Arg}$)	Nif^-	4	2(67%)	0	1(33%)

[a] MoFe-protein specific activities in the crude extract are listed as nmol of the product evolved per min×mg of total protein in the crude extract either under a 100% argon atmosphere or under 10% C_2H_2/90% argon atmosphere. All assays were performed with an optimal amount of purified complementary protein present.

[b] Numbers in parentheses represent the percentage of total electron flux to each product.

Table 9.3 Comparisons of the purification for the wild type and the altered $\alpha 442^{Cys}$ MoFe proteins by the traditional method.

Purification Step		**Crude extract**	**Q-Sepharose**	**Sephacryl-200**	**Phenyl Sepharose**
Specific Activity [a] (nmols H_2/mg×min)	WT	110	620	930	2530
	$\alpha 442^{Cys}$	2.5	8.3	24	44
Fold purified	WT	1	6	9	23
	$\alpha 442^{Cys}$	1	3	9	17

[a] MoFe-protein specific activities are listed as nmols of H_2 (min×mg MoFe protein)$^{-1}$ under a 100% argon atmosphere. All assays were performed with an optimal amount of purified wild type Fe protein present.

Table 9.4 Specific activities[a] of the purified wild type and $\alpha 442^{Cys}$ MoFe proteins and the effect of 10% CO.

MoFe Protein	**Addition**	**Product**	**Atmosphere**		
			10% C_2H_2	**100% Ar**	**100% N_2**
Wild Type	None	C_2H_4 C_2H_6 H_2 NH_3	2130 0 270	2450	760 1130
		$ATP/2e^-$	4.3	4.7	4.7
	+10%CO	C_2H_4 C_2H_6 H_2 NH_3	9 0 2530	2610	2580 0
		$ATP/2e^-$	4.5	4.5	5.0
$\alpha 442^{Cys}$	None	C_2H_4 C_2H_6 H_2 NH_3	20 2 18	41	44 0
		$ATP/2e^-$	62	56	50
	+10%CO	C_2H_4 C_2H_6 H_2 NH_3	0.2 0 50	49	65 0
		$ATP/2e^-$	48	45	47

[a] Specific activities are expressed as nmols of electron pairs(min×mg MoFe protein)$^{-1}$ under the indicated atmosphere and all assays were performed with an optimal amount of purified wild type Fe protein present.

type. However, unlike the wild type under 10% C_2H_2, only about 50% of the total electron flux goes to C_2H_4 formation and about 5% goes to C_2H_6 formation with this altered MoFe protein. Another difference is the ATP/$2e^-$ ratio for the $\alpha 442^{Cys}$ MoFe protein in these assays. The ratios are about 10-times higher than those of the wild type. Consistent with the results from the crude extracts, H^+-reduction catalyzed by this altered MoFe protein is not sensitive to CO. When 10% CO is added to the assays under either 10%C_2H_2 or 100% N_2, all of the electron flux is diverted to proton reduction with this altered MoFe protein (Table 9.4).

Metal affinity chromatography was also used to purify the $\alpha 442^{Cys}$ MoFe protein with a His-tag at the carboxyl terminus. After purifying the wild type MoFe protein from the DJ995 strain, which has seven His residues at the carboxyl terminus on the α-subunit of the MoFe protein, the product had a H_2-evolution activity of about 1800 nmols of H_2 (min×mg MoFe protein)$^{-1}$, compared to 2200-2400 nmols of H_2 (min×mg MoFe protein)$^{-1}$ for the non-His-tag wild type MoFe protein purified by the traditional method. Other comparisons between these two types of wild type MoFe proteins have been reported (Christiansen J *et al.*, 1998). Those experiments included determination of some catalytic, kinetic and spectroscopic parameters. The results indicate that the poly-His wild type MoFe protein is not appreciably different from the normal wild type MoFe protein in terms of either the diazotrophic growth rate of the cells containing it or in its major catalytic and biophysical properties.

When seven histidine residues were similarly attached to the carboxyl end of the α subunit of the MoFe protein, which has the $\alpha 442^{Cys}$ substitution, followed by the metal affinity chromatography purification, the poly-His $\alpha 442^{Cys}$ MoFe protein had an H_2 evolution activity of only about 25 nmols of H_2 (min×mg MoFe protein)$^{-1}$ (Table 9.5). Moreover, when the two $\alpha 442^{Cys}$ MoFe proteins purified by the two different methods were compared, not only was the activity of the poly-His MoFe protein about half that of the normally purified $\alpha 442^{Cys}$ MoFe protein, but the electron distribution among the products under 10% C_2H_2 was also changed (Table 9.5). The normal $\alpha 442^{Cys}$ MoFe protein used more of its total electron flux for the C_2H_4 and C_2H_6 production, whereas the poly-His $\alpha 442^{Cys}$ MoFe protein reduced C_2H_2 quite poorly. The ATP/$2e^-$ ratio in the

Table 9.5 Specific activity, product formation and metal content comparisons of the two $\alpha 442^{Cys}$ MoFe proteins either without or with the poly-His tag.

MoFe protein	**Product**	**10% C_2H_2/90% argon Activity (% e^-) [a,b]**	**100% argon Activity [b]**	**Mo[c]/MoFe**	**[Fe][c]/[Mo]**
$\alpha 442^{Cys}$ (– His tag)	C_2H_4	20 (49%)			
	C_2H_6	2.0 (5%)			
	H_2	19 (46%)	45	0.48	12
	ATP/$2e^-$	60	50		
$\alpha 442^{Cys}$ (+ His tag)	C_2H_4	3.3(13%)			
	C_2H_6	<1%			
	H_2	23(87%)	25	0.66	11
	ATP/$2e^-$	170	180		

[a] Numbers in parentheses represent the percentage of total electron flux to each product.

[b] All assays were performed with an optimal amount of purified wild type Fe protein present.

[c] Inductively coupled plasma atomic emission spectroscopy was utilized to determine the Mo and Fe contents (in the units of g atoms/mole MoFe protein) of the purified MoFe proteins.

assays with the His-tagged MoFe protein was about three-times those for the MoFe protein without the poly-His-tag.

Mo and Fe content were also determined for these two altered MoFe proteins (Table 9.5). The non-His $\alpha 442^{Cys}$ MoFe protein contained only about 25% of the expected Mo content, whereas the poly-His $\alpha 442^{Cys}$ had about 33%. The ratio of [Fe]/[Mo] with both MoFe proteins were about 12:1 versus the 15:1 found for the wild type.

4. Attempted reconstitution of the DJ42 mutant strain with the $\alpha 442^{Cys}$ crude extract

To find out if there is free FeMo cofactor available in the crude extract of $\alpha 442^{Cys}$ mutant strain, we mixed the crude extracts from both the DJ42 and the $\alpha 442^{Cys}$ strains using different ratios. Then, we calculated the specific activity for each crude extract by using the actual amount of that crude extract in the mixture compared to their individual crude extract activity. Table 9.6 shows the individual specific activity of the DJ42 and the $\alpha 442^{Cys}$ mutant strains and their activities in the mixed crude extracts.

Unlike the results with the $\alpha 275^{Ala}$ mutant strain (Kent HM *et al.*, 1989), the results obtained here indicated there were no significant interactions between the two extracts. When four volumes of the DJ42 crude extract were mixed with one volume of the $\alpha 442^{Cys}$ crude extract, the calculated $\alpha 442^{Cys}$ activity in the mixture was about four times the activity when measured alone, whereas the DJ42 activity seemed not changed. As the amount of the $\alpha 442^{Cys}$ crude extract was increased, the DJ42 activity increased whereas the activity of the $\alpha 442^{Cys}$ crude extract was not changed much. These results suggest that the apparent increase of the DJ42 crude extract was not because the insertion of $\alpha 442^{Cys}$ FeMo cofactor. Apparently, there was not much interaction between the two crude extracts.

D. Discussion

1. Substitutions at the $\alpha 440^{Gln}$ position

Among the four α-440 mutant strains, only the strain with the Arg substitution cannot fix N_2. Substitution of Gln by Glu has no apparent effect on either the diazotrophic growth rate of the mutant strain or the catalytic activity of its crude extract.

Table 9.6 Attempted reconstitution of DJ42 mutant strain crude extract with an extract of the $\alpha 442^{Cys}$ mutant strain.

Crude extract volume ratio DJ 42 to $\alpha 442^{Cys}$	**DJ 42 Crude extract [a,b,c]**		**$\alpha 442^{Cys}$ Crude extract [a,b,c]**	
	H_2	**C_2H_4**	**H_2**	**C_2H_4**
Not mix	1.7	0.8	2.3	0.6
4:1	2.0	1.2	8.5	5.3
2:1	2.4	1.3	5.5	3.0
1:1	2.9	1.5	3.3	1.7
1:2	3.7	1.8	2.1	1.0
1:4	7.5	3.0	2.1	0.9

[a] Crude extracts activities are listed as nmols of product (min×mg total crude extract proteins)$^{-1}$.

[b] Assays were performed under 10% C_2H_2 /90% argon atmosphere. A saturating amount of the wild type Fe protein was present in the assays.

[c] Specific activities of each mutant-strain crude extract in the mixture were calculated using the total protein in each individual crude extract.

This result might be expected if αGln440 is indeed hydrogen-bonded to the homocitrate as Glu should be able to duplicate this interaction. However, the substitution of Gln by Asn decreases the length of the amino acid side chain by a single carbon unit, and might affect the catalytic capacities of the resulting nitrogenase. The impact of a similar shortening was clearly demonstrated in the NifV$^-$ mutant strain (McLean PA *et al.*, 1983; Liang J *et al.*, 1990). The NifV$^-$ nitrogenase has a citrate, a single carbon shorter, in place of homocitrate. However, unlike the NifV$^-$ strain, the α440^{Asn} strain grows well on N_2 and the extracts do not show other NifV$^-$ effects, like CO-sensitive H_2 evolution. The rationale for constructing MoFe protein with the Arg and Lys substitutions was to explore the possibility that their longer side chains may be able to hydrogen bond to the shorter citrate and so rescue the NifV$^-$ phenotype. However, the Lys substituted mutant is Nif$^+$ making it impossible to select for a suppressor mutant. The Arg mutant is Nif$^-$, but after transformation with NifV$^-$ DNA, rescue of the NifV$^-$ phenotype was unsuccessful (Peters JW, Newton WE and Dean DR, unpublished data).

The crystal structure of the MoFe protein shows that the two Gln residues (αGln191 and αGln440) hydrogen bond to the terminal carboxylates on the α-carbon and δ-carbon atoms, respectively, of the homocitrate moiety of the FeMo cofactor. As shown in Figure 9.1, these two Gln residues both approach the homocitrate, one from each side. It has been suggested that αGln191 has a critical impact on the binding, protonation, and/or reduction of all nitrogenase substrates (Fisher K *et al.*, 2000b). Therefore, it brought up a question about the αGln440 residue. Is it also involved in proton/electron transfer to the FeMo cofactor? The crystal structure indicates that a potential pathway could funnel protons through αGln440 to homocitrate and then to the FeMo cofactor and substrate (Howard JB and Rees DC, 1996). In Chapter 7, specific activity vs. pH experiments were described to look for the possible amino acid residues whose deprotonation/protonation is required for nitrogenase activity. What would be the effects of substitution at the α-440 position on these acid-base groups? To answer this question, further purification and characterization of the altered MoFe proteins from the α-440 mutant strains would be necessary and specific activity vs. pH experiments under different atmospheres need to

be conducted to gain insights into the possible proton-delivery function of the αGln440 residue.

2. Role of the αHis442 residue

All of the α-442 mutant strains cannot fix N_2, and all substitutions resulted in very low or no MoFe protein activity (Table 9.1). It is obvious that the αHis442 residue, one of the direct ligands to the FeMo cofactor, plays an important role in nitrogenase catalysis. The $\alpha 442^{Cys}$ MoFe protein had the highest H_2-evolution and C_2H_2-reduction activity among all the α-442 altered MoFe proteins studied, but the activities were only about 2% of the wild type. In no case could a whole-cell EPR spectrum be obtained (data not shown). Although the $\alpha 442^{Cys}$ altered MoFe protein had a very low specific activity under a 10% C_2H_2 atmosphere, it was able to produce both C_2H_4 and C_2H_6 (Tables 9.1 and 9.4). The ability to produce C_2H_6 was also confirmed by the whole-cell C_2H_2 assay during growth of the $\alpha 442^{Cys}$ mutant strain (Figure 9.2). The formation of the C_2H_6 by the $\alpha 442^{Cys}$ MoFe protein is different from that by the V-nitrogenase (Dilworth MJ *et al.*, 1988). There was no lag phase before C_2H_6 was formed in a time-dependent C_2H_2 reduction assay (data not shown). Using the purified $\alpha 442^{Cys}$ MoFe protein, an EPR signal for the FeMo cofactor that was slightly more rhombic than that of the wild type was observed, indicating changes in the environment around the FeMo cofactor. The intensity of the signal was much lower than that of the wild type (data not shown).

When this altered MoFe protein was purified by the traditional method, many steps of freezing and thawing of the sample are involved. It may be that, during the purification, one (or both) of the metallocluster prosthetic groups can be either lost or decomposed because the αHis442 residue is one of the ligands for the FeMo cofactor to attach to the protein matrix. One criteria of instability is how heat sensitive the altered MoFe is. The $\alpha 442^{Cys}$ MoFe protein lost considerable activity at 40°C, whereas the wild type MoFe protein is heat stable up to 55°C. Possibly the substitution causes the FeMo cofactor to be loosely bound to the protein and so easily lost or decomposed. Therefore, metal affinity chromatography was introduced both to reduce the number of

chromatography steps and to eliminate the repeated freeze/thaw process, all of which could cause damage to the altered nitrogenase.

Metal affinity chromatography has proved to be a rapid and gentle method to purify the MoFe protein, especially for some altered MoFe proteins labile in the traditional procedures (Christiansen J *et al.*, 1998). Surprisingly, the purified poly-His $\alpha 442^{Cys}$ MoFe protein had an even lower H_2-evolution specific activity than the non-His MoFe protein. In addition, the His-tagged $\alpha 442^{Cys}$ MoFe protein could not reduce C_2H_2 as effectively as the non-His MoFe protein, and produced much less C_2H_6, too. Although the specific activity of the His-$\alpha 442^{Cys}$ MoFe protein might be improved by modifying the metal affinity chromatography method, for example, changing the imidazole concentration for washing off the protein from the column, the change in phenotype of the altered MoFe protein was not expected. The DNA sequences in the plasmids used in the site-directed mutagenesis experiments were checked. The only difference was the inclusion of nucleotides encoding the seven histidine residues attached to the carboxyl end of the α subunit. This inclusion should be insignificant because, with the wild type MoFe protein, there are no significant differences between the His- and non-His proteins. The problem then might have occurred during the transformation process and/or the growth of the mutant strains, in which the mutant strain picks up another mutation to cause the change in phenotype. An alternative explanation is that metal-affinity chromatography accumulates all His-tagged species, holo-protein, apo-protein and others. The accumulated inactive species would lower the overall purity of and activity of the preparation. However, the metal contents of the two preparations would be more different than those found.

Nevertheless, being one of the direct ligands to the FeMo cofactor, the αHis442 residue certainly plays a critical role in binding the FeMo cofactor to its protein matrix. The NifEN complex provides a scaffold for FeMo cofactor assembly before its insertion to the MoFe protein (Brigle KE *et al.*, 1987). Once the FeMo cofactor is assembled, it must escape from the NifEN complex during maturation. Residues that are found within the FeMo cofactor-binding regions of the MoFe protein, but not at the corresponding regions within the NifEN complex, might have either functional or structural significance for the MoFe protein's catalytic properties. Corresponding to the MoFe protein's

αCys275 and αHis442 residues are Cys and Asn, respectively, in the NifEN complex. Therefore, because the $\alpha 442^{Asn}$ is inactive, the αHis442 seems not only play a role in binding the FeMo cofactor to the MoFe protein, but is also an important contributor to the catalytic properties of the MoFe protein.

Free or loosely bound FeMo cofactor in the crude extract of a mutant strain should be detected by EPR spectroscopy as shown for the $\alpha 275^{Ala}$ crude extract. The crude extract from this mutant strain could also be used to reconstitute an extract from a mutant strain ($NifB^{-}$) that was deficient in FeMo cofactor biosynthesis (Kent HM *et al.*, 1989). No EPR signals for the FeMo cofactor were observed with any crude extracts from the α-442 mutant strains (data not shown). Moreover, the crude extract of the $\alpha 442^{Cys}$ mutant strain could not reconstitute the crude extract of DJ42, which is a mutant strain that cannot synthesize the FeMo cofactor. Therefore, unlike the crude extract of the $\alpha 275^{Ala}$ mutant strain (Kent HM *et al.*, 1989), there is apparently no free (or loosely bound) FeMo cofactor in the $\alpha 442^{Cys}$ crude extract. It appears that the cysteine substitution can still hold the FeMo cofactor in the altered MoFe protein, as indicated by the Mo content in the purified $\alpha 442^{Cys}$ MoFe protein. However, the cysteine substitution either allows easy decomposition of the FeMo cofactor in the altered MoFe protein or functions not nearly as efficiently as a histidine at this position if the αHis442 really has a significant catalytic role in the nitrogenase mechanism (Burgess BK and Lowe DJ, 1996; Grönberg KLC *et al.*, 1998) or both. Together, our results and those with the $\alpha 275^{Ala}$ mutant strain suggest that both the αCys275 and the αHis442 residues are essential for the binding of the FeMo cofactor to the protein. It may be that the αCys275 is more important for anchoring the cofactor to the α-subunit, whereas the αHis442 could be more involved in nitrogenase catalysis.

References

Alberty RA. 1994 Thermodynamics of the nitrogenase reactions. *J. Biol.Chem*. 269: 7099-102

Allen RM, Chatterjee R, Madden MS, Ludden PW, Shah VK. 1994 Biosynthesis of the iron-molybdenum cofactor of nitrogenase. *Crit. Rev. Biotechnol*. 14:225-249

Anderson GL, Howard JB. 1984 Reactions with the oxidized iron protein of *Azotobacter vinelandii* nitrogenase: formation of a 2Fe center. *Biochemistry* 23:2118-2122

Angove HC, Yoo SJ, Burgess BK, Münck E. 1997 Mössbauer and EPR evidence for an all-ferrous Fe_4S_4 cluster with S=4 in the Fe protein of nitrogenase. *J. Am. Chem. Soc.* 119:8730-8731

Arnold W, Rump A, Klipp W, Priefer UB, Puhler A. 1988 Nucleotide sequence of a 24,206-base-pair DNA fragment carrying the entire nitrogen fixation gene cluster of *Klebsiella pneumoniae. J. Mol. Biol.* 203:715-738

Ashby GA, Dilworth MJ, Thorneley RNF. 1987 *Klebsiella pneumoniae* nitrogenase: Inhibition of hydrogen evolution by ethylene and the reduction of ethylene to ethane. *Biochem. J.* 247:547-554

Austin S, Buck M, Cannon W, Eydmann T, Dixon R. 1994 Purification and in vitro activities of the native nitrogen fixation control proteins NifA and NifL. *J. Bacteriol*. 176:3460-3465

Bennett LT, Cannon F, Dean DR. 1988 Nucleotide sequence and mutagenesis of the *nifA* gene from *Azotobacter vinelandii. Mol. Microbiol*. 2:315-321

Biggins DR, Kelly M. 1970 Interaction of nitrogenase from *Klebsiella pneumoniae* with ATP or cyanide. *Biochim. Biophys. Acta* 205:288-299

Bishop PE, Premakumar R, Dean DR, Jacobson MR, Chisnell JR, Rizzo TM, Kopczynski J. 1986 Nitrogen fixation by *Azotobacter vinelandii* strains having deletion in structural genes for nitrogenase. *Science* 232:92-94

Blanchard CZ, Hales B 1996 Isolation of two forms of the nitrogenase VFe protein from *Azotobacter vinelandii. Biochemistry* 35:472-478

Bockman OC 1997 Agriculture, Fertilizers and Environment. *Plant and Soil* 194:11-14

Bolin JT, Campobasso N, Muchmore SW, Morgan TV, Mortenson LE. 1993 In *Molybdenum Enzymes, Cofactors and Model Systems* (Stiefel EI, Coucouvanis D & Newton WE, Eds.) pp 186-195, American Chemical Society, Washington, DC.

Brigle KE, Newton WE, Dean DR. 1985 Complete nucleotide sequence of the *Azotobactor vinelandii* nitrogenase structural gene cluster. *Gene* 37:37-44

Brigle KE, Setterquist RA, Dean DR, Cantwell JS, Weiss MC, Newton WE. 1987 Site-directed mutagenesis of the nitrogenase MoFe protein of *Azotobacter vinelandii*. *Proc. Natl. Acad. Sci. USA* 84:7066-7069

Bushcanan-Wollaston V, Cannon MC, Beynon JL, Cannon FC. 1981 Role of the *nif A* gene product in the regulation of *nif* gene expression in *Klebsiella pneumoniae*. *Nature* 294:776-778

Bulen WA, Burns RC, LeComte JR. 1965 Nitrogen fixation: Hydrosulfite as electron donor with cell-free preparations of *Azotobacter vinelandii* and *Rhodospirillum rubrum. Proc. Natl. Acad. Sci. USA* 56:979-986

Bulen WA 1976 Nitrogenase from *Azotobacter vinelandii* and reactions affecting mechanistic interpretations. *Proc. 1st Symp. Nitrogen Fixation,* Vol 1, (Newton WE and Nyman CJ eds.) Washington State University Press, pp177-186

Burgess BK, Wherland S, Newton WE, Stiedel EI. 1981 Nitrogenase reactivity: insight into the nitrogen-fixing process through hydrogen-inhibition and HD-forming reactions. *Biochemistry* 20:5140-5146

Burgess, BK. 1984 In *Advances in Nitrogenase Fixation Research* Veeger C, Newton WE. Eds. Nijhoff/Junk Publishers: Dordrecht. pp103.

Burgess BK, Corbin JL, Rubinson JF, Li JG, Dilworth MJ, Newton WE. 1984b *In advances in Nitrogen Fixation Research* (Veeger SC and Newton WE, Eds.) pp146, Nijhoff/Junk, The Hague, The Netherlands.

Burgess BK 1985 In Metal Ions in Biology Series, vol.7: *Molybdenum Enzymes* (Spiro TG, ed.), pp161-219, Wiley-Interscience, New York

Burgess BK 1990 and references therein. The iron-Molybdenum cofactor of nitrogenase *Chem. Rev*. 90:1371406

Burgess BK 1992 In *Molybdenum Enzymes, Cofactors and Model Systems*. Stiefel EI, Coucouvanis D, Newton WE, Eds. American Chemical Society: Washington DC. pp144

Burgess BK and Lowe DJ. 1996 Mechanism of molybdenum nitrogenase. *Chem. Rev.* 96:2983-3011

Burns RC and Bullen WA 1965. ATP-dependent hydrogen evolution by cell-free preparations of *Azotobacter vinelandii. Biochim. Biophys. Acta* 105:437-445

Burns RC and Hardy RWF 1975 Nitrogen Fixation in Bacteria and Higher Plants, Springer-Verlag, Berlin. pp43

Burris RH, Winter HC, Munson TO, Garcia-Rivera J. 1965 *Nonheme iron proteins, role in energy conversation* (San Pietro, A. ed) Antioch Press, Yellow Springs, OH, pp 135. Burris RH, Orme-Johnson WH 1976 *In proceedings 1st International Symposium on Nitrogen Fixation* (Newton WE and Nyman CJ, eds.) Vol 1. pp208-233, Washington State University Press, Pullman WA.

Bursey EH, Burgess BK. 1998 Characterization of a variant iron protein of nitrogenase that is impaired in its ability to adopt the MgATP-induced conformational change. *J. Biol. Chem*. 273:16927-16934

Cameron L, Hales BJ. 1998 Investigation of CO binding and release from Mo-nitrogenase during catalytic turnover. *Biochemistry* 37: 9449-9456

Carnahan JE, Mortenson LE, Mower HF, Castle JE. 1960 Nitrogen fixation in cell-free extracts of *Clostridium pasteurianum. Biochim. Biophys. Acta* 44:520-535

Chan JM, Christiansen J, Dean DR, Seefeldt LC. 1999 Spectroscopic evidence for changes in the redox state of the nitrogenase P-cluster during turnover. *Biochemistry* 38:5779-5785

Chan MK, Kim J, Rees DC. 1993. The nitrogenase FeMo-cofactor and P-cluster pair: 2.2 Å resolution structures. *Science* 260:792-794

Chaney AL, Marbach EP. 1962 Modified reagents for determination of urea and ammonia. *Clin Chem*. 8:130-132

Chat J. 1980 Chemistry relevant to the biological fixation of nitrogen. pp. 1-18 in *Proc. Phytochem. Soc. Eur.* Stewart WDP, Gallon JR eds. London: Academic Press

Chen L, Gavini N, Tsuruta H, Eliezer D, Burgess BK, Doniach S, Hodgson KO. 1994 MgATP-induced conformational changes in the iron protein from *Azotobacter vinelandii,* as studied by small-angle x-ray scattering. *J. Biol. Chem*. 269:3290-3294

Chisnell JR, Premakumar R, Bishop PE 1988 Purification of a second alternative nitrogenase from a *nifHDK* deletion strain of *Azotobacter vinelandii*. *J. Bacteriol*. 170:27-33

Chiu H-J, Peters JW, Lanzilotta WN, Ryle MJ, Seefeldt LC, Howard JB, Rees DC. 2001 MgATP-Bound and nucleotide-free structures of a nitrogenase protein complex between the Leu 127 Delta-Fe-protein and the MoFe-protein. *Biochemistry* 40:641-650

Christiansen J, Tittsworth RC, hales BJ, Cramer SP. 1995 Fe and Mo EXAFS of *Azotobacter vinelandii* nitrogenase in partially oxidized and singly reduced forms. *J. Am. Chem. Soc.* 109:7507-7515

Christiansen J, Goodwin PJ, Lanzilotta WN, Seedfeldt LC, Dean DR 1998 Catalytic and biophysical properties of a nitrogenase apo-MoFe protein produced by a *nifB*-deletion mutant of *Azotobacter vinelandii. Biochemistry* 37:12611-12623

Christiansen J, Cash VL, Seefeldt LC, Dean DR. 2000 Isolation and characterization of an acetylene-resistant nitrogenase. *J. Bacteriol*. 275:11459-11464

Christie PD, Lee H-I, Cameron LM, Hales BJ, Orme-Johnson WH, Hoffman BM. 1996 Identification of the CO-Binding Cluster in Nitrogenase MoFe Protein by ENDOR of ^{57}Fe Isotopomers. *J. Am. Chem. Soc*. 118:8707-8709

Clarke TA, Yousafzai FKY, Eady RR. 1999 *Klebsiella pneumoniae* nitrogenase: formation and stability of putative beryllium fluoride-ADP transition state complexes. *Biochemistry* 38:9906-9913

Clarke TA, Maritano S, Eady RR. 2000 Formation of a tight 1:1 complex of *Clostridium pasteurianum* Fe protein-*Azotobacter vinelandii* MoFe protein: Evidence for long-range interaction between the Fe protein binding sites during catalytic hydrogen evolution. *Biochemistry* 39:11434-11440

Coleman DE, Berghuis AM, Lee E, Linder ME, Gilman AG, Sprang SR 1994 Structures of active conformations of Gi alpha 1 and the mechanism of GTP hydrolysis. *Science* 265:1405-1412

Conradson SD, Burgess BK, Newton WE, Mortenson LE, Hodgson KO. 1987 Structural studies of the molybdenum site in the more protein and its FeMo cofactor by EXFAS. *J. Am. Chem. Soc.* 109:7507-7515

Corbin JL 1978. A simple, automated apparatus for the rapid multiple flushes of reaction (assay) vessels with gases. *Anal. Biochem*. 84:340-342

Cordewener J, Haaker H, Veeger C. 1983 Binding of MgATP to the nitrogenase proteins from *Azotobacter vinelandii. Eur. J. Biochem*. 132:47-54

Dao C.J-F 1990 Self-oxidation of dithionite-Av2 solutions. A Ph.D. dissertation from the graduate school of University of Southern California.

Davis LC, Henzl MT, Burris RH, Orme-Johnson WH. 1979 Iron-sulfur clusters in the molybdenum-iron protein component of nitrogenase. Electron paramagnetic resonance of the carbon monoxide inhibited state. *Biochemistry* 18:4860-4869

Davis LC 1980 Hydrazine as a substrate and inhibitor of *Azotobacter vienlandii* nitrogenase. *Arch. Biochem. Biophys*. 204:270-276

Davis LC, Wang YL. 1980 *In vivo* and *in vitro* kinetics of nitrogenase. *J. Bacteriol.* 141:1230-1238

Davis R, Lehman L, Petrovich R, Shah VK, Roberts GP, Ludden PW 1996 Purification and characterization of the alternative nitrogenase from the photosynthetic bacterium *Rhodospirillum rubrum. J. Bacteriol.* 178:1445-1450

Dean DR, Setterquist RA, Brigle KE, Scott DJ, Laird, NF, Newton WE. 1990 Evidence that conserved residues Cys-62 and Cys-154 within the *Azotobacter vinelandii* nitrogenase MoFe protein alpha-subunit are essential for nitrogenase activity but conserved residues His-83 and Cys-88 are not. *Mol. Microbiol*. 4:1505-1512

Dean DR, Jacobson MR. 1992 Biochemical genetics of nitrogenase. *Biological Nitrogen Fixation*, NewYork: Chapman and Hall. pp763-834

Dean DR, Bolin JT, Zheng L. 1993 Nitrogenase metalloclusters: Structures, organizations, and synthesis. *J. Bacteriol*. 175:6737-6744

DeRose VJ, Kim C-H, Newton WE, Dean DR, Hoffman BM. 1995 Electron spin echo envelope modulation spectroscopic analysis of altered nitrogenase MoFe proteins from *Azotobacter vinelandii*. *Biochemistry* 34:2809-2814

Diets TL, Howard JB. 1989 Kinetics of MgATP-dependent iron chelation from the Fe-protein of the *Azotobacter vinelandii* nitrogenase complex. Evidence for two states. *J. Biol. Chem*. 264:6619-6628

Diets TL, Howard JB. 1990 Effects of slats on *Azotobacter vinelandii* nitrogenase activities. *J. Biol. Chem*. 265:3859-3867

Dilworth MJ, 1966 Acetylene reduction by nitrogen-fixing preparations from *Clostridium pasteurianum. Biochem. Biophys. Acta* 127:285-294

Dilworth MJ, Thorneley RNF. 1981 Nitrogenase of *Klebsiella pneumoniae*: Hydrazine is a product of azide reduction. *Biochem. J*. 193:971-983

Dilworth MJ, Eady RR, Robson RL, Miller RW. 1987 Ethane formation from acetylene as a potential test for vanadium nitrogenase *in vivo*. *Nature* (London) 327:167-168

Dilworth MJ, Eady RR, Eldridge ME. 1988 The vanadium nitrogenase of *Azotobacter chroococcum*: Reduction of acetylene and ethylene to ethane. *Biochem. J.* 249:745-751

Dilworth MJ, Eady RR. 1991 Hydrazine is a product of dinitrogen reduction by the vanadium-nitrogenase from *Azotobacter chroococcum. Biochem. J.* 277:465-468

Dilworth MJ, Eldridge ME. 1992 Correction for creatine interference with the direct indophenol measurement of NH_3 in steady-state nitrogenase assays. *Anal. Biochem*. 207:6-10

Dilworth MJ and Fisher K. 1998 Elimination of creatine interference with the indophenol measurement of NH3 produced during nitrogenase assays. *Analytical Biochemistry* 256:242-244

Dilworth MJ , Fisher K, Kim C-H, Newton WE. 1998 Effects on substrate reduction of substitution of Histidine-195 by Glutamine in the α-subunit of the MoFe protein of *Azotobacter vinelandii* nitrogenase. *Biochemistry* 37:17495-17505

Dixon RA, Eady RR, Espin G, Hill S, Iaccario M, Kahn D, Merrick M. 1980 Analysis of regulation of *Klebsiella pneumoniae* nitrogen fixation (*nif*) gene cluster with gene fusions. *Nature* 286:128-132

Dixon R, Cheng Q, Dowson-Day M, Day A. 2000 In *Nitrogen Fixation: From Molecules to Crop Productivity*. Pedrosa FO, Hungria M, Yates MG, Newton WE, eds. Kluwer Academic Publishers. pp635-639

Durrant MC 2001a Controlled protonation of iron-molybdenum cofactor by nitrogense: a structural and theoretical analysis. *Biochem. J.* 355:569-576

Durrant MC, 2001b A molybdenum-centered model for nitrogenase catalysis. Inorganic Chemistry Communications 4:60-62

Duyvis MG, Wassink H, Haaker H. 1998 Nitrogenase of *Azotobacter vinelandii*: Kinetic analysis of the Fe protein redox cycle. *Biochemistry* 37:17345-17354

Eady RR, Lowe DJ, Thorneley RNF. 1978 Nitrogenase of *Klebsiella pneumoniae*: A pre-steady-state burst of ATP hydrolysis is coupled to electron transfer between the component protein. *FEBS Lett*. 95:211-213

Eady RR, Robson RL, Richardson TH, Millere RW, Hawkins M. 1987 The vanadium nitrogenase of *Azotobacter chroococcum*. Purification and properties of the VFe protein. *Biochem. J*. 244:197-207

Eady RR 1996 Structure-function relationships of alternative nitrogenases *Chem. Rev*. 96:3013-3030

Eidsness MK, Flank AM, Smith BE, Flood AC, Garner CD, Cramer SP. 1986 EXFAS of *Klebsiella pneumoniae* nitrogenase MoFe protein from wild type and *nifV* mutant strains. *J. Am. Chem. Soc.* 108:2746-2748

Emerich DW and Burris RH. 1976 Interactions of heterologous nitrogenase components that generate catalytically inactive complexes. *Proc. Natl. Acad. Sci. USA* 73:4369-4373

Emerich DW, Ljones T, Burris RH. 1978 Nitrogenase: Properties of the catalytically inactive complex between the *Azotobacter vinelandii* MoFe protein and the *Clostridium pasteurianum* Fe protein. *Biochem. Biophys. Acta* 527:359-369

Ennor AH 1975 Determination and preparation of N-phosphates of biological origin. *Methods in Enzymol*. 3:850-856

Erickson JA, Nyborg AC, Johnson JL, Truscott SM, Gunn A, Nordmeyer FR, Watt GD. 1999 Enhanced efficiency of ATP hydrolysis during nitrogenase catalysis utilizing reductants that form the all-ferrous redox state of the Fe protein. *Biochemistry* 38:14279-14285

Filler WA, Kemp RM, Ng. JG, Hawkes TR, Dixon RA, Smith BE. 1986 The *nifH* gene product is required for the synthesis or stability of the iron-molybdenum cofactor of nitrogenase from *Klebsiella pneumoniae. Eur. J. Biochem*. 160:371-377

Fisher AJ, Smith CA, Thoden JB, Smith R, Sutoh K, Holden HM, Rayment I. 1995 X-ray structures of the myosin motor domain of Dictyostelium discoideum complexed with MgADP.BeFx and MgADP.AlF_4^-. *Biochemistry* 34:8960-8972.

Fisher K, Lowe DJ, Thorneley RNF. 1991 *Klebsiella pneumoniae* nitrogenase: The pre-steady-state kinetics of MoFe protein reduction and hydrogen evolution under conditions of limiting electron flux show that the rates of association with the Fe protein and electron transfer are independent of the oxidation level of the MoFe protein. *Biochem. J.* 279:81-85

Fisher K, Hare ND, Newton WE. 1998 Mapping the catalytic surface of *A. vinelandii* MoFe protein by site specific mutagenesis. In *Biological Nitrogen Fixation for the 21st Century* (Elmerich C, Kondorosi A, Newton WE.) pp23-26, Kluwer Academic Publishers, Dordrecht, the Netherlands.

Fisher K, Dilworth MJ, Newton WE. 2000a Differential effects on N_2 binding and reduction, HD formation, and azide reduction with α-195^{His} and α-191^{Gln}-substituted MoFe proteins of *Azotobacter vinelandii* nitrogenase. *Biochemistry* 39:15570-15577

Fisher K, Dilworth MJ, Kim H-C, Newton WE. 2000b *Azotobacter vinelandii* nitrogenases with substitutions in the FeMo-cofactor environment of the MoFe protein: Effects of acetylene or ethylene on interactions with H^+, HCN and CN^-. *Biochemistry* 39: 10855-10865

Fisher K, Dilworth MJ, Kim H-C, Newton WE. 2000c *Azotobacter vinelandii* nitrogenase containing altered MoFe proteins with substitutions in the FeMo cofactor environment: Effects on the catalyzed reduction of acetylene and ethylene. *Biochemistry* 39:2970-2979

Fisher K, Newton WE, Lowe DJ. 2001 Electron paramagnetic resonance analysis of different *Azotobacter vinelandii* nitrogenase MoFe protein conformations generated during enzyme turnover: Evidence for S=3/2 spin states from reduced MoFe protein intermediates. *Biochemistry* 40:3333-3339

Fu w, Jack RF, Morgan TV, Dean DR, Johnson MK. 1994 *nifU* gene product from *Azotobacter vinelandii* is a homodimer that contains two identical [2Fe-2S] clusters. *Biochemistry* 33:13455-13463

Galloway JN, Schlesinger HW, Levy II H, Michaels A, Schnoor JL. 1995 Nitrogen fixation: atmospheric enhancement-environmental response. *Global Biogeochemical Cycles* 9:235-252

Gavini N, Burgess BK. 1992 FeMo cofactor synthesis by a *nifH* mutant with altered MgATP reactivity. *J. Biol. Chem.* 267:21179-86

George SJ, Richards AJM, Thomson AJ, Yates MG, 1984 *Azotobacter chroococcum* 7Fe ferredoxin. Two pH-dependent forms of the reduced 3Fe clusters and its conversion to a 4Fe cluster. *Biochem. J.* 224:247-251

George SJ, Ashby GA, Wharton CW, Thorneley RNF. 1997 Time-Resolved Binding of Carbon Monoxide to Nitrogenase Monitored by Stopped-Flow Infrared Spectroscopy. *J. Am. Chem. Soci*. 119:6450 -6451

Georgiadis MM, Komiya H, Woo D, Kornuc JJ, Rees DC. 1992 Crystallographic structure of the nirtogenase iron protein from *Azotobacter vinelandii*. *Science* 257:1653-1659

Grönberg KLC, Gormal CA, Durrant MC, Smith BE, Henderson RA. 1998 Why R-homocitrate is essential to the reactivity of FeMo cofactor of nitrogenase: Studies on $NifV^-$ extracted FeMo cofactor. *J. Am. Chem. Soc. USA* 120:10613-10621

Guex, N. and Peitsch, M.C. 1997 SWISS-MODEL and the Swiss-PdbViewer: An environment for comparative protein modeling. *Electrophoresis* 18, 2714-2723

Guth JH, Burris RH. 1983 Inhibition of nitrogenase catalyzed NH_3 formation by H_2. *Biochemistry* 22:5111-5122

Hadfield KL, Bulen WA. 1969 Adenosine triphosphate requirement of nitrogenase from *Azotobacter vinelandii. Biochemistry* 8:5103-5108

Hageman RV, Burris RH. 1978 Nitrogenase ans nitrogenase reductase associate and dissociate with each catalytic cycle. *Proc. Natl. Acad. Sci. USA* 75:2699-2702

Hageman RV, Orme-Johnson WH, Burris RH. 1980 Role of magnesium adenosine 5' triphosphate in the hydrogen evolution reaction catalyzed by nitrogenase from *Azotobacter vinelandii*. *Biochemistry* 19:2333-2342

Hagen WR, Wassink H, Eady RR, Smith BE, Haaker H. 1987 Quantitative EPR of an S=7/2 system in thionine-oxidized MoFe proteins of nitrogenase. *Eur. J. Biochem.* 169:457-465

Hardy RWF, Knight E Jr, D'Eustachio AJ. 1965 An energy-dependent hydrogen-evolution from dithionite in nitrogen-fixing extracts of *Clostridium pasteurianum. Biochem. Biophys. Res. Commun*. 20:539-544

Hardy RWF and Knight E Jr, 1967 ATP-dependent reduction of azide and HCN by N_2-fixing enzymes of *Azotobacter vinelandii and Clostridium pasteurianum*. *Biochim. Biophys. Acta* 139:69-90

Hardy RWF, Holsten RD, Jackson EK, Burns RC. 1968 The acetylene-ethylene assay for measurements of nitrogen fixation: Laboratory and field evaluation. *Plant Physiol*. 43:1185-1207

Hardy RWF. 1979 *A Treatise on Nitrogen Fixation*, Section 2, (Hardy RWF and Burns RC, eds.) Wiley and Sons, New York, pp515-568

Hausinger RP, Howard JB. 1983 Thiol reactivity of the nirogenase Fe-protein from *Azotobacter vinelandii*. *J. Biol. Chem.* 258:13486-13492

Hawkes TR, McLean PA, Smith BE. 1984 Nitrogenase from *nifV* mutants of *Klebsiella pneumoniae* contains an altered form of the iron-molybdenum cofactor. *Biochem. J.* 217:317-321

Hill S, Austin S, Eydmann T, Jones T, Dixon R 1996 *Azotobacter vinelandii* NIFL is a flavoprotein that modulates transcriptional activation of nitrogen-fixation genes via a redox-sensitive switch. *Proc. Natl. Acad. Sci. USA* 93:2143-2148

Hofmann-Findeklee C, Gadkari D, Meyer O. 2000 Superoxide-dependent nitrogen fixation. In *Nitrogen Fixation: From Molecular to Crop Productivity*. Pedrosa FO, Hungria M, Yates MG, Newton WE, eds. Kluwer Academic Publishers. pp23-30

Holtel A, Merrick MJ 1989 The *Klebsiella pneumoniae* P_{II} protein (*glnB* gene product) is not absolutely required for nitrogen regulation and is not involved in NifL-mediated *nif* gene regulation. *Mol. Gen. Genet.* 217:474-480

Homer MJ, Paustian TD, Shah VK, Roberts GP 1993 The *nifY* product of *Klebsiella pneumoniae* is associated with apodinitrogenase and dissociates upon activation with the iron-molybdenum cofactor. *J. Bacteriol*. 175:4907-4910

Homer MJ, Dean DR, Roberts GP. 1995 Characterization of the gamma protein and its involvement in the metallocluster assembly and maturation of dinitrogenase from *Azotobacter vinelandii. J. Biol. Chem.* 270:24745-24752

Hoover TR, Robertson AD, Cerny RL, Hayes EN, Imperial J, Shah VK, Ludden PW 1987 Identification of the V factor needed for synthesis of the iron-molybdenum cofactor of nitrogenase as homocitrate. *Nature* 329:855-857

Hoover TR, Imperial J, Liang JH, Ludden PW, Shah VK 1988 Dinitrogenase with altered substrate specificity results from the use of homocitrate analogues for in vitro synthesis of the iron-molybdenum cofactor. *Biochemistry* 27:3647-3652

Hoover TR, Imperial J, Ludden PW, Shah VK. 1989 Homocitrate cures the *NifV* phenotype in *Klebsiella pneumoniae*. *J. Bacteriol*. 170:1978-1979

Howard JB, Rees DC. 1994 Nitrogenase: a nucleotide-dependent molecular switch. *Ann. Rev. Biochem*. 63:235-264

Howard JB, Rees DC. 1996 Structural basis of biological nitrogen fixation. *Chem. Rev.* 96:2965-2982

Howard KS, McLean PA, Hansen FB, Lemley PV, Koblan KS, Orme-Johnson WH 1986 *Klebsiella pneumoniae nifM* gene product is required for stabilization and activation of nitrogenase iron protein in *Escherichia coli. J. Biol. Chem*. 261:772-778

Howes BD, Fisher K, Lowe DJ. 1994 Nitrogenase of *Klebsiella pneumoniae*: electron nuclear double resonance (ENDOR) studies on the substrate reduction site. *Biochem. J*. 297:261-264

Hwang JC, Burris RH 1972 Nitrogenase-catalyzed reactions. *Biochim. Biophys. Acta* 283:339-350

Hwang JC, Chen CH, Burris RH. 1973 Inhibition of nitrogenase catalyzed reductions. *Biochim. Biophys. Acta* 292:256-270

Hyman MR, Seefledt LC, Morgan TV, Arp DJ, Mortenson LE 1992 Kinetic and spectroscopic analysis of the inactivating effects of nitric oxide on the individual components of *Azotobacter vinelandii* nitrogenase. *Biochemistry* 31:2947-2955

Imam S, Eady RR. 1980 Nitrogenase of *Klebsiella pneumoniae*: Reductant-independent ATP hydrolysis and the effect of pH on the efficiency of coupling of ATP hydrolysis to substrate reduction. *FEBS Lett*. 110:35-38

Imperial J, Ugalde RA, Shah VK, Brill WJ. 1984 Role of the *nifQ* gene product in the incorporation of molybdenum into nitrogenase in *Klebsiella pneumoniae*. *J. Bacteriol*. 158:187-194

Jackson EK, Parshall GW, Hardy RWF. 1968 Hydrogen reactions of nitrogenase: Formation of the molecule HD by nitrogenase and by an inorganic model. *J. Biol. Chem.* 243:4952-4958

Jacobson MR, Cash VL, Weiss MC, Laird NF, Newton WE, Dean DR. 1989a Biochemical and genetic analysis of the *nifUSVWZM* cluster from *Azotobacter vinelandii. Molec. Gen. Genet.* 219:49-57

Jacobson MR, Brigle KE, Bennett LT, Setterquist RA, Wilson MS, Cash VL, Beynon J, Newton WE, Dean DR 1989b Physical and genetic map of the major *nif* gene cluster from *Azotobacter vinelandii. J. Bacteriol*. 171:1017-1027

Jacobson MR, Cantwell, JS, Dean DR. 1990 A hybrid *Azotobacter vinelandii–Clostridium pasteurianum* nitrogenase iron protein that has *in vivo* and *in vitro* catalytic activity. *J. Biol. Chem*. 265:19429-19433

Jang SB, Seefeldt LC, Peters JW. 2000 Insights into nucleotide signal transduction in nitrogenase: structure of an iron protein with MgADP bound. *Biochemistry* 39:14745-14752

Jeng DY, Morris JA, Mortenson LE. 1970 The effect of reductant in inorganic phosphate release from adenosine 5'-triphosphate by purified nitrogenase of *Clostridium pasteurianum. J. Biol. Chem*. 245:2809-2813

Joerger RD, Bishop PE 1988 Nucleotide sequence and genetic analysis of the *nifB-nifQ* region from *Azotobacter vinelandii. J. Bacteriol*. 170:1475-1487

Johnson MK 1988 Variable temperature magnetic circular dichroism studies of metalloproteins. In *Metal Clusters in Proteins*. ed. L Que pp. 326-342 Washington DC:ACS Books Symposium Series.

Kelly M, Postgate JR, Richards RL 1967 Reduction of cyanide and isocyanide by nitrogenase of *Azotobacter chroococcum. Biochem. J.* 102:1C-3C

Kelly M, 1969 Comparisons and cross reactions of nitrogenase from *Klebsiella pneumoniae, Azotobacter chroococcum* and *Bacillus polymyza. Biochim. Biophys. Acta* 191:527-540

Kent HM, Ioannidis I, Gormal C, Smith BE, Buck M. 1989 Site-directed mutagenesis of *Klebsiella pneumoniae* nitrogenase. *Biochem. J.* 264:257-264

Kent HM, Baines M, Gormal C, Smith BE, Buck M. 1990 Analysis of site-directed mutations in the α- and β- subunits of *Klebseilla pneumoniae* nitrogenase. *Mol. Microbiol*. 4:1497-1504

Kim H-C, Zheng L, Newton WE, Dean DR. 1993 Intermolecular electron transfer and substrate reduction properties of MoFe proteins altered by site-specific amino acid substitution. *New Horizons in Nitrogen Fixation*. Dordrecht, Netherlands: Kluwer Academic. pp 105-110

Kim H-C, Newton WE, Dean DR. 1995 Role of the MoFe protein alpha-subunit histidine-195 residue in FeMo-cofactor binding and nitrogenase catalysis. *Biochemistry* 34:2798-2808

Kim J, Rees DC. 1992a. Structural models for the metal centers in the nitrogenase molybdenum-iron protein. *Science* 257:1677-1682

Kim J, Rees DC. 1992b. Crystallographic structure and functional implications of the nitrogenase molybdenum-iron protein from *Azotobacter vinelandii*. *Nature* 360:553-560

Kraulis, P.J. (1991) MOLSCRIPT: a program to produce both detailed and schematic plots of protein structure. *J. Appl. Crystallogr*. 24, 946-950

Laemmli UK. 1970 Cleavage of structural proteins during assembly of the head of bacteriophage T_4. *Nature* 227:680-685

Lanzilotta WN, Ryle MJ, Seefeldt LC. 1995 Nucleotide hydrolysis and protein conformational changes in *Azotobacter vinelandii* nitrogenase iron protein: defining the function of aspartate 129. *Biochemistry* 34:10713-10723

Lanzilotta WN, Seefeldt LC. 1996 Electron transfer from the nitrogenase iron protein to the [8Fe-(7/8)S] clusters of the molybdenum-iron protein. *Biochemistry* 35:16770-16776

Lanzillota WN, Fisher K, Seefeldt LC. 1996 Evidence for electron transfer from the nitrogenase iron protein to the molybdenum0iron protein without MgATP hydrolysis: Characterization of a tight protein-protein complex. *Biochemistry* 35:7188-7196

Lanzilotta WN, Fisher K, Seefeldt LC. 1997 Evidence for electron transfer-dependent formation of a nitrogenase iron protein-molybdenum-iron protein tight complex. The role of aspartate 39. *J. Biol. Chem*. 272:4157-4165

Lanzilotta WN, Christiansen J, Dean DR, Seefeldt LC. 1998 Evidence for coupled electron and proton transfer in the [8Fe-7S] cluster of nitrogenase. *Biochemistry* 37:11376-11384

Larson C, Christensen S, Watt GD. 1995 Reductant-independent ATP hydrolysis catalyzed by homologous nitrogenase proteins from *Azotobacter vinelandii* and heterologous crosses with *Clostridium pasterianum*. *Arch. Biochem. Biophys*. 323:215-222

Lee H-I, Cameron LM, Hales BJ, Hoffman BM 1997 CO binding to the FeMo cofactor of CO-inhibited nitrogenase: ^{13}CO and ^{1}H Q-band ENDOR investigation. *J. Am. Chem. Soc.* 119:10121-10126

Lee H-I, Kristin ST, Dean DR, Newton WE, Hoffman BM. 1998 14N electron spin –echo envelope modulation of the S=3/2 spin system of the *Azotobacter vinelandii* nitrogenase iron-molybdenum cofactor. *Biochemistry* 37:13370-13378

Lee H-I, Sorlie M, Christiansen J, Song R, Dean DR, Hales BJ, Hoffman BM. 2000 Characterization of an intermediate in the reduction of acetylene by the nitrogenase α-Gln ^{195} MoFe protein by Q-band EPR and ^{13}C, ^{1}H ENDOR. *J. Am. Chem. Soc*. 122:5582-5587

Lehman LJ, Roberts GP 1991 Identification of an alternative nitrogenase system in *Rhodospirillum rubrum. J. Bacteriol*. 173:5705-5711

Li JG, Burgess BK, Corbin JL 1982 Nitrogenase reactivity: Cyanide as substrate and inhibitor. *Biochemistry* 21:4393-4402

Li J-H, Burris RH 1983 Influence of pN_2 and pD_2 on HD formation by various nitrogenases. *Biochemistry* 22:4472-4480

Liang JH, Burris RH. 1988a Hydrogen burst association with nitrogenase catalyzed reaction. *Proc. Natl. Acad. Sci. USA* 85:9446-9450

Liang JH, Burris RH 1988b Inhibition of nitrogenase by NO. *Indian J. Biochem. Biophys*. 25:636-641

Lindahl PA, Day EP, Kent TA, Orme-Johnson WH, Munck E. 1985 Mössbauer, EPR, and magnetization studies of the *Azotobacter vinelandii* Fe protein. Evidence for a [4Fe-4S]$^{1+}$ cluster with spin S = 3/2. *J. Biol. Chem.* 260:11160-11173

Lindahl PA, Gorelick NJ, Münck E, Orme-Johnson WH. 1987 EPR and Mössbauer studies of nucleotide-bound nitrogenase iron protein from *Azotobacter vinelandii*. *J. Biol. Chem.* 262:14945-14953

Lindahl PA, Papaefthymiou V, Orme-Johnson WH, Munck E. 1988 Mössbauer studies of solid thionin-oxidized MoFe protein of nitrogenase. *J. Biol Chem*. 263:19412-19418

Little R, Reyes-Ramirez F, Zhang Y, van Heeswijk WC, Dixon R 2000 Signal transduction to the *Azotobacter vinelandii* NifL-NifA regulatory system is influenced directly by interaction with 2-oxoglutarate and the PII regulatory protein. *EMBO J.* 19:6041-6050

Liu HI, Filippani A, Gavini N, Burgess BK, Hedman B, Cicco AD, Natoli CR, Hodgson KO. 1994 EXAFS studies of FeMo-cofactor and MoFe protein: Direct evidence for the

long-range Mo-Fe-Fe interaction and cyanide binding to the Mo in FeMo-cofactor. *J. Am. Chem. Soc.* 116:2418-2423

Lowe DJ, Eady RR, Thorneley RNF 1978 Electron-paramagnetic-resonance studies on nitrogenase of *Klebsiella pneumoniae*. Evidence for acetylene- and ethylene-nitrogenase transient complexes. *Biochem. J.* 173:277-290

Lowe DJ and Thorneley RNF 1984 The mechanism of *Klebsiella pneumoniae* nitrogenase action: The determination of rate constants required for the simulation of the kinetics of N_2 reduction and H_2 evolution. *Biochem. J*. 224:887-911

Lowe DJ, Fisher K, Thorneley RNF, Vaughn SA, Burgess BK. 1989 Kinetics and mechanism of the reaction of cyanide with molybdenum nitrogenase from *Azotobacter vinelandii. Biochemistry* 28:8640-8466

Lowe DJ, Fisher K, Thorenley RNF. 1990 *Klebsiella pneumoniae* nitrogenase mechanism of acetylene reduction and its inhibition by carbon monoxide. *Biochem. J.* 272:621-625

Lowe DJ, Fisher K, Thorneley RNF. 1993 *Klebsiella pneumoniae* nitrogenase: pre-steady-state absorbance changes show that redox changes occur in the MoFe protein that depend on substrate and component protein ratio; a role for P-centres in reducing dinitrogen? *Biochem. J.* 292:93-98

Lowe DJ, Ashby GA, Brune M, Knights H, Webb MR, Thorneley RNF. 1995 ATP hydrolysis and energy transduction by nitrogenase: Tikhonovich IA, Provorov NA, Romanov VI, Newton WE (Eds.) *Nitrogen Fixation*: *Fundamentals and Applications*, 27, Kluwer Academic, London. pp103-108

Lowry OH, Rosebrough NJ, Farr AL, Randall RH. 1951 Protein measurement with the folin phenol reagent. *J. Biol. Chem*. 193:265-275

Macheroux P, Hill S, Austin S, Eydmann T, Jones T, Kim SO, Poole R, Dixon R**.** 1998 Electron donation to the flavoprotein NifL, a redox-sensing transcriptional regulator. *Biochem. J.* 332:413-419

Ma L, Brosius MA, Burgess BK. 1996 Construction of a form of the MoFe protein of nitrogenase that accepts electrons from the Fe protein but does not reduce substrate. *J. Biol. Chem.* 271:10528-10532

Maritano S, Fairgurst SA, Eady RR. 2001 Long-range interactions between the Fe protein binding sites of the MoFe protein of nitrogenase. *J. Biol. Inorg. Chem*. 6:590-600

May HD, Dean DR, Newton WE. 1991 Altered nitrogenase MoFe proteins from *Azotobacter vinelandii. Biochem. J*. 277:457-464

Mayer SM, Lawson DM, Gormal CA, Roe SM, Smith BE. 1999 New insights into structure-function relationships in nitrogenase: A 1.6 angstrom resolution X-Ray crystallographic study of *Klebsiella pneumoniae* MoFe protein *J. Mol. Biol.* 292:871-891

Mayer SM, Niehaus WG, Dean DR. 2002 Reduction of short chain alkynes by a nitrogenase α-70^{Ala}-substituted MoFe protein. *J. Chem. Soc.* In press.

McKenna CE, McKenna MC, Higa MT. 1976 Letter: Chemical probes of nitrogenase. 1. Cyclopropene. Nitrogenase-catalyzed reduction to propene and cyclopropane. *J. Am. Chem. Soc.* 98:4657-4659

McLean PA, Smith BE, Dixon RA. 1983 Nitrogenase of *Klebsiella pneumoniae* nifV mutants. *Biochem. J.* 211:589-97

Mensink RE, Wassink H, Haaker H. 1992 A reinvestigation of the pre-steady-state ATPase activity of the nitrogenase from *Azotobacter vinelandii*. *Eur. J. Biochem.* 208:289-294

Merrick M, Dixon R 1984 Why don't plants fix nitrogen? *Trends in Biotech*. 2:162-167

Merrick MJ, Edwards RA 1995 Nitrogen control in bacteria. *Microbiol. Rev*. 59:604-622

Merrick MJ, Arcondeguy T, van Heeswijk WC. 2000 Regulation of *nif* gene expression in free-living diazotrophs: Recent advances. In Nitrogen Fixation: From Molecules to crop productivity. Pedrosa FO, Hungria M, Yates MG, Newton WE, eds. Kluwer Academic Publishers. pp 67-72

Meyer J, Gaillard J, Moulis JM. 1988 Hydrogen-1 nuclear magnetic resonance of the nitrogenase iron protein (Cp2) from *Clostridium pasteurianum*. *Biochemistry* 27:6150-6156

Morett E, Buck M. 1989 In vivo studies on the interaction of RNA polymerase σ^{54} with the *Klbsiella pneumoniae* and *Rhizobium meliloti nifH* promoters: The role of NifA in the formation of an open promoter complex. *J. Mol. Biol*. 210:65-77

Morgan TV, McCracken J, Orme-Johnson WH, Mims WB, Mortenson LE, Peisach J 1990 Pulsed electron paramagnetic resonance studies of the interaction of Mg-ATP and D2O with the iron protein of nitrogenase. *Biochemistry* 29:3077-3082

Mortenson LE. Ferredoxin and ATP, requirement for nitrogen fixation in cell-free extracts of *Clostridium pasteurianum.* 1964 *Proc. Natl. Acad. Sci. USA* 52:272-279

Newton WE, 1975 Corbin JL, McDonald JW. In *Proceeding of the First International Symposium on Nitrogen Fixation*. Newton WE, Nyman CJ eds. Washington State University Press. Pullman WA. pp53

Newton WE, Dean DR. 1993 Role of the iron-molybdenum cofactor polypeptide environment in *Azotobacter vinelandii* molybdenum-nitrogenase catalysis. In *Molybdenum Enzymes, Cofactors and model Systems*. Stiefel EI, Coucouvanis D, Newton WE, Eds. American Chemical Society: Washington DC. pp216-230

Newton WE, Fisher K, Kim H-C, Shen J, Cantwell JS, Thrasher KS, Dean DR. 1995 In *Nitrogen Fixation: Fundamentals and Applications*. Tiknonovich IA, Provorov NA, Romanov VI, Newton WE, eds. Kluwer Academic Publishers. Boston pp91

Newton WE. 1996 In Kirk-Othmer Encyclopedia of Chemical Technology, 4th Edit. Vol. 17, pp172-204, John Wiley & Sons, Inc., New York.

Newton WE. 2000 In *Nitrogen Fixation: From Molecular to Crop Productivity*. Pedrosa FO, Hungria M, Yates MG, Newton WE, eds. Kluwer Academic Publishers. pp3-8

Newton WE, Vichitphan K, Fisher K 2002 *In Nitrogen Fixation: Global Perspectives,* CABI Publishing, Wallingford, in press. Finan T, O'Brian MR, Layzell DB, Vessey JK, Newton WE (eds.)

Nyborg AC, Erickson JL, Johnson A, Gunn SM, Watt GD. 2000 Reactions of *Azotobactor vinelandii* nitrogenase using Ti(III) as reductant. *J. Inorg. Biochem*. 78:371-381

Oliver ME, Hales BJ. 1993 Using dysprosium complexes to probe the nitrogenase paramagnetic centers. *Biochemistry* 32:6058-6064

Orme-Johnson WH, Hamilton WD, Jones TL, Tso MY, Burris RH, Shah VK, Brill WJ 1972 Electron paramagnetic resonance of nitrogenase and nitrogenase components from *Clostridium pasteurianum* W5 and *Azotobacter vinelandii* OP. *Proc. Natl. Acad. Sci. USA* 69:3142-3145

Page WJ, von Tigerstorm M. 1979 Optimal conditions for transformation of *Azotobacter vinelandii. J. Bacteriol.* 139: 1058-1061

Peters JW, Fisher K, Dean DR. 1994 Identification of a nitrogenase protein-protein interaction site defined by residue 59 through 67 within the *Azotobacter vinelandii* Fe protein. *J. Biol. Chem*. 269:28076-28083

Peters JW, Fisher K, Newton WE, Dean DR. 1995a Involvement of the P cluster in intramolecular electron transfer within the nitrogenase MoFe protein. *J. Biol. Chem.* 270:27007-27013

Peters JW, Fisher K, Dean DR. 1995b Nitrogenase structure and function: A biochemical-genetic perspective. *Annu. Rev. Microbiol*. 49:335-366

Peters JW, Stowell MHB, Soltis SM, Finnegan MG, Johnson MK, Rees DC. 1997 Redox dependent structural changes in the nitrogenase P-cluster. *Biochemistry* 36: 1181-1187

Pham DN, Burgess BK. 1993 Nitrogenase reactivity: Effeccts of pH on substrate reduction and CO inhibition. *Biochemistry* 32:13725-13731

Pierik AJ, Wassink H, Haaker H, Hagen WR. 1993 Redox properties and EPR spectroscopy of the P clusters of *Azotobacter vinelandii* MoFe protein. *Eur. J. Biochem*. 212:51-61

Pollock RC, Lee H-I, Cameron LM, Deroase VJ, Hales BJ, Orme-Johnson WH, Hoffman BM. 1995 Investigation of CO bound to inhibited forms of nitrogenase MoFe protein by 13C ENDOR. *J. Am. Chem. Soc.* 117:8686-8687

Pope MR, Murrell SA, Ludden PW. 1985 Covalent modification of the iron protein of nitrogenase from *Rhodospirillum rubrum* by adenosine diphosphoribosylation of a specific arginine residue. *Proc. Natl. Acad. Sci. USA* 82:3173-3177

Ramos JL and Robson RL, 1985 Lesions in citrate synthase that affect aerobic nitrogen fixation by *Azotobacter chroococcum*. *J. Bacteriol*. 162:746-751

Rasche ME, Seefeldt LC. 1997 Reduction of thiocyanate, cyanate, and carbon disulfide by nitrogenase: kinetic characterization and EPR spectroscopic analysis. *Biochemistry* 36:8574-8585

Rees DC. 1993 Dinitrogen reduction by nitrogenase: if N_2 isn't broken, it can't be fixed *Curr. Opin. Struct. Biol*. 3:921-928

Rees DC, Schindelin H, Kisker C, Schlessman JL, Peters JW, Seefeldt LC, Howard JB. 1998 Complex structures of nitrogenase. In *Biological Nitrogen Fixation for the 21st Century* (Elmerich C, Kondorosi A, Newton WE eds.) pp11-16, Kluwer Academic Publishers, Dordrecht, the Netherlands.

Rees DC, Howard JB. 2000 Nitrogenase: standing at the crossroads. *Currt. Opin. in chem. Biol*. 4:559-566

Ribbe M, Gadkari D, Meyer O. 1997 N_2 fixation by *Streptomyces thermoautotrophicus* involves a molybdenum-dinitrogenase and a manganese-superoxide oxidoreductase that couple N_2 reduction to the oxidation of superoxide produced from O_2 by a molybdenum-CO dehydrogenase. *J. Biol. Chem*. 272:26627-26633

Richards AJM, Lowe DJ, Richards RL, Thomson AJ, Smith BE. 1994 Electron-paramagnetic-resonance and magnetic-circular-dichroism studies of the binding of cyanide and thiols to the thiols to the iron-molybdenum cofactor from *Klebsiella pneumoniae* nitrogenase. *Biochem. J.* 297:373-378

Rivera-Ortiz JM and Burris RH 1975 Interactions among substrates and inhibitors of nitrogenase. *J. Bacterial*. 123:537-545

Roberts GP, MacNeil T, MacNeil D, Brill WJ 1978 Regulation and characterization of protein products coded by the *nif* (nitrogen fixation) genes of *Klebsiella pneumoniae*. *J. Bacteriol.* 136:267-279

Robinson AC, Burgess BK, Dean DR. 1987 Rion-molybdenum cofactor biosynthesis in *Azotobacter vinelandii* requires the iron protein of nitrogenase. *J. Biol. Chem.* 262:14327-14332

Robson RL. 1984 Identification of possible adenine nucleotide-binding sites in nitrogenase Fe- and MoFe-proteins by amino acid sequence comparison. *FEBS lett*.173:394-398

Robson RL, Woodly PR, Pau RN, Eady RR. 1989 Structural genes for the vanadium nitrogenase from *Azotobater chroococcum*. *EMBO J*. 8:1217-1224

Rod TH, Hammer B, Norskov JK 2000. Modeling the nitrogenase: FeMo cofactor. *J. Am. Chem. Soc.* 122:12751-12763

Rubinson JF, Burgess BK, Corbin JL, Dilworth MJ. 1985 Nitrogenase reactivity: Azide reduction. *Biochemistry* 24:273-283

Rudd KE, Sofia HJ, Koonin EV, Plunkett G 3rd, Lazar S, Rouviere PE 1995 A new family of peptidyl-prolyl isomerases. *Trends Biochem. Sci*. 20:12-14

Ryle MJ, Lanzilotta WN, Mortenson LE, Watt GD, Seefeldt LC. 1995 Evidence for a central role of lysine 15 of *Azotobacter vinelandii* nitrogenase iron protein in nucleotide binding and protein conformational changes. *J. Biol. Chem*. 270:13112-13117

Ryle MJ, Seefeldt LC. 1996a Elucidation of a MgATP signal transduction pathway in the nitrogenase iron protein: formation of a conformation resembling the MgATP-bound state by protein engineering. *Biochemistry* 35:4766-4775

Ryle MJ, Lanzilotta WN, Seefeldt LC, Scarrow RC, Jensen GM. 1996b Circular dichroism and x-ray spectroscopies of *Azotobacter vinelandii* nitrogenase iron protein. MgATP and MgADP induced protein conformational changes affecting the [4Fe-4S] cluster and characterization of a [2Fe-2S] form. *J. Biol. Chem*. 271:1551-1557

Ryle MJ, Lee H-I, Seefeldt LC, Hoffman BM. 2000 Nitrogenase reduction of carbon disulfide: Freeze-quench EPR and ENDOR evidence for three sequential intermediates with cluster-bound carbon moieties. *Biochemistry* 39:1114-1119

Schindelin H, Kisker C, Schlessman JL, Howard JB, Rees DC. 1997 Structure of ADP·AlF^-_4 stabilized nitrogenase complex and its implications for signal transduction. *Nature* 387: 370-376

Schmitz RA, He L, Kustu S. 1996 Iron is required to relieve inhibitory effects on NifL on transcriptional activation by NifA in *Klebsiella pneumoniae*. *J. Bacteriol*. 178:4679-4687

Schmitz RA. 1997 NifL of *Klebsiella pneumoniae* carries an N-terminally bound FAD cofactor, which is not directly required for the inhibitory function of NifL. *FEMS Microbiol Lett.* 157:313-318

Schneider K, Muller A, Schramm U, Klipp W 1991 Demonstration of a molybdenum- and vanadium-independent nitrogenase in a *nifHDK*-deletion mutant of *Rhodobacter capsulatus. Eur. J. Biochem.* 195:653-661

Schneider K, Gollan U, Drottboom M, Selsemeier-Voigt S, Muller A. 1997 Comparative biochemical characterization of the iron-only nitrogenase and the molybdenum nitrogenase from *Rhodobacter capsulatus. Eur. J. Biochem.* 244:789-800

Schöllhorn R, Burris RH. 1967 Acetylene as a competitive inhibitor of N_2 fixation. *Proc. Natl. Scad. Sci. USA* 58:213-216

Scott DJ, May HD, Newton WE, Brigle KE, Dean DR. 1990 Role for the nitrogenase MoFe protein α-subunit in FeMo-cofactor binding and catalysis. *Nature* 343:188-190

Scott DJ, Dean DR, Newton WE. 1992 Nitrogenase-catalyzed ethane production and CO-sensitive hydrogen evolution from MoFe proteins having amino acids substitutions in an α-subunit FeMo cofactor-binding domain. *J. Biol. Chem*. 267:20002-20010

Seefeldt LC, Morgan TV, Dean DR, Mortenson LE. 1992 Mapping the site(s) of MgATP and MgADP interaction with the nitrogenase of *Azotobacter vinelandii*. Lysine 15 of the iron protein plays a major role in MgATP interaction. *J. Biol. Chem*. 267:6680-6688

Seefeldt LC 1994 Docking of nitrogenase iron- and molybdenum-iron proteins for electron transfer and MgATP hydrolysis: The role of arginine 140 and lysine143 of *Azotobacter vinelandii* iron protein. *Protein Sci.* 3:2073-2081

Seefeldt LC, Rasche ME, Ensign SA 1995 Carbonyl sulfide and carbon dioxide as new substrates, and carbon disulfide as a new inhibitor, of nitrogenase. *Biochemistry* 34:5382-5389

Seefeldt LC, Dean DR 1997 Role of nucleotides in nitrogenase catalysis. *Acc. Chem. Res*. 30:260-266.

Shah VK, Brill WJ. 1977 Isolation of an iron-molybdenum cofactor from nitrogenase. *Proc. Natl. Acad. Sci. USA* 78:3249-3253

Shah VK, Hoover TR, Imperial J, Paustian TD, Roberts GP, Ludden PW. In *Nitrogen Fixation: Hundred Years After*. Bothe E, de Bruijn FJ, Newton WE eds. Gustav Fischer: Stuttgart 1988 pp115-120

Shah VK, Allen JR, Spangler NJ, Ludden PW. 1994 *In vitro* synthesis of the iron-molybdenum cofactor of nitrogenase. Purification and characterization of NifB cofactor, the product of NIFB protein. *J. Biol Chem*. 269:1154-1158

Shah VK, Rangaraj P, Chatterjee R, Allen RM, Roll JT, Roberts GP, Ludden PW. 1998 Requirement of NIFX for the in vitro biosynthesis of the iron-molybdenum cofactor of nitrogenase. In *Nitrogen Fixation for the 21st Century*. Elmerich C, Kondorsi A, Newton WE, eds. Kluwer Academic Press, Dordrecht, The Netherlands. pp51-52

Shen J, Dean DR, Newton WE. 1997 Evidence for multiple substrate-reduction sites and distinct inhibitor-binding sites from an altered *Azotobacter vinelandii* nitrogenase MoFe protein. *Biochemistry* 36:4884-4894

Shi L, Pulakat L, Gavini N. 1999 Genetic analysis of *nif* regulatory genes by utilizing the yeast two-hybrid system detected formation of a NifL-NifA complex that is implicated in regulated expression of *nif* genes. *J. Bacteriol*. 181:6535-6539

Simon HM, Homer MJ, Roberts GP 1996 Perturbation of *nifT* expression in *Klebsiella pneumoniae* has limited effect on nitrogen fixation. *J. Bacteriol*. 178:2975-2977

Simpson FB, Burris RH 1984 A nitrogen pressure of 50 atmospheres does not prevent evolution of hydrogen by nitrogenase. *Science* 224:1095-1097

Smil V 1991 Population growth and nitrogen: an exploration of a critical existential link. *Population and Development Reviews* 17:569-601

Smith BE, Lowe DJ, Bray RC. 1973 Studies by electron paramagnetic resonance on the catalytic mechanism of nitrogenase of *Klebsiella pneumoniae. Biochem. J.* 135:331-341

Smith BE, Lang G. 1974 Mössbauer spectroscopy of the nitrogenase proteins from *Klebsiella pneumoniae*. Structural assignments and mechanistic conclusions. *Biochem. J.* 137:169-180

Smith BE, O'Donnell MJ, Lang G, Spartalain K. 1980 A Mössbauer spectroscopic investigation of the redox behaviour of the molybdenum-iron protein from *Klebsiella pneumoniae* nitrogenase. Mechanistic and structural implications. *Biochem. J.* 191:449-455

Smith BE, Eady RR. 1992 Metalloclusters of the nitrogenases. *Eur. J. Biochem.* 205:1-15

Smith BE, 1999 Structure, function, and biosynthesis of the metallosulfur clusters in nitrogenases. *Advances in Inorganic Chemistry* 47:159-219

Smith JP, Emptage MH, Orme-Johnson WH. 1982 Magnetic susceptibility studies of native and thionine-oxidized molybdenum-iron protein from *Azotobacter vinelandii* nitrogenase. *J. Biol. Chem*. 257:2310-2313

Sondek J, Lambright DG, Noel JP, Hamm HE, Sigler PB. 1994 GTPase mechanism of G-proteins from the 1.7-Å crystal structure of transducin alpha-GDP-AlF^-_4. *Nature* 372:276-279

Sorlie M, Christiansen J, Lemon BJ, Peters JW, Dean DR, Hales BJ. 2001 Mechanistic features and structure of the nitrogenase alpha-Gln195 MoFe protein. *Biochemistry* 40:1540-1549

Sprang SR 1997 G proteins, effectors and GAPs: structure and mechanism. *Curr. Opin. Struct. Biol.* 7:849-856

Stephens PJ, Jensen GM, Devlin FJ, Morgan TV, Stout CD, Martin AE, Burgess BK 1991 Circular dichroism and magnetic circular dichroism of *Azotobacter vinelandii* ferredoxin I. *Biochemistry* 30:3200-3209

Strandberg GW, Wilson PW. 1968 Formation of the nitrogen-fixing enzyme system in *Azotobacter vinelandii. Can. J. Microbiol*. 14:25-31

Strop P, Takahara PM, Chiu HJ, Hayley C, Angove HC, Burgess BK, Rees DC. 2001 Crystal structure of the all-ferrous $[4Fe\text{-}4S]^0$ form of the nitrogenase iron protein from *Azotobacter vinelandii*. *Biochemistry* 40:651-656

Surerus KK, Hendruch MP, Christie PD, Rottgardt D, Orme-Johnson WH, Münck E. Mössbauer and integer-spin EPR of the oxidized P clusters of nitrogenase: P^{ox} is a non-Kramers system with a nearly degenerate ground doublet. *J. Am. Chem. Soc*. 114:8580-8590

Thomann H, Morgan TV, Jin H, Burgmayer SJN, Bare RE, Stiefel EI. 1987 Protein Nitrogen Coordination to the FeMo Center of Nitrogenase from *Clostridium pasteurianum. J. Am. Chem. Soc.* 109:7913-7914

Thomann H, Bernardo M, Newton WE, Dean DR. 1991 N coordination of FeMo cofactor requires His-195 of the MoFe protein α subunit and is essential for biological nitrogen fixation. *Proc. Natl. Acad. Sci. USA* 88:6620-6623

Thorneley RNF 1975 Nitrogenase of *Klebsiella pneumoniae*: A stopped-flow study of magnesium-adenosine triphosphate-induced electron transfer between the component proteins. *Biochem. J.* 145:391-396

Thorneley RNF, Lowe DJ, Eady RR. 1978 Biological nitrogen fixation by way of an enzyme-bound dinitrogen-hydride intermediate. *Nature* 272:557-558

Thorneley RNF, Lowe DJ. 1983 Nitrogenase of *Klebsiella pneumoniae*: Kinetics of the dissociation of oxidized iron protein from molybdenum-iron protein, identification of the rate-limiting step for substrate reduction. *Biochem. J.* 215:393-403

Thorneley RNF and Lowe DJ 1984a The mechanism of *Klebsiella pneumoniae* nitrogenase action: Simulation of the dependence of the H_2 evolution rate on component-protein concentration and ratio and sodium dithionite concentration. *Biochem. J.* 224:903-909

Thorneley RNF, Lowe DJ. 1984b The mechanism of *Klebsiella pneumoniae* nitrogenase action: Pre-steady-state kinetics of an enzyme-bound intermediate in N_2 reduction and of NH3 formation. *Biochem. J.* 224:887-894

Thorneley RNF, Lowe DJ 1985 Kinetics and mechanism of the nitrogenase enzyme system: T. Spiro (*Ed.*), *Molybdenum Enzymes*, 1, Wiley-Interscience, New York, pp 221-284

Thorneley RNF, Ashby GA, Howarth JV, Millar NC, Gutfreund H. 1989 A transient kinetic study of the nitrogenase of *Klebsiella pneumoniae* by stopped-flow calorimetry. *Biochem. J.* 264:657-661

Thorneley RNF, Ashby GA. 1989 Oxidation of nitrogenase iron protein by dioxygen without inactivation could contribute to high respiration rates of *Azotobacter* species and facilitate nitrogen fixation in other aerobic environments. *Biochem. J*. 261:181-187

Thorneley RNF, Bergström J, Eady RR, Lowe DJ 1989b Vanadium nitrogenase of *Azotobacter chroococcum*. MgATP-dependent electron transfer within the protein complex. *Biochem. J*. 257:789-794

Thorneley RNF, Ahsby GA, Julius C, Hunter JL, Webb MR. 1991 Nitrogenase of *Klebsiella pneumoniae*. Reversibility of the reductant-independent MgATP-cleavage reaction is shown by MgADP-catalyzed phosphate / water oxygen exchange. *Biochem. J*. 277:735-741

van Heeswijk WC, Stegeman B, Hoving S, Molenaar D, Kahn D, Westerhoff HV 1995 An additional P_{II} in *Escherichia coli*: a new regulatory protein in the glutamine synthetase cascade. *FEMS Microbiol Lett.* 132:153-157

Vaughn SA, Burgess BK, 1989 Nitrite, a new substrate for nitrogenase. *Biochemistry* 28:419-424

Walker GA and Mortenson LE. 1974 Effect of magnesium adenosine 5'-triphosphate on the accessibility of the iron of *Clostridium* azoferredoxin, a component of nitrogenase. *Biochemistry* 13:2382-2388

Walker JE, Saraste M, Runswick M. J, Gay N. J. 1982 Distantly related sequences in the α- and β-subunits of ATP synthase, myosin, kinases and other ATP-requiring enzymes and a common nucleotide binding fold. *EMBO J.* 8:945-981

Watt GD, Reddy KRN. 1994 Formation of an all ferrous Fe_4S_4 cluster in the iron protein –component of *Azotobacter vinelandii* nitrogenase. *J. Inorg. Biochem*. 53:281-294

Waugh SI, Paulson DM, Mylona PV, Maynard RH, Premakumar R, Bishop PE 1995 The genes encoding the delta subunits of dinitrogenases 2 and 3 are required for Mo-independent diazotrophic growth by *Azotobacter vinelandii. J. Bacteriol*. 177:1505-1510.

Wherland S, Burgess BK, Stiefel EI, Newton WE. 1981 Nitrogenase reactivity: Effects of component ratio on electron flow and distribution during nitrogen fixation. *Biochemistry* 20:5132-5140

White TC, Harris GS, Orme-Johnson WH 1992 Electrophoretic studies on the assembly of the nitrogenase molybdenum-iron protein from the *Klebsiella pneumoniae nifD* and *nifK* gene products. *J. Biol. Chem*. 267:24007-24016.

Willing A, Georgiadis MM, Rees DC, Howard JB. 1989 Cross-linking of nitrogenase components. *J. Biol. Chem*. 264:8499-8503

Willing A, Howard JB. 1990 Cross-linking site in *Azotobacter vinelandii* complex. *J. Biol. Chem*. 265:6569-6599

Willson PE, Nyborg AC, Watt GD. 2001 Duplication and extension of the Thorneley and Lowe kinetic model for *Klebsiella pneumoniae* nitrogense catalysis using a MATHEMATICA software platform. *Biophs. Chem*. 91:281-304

Wolle D, Dean DR, Howard JB. 1992a Nucleotide-iron-sulfur cluster signal transduction in the nitrogenase iron-protein: the role of Asp125. *Science* 258:992-995

Wolle D, Kim H-C, Dean DR, Howard JB 1992b Ionic interactions in the nitrogenase complex: Properties of Fe protein containing substitutions for 100Arg. *J. Biol. Chem.* 267:3667-3673

Yates MG, Lowe DJ. 1976 Nitrogenase of *Azotobacter chroococcum*: a new electron-paramagnetic-resonance signal associated with a transient species of the Mo-Fe protein during catalysis. *FEBS Lett*. 72:121-126

Yates MG. 1992 In Biological Nitrogen Fixation; Stacey G, Burris RH, Evans HJ. Eds. Chapman and Hall: New York. P685

Yoo SJ, Angove HC, Burgess BK, Hendrich MP, Munck E. 1999 Mössbauer and integer-spin EPR studies and spin-coupling analysis of the [4Fe-4S]0 cluster if the Fe protein from *Azotobacter vinelandii* nitrogenase. *J. Am. Chem. Soc*. 121:2534-2545

Young JPW 1992 In: *Biological Nitrogen Fixation*. Stacey G, Burris RH, Evans HJ, eds. New York: Chapman and Hall. pp43

Yuvaniyama P, Agar JN, Cash VL, Johnson MK, Dean DR 2000 NifS-directed assembly of a transient [2Fe-2S] cluster within the NifU protein. *Proc. Natl. Acad. Sci. USA* 97:599-604

Zheng L, Dean DR. 1994 Catalytic formation of a nitrogenase iron-sulfur cluster. *J. Biol. Chem.* 269:18723-18726

Zheng L, White RH, Dean DR. 1997 Purification of the *Azotobacter vinelnadii nifV*-encoded homocitrate synthase. *J. Bacteriol*. 179:5963-5966

Vita

Hong Li was born on October 13, 1972, in He Fei, China. She graduated from Beijing Normal University with a Bachelor of Science in Biochemistry in 1994, and a master's degree of Science in Biochemistry in 1997. She came to Virginia Polytechnic Institute and State University in August of 1997 and started her graduate program in the Biochemistry Department. In the summer of 1998, she entered the laboratory of Dr. William E Newton to work on the Mo-nitrogenase from *Azotobacter vinelandii*, and she completed her Ph.D. requirement in April 2002.